Anatomy of the *Bacillus subtilis* Cell Envelope Stress Response

Dissertation zur Erlangung des Doktorgrades der Naturwissenschaften Dr. rer. nat. an der Fakultät für Biologie der Ludwig-Maximilians-Universität München

von

Jara Marina Radeck

München, 2017

Diese Dissertation wurde angefertigt

unter der Leitung von Prof. Dr. Thorsten Mascher

im Bereich der Mikrobiologie

an der Ludwig-Maximilians-Universität München

Erstgutachter: Prof. Dr. Thorsten Mascher

Zweitgutachter: PD Dr. Ralf Heermann

Tag der Abgabe: 19.09.2017

Tag der mündlichen Prüfung: 15.12.2017

Erklärung

Ich versichere hiermit an Eides statt, dass meine Dissertation selbständig und ohne unerlaubte Hilfsmittel angefertigt worden ist.

Die vorliegende Dissertation wurde weder ganz, noch teilweise bei einer anderen Prüfungskommission vorgelegt.

Ich habe noch zu keinem früheren Zeitpunkt versucht, eine Dissertation einzureichen oder an einer Doktorprüfung teilzunehmen.

München, den_____ _____

Jara Radeck

TABLE OF CONTENTS

ABBREVIATIONS

1CS	*One-c*omponent *s*ystem
2CS	*Two-c*omponent *s*ystem
ABC-transporter	*A*TP-*b*inding *c*assette-transporter
AMP	*A*nti-*m*icrobial *p*eptide
ATP	*A*denosine *t*ri*p*hosphate
CES	*C*ell *e*nvelope *s*tress
CESR	*C*ell *e*nvelope *s*tress *r*esponse
DAGK	*D*i*ac*yl *g*lycerol *k*inase
DNA	*D*eoxyribo*n*ucleic *a*cid
ECF	*E*xtra*c*ytoplasmic *f*unction sigma factor
GlcNAc	*N-ac*etyl*glu*cosamine
LB	*L*ysogeny *b*roth
LTA	*L*ipo*t*eichoic *a*cid
MurNAc	*N-ac*etyl*mur*amic acid
PAP2	Plasma membrane-bound *p*hosphatidic *a*cid *p*hosphatase
PBP	*P*enicillin-*b*inding *p*rotein
PG	*P*eptido*g*lycan
Psp	*P*hage-*s*hock-*p*rotein
PspA	*P*hage-*s*hock-*p*rotein *A*
IM30	*I*nner *m*embrane-associated protein of *30* kDa
UDPK	*U*n*d*eca*p*renol *k*inase
UP	*U*ndecaprenyl *p*hosphate
UPP	*U*ndecaprenyl *p*yro*p*hosphate
WTA	*W*all *t*eichoic acid

LIST OF PUBLICATIONS (SEE APPENDIX)

Publications and manuscripts presented in this thesis:

Publication I:

Fritz G, Dintner S, Treichel N S, **Radeck J**, Gerland U, Mascher T, Gebhard S (2015) A new way of sensing: need-based activation of antibiotic resistance by a flux-sensing mechanism. **mBio**. 6(4):e00975. doi: 10.1128/mBio.00975-15.

Publication II:

Radeck J, Gebhard S, Orchard P, Kirchner M, Bauer S, Mascher T, Fritz G (2016) Anatomy of the bacitracin resistance network in *Bacillus subtilis*. **Mol Micro**. 100(4):607-20. doi: 10.1111/mmi.13336.

Publication III (review): (with permission of the Springer Nature publishing group)

Radeck J, Fritz G, Mascher T (2016) The cell envelope stress response of *Bacillus subtilis*: from static signaling devices to dynamic regulatory network. **Curr Genet**. 63(1):79-90. doi: 10.1007/s00294-016-0624-0

Manuscript I: [&]

Radeck J*, Lautenschläger N*, Mascher T (2017) The essential UPP phosphatase pair BcrC and UppP connects cell wall homeostasis with cell envelope stress response in *Bacillus subtilis*. (submitted to Frontiers in Microbiology)
* contributed equally to this work

Publications and manuscripts not presented in this thesis:

Manuscript II: [&&]

Radeck J, Meyer D, Lautenschläger N, Mascher T (2017) *Bacillus* SEVA siblings: A Golden Gate-based toolbox to create personalized integrative vectors for *Bacillus subtilis*. (submitted to Scientific Reports)

[&] was published in a revised form as: **Radeck J***, Lautenschläger N*, Mascher T (2017) The Essential UPP Phosphatase Pair BcrC and UppP Connects Cell Wall Homeostasis during Growth and Sporulation with Cell Envelope Stress Response in *Bacillus subtilis*. **Front. Microbiol.**, 8:2403. doi: 10.3389/fmicb.2017.02403

[&&] was published in a revised form in: **Sci. Rep.** 7:14134. doi: 10.1038/s41598-017-14329-5

AUTHOR CONTRIBUTIONS

Publication I: Fritz G, Dintner S, Treichel N S, **Radeck J**, Gerland U, Mascher T, Gebhard S (2015) A new way of sensing: need-based activation of antibiotic resistance by a flux-sensing mechanism.

Thorsten Mascher, Ulrich Gerland, Georg Fritz, and Susanne Gebhard designed the study. Sebastian Dintner, Nicole Treichel, and Jara Radeck performed the experiments, Susanne Gebhard coordinated the experimental work. Georg Fritz performed mathematical modeling. Georg Fritz and Susanne Gebhard created the figures and wrote the manuscript.

Publication II: Radeck J, Gebhard S, Orchard P, Kirchner M, Bauer S, Mascher T, Fritz G (2016) Anatomy of the bacitracin resistance network in *Bacillus subtilis*.

Georg Fritz, Jara Radeck, Susanne Gebhard, and Thorsten Mascher conceived and designed the experiments. Jara Radeck, Peter Orchard, Marion Kirchner and Stephanie Bauer performed the experiments. Jara Radeck and Georg Fritz coordinated the experiments, analyzed the data, created the figures and wrote the manuscript.

Publication III (review): Radeck J, Fritz G, Mascher T (2016) The cell envelope stress response of *Bacillus subtilis*: from static signaling devices to dynamic regulatory network.

Georg Fritz, Thorsten Mascher, and Jara Radeck performed the literature search and wrote the manuscript.

Manuscript I: Radeck J*, Lautenschläger N*, Mascher T (2017) The essential UPP phosphatase pair BcrC and UppP connects cell wall homeostasis with cell envelope stress response in *Bacillus subtilis*. * contributed equally to this work

Jara Radeck and Thorsten Mascher conceived and designed the experiments. Nina Lautenschläger and Jara Radeck performed the experiments. Jara Radeck coordinated the experimental work and created the figures. Jara Radeck and Thorsten Mascher wrote the manuscript.

Manuscript II: Radeck J, Meyer D, Lautenschläger N, Mascher T (2017) *Bacillus* SEVA siblings: A Golden Gate-based toolbox to create personalized integrative vectors for *Bacillus subtilis*.

Jara Radeck and Thorsten Mascher conceptualized the study. Jara Radeck, Daniel Meyer, and Nina Lautenschläger performed the experiments. Jara Radeck coordinated the experimental work and created the figures. Jara Radeck and Thorsten Mascher wrote the manuscript.

We hereby confirm the above-mentioned declarations:

_____	_____
Jara Radeck	Prof. Dr. Thorsten Mascher

Additional declaration for shared first authorship:

Manuscript I: Radeck J*, Lautenschläger N*, Mascher T (2017) The essential UPP phosphatase pair BcrC and UppP connects cell wall homeostasis with cell envelope stress response in *Bacillus subtilis*. * contributed equally to this work

Jara Radeck and Thorsten Mascher conceived and designed the experiments. Nina Lautenschläger and Jara Radeck performed the experiments. Jara Radeck coordinated the experimental work and created the figures. Jara Radeck and Thorsten Mascher wrote the manuscript.

The experimental workload was shared as followed:

Jara Radeck generated UPP phosphatase deletion and depletion strains and performed the MIC assay. She outlined and coordinated the experimental work, processed, analyzed, and visualized all data generated for this study.

Nina Lautenschläger created the reporter strains and *dgkA* mutants. She performed and optimized the plate reader assays and microscopic documentation, and created a preliminary structure for the data to ease its evaluation.

We share the first authorship because the workload of this study was comparably high for both of us. Jara Radeck's name is in the first position because of her significantly higher share in intellectual contribution.

We hereby confirm the above-mentioned declarations:

_____	_____
Jara Radeck	Nina Lautenschläger

SUMMARY

The bacterial cell wall withstands the turgor pressure and is an essential structure for most bacteria. The lipid II cycle is responsible for transporting cell wall building blocks across the cytoplasmic membrane by means of the carrier molecule undecaprenyl phosphate (UP). One essential step is the recycling of undecaprenyl pyrophosphate (UPP) to UP by UPP phosphatases. This step is targeted by bacitracin, an UPP-binding anti-microbial peptide (AMP). In the course of this thesis, the effect of deletion and depletion of bacitracin resistance modules and UPP phosphatase genes on the cell envelope stress response in *Bacillus subtilis* was evaluated.

The main resistance determinant against bacitracin, the ABC-transporter BceAB was found to be homeostatically regulated "to need" by flux-sensing of its own activity. The full effect of the secondary layer of resistance determinants, consisting of the UPP phosphatase BcrC and the phage shock protein-like response of the Lia-system, is only revealed in the absence of BceAB. For the first time, a resistance phenotype for LiaIH toward bacitracin was reported. The genes *uppP* and *bcrC* encode UPP phosphatases and were found to be synthetic lethal. Depletion of either UPP phosphatase in a double mutant background lead to bulging cells in exponential growth phase. BcrC is the main UPP phosphatase during growth. In contrast, UppP is primarily responsible for normal sporulation.

The generation of UP in the lipid II cycle is essential and can be impaired by (i) addition of the UPP-binding AMP bacitracin, (ii) deletion and depletion of UPP phosphatases (BcrC and UppP), or, to a limited degree, (iii) deletion of the undecaprenol kinase (UDPK) DgkA. There is a marked difference in the CESR toward these challenges: while the addition of bacitracin activates two damage driven promoters, P_{lial} and P_{bcrC}, a lack of UPP phosphatases or DgkA is only detected by the latter. This indicates that the blocking of UPP with bacitracin has a different effect on the cell envelope than the shortage of UPP phosphatases. Our analysis of the dephosphorylation of UPP in *B. subtilis* lays another cornerstone for the holistic understanding of the lipid II cycle.

ZUSAMMENFASSUNG

Die bakterielle Zellwand ist für die meisten Bakterien überlebensnotwendig, zum Beispiel um dem Turgor entgegenzuwirken. Sie besteht aus Zucker-Peptidbausteinen, deren Auf- und Abbau komplex reguliert ist. Für die Anlieferung der Bausteine ist der Lipid II-Zyklus mit dem Transportmolekül Undecaprenylphosphat (UP) zuständig. Nach Einbau des Zellwandbausteins liegt das Transportmolekül als Undecaprenylpyrophosphat (UPP) vor und wird von UPP-Phosphatasen zu UP dephosphoryliert, um wiederverwendet werden zu können. An diesem essentiellen Schritt greift das Peptidantibiotikum Bacitracin an, indem es an UPP bindet und so das Recycling verhindert. Eine Blockade des Lipid II-Zyklus führt zu fehlerhafter Zellwandsynthese mit entsprechenden morphologischen Phänotypen, sowie zur Aktivierung der Zellwandstressantwort. In dieser Arbeit wird die Dephosphorylierung von UPP in *Bacillus subtilis* in zwei Aspekten genetisch untersucht. Zum einen wird unter Bacitracinstress beobachtet, wie die nativen Sensoren und Resistenzmechanismen in Abhängigkeit voneinander reagieren. Zum anderen werden die Auswirkungen eines UPP-Phosphatase-Defizits beleuchtet.

Der ABC-Transporter BceAB ist die primäre Resistenzdeterminante gegen Bacitracin. Seine Anzahl wird durch homöostatische Selbstregulierung an den aktuellen Bedarf angepasst, indem die Aktivität der Transporter als Signal für deren Auslastung verwendet wird. Die sekundären Resistenzdeterminanten, die UPP-Phosphatase BcrC und LiaIH (wobei LiaH Ähnlichkeit zum Phagenschockprotein A aufweist), werden schadensabhängig induziert. Ihr volles Potential wird nur in Abwesenheit von BceAB sichtbar. Zum ersten Mal wurde gezeigt, dass LiaIH Resistenz gegen Bacitracin vermitteln kann, obwohl deren Expression bei Bacitracinstress schon seit über zehn Jahren bekannt ist. Außerdem konnte gezeigt werden, dass die Gene *bcrC* und *uppP* der UPP-Phosphatasen BcrC und UppP ein essentielles Paar bilden. Die Depletion dieser Phosphatasen in einer *bcrC uppP* Doppelmutante führte zu gewölbten Zellen in der exponentiellen Wachstumsphase. BcrC stellt die Haupt-UPP-Phosphatase während des Wachstums dar, wohingegen UppP für die ordnungsgemäße Sporulation benötigt wird.

Die (Wieder-)Herstellung von UP ist für den Lipid II Zyklus essentiell und kann auf drei Arten gestört werden: (i) Zugabe von Bacitracin, welches UPP bindet und die Dephosphorylierung verhindert, (ii) Deletion und Depletion der UPP-Phosphatasen BcrC und UppP, oder, in geringem Umfang, (iii) Deletion der Undecaprenol-Kinase DgkA. Hierbei zeigt sich ein drastischer Unterschied in der Zellwandstressantwort. Während durch Bacitracin zwei schadensabhängige Promotoren aktiviert werden, P_{lial} und P_{bcrC}, ist bei UPP-Phosphatase- oder DgkA-Mangel nur letzterer aktiv. Dies deutet darauf hin, dass diese Eingriffe auf die Bildung von UP verschiedene molekulare Konsequenzen haben, die unterschiedlich detektiert werden. Unsere Untersuchung der UPP-Dephosphorylierung legt einen weiteren Grundstein für das umfängliche Verständnis der Funktion und Regulation des Lipid II Zyklus und der Zellwandbiosynthese.

PREFACE

"Zwei Seelen wohnen, ach! In meiner Brust,

Die eine will sich von der andern trennen" – J. W. v. Goethe, Faust I

"Two souls, alas, are housed within my breast,

And each will wrestle for the mastery there"

My heart, it beats for basic science. My heart, it beats for applied science and Synthetic Biology. I was fortunate enough that in the course of my thesis, I did not have to choose one of the wishes above the other – I could pleasure both hearts, which were linked by the organism of choice: *Bacillus subtilis*. The order of events did not allow me to use the vector toolbox "*Bacillus* SEVA siblings" for the cell envelope stress project, so in this thesis, I will only focus on cell envelope stress and undecaprenyl pyrophosphate phosphatases.

1 INTRODUCTION

Parts of this chapter have been adapted from:

Radeck J, Gebhard S, Orchard P, Kirchner M, Bauer S, Mascher T, Fritz G (2016) Anatomy of the bacitracin resistance network in *Bacillus subtilis*. **Mol Micro**.100(4):607-20. doi: 10.1111/mmi.13336.

And:

Radeck J, Fritz G, Mascher T (2016) The cell envelope stress response of *Bacillus subtilis*: from static signaling devices to dynamic regulatory network. **Curr Genet**. 63(1):79-90. doi: 10.1007/s00294-016-0624-0

1.1 THE BACTERIAL CELL ENVELOPE

The cell envelope is an essential complex multilayered structure to separate bacteria from the environment and protect their content. Gram-positive bacteria, such as *Bacillus subtilis*, are surrounded by (i) an inner membrane and (ii) a thick cell wall (~30 nm). The membrane consists of a phospholipid bilayer where proteins and lipoteichoic acids (LTAs) can be anchored. To name just a few functions, the membrane serves as a diffusion barrier, allows the formation of a membrane potential, and is a platform for protein interaction, e.g. for signaling pathways or chemical synthesis which involves multiple enzymes (Hurdle *et al.*, 2011). The cell wall contains mainly peptidoglycan (PG) and wall teichoic acids (WTAs), but also LTAs, and proteins (Dufresne & Paradis-Bleau, 2015; Silhavy *et al.*, 2010). PG forms a sieve-structured network of glycan chains composed of *N*-acetylglucosamine (GlcNAc) and *N*-acetylmuramic acid (MurNAc), cross-linked by short peptide bridges (Vollmer & Höltje, 2004). It determines the cell shape, counteracts the cellular turgor pressure, and is negatively charged due to the presence of teichoic acids. Both, membrane and cell wall compositions, are actively changed by the bacteria according to environmental conditions and needs. For example, under phosphate-depleting conditions, teichuronic acids instead of teichoic acids are utilized (Bhavsar *et al.*, 2004; Botella *et al.*, 2014). The essential functions fulfilled by the cell envelope and its accessibility make it a perfect target for antibiotics: almost every single step of its biosynthesis pathway is targeted by at least one antibiotic (Bugg *et al.*, 2011; Schneider & Sahl, 2010), see Figure 1. Since the bacterial cell envelope is distinct from eukaryotic cells, the cell wall active antibiotics are suitable candidates for clinical use.

1.1.1 CELL WALL BIOSYNTHESIS

The PG biosynthesis can be separated into three stages: (i) intracellular assembly of PG precursors, (ii) their shuttling across the membrane (lipid II cycle), and (iii) their incorporation into the existing cell wall. Especially the last step needs to be highly regulated in a spatio-temporal manner, since the insertion of new building blocks for cell elongation requires the hydrolysis of the pre-existing PG in a turgor-strained setting; see (Typas *et al.*, 2012) for a recent review. Further structural changes, like

the extrusion of flagella and pili or DNA uptake in competent cells, require PG modification, as well (Carballido-Lopez *et al.*, 2006).

1.1.2 LIPID II CYCLE

The carrier molecule for cell wall components (PG, WTAs, or (in Gram-negative bacteria) lipopolysaccharide O-antigen) in most bacteria is undecaprenyl phosphate (UP), a linear-chain polyprenyl-phosphate (Manat *et al.*, 2014). The respective precursors are attached to the carrier which shuttles them from the inner to the outer leaflet of the cytoplasmic membrane. For PG, this process is called lipid II cycle (Figure 1), in reference to the mature molecule used for cell wall assembly: lipid II (Scheffers & Tol, 2015).

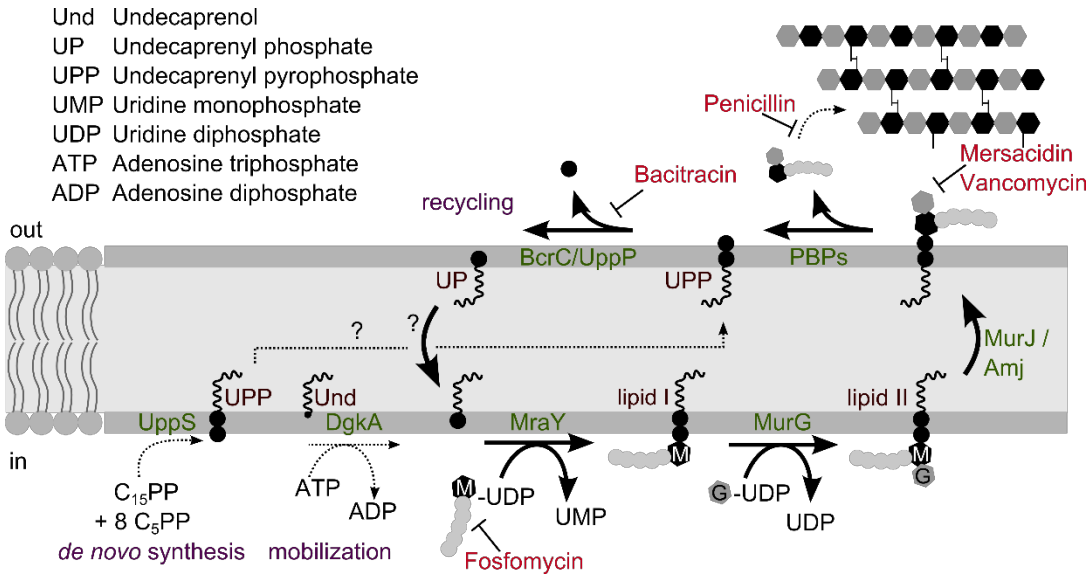

Figure 1. The lipid II cycle and a few interfering antibiotics. The first step of the lipid II cycle is catalyzed by MraY: the soluble precursor molecule *N*-acetyl-muramic acid-pentapeptide (MurNAc-pentapeptide, M) is loaded onto UP, forming lipid I. Subsequently, *N*-acetyl-glucosamine (GlcNAc, G) is added by MurG and lipid II is generated. The flippases MurJ and Amj flip lipid II to the outer leaflet of the cytoplasmic membrane (Laddomada *et al.*, 2016; Meeske *et al.*, 2015) where the MurNac-GlcNAc-pentapeptide is linked to the cell wall by β-(1→4) glycosylation and transpeptidation, carried out by Penicillin-binding proteins (PBPs) (Goffin & Ghuysen, 1998; Schneider & Sahl, 2010). Thus, UPP is released on the outer leaflet and dephosphorylated by designated UPP phosphatases to UP. To be accessible for recycling, UP needs to be flipped back to the inner leaflet by a yet unknown mechanism (Manat *et al.*, 2014). Feeding into the lipid II cycle are *de novo* synthesis of UPP via UppS and (probably) phosphorylation of undecaprenol via DgkA. Molecules (black) and relevant enzymes in *B. subtilis* (green) are named in the figure. Modified from (Breukink & de Kruijff, 2006).

UP is loaded on the cytosolic side of the membrane, flipped to the outside by specific flippases and released as undecaprenyl pyrophosphate (UPP) upon polymerization of

the transported building block (Manat *et al.*, 2014). UPP is dephosphorylated to UP by UPP phosphatases and – potentially in this process – flipped back to the inner leaflet of the cytoplasmic membrane. *De novo* assembly of UPP takes place at the inner leaflet of the cytoplasmic membrane by the essential UPP synthase UppS: eight isoprene units (derived from isoprenyl pyrophosphate) are added to farnesyl pyrophosphate (Barreteau *et al.*, 2009). Both, newly synthesized and recycled UPP, need to be dephosphorylated to UP by UPP phosphatases to be (re)loaded with new building blocks. This process, especially the membrane orientation, is not yet fully understood (Manat *et al.*, 2014). The lipid II cycle is a prime target of clinically relevant anti-microbial peptides (AMPs), such as tunicamycin, vancomycin, bacitracin or mersacidin (Field *et al.*, 2015; Schneider & Sahl, 2010).

In *B. subtilis*, UP is responsible for the transport of WTAs and PG (Barreteau *et al.*, 2009; Bouhss *et al.*, 2008). When the teichoic acid is attached to the PG, UP (instead of UPP) is released, in contrast to the lipid II cycle (Anderson *et al.*, 1972; Brown *et al.*, 2013).

1.2 BACTERIAL CELL ENVELOPE STRESS RESPONSE (CESR)

B. subtilis belongs to the phylum of *Firmicutes*, which comprises Gram-positive bacteria with a low GC-content. It is a model organism for cellular differentiation, division and cell shape determination, among others (Jensen *et al.*, 2005; Muchova *et al.*, 2013; van Gestel *et al.*, 2015). *B. subtilis* lives in the soil, one of the most competitive environments for bacteria. It is exposed not only to changing environmental conditions, like temperature, humidity, nutrients, salinity or pH, but also to AMPs, which are produced by competitors to suppress proliferation (Eijsink *et al.*, 2002). Their main target is the cell envelope integrity and biosynthesis (Breukink & de Kruijff, 2006). In order to survive, cells have to respond immediately and usually with differential gene expression. Accordingly, important cues, such as AMPs or cell envelope damage, need to be sensed, signals have to be transduced to the cytoplasm and the correct protective countermeasures must be taken. This is collectively referred to cell envelope stress response (CESR) (Jordan *et al.*, 2008; Schrecke *et al.*, 2012).

There are three bacterial regulatory principles and representatives of all of them are involved in CESR. (i) Extracytoplasmic function sigma factors (ECFs) are activated in response to extracellular stress and have evolved diverse mechanisms of signal transduction (Mascher, 2013). A cognate, often membrane bound, anti-σ factor is responsible for the regulation of σ factor activity. For instance, under non-inducing conditions, the anti-σ factor binds and inactivates the σ factor, and releases it upon stimulus perception under inducing conditions (Hughes & Mathee, 1998). (ii) One-component systems (1CS) combine an extracellular input domain with an intracellular effector domain in a single protein. The bacitracin-responsive regulator BcrR of *Enterococcus faecalis* (Gauntlett *et al.*, 2008; Gebhard *et al.*, 2009) is so far the only known example of a membrane-anchored transcriptional regulator that responds to envelope stress. The scarcity of 1CS in the CESR, despite the dominating abundance of 1CS in general, is explained by the molecular restrictions of simultaneous membrane localization and DNA binding (Ulrich *et al.*, 2005). (iii) This restriction is overcome in two-component systems (2CS), in which the input and effector domains are located on two separate proteins. One is the membrane-anchored signal sensor, a histidine kinase, the other a soluble transcriptional response regulator. The signal is communicated via phosphoryl group transfer (Gao *et al.*, 2007). ECFs and 2CSs are commonly found amongst the signaling devices mediating the cellular response to AMP challenge (Jordan *et al.*, 2008).

Regarding resistance determinants, there are two general principles at work: (i) specific resistance determinants that either transport or sequester AMPs from their molecular targets, like ATP binding cassette (ABC)-transporters (Gebhard, 2012) or lipoproteins (Aso *et al.*, 2005; Khosa *et al.*, 2016), and (ii) unspecific resistance determinants that alter the composition and charge of the cell envelope to exacerbate the access of AMPs to their targets (Revilla-Guarinos *et al.*, 2014) or cope with the physiological damage that already occurred, e.g. using phage-shock-proteins (Psps) (Joly *et al.*, 2010). Especially specific resistance determinants act most efficiently if activated before severe damage occurs, so they rely on very sensitive sensing of AMPs – at concentrations far below lethality.

1.2.1 THE BACITRACIN-INDUCED CESR IN *B. SUBTILIS*

In this work, I will focus on the CESR of *B. subtilis* toward the peptide antibiotic bacitracin, and especially how the regulation of resistance determinants interdepends. Bacitracin is a cyclic AMP, produced by nonribosomal peptide synthesis in some strains of *Bacillus licheniformis* and *B. subtilis* (Azevedo *et al.*, 1993; Ishihara *et al.*, 2002; Konz *et al.*, 1997), but not the W168 strain used in this study. Bacitracin coordinates a divalent cation (optimal is Zn^{2+}), binds UPP tightly and blocks its dephosphorylation (Economou *et al.*, 2013; Storm & Strominger, 1973), thereby inhibiting an essential step in the preparation or recycling of the carrier molecule to transport cell wall building blocks. It is clinically used as broad spectrum antibiotic against skin infections (Trookman *et al.*, 2011).

To enable progression of the lipid II cycle and protect against cell envelope damage, there are three known resistance mechanisms against bacitracin in bacteria: (i) specific ABC-transporters (Manson *et al.*, 2004; Ohki *et al.*, 2003a; Podlesek *et al.*, 1995), (ii) (over)expression of (alternative) UPP phosphatases (Bernard *et al.*, 2005; Cain *et al.*, 1993; Cao & Helmann, 2002; Ohki *et al.*, 2003b), and (iii) variation of exopolysaccharide production (Pollock *et al.*, 1994; Tsuda *et al.*, 2002).

Upon bacitracin addition, *B. subtilis* upregulates σ^B (general stress response) and the ECF σ^M (CESR). Furthermore, several 2CS are activated, which orchestrate the upregulation of the following proteins (Mascher *et al.*, 2003; Rietkötter *et al.*, 2008; Wolf *et al.*, 2010): (i) the phage-shock-protein A (PspA)-like LiaH, and LiaI, (ii) the ABC-transporters BceAB and (iii) PsdAB[1], (iv) the ZneR-regulon[2], (v) YhcYZ and YhdA[3], and (vi) YdhE[4]. Systems iii-vi are either not relevant in bacitracin sensing or mediating

[1] PsdAB has been shown to be activated by crosstalk of BceS to the response regulator of the Psd-system PsdR (Rietkötter *et al*., 2008).
[2] The ZneR-regulon is suspected to be activated by Zn^{2+}, which is present in the biologically active bacitracin salt (Mascher *et al*., 2003).
[3] The *yhcYZ-yhdA*-operon and *ydhE* are regulated by LiaFSR (Wolf *et al*., 2010). YhcYZ are predicted to be a sensor kinase and response regulator, but their target is not known (Jordan *et al*., 2006; Wolf *et al*., 2010). *yhdA* is part of the same operon and encodes a putative NADPH-dependent azobenzene FMN reductase (Deller *et al*., 2006)
[4] YdhE is a putative macrolide glycosyltransferase, so it could be involved in the inactivation of macrolide antibiotics (Liu *et al*., 2016)

resistance (iii, iv), or too little is known about them so far (v, vi), so they are excluded from further study on the *B. subtilis* CESR toward bacitracin.

We included the following proteins in our study, due to their strong upregulation in the presence of bacitracin and/or known involvement in bacitracin resistance:

- BceAB, an ABC-transporter known to be upregulated in the presence of bacitracin and involved in bacitracin resistance (Mascher *et al.*, 2003)
- LiaIH, two proteins strongly induced in the presence of bacitracin (Mascher *et al.*, 2003), but not yet shown to be involved in resistance toward bacitracin (Wolf *et al.*, 2010)
- BcrC, a UPP phosphatase known to be involved in bacitracin resistance (Bernard *et al.*, 2003) and regulated by the CESR-related ECF σ^M (Cao & Helmann, 2002).

The current knowledge on BceAB, LiaIH and BcrC and their regulation will be described in the following sections.

1.2.2 THE ABC-TRANSPORTER BCEAB MEDIATES BACITRACIN-RESISTANCE

The ABC transporter BceAB (bacitracin efflux) is formed by the cytoplasmic ATPase BceA and the permease BceB, which consists of 10 transmembrane helices and a large unstructured extracellular loop between helices seven and eight. Its expression is regulated by the histidine kinase BceS and the response regulator BceR, which are encoded in an operon upstream of *bceAB*, see Figure 2 (Bernard *et al.*, 2003; Mascher *et al.*, 2003; Ohki *et al.*, 2003a). Deletion of *bceAB* leads to approximately 50-fold increased bacitracin sensitivity (Bernard *et al.*, 2003; Mascher *et al.*, 2003). While *bceRS* are constitutively expressed via the weak promoter P_{bceR}, the usually low expression of *bceAB* can be induced >100-fold upon addition of certain AMPs (Rietkötter *et al.*, 2008). The permease BceB has a dual role, which depends on the ATP-hydrolysing activity of the BceA subunit (Bernard *et al.*, 2007): (i) Transport of bacitracin and several other antibiotics interfering with the lipid II cycle, like plectasin, actagardin, and mersacidin (Staroń *et al.*, 2011). (ii) Acting as their sensor to control its own production (Bernard *et al.*, 2007; Rietkötter *et al.*, 2008). While the coupling

of the sensing and resistance mechanism in one specific transporter (in this case BceAB) can be advantageous, in most systems both actions are strictly separated as sensors and effectors, connected by regulators, as described in 1.2. The dual mode-of-action of BceAB is rare and was therefore further investigated.

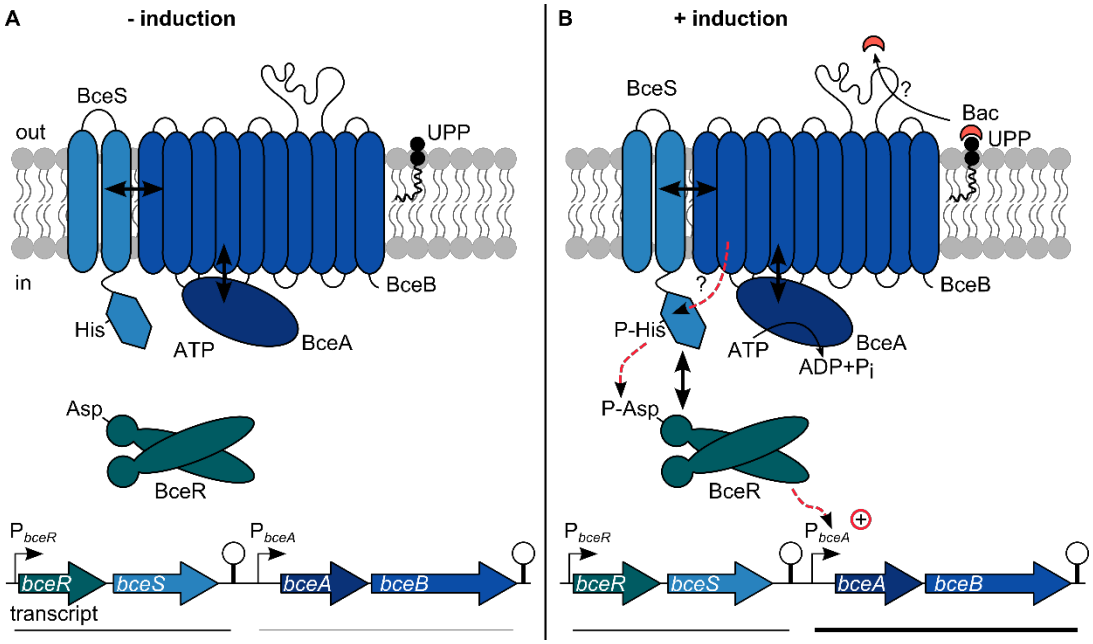

Figure 2. **Schematic representation of the regulation of the BceAB-resistance determinant.** Configurations are shown in the absence (A) and presence (B) of inducer. Relevant molecules, proteins and their corresponding genes are depicted and named. UPP. Undecaprenyl pyrophosphate. Bac. Bacitracin. Double-pointing arrows indicate protein-protein interaction between BceA and BceB as well as BceB and BceS. **A.** Low levels of BceABRS are present in the cell. BceS and BceR are inactive. **B.** BceB removes bacitracin from its target UPP (depending on ATP-ase activity of BceA) and BceS receives a stimulus from the transporter, which is not yet understood. BceS subsequently autophosphorylates and transfers the phosphate residue to the response regulator BceR. Consequently, the BceR dimer conformation is changed and BceR activates the promoter P_{bceA} to increase the transcription of *bceAB*. The transcription of *bceRS* remains at a constant low level. Schematic genes and transcripts are not drawn to scale. (Dintner *et al.*, 2014; Mascher *et al.*, 2003; Ohki *et al.*, 2003b)

It was shown that BceAB binds bacitracin *in vitro* and interacts with BceS *in vivo* and *in vitro* (Dintner *et al.*, 2014) and some residues potentially involved in signaling and/or bacitracin resistance could be identified (Kallenberg *et al.*, 2013). But, the exact mechanism of signal transfer is still elusive.

In Gram-positive bacteria, including important pathogens like *Staphylococcus aureus* and *E. faecalis*, there are several examples for such Bce-like systems, which are named after their best-studied example from *B. subtilis* (Gebhard *et al.*, 2014; Hiron *et al.*, 2011). These transporters mediate resistance against a range of AMPs and are regulated by 2CS in which the intermembrane histidine-kinase lacks a recognizable

ligand-binding domain (Mascher, 2014). Instead, transporter and kinase form a sensory complex (Dintner *et al.*, 2014; Kallenberg *et al.*, 2013). The transporter can be simultaneously involved in mediating resistance (e.g. in *B. subtilis*), or one transporter is used for sensing and another one for mediating resistance (e.g. in *E. faecalis*) (Gebhard *et al.*, 2014; Rietkötter *et al.*, 2008). For the Bce-system in *B. subtilis*, it was also shown that ATP-hydrolysis by BceA, i.e. active transport by BceB, is required for signaling, although the exact stimulus and direction of transport it is not yet known (Ouyang *et al.*, 2010; Rietkötter *et al.*, 2008).

1.2.3 ACTIVATION OF THE PHAGE-SHOCK-PROTEIN-LIKE RESPONSE LIAIH

The *B. subtilis* promoter P_{lial} is controlled by the 2CS LiaRS (for lipid II cycle interfering antibiotic response regulator and sensor) and represents a very sensitive indicator of cell envelope stress (CES) (Mascher *et al.*, 2004). Surprisingly, the deletion of the target genes *liaIH* lead to no or only very weak resistance phenotypes toward the inducers (Wolf *et al.*, 2010). The reason for their induction remained so far elusive.

The LiaRS 2CS is regulated by the LiaS-inhibitor LiaF and reacts to a broad range of cell envelope stressors, including oxidative stress, alkaline shock, or bacitracin addition (Jordan *et al.*, 2006; Wolf *et al.*, 2010). LiaRS respond to the disruption of active cell wall synthesis and are therefore “damage-sensing” (Wolf *et al.*, 2012). The actual stimulus for the Lia system remains to be identified.

While LiaFSR represent a well-conserved sensor in *Firmicutes* CESR, neither their regulon nor its size is conserved between species, which indicates its adaptation toward the lifestyle and regulatory needs (Jordan *et al.*, 2008). In *B. subtilis*, the relevant target of LiaRS is P_{lial}, which regulates the transcription of the hexacistronic operon *liaIH-liaGFSR*, see Figure 3 (Jordan *et al.*, 2006; Wolf *et al.*, 2010). In the absence of CES, P_{liaG}, the weak constitutive promoter upstream of *liaG* ensures a basal expression level of *liaGFSR*. Upon up-regulating conditions, P_{lial} activity is increased up to ~300-fold, resulting in a major 1.1-kb transcript containing *liaIH* and a 4-kb transcript encompassing the entire locus. LiaG is a predicted membrane

protein with a large extracellular domain of unknown function (DUF4097, Pfam[5], (Finn *et al.*, 2016)). It is only present in close relatives of *B. subtilis* and its function is still elusive (Jordan *et al.*, 2006). LiaF is a membrane protein, which is predicted to contain four transmembrane helices (TMHs) and a domain of unknown function (DUF2154, Pfam) in its cytoplasmic C-terminus. It was further shown that LiaF serves as inhibitor of LiaS if present in excess stoichiometry (approx. 9:2 = LiaF:LiaS), as is the case under non-inducing conditions *in vivo* (Schrecke *et al.*, 2013). The LiaF C-terminus seems to be important for stimulus perception and/or signaling (Jordan *et al.*, 2006).

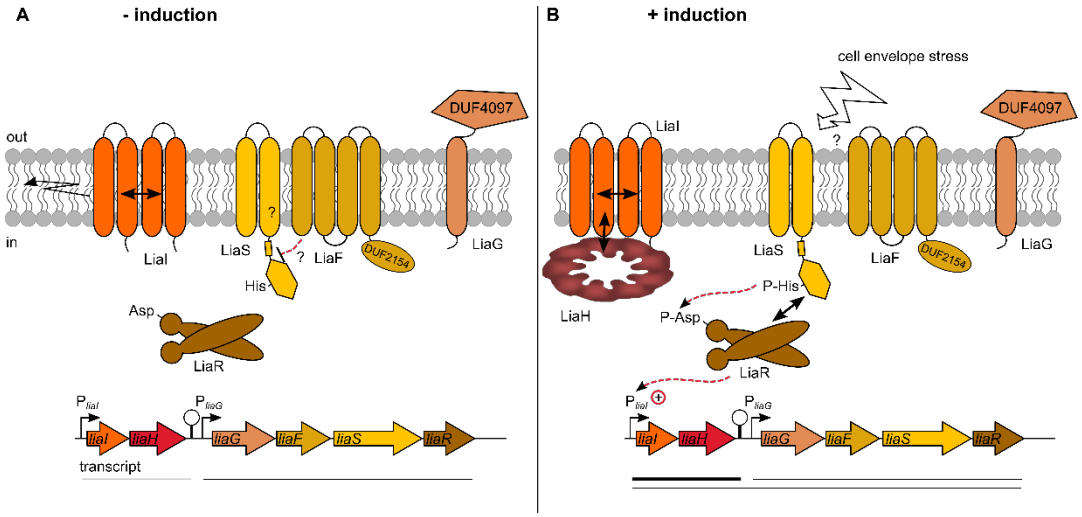

Figure 3. **Schematic representation of the regulation of the LiaIH-stress response.** Configurations are shown in the absence (A) and presence (B) of inducing CES. Relevant molecules, proteins and there encoding genes are depicted and named. Double-pointing arrows indicate permanent interaction between LiaI proteins. **A.** LiaI forms fast-moving patches at the membrane. LiaF inhibits the histidin kinase LiaS. LiaR is therefore inactive. LiaG is a protein of unknown function, seemingly neither involved in sensing nor resistance determination. **B.** Under inducing conditions, e.g. in the presence of bacitracin, LiaS is active and phosphorylates the response regulator LiaR, which in turn upregulates transcription of P_{liaI}. This results in a high production level of LiaI and LiaH as well as a moderate increase of LiaGFSR. The membrane patches of LiaI become static (presumably at locations of defect cell wall) and recruit LiaH oligomers to the membrane. Schematic genes and transcripts are not drawn to scale. (Dominguez-Escobar *et al.*, 2014; Wolf *et al.*, 2010)

Without CES, LiaI proteins can be detected as GFP-fusions in fluorescence microscopy (Dominguez-Escobar *et al.*, 2014). These oligomerize and form motile membrane patches. LiaH, a PspA/IM30 (inner membrane-associated protein of 30 kDa) protein

[5] Protein families database http://pfam.xfam.org/

family member, is spread dispersedly (Dominguez-Escobar *et al.*, 2014). Under CES conditions, LiaIH are strongly produced, the small membrane anchor protein LiaI recruits the cytosolic LiaH, and the membrane-associated patches become static (Dominguez-Escobar *et al.*, 2014). While the corresponding molecular cue for the location of static patches remains elusive, no co-localization with MreB was detected, which is important for the localization of the cell wall biosynthesis machine (Dominguez-Escobar *et al.*, 2014). LiaH forms rings (potentially nonamers of tetramers) similar to the homologous PspA in *E. coli* (Wolf *et al.*, 2010). The *E. coli* Psp-system supports maintenance of the proton motive force in the presence of detergents, mediated by oligomeric PspA (Kleerebezem *et al.*, 1996; Kobayashi *et al.*, 2007).

Despite first insights into the role of PspA in *E. coli* and the strong induction of *liaIH* under bacitracin stress, no link to bacitracin resistance was detected so far (Wolf *et al.*, 2010). In fact, only mild contributions to the resistance against some of the inducing antibiotics (e.g. daptomycin, fosfomycin, and hydrogen peroxide, but not bacitracin, nisin or vancomycin) were demonstrated to date (Hachmann *et al.*, 2009; Wolf *et al.*, 2010).

1.2.4 THE UPP PHOSPHATASE BCRC MEDIATES BACITRACIN RESISTANCE

The third player in the bacitracin stress response network is the UPP phosphatase BcrC. It provides resistance by competing with bacitracin for the target UPP, and consequently, a *bcrC* deletion mutant is about five times more sensitive toward bacitracin than the wild type (Bernard *et al.*, 2003; Bernard *et al.*, 2005). *bcrC* is controlled by multiple stress-inducible alternative sigma factors, including σ^M, σ^I, σ^X, σ^V, and potentially also σ^W (Cao & Helmann, 2002; Guariglia-Oropeza & Helmann, 2011; Tseng & Shaw, 2008; Zweers *et al.*, 2012). Under CES conditions caused by bacitracin, *bcrC* is under control of σ^M, which controls approx. 60 genes involved in cell wall synthesis, shape determination, DNA damage response and detoxification (Bernard *et al.*, 2005; Cao & Helmann, 2002; Eiamphungporn & Helmann, 2008). It was shown that the resistance toward bacitracin mainly depends on the additional transcription of *bcrC* mediated by σ^M in the presence of bacitracin (Cao & Helmann,

2002). Consequently, the regulation of σ^M is important to understand the regulation of *bcrC*.

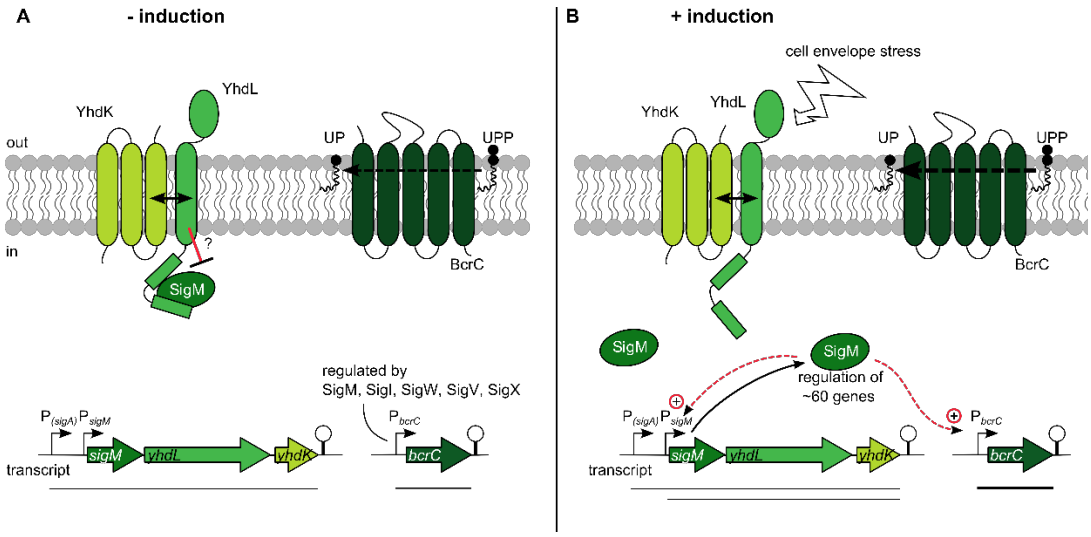

Figure 4. Regulation of BcrC at CES conditions. A. *bcrC* is under transcriptional control of five ECFs, among them σ^M, which is active upon bacitracin addition. The corresponding gene *σ^M^* is controlled by the housekeeping sigma factor σ^A, and σ^M itself in a positive feedback loop. *yhdLK* are co-transcribed with *σ^M^* and the encoded proteins act as anti-σ-factors, sequestering σ^M in the absence of membrane stress. All depicted genes are transcribed and the corresponding proteins are present in cell membranes also in the absence of CES. **B.** Under CES conditions, σ^M is released from YhdLK to regulate approx. 60 genes. The transcription of *σ^M^-yhdLK* and *bcrC* is increased. Schematic genes and transcripts are not drawn to scale (Cao & Helmann, 2002; Hahne *et al.*, 2008; Horsburgh & Moir, 1999; Yoshimura *et al.*, 2004)

The gene encoding σ^M is co-transcribed in an operon with the genes of the cognate anti-*σ* factors YhdL and YhdK, which tightly control the activity of σ^M (Figure 4) (Horsburgh & Moir, 1999; Jervis *et al.*, 2007). In the absence of membrane stress, YhdK, a small membrane protein with three TMHs, was shown to interact with YhdL to negatively regulate *σ^M^* (Yoshimura *et al.*, 2004). It was demonstrated that the cytoplasmic N-terminus of YhdL is involved in σ^M binding, while the single TMH of YhdL is required for interaction with YhdK. The extracytoplasmic C-terminus of YhdL might function as sensory domain, but the precise molecular cues detected by YhdLK/σ^M remain to be identified and are still a matter of debate (Helmann, 2016; Yoshimura *et al.*, 2004).

1.3 THE LINK BETWEEN CESR CAUSED BY BACITRACIN AND UPP PHOSPHATASES

Bacitracin blocks the generation of the essential carrier molecule UP from UPP – UPP dephosphorylation – and is known to elicit a CESR. UPP itself is generated by *de novo* synthesis or recycling after incorporation of a cell wall building block into the existing PG network. In the first part of this study, I focused on the *B. subtilis* CESR caused by bacitracin and especially the interdependence of the three well-known players involved in stress perception and resistance mediation, BceABRS, BcrC/σ^M and LiaIHGFSR. In the second part, I took a different look at this reaction (UPP dephosphorylation to UP) by reducing the UPP phosphatase activity, which might have a similar effect on *B. subtilis* like bacitracin addition.

1.3.1 UP AS A BOTTLENECK IN CELL WALL BIOSYNTHESIS

UP is the carrier for both PG and WTA building blocks and its availability might represent the central bottleneck for the synthesis of lipid II both *in vitro* and *in vivo* (Breukink & de Kruijff, 2006; Egan *et al.*, 2015). Only ~ $2*10^5$ UP molecules (0.5-1 % of all phospholipids) are present per cell (Kramer *et al.*, 2004). The amount of WTA and PG synthesis is reduced under UP-limiting conditions; especially if the culturing conditions favor the competing pathway (PG if WTA are measured and *vice versa*), which leads to a further decrease of available UP (Anderson *et al.*, 1972). Blocking any step of the lipid II cycle will lead to accumulation of intermediates, shortage of free carrier molecules and impaired cell wall biosynthesis that depends on UP. The availability of lipid carrier is a bottleneck, which is exemplified in Gram-negative bacteria that can gain bacitracin resistance by losing pathways for generating exopolysaccharides that also use UP as a carrier (Pollock *et al.*, 1994).

1.3.2 UPP PHOSPHATASES IN *B. SUBTILIS*

There are two known (BcrC and UppP) and one putative (YodM) UPP phosphatase encoded in the *B. subtilis* genome. BcrC was originally suspected to be a permease, because it is mediating resistance against bacitracin and is in parts similar to the BcrC-component of the *B. licheniformis* ABC-transporter BcrABC (Cao & Helmann, 2002;

Ohki *et al.*, 2003b). Biochemical analysis however revealed its UPP phosphatase activity and therefore its resistance mechanism: BcrC and bacitracin compete for the same target UPP (Bernard *et al.*, 2005). The equilibria of UPP dephosphorylation by BcrC and UPP binding by bacitracin are shifted toward dephosphorylation with increasing concentrations of BcrC. By scrutinizing how the *bcrC*-promoter is regulated, it was also shown that the σ^M-mediated upregulation of P_{bcrC} in the presence of bacitracin is responsible for the higher resistance against bacitracin – not its basal activity (Cao & Helmann, 2002).

The location of UPP dephosphorylation at the inner, outer or both leaflets of the cytoplasmic membrane, as well as the translocation of UP from the outer to the inner leaflet are still under investigation. Until 2015, it was assumed that dephosphorylation of recycled UPP takes place at the outer leaflet of the cytoplasmic membrane and dephosphorylation of *de novo* synthesized UPP at the inner leaflet (Manat *et al.*, 2014). This was supported by the finding that there are two known families of UPP phosphatases, BacA and PAP2, which are best studied in *E. coli*.

The BacA-type is named after the *E. coli* BacA UPP phosphatase and carries two motives (BacA1 and BacA2) that form the catalyzing center (Manat *et al.*, 2015). Using TMH predictions and topology studies with the β-lactamase BlaM, BacA is predicted to contain 7 TMHs with a cytosolic N-terminus, a periplasmic C-terminus and the active center facing the periplasm (Manat *et al.*, 2015). BacA is the "house-keeping" UPP phosphatase in *E. coli* and contributes ~70% to the total UPP phosphatase-activity (El Ghachi *et al.*, 2004). For the *B. subtilis* homolog UppP no topology studies are available, but it is assumed to be similar, due to their high identity (47%) and similarity (63% [6])(Bernard *et al.*, 2005; Inaoka & Ochi, 2012).

There are three additional UPP phosphatases in *E. coli*, LpxT, YbjG and PgpB, which all belong to the superfamily of plasma membrane-bound (type 2) phosphatidic acid phosphatases (PAP2). A crystal structure for PgpB revealed that the cytoplasmic N- and C-termini are connected by 6 TMHs and that the catalytic center is localized at the periplasmic leaflet of the cytoplasmic membrane (Touze *et al.*, 2008a).

[6] Sequence Identity and Similiarity tool, SIAS, http://imed.med.ucm.es/Tools/sias.html

Superimposition of the *B. subtilis* BcrC and YodM protein sequences to the PgpB crystal structure is possible and predicts two missing parts in both *B. subtilis* proteins: the first TMH, including part of the periplasmic loop and parts of the C-terminus (based on Phyre2 analysis, data not shown; Kelley *et al.*, 2015). Compared to UppP/BacA, the sequence is less well conserved (based on SIAS analysis, data not shown). It is assumed that the topology is similar enough to postulate a UPP phosphatase activity on the outer leaflet of the cytoplasmic membrane.

In summary, both types of UPP phosphatases are active at the outer leaflet of the cytoplasmic membrane, where UPP-recycling takes place. However, *de novo* synthesized UPP is generated at the inner leaflet of membrane, so it remains elusive how this fraction of UPP is dephosphorylated. Additionally, the mechanism for flipping of UP from the outer to the inner leaflet of the plasma membrane is unknown.

1.3.3 AN ADDITIONAL SOURCE OF THE LIPID CARRIER UP: PHOSPHORYLATION OF UNDECAPRENOL

As described above, the most-studied source of UP originates from UPP dephosphorylation. UPP is recycled after releasing the PG building blocks to the cell wall, or *de novo* synthesized via UppS (Guo *et al.*, 2005). In Gram-positive bacteria, UP can also be generated by phosphorylating undecaprenol, e.g. by the UDPK DgkA in *B. subtilis* (Higashi *et al.*, 1970; Jerga *et al.*, 2007). Prokaryotic UDPKs and diacylglycerol kinases (DAGKs) are membrane proteins that form homotrimers (Sandermann & Strominger, 1971; Van Horn & Sanders, 2012). Their catalytic centers face the cytoplasm (Abe *et al.*, 2003), in contrast to the UPP phosphatases described above. It was discovered that *dgkA* is expressed during vegetative growth before sporulation (Amiteye *et al.*, 2003). In a *dgkA* mutant the following sporulation phenotypes were observed: less bright endospores, a defective spore cortex in some spores, and reduced levels of dipicolinic acid, suggesting a supporting role of DgkA for efficient sporulation and cortex (spore-specific PG) formation (Amiteye *et al.*, 2003). The DgkA substrate undecaprenol was only studied in few bacteria to date, excluding *B. subtilis*, and its source remains unclear (Barreteau *et al.*, 2009; Higashi

et al., 1970; Siewert & Strominger, 1967). The available data suggests that undecaprenol is only present in Gram-positive bacteria (Barreteau *et al.*, 2009). For *S. aureus*, the amounts of undecaprenol (~23%), UP (~19%) and UPP (~58%) were measured, demonstrating that undecaprenol substantially contributes to the C_{55}-isoprenoid pool in this organism (Barreteau *et al.*, 2009).

Additionally to the previously described UPP dephosphorylation and undecaprenol phosphorylation, UP is also generated from recycling the carrier of WTA-shuttling. In this pathway, teichoic acids are linked to PG and UP is released as a carrier molecule (instead of UPP in case of the lipid II cycle). While the recycling of UP in this case is UPP phosphatase-independent, the generation of WTA-precursors itself depends on UP and is therefore not self-sustaining (Brown *et al.*, 2013). Consequently, this was not part of our study.

1.4 OPEN QUESTIONS THAT WERE ADDRESSED IN THIS THESIS

1.4.1 IS BCEAB A FLUX SENSOR?

The regulation of the *bceAB* operon depends on the 2CS BceRS and an active BceAB transporter, but the type of input remained elusive. Here, a mathematical approach was taken to further characterize the signaling input in mutants with fixed levels of BceAB that are challenged with increasing amounts of bacitracin.

See **Publication I**:

Fritz G, Dintner S, Treichel N S, **Radeck J**, Gerland U, Mascher T, Gebhard S (2015) A new way of sensing: need-based activation of antibiotic resistance by a flux-sensing mechanism. **mBio**. 6(4):e00975. doi: 10.1128/mBio.00975-15.

1.4.2 INTERDEPENDENCE OF CESR TOWARD BACITRACIN

Of three known strategies to counteract a bacitracin attack (ABC-transporters, UPP phosphatases, and variation of exopolysaccharide production), the first two (ABC-transporter BceAB, UPP phosphatase BcrC) are known to be employed by *B. subtilis*. These two, and a third player (LiaIH, which was chosen due to its strong activation in

the presence of bacitracin) were included in this study. We investigated if LiaIH contributes to bacitracin resistance in the absence of BceAB or BcrC.

There is only little knowledge on how the cell orchestrates the activity of individual modules, although a certain degree of interdependence is expected, because of their activation by the same stimulus. For example, it was observed that a *bcrC bceAB* double mutant was more sensitive than either of the single mutants (Bernard *et al.*, 2003). Furthermore, it was shown that their signaling is independent, but this was not investigated further (Bernard *et al.*, 2003). Here, a systematic investigation of the functional and regulatory interdependence of all three systems that are strongly upregulated upon bacitracin addition (BceAB, LiaIH, BcrC) was performed.

See **Publication II**:

Radeck J, Gebhard S, Orchard P, Kirchner M, Bauer S, Mascher T, Fritz G (2016) Anatomy of the bacitracin resistance network in *Bacillus subtilis*. **Mol Micro**.100(4):607-20. doi: 10.1111/mmi.13336.

1.4.3 EFFECT OF UPP PHOSPHATASE REDUCTION ON CESR

The putative link between CESR and cell wall homeostasis (as exemplified by UP turnover) was further investigated in a follow-up study. For both UPP phosphatases known to be relevant *in vivo*, BcrC and UppP (Zhao *et al.*, 2016), we verified the gene pair *bcrC* and *uppP* to be synthetic lethal[7]. A comprehensive set of deletion, complementation and depletion strains was constructed and studied for morphology, sporulation, CESR and bacitracin MIC.

See **Manuscript I**:

Radeck J*, Lautenschläger N*, Mascher T (2017) The essential UPP phosphatase pair BcrC and UppP connects cell wall homeostasis with cell envelope stress response in *Bacillus subtilis*. (submitted to Frontiers in Microbiology)
* contributed equally to this work

[7] "**Synthetic lethality** arises when a combination of deficiencies in the expression of two or more genes leads to cell death, whereas a deficiency in only one of these genes does not." (https://en.wikipedia.org/wiki/Synthetic_lethality, Aug 21, 2017)

2 RESULTS

The results are presented in the following publications (see appendix):

Publication I (p. 77-95):

Fritz G, Dintner S, Treichel N S, **Radeck J**, Gerland U, Mascher T, Gebhard S (2015) A new way of sensing: need-based activation of antibiotic resistance by a flux-sensing mechanism. **mBio**. 6(4):e00975. doi: 10.1128/mBio.00975-15.

Publication II (p. 97-121):

Radeck J, Gebhard S, Orchard P, Kirchner M, Bauer S, Mascher T, Fritz G (2016) Anatomy of the bacitracin resistance network in *Bacillus subtilis*. **Mol Micro**.100(4):607-20. doi: 10.1111/mmi.13336.

Manuscript I (p. 125-136):

Radeck J*, Lautenschläger N*, Mascher T (2017) The essential UPP phosphatase pair BcrC and UppP connects cell wall homeostasis with cell envelope stress response in *Bacillus subtilis*. (submitted to Frontiers in Microbiology)
* contributed equally to this work

3 DISCUSSION

Parts of this chapter have been adapted from:

Radeck J, Gebhard S, Orchard P, Kirchner M, Bauer S, Mascher T, Fritz G (2016) Anatomy of the bacitracin resistance network in *Bacillus subtilis*. **Mol Micro**.100(4):607-20. doi: 10.1111/mmi.13336.

Radeck J, Fritz G, Mascher T (2016) The cell envelope stress response of *Bacillus subtilis*: from static signaling devices to dynamic regulatory network. **Curr Genet**. 63(1):79-90. doi: 10.1007/s00294-016-0624-0

Radeck J*, Lautenschläger N*, Mascher T (2017) The essential UPP phosphatase pair BcrC and UppP connects cell wall homeostasis with cell envelope stress response in *Bacillus subtilis*. (submitted to Frontiers in Microbiology)

* contributed equally to this work

3.1 RATIONALE OF THIS STUDY

Bacterial survival in competitive environments is determined by resistance to AMPs, such as bacitracin, among others. The resistance mechanisms in *B. subtilis* against bacitracin include the highly-specific ABC-transporter BceAB (Ohki *et al.*, 2003a), the UPP phosphatase BcrC (Bernard *et al.*, 2005), and LiaIH (**publication II**). Although the single resistance modules, their regulation and orchestration had already been characterized to some extent, their interdependence in the CESR network remained unclear. Bacitracin's mode of action – binding to the lipid carrier UPP and therefore blocking the lipid II cycle – is similar to a lack of UPP phosphatases, which catalyze the dephosphorylation of UPP to UP. This bottleneck could represent a link between homeostatic regulation of cell wall synthesis and the CESR. In this thesis, I aimed at characterizing the bacitracin perception by the Bce system, the interdependence of modules that perceive and/or relieve CES caused by bacitracin, and the impact of UPP phosphatase limitations on *B. subtilis*.

3.2 MAIN FINDINGS

3.2.1 BCEAB IS A FLUX SENSOR

In Bce-like systems, the ABC-transporter is strictly necessary for sensing, while the histidine kinase and response regulator are responsible for signal transfer and activation of the target promoter (Dintner *et al.*, 2011; Mascher *et al.*, 2006; Mascher, 2013). We exploited mathematical modeling to show for the first time that indeed the transport activity, or flux, is the stimulus of the *B. subtilis* Bce-system BceABRS in the presence of bacitracin. This new produce-to-demand strategy provides important insight in the kind of stimulus perceived by of all Bce-like systems (**publication I**).

3.2.2 THE *B. SUBTILIS* CESR TOWARD BACITRACIN IS ORGANIZED IN TWO LAYERS

A two-layered, partially redundant CESR network architecture in *B. subtilis* was identified by scrutinizing the bacitracin resistance and promoter activity of a comprehensive set of *B. subtilis* mutants (*bceAB*, *bcrC* and *liaIH;* **publication II**). We further demonstrated that the bacitracin resistance determinants confer resistance in a redundant manner.

3.2.3 LIAIH CONTRIBUTES TO BACITRACIN RESISTANCE IN *B. SUBTILIS*

For the first time, a contribution of LiaIH to the resistance against bacitracin was discovered, which was only revealed in the absence of the main resistance determinant BceAB. Therefore, we introduced the concept of a primary (drug-sensing, BceAB) and secondary (damage sensing, BcrC and LiaIH) layer of resistance. This finding highlighted the redundancy and interdependence in this CESR network, which might be a widespread principle (**publication II**).

3.2.4 DEPLETION OF UPP PHOSPHATASES LEADS TO MORPHOLOGICAL DEFECTS AND ACTIVATION OF P_{BCRC}

Publication II also presented data on the activation of CESR at reduced UPP phosphatase levels. We investigated this essential part of the lipid II cycle by genetically reducing the levels of UPP phosphatases further and identified pleiotropic effects on growth, cell morphology, CESR, bacitracin sensitivity and sporulation (**manuscript I**). In depletion mutants, where only one of the UPP phosphatases was present at low levels, morphological defects during fast growth were observed. Surprisingly, only P_{bcrC}, but not P_{liaI} was induced in these strains, although both promoters were activated in presence of bacitracin, which targets the same reaction (**publication II**). Overall, the homeostatically regulated BcrC was more important for the prevention of CES and normal growth, whereas UppP was necessary for efficient sporulation (**manuscript I**).

3.2.5 PHOSPHORYLATION OF UNDECAPRENOL BY DGKA CONTRIBUTES TO THE UP POOL

Furthermore, we could show that DgkA (as part of an UPP-phosphatase independent pathway) contributes to the cellular UP pool during late stationary phase as indicated by increased P_{bcrC} activity in a *dgkA* mutant (**manuscript I**). Taken together, our data provides the first insight into the fine-tuning of UP homeostasis that adjusts the lipid II cycle (and therefore cell wall biosynthesis) in response to growth rates and envelope stress levels.

3.3 THE CESR TOWARD BACITRACIN IS ORGANIZED REDUNDANTLY

B. subtilis combats the AMP bacitracin by using three resistance modules which act with principle redundancy (**publication II**). Upon increasing concentrations of bacitracin, three different resistance mechanisms are (increasingly) activated, starting with the lowest induction threshold: (i) the ABC-transporter BceAB, (ii) the Psp-like LiaIH response, and (iii) the UPP phosphatase BcrC (Rietkötter *et al.*, 2008). BceAB represents the primary layer of bacitracin-induced CESR, due to its drug-sensing and highly effective resistance mechanism. BcrC and LiaIH are both activated by secondary effects caused by bacitracin (also referred to as "damage-sensing" (Wolf *et al.*, 2012)) and confer less resistance toward this antibiotic. We elucidated that the effect of LiaIH and BcrC is (partially) masked in the presence of BceAB. In fact, the activation of the Lia and Bce-system is strongly anticorrelated with the amount of BceAB (and BcrC, to a lower extent) present in the cell. For example, in the presence of high levels of BceAB, LiaIH is produced in smaller amounts upon the addition of bacitracin than in the presence of low levels of BceAB. The levels of LiaIH, in contrast, have no influence on the activation of P_{bcrC} and P_{bceA} (**publication II** and Figure 6 of supplemental data).

The activation (BceAB, LiaIH) or elevated activation (BcrC) of resistance determinants upon need is a key feature of "active redundancy", in contrast to "passive redundancy", in which excess capacity is used steadily to reduce the impact of component failures (Pahl *et al.*, 2007). In fact, the principle of redundancy is found in different stress contexts, like the oxidative stress responses in *Ralstonia solanacearum* and *Salmonella enterica* (Flores-Cruz & Allen, 2009; Hebrard *et al.*, 2009), to name but a few examples (Storz *et al.*, 2011).

3.3.1 THE ABC TRANSPORTER BCEAB IS A FLUX SENSOR

Bacteria can monitor their environment by either perceiving the concentration of a relevant substance directly, or the downstream effects on cellular physiology (Helmann, 2016; Jordan *et al.*, 2008; Staroń *et al.*, 2011). In **publication I**, we demonstrated that sensing of the transport flux is a third option. By this means, the cell monitors its current detoxification capacity. To elucidate this novel mechanism

of sensing, we combined mathematical modeling of the regulatory pathway of BceAB with quantitative, time-resolved dose-response promoter dynamics. We found that the resistance pump BceAB uses its bacitracin transport activity as input for the regulation of transporter abundance. This is an elegant example of negative feedback regulation, which allows continuous monitoring of the most relevant parameter for survival: the cells current ability to cope with the inhibitory effects caused by the drug. In concentration sensing, the transcriptional response correlates with the inducer concentration, whereas in flux sensing, the amount of transporters is only upregulated if the transport activity is insufficient, even at high antibiotic concentrations. This leads to the assumption that flux sensing is a very cost-effective strategy for regulation in any physiological context.

Additionally, the model could predict the bacitracin sensitivity based on the number of expressed transporters and shows the expected behavior for flux-sensing mechanisms in general. Therefore, it can be used to identify further flux-regulated sensors, which seem to be a cost-effective assessment in changing environments. This is an efficient way to minimize costs by adjusting the response flexible to demand (Kwun & Hong, 2014; Melnyk *et al.*, 2015).

3.3.1.1 FLUX SENSING MIGHT BE A GENERAL PRINCIPLE FOR BCE-LIKE SYSTEMS

Over 200 Bce-like systems are distributed in the *Firmicutes* phylum, in which the histidine kinase and permease have coevolved (Dintner *et al.*, 2011). Together with experimental evidence of the transporter's sensory role in all systems studied to date (Gebhard *et al.*, 2014; Hiron *et al.*, 2011; Ouyang *et al.*, 2010; Revilla-Guarinos *et al.*, 2013; Staroń *et al.*, 2011), this tight evolutionary correlation suggests a conserved signaling mechanism. The flux sensing activity of BceAB, as shown in **publication I**, might therefore be just one example of a widespread regulatory principle with regards to AMP resistance.

3.3.1.2 MATHEMATICAL MODELING IS AN EFFICIENT TOOL TO CALCULATE "HIDDEN" PARAMETERS

The mathematical modeling approach not only revealed a novel flux-sensing mechanism, but also gave access to important system variables. In our case, we

calculated that the fraction of bacitracin-bound UPP that leads to growth inhibition is ~ 90% (**publication I**). This insight could be used to predict the bacitracin concentrations needed for growth inhibition in strains with fixed levels of BceAB. Such "hidden" parameters, which are difficult to quantify experimentally, can be used for highly relevant predictions of bacterial physiology and a better understanding of cellular processes. For example, Bce-like systems respond to diverse peptide antibiotics that interfere with cell wall biosynthesis, like nisin, vancomycin or teicoplanin, which are used as food preservatives or in clinical settings (Gebhard & Mascher, 2011; Meehl *et al.*, 2007; Pietiäinen *et al.*, 2009). Knowledge derived from mathematical modeling of these and further systems can help to develop of new treatments against pathogenic bacteria, against which current strategies fail.

3.3.1.3 INDUCTION AND SPECIFICITY OF BCE-LIKE SYSTEMS

In *B. subtilis*, BceAB not only confers resistance to bacitracin, but also to the lantibiotics with globular structure actagardin and mersacidin (Mascher *et al.*, 2003; Ohki *et al.*, 2003a; Staroń *et al.*, 2011). While bacitracin targets UPP, the latter bind to lipid II (Brötz *et al.*, 1998). Surprisingly, structurally similar antibiotics like ramoplanin do not induce the Bce-system (Cudic *et al.*, 2002; Staroń *et al.*, 2011). Bce-like transporters, in general, can detoxify antibiotics which belong to these additional classes: defensins or β-lactams, as summarized in (Gebhard, 2012). In the last 15 years, important progress has been made in identifying the structures involved in mediating resistance, like the dependence on BceA ATPase activity, and the presence of the large extracellular unstructured region of BceB that is important for mediating specificity (Gebhard & Mascher, 2011; Hiron *et al.*, 2011; Rietkötter *et al.*, 2008). Crucial residues for sensing and resistance mediation were further identified (Kallenberg *et al.*, 2013) and it was shown that BceB binds bacitracin *in vitro* (Dintner *et al.*, 2014). In **publication I**, we determined that the transport activity of BceAB is the signal for BceRS.

However, in **publication II**, we found that P_{bceA}-activity is elevated in a *bcrC* mutant even without the addition of bacitracin. We speculated that this effect could be caused by increased levels of UPP or endogenous production of AMPs. For a set of

known AMPs produced in *B. subtilis* that activate P_{bceA} during stationary phase (Höfler *et al.*, 2016), we tested this hypothesis: YydF (Butcher *et al.*, 2007), SdpC (sporulation delaying protein) and SkfA (sporulation killing factor) (Gonzalez-Pastor *et al.*, 2003). Supplemental data (Figure 7) shows that P_{bceA}-activity depended on *bcrC*, but not on the AMPs mentioned above, under the conditions of the study presented in **publication II**. Consequently, another explanation for elevated P_{bceA} activity in a *bcrC* loss mutant is favored: the accumulation of UPP. While the UPP-bacitracin complex is the physiological substrate of BceAB, still both individual molecules, UPP and bacitracin, might be able to interact with BceAB with lower affinity. The UPP accumulation due to the lack of the UPP phosphatase BcrC might therefore cause an increased basal activity of P_{bceA}.

3.3.1.4 DIRECTION OF TRANSPORT OF BCEAB

The direction (and molecule) of transport and specific residues that interact with the target molecule(s) are still elusive. It was speculated that BceAB is (i) an exporter (Bernard *et al.*, 2007), or (ii) importer of bacitracin (Dawson *et al.*, 2007; Rietkötter *et al.*, 2008), or (iii) an importer of UPP, thereby separating antibiotic and target (Kingston *et al.*, 2014), or (iv) that it removes the AMP from its target into the extracellular space, similar to LanFEG-type transporters (Dintner *et al.*, 2014; Gebhard, 2012).

While the translocation of UPP could explain how BceAB confers resistance against the UPP-binding bacitracin, it cannot describe a resistance mechanism toward antibiotics with different targets, like lipid II (Staroń *et al.*, 2011). If the antibiotics are removed from their target without translocation through the membrane, resistance to different classes of antibiotics that even bind to different target molecules could be explained (as outlined in 3.3.1.3). This theory is in accordance with the finding of flux sensing, but unfortunately no experimental data on transport direction is available, yet.

3.3.2 THE LIAIH PHAGE SHOCK-LIKE RESPONSE CONTRIBUTES TO BACITRACIN RESISTANCE AND FEEDS BACK ON ITS OWN REGULATION

P_{bceA} is the most sensitive bacitracin-responsive promoter, followed by P_{liaI} and P_{bcrC} (Rietkötter *et al.*, 2008). While BceAB is a specific transporter with high detoxification capacity, the role of the strongly produced proteins LiaIH was elusive for the longest time (Wolf *et al.*, 2010). In **publication II**, we could show for the first time that LiaIH actually contribute to the bacitracin resistance properties of *B. subtilis*, but their capacity is only revealed in the absence of BceAB. A *bceAB liaIH* double mutant was six times more sensitive to bacitracin than a *bceAB* mutant, while a *liaIH* mutant and the wild type had the same level of resistance. Finally, a contribution of LiaIH to the bacitracin resistance capacities of *B. subtilis* was shown. Since LiaH is a PspA homologue, a comparison to other Psp-like responses might help revealing the resistance mechanism provided by LiaIH.

3.3.2.1 THE PSP RESPONSE HELPS MAINTAINING THE ENERGY STATE OF STRESSED CELLS

Psp-like proteins are ancient and widely conserved, occur in Gram-positive and -negative bacteria, as well as in archaea and plant chloroplasts, and are best studied in *E. coli* and *Yersinia enterocolitica* (Darwin, 2005; Huvet *et al.*, 2011; Joly *et al.*, 2010). However, little is known about their induction and how they can protect the cells. Cells missing the Psp system are still viable, but less tolerant against envelope stress, in case of a reduced energy state of the cell (Darwin, 2005; Darwin, 2007; Model *et al.*, 1997). For example, ATP- and proton motive force-dependent protein secretion are reduced (Kleerebezem & Tommassen, 1993; Kleerebezem *et al.*, 1996) and growth is impaired during stationary phase at alkaline pH (Weiner & Model, 1994) or in the presence of bile salts (Adams *et al.*, 2003). Accumulating data suggests that the formation of large protein complexes at the membrane interface is crucial for the function of PspA proteins, which (at least in *E. coli* and *Y. enterocolitica*) prevents proton leakage across the inner membrane (as reviewed in Flores-Kim & Darwin, 2016). This indicates that there might be a PspA-mediated resistance mechanism that prevents proton leakage caused by various molecules that interfere with cell envelope integrity. The Psp systems seem to provide a general, but low-level resistance under various conditions. This is in stark contrast to evolutionary “newer”

systems, like Bce-like ABC transporters that are almost exclusively found in *Firmicutes* (Dintner *et al.*, 2011). These are drug transporters with a narrow range of specificity that confer a high level of resistance against few antibiotics. The specific (drug-acting) resistance modules might have evolved "on top" of the ancient, general (damage-acting) stress response, which could explain their redundancy in conditions, in which both systems can provide some resistance.

Another explanation is based the close relationship between the producers of bacitracin and the strains which are resistant against this AMP (in this case, some strains of *B. licheniformis* and B*. subtilis* (Azevedo *et al.*, 1993; Frøyshov & Laland, 1974; Ishihara *et al.*, 2002)). The producer of an antibiotic needs to be resistant against this compound, so that the genes responsible for bacitracin production and bacitracin resistance might have evolved in the same bacteria. Some strains, like *B. subtilis* W168, might have lost the genes responsible for bacitracin production but kept the genes responsible for resistance.

In both cases, the deletion of main, drug-specific resistance determinants might reveal further conditions under which the Psp response confers resistance that was merely masked.

3.3.2.2 REGULATION OF THE PSP RESPONSE IN *E. COLI* COMPARED TO LIAIH IN *B. SUBTILIS*

The Psp-like response has been most studied in *E. coli* and *Y. enterocolitica*, in which it includes the proteins PspABCDEFG (as reviewed in Flores-Kim & Darwin, 2016). In these organisms, under non-inducing conditions, PspA interacts with and inhibits the transcriptional enhancer PspF. Under inducing conditions, PspA multimerizes, becomes membrane located (in part through interaction with PspBC), and PspF upregulates transcription of *pspABCDE* and *pspG* (Brissette *et al.*, 1990; Flores-Kim & Darwin, 2016; Jovanovic *et al.*, 1996). This response is induced by ethanol shock, osmotic shock, or secretin proteins that mislocalize in the inner membrane, among others (Joly *et al.*, 2010). PspA in its 36-meric form can help to maintain the proton motive force by reducing proton loss through the inner membrane (Kobayashi *et al.*, 2007) and PspBC can prevent plasmolysis caused by secretin (Horstman & Darwin, 2012).

We found evidence that the *B. subtilis* LiaIH also play a partial positive autoregulatory role in activating P_{liaI}, although there is no strict dependence involved (**publication II**). It is conceivable that the high levels of LiaIH in the plasma membrane (Dominguez-Escobar *et al.*, 2014) generate the kind of CES that is detected by the Lia system. This could explain, why the regulation of LiaIH is so fine-tuned, but also highly dynamic.

In *E. coli* and *Y. enterocolitica*, an autoregulatory loop of Psp systems exists, as described above, in which PspA directly negatively regulates the transcriptional activator PspF by forming hetero-oligomers (Joly *et al.*, 2010). However, this regulation bears no similarity to *B. subtilis*, in which the regulation of *liaIH* is carried out through LiaFSR, which are not homologous to PspA or PspF. So even if a similar regulatory principle is part of the regulation in both systems, the analogy to PspAF can only be on a functional level. All in all, the role of LiaIH in modifying its own regulation needs to be further investigated.

Unfortunately, the molecular cue of the Psp response in general remains elusive. There is ongoing discussion about the (unifying) stimulus that seems to be sensed in the inner membrane: experimental evidence argues against earlier hypotheses (reduced proton motive force or an altered redox state), and membrane-stored curvature elastic stress is currently debated (as reviewed in Flores-Kim & Darwin, 2016). Due to the different regulation of the *B. subtilis* Lia-system, it is conceivable that its stimulus differs from that in the γ-proteobacteria *E. coli* and *Y. enterocolitica*. Further investigation of the induction, regulation and resistance mechanism of the Psp response will hopefully give new insights into this ancient and wide-spread system.

3.3.3 THE (REDUNDANT) UPP PHOSPHATASES RECYCLE UPP AND CONTRIBUTE TO BACITRACIN RESISTANCE

The reaction catalyzed by UPP phosphatases, dephosphorylation of UPP to UP, is blocked by bacitracin binding to UPP. By competition for the same target, UPP phosphatases can reduce the level of bacitracin toxicity. BcrC levels are increased upon bacitracin addition via σ^M (Cao & Helmann, 2002). BcrC accounts for a 5-fold increased resistance toward that antibiotic in the wild type, or 24-fold in a *bceAB*

mutant (**publication II**). In contrast, UppP only mediates bacitracin resistance in the absence or at very low levels of BcrC and it is not upregulated upon bacitracin addition (**publication II**; Cao & Helmann, 2002). At the same time, both UPP phosphatases pursue an essential function for the cell, which is exemplified by the synthetic lethality of *bcrC* and *uppP* and severe morphological defects in depletion strains (**manuscript I**; Zhao *et al.*, 2016)).

UPP dephosphorylation is usually performed by at least two proteins in a (partially) redundant manner in many of the bacteria studied (*S. aureus*, *Streptococcus pneumoniae*, *Mycobacterium smegmatis*, *E. coli*, *B. subtilis*): each individual gene is not essential by itself, but single deletion mutants may exhibit increased bacitracin sensitivity or reduced pathogenicity (Chalker *et al.*, 2000; El Ghachi *et al.*, 2004; Röse *et al.*, 2004; Zhao *et al.*, 2016). Quite remarkably, in an *E. coli* K12 *bacA* deletion mutant, UPP phosphatase activity was reduced by 75%, but no growth abnormalities were observed under laboratory conditions (El Ghachi *et al.*, 2004). There is accumulating data that BcrC (PAP2-type) is the main and UppP (BacA-type) the minor UPP phosphatase in *B. subtilis* during normal growth (**manuscript I**; Inaoka & Ochi, 2012; Zhao *et al.*, 2016), while UppP is necessary for sporulation (**manuscript I**; Meeske *et al.*, 2016). But so far, no direct measurement of UPP phosphatase activity is available for this organism. Under most conditions, strains with either *bcrC* or *uppP* deletions exhibit no growth defects (**manuscript I**; Inaoka & Ochi, 2012; Zhao *et al.*, 2016), with the exception of a *bcrC* mutant in liquid LB medium (**publication II**).

YodM is the third known UPP phosphatase of *B. subtilis*, and of only little relevance, as judged by the available data. While its native expression levels are not sufficient to support growth, Zhao *et al*. showed that in the presence of strongly enhanced transcription and translation of *yodM*, both *uppP* and *bcrC* can be deleted (Zhao *et al.*, 2016). This experiment showed that *yodM* encodes an intact UPP phosphatase. During growth under extremely limited UPP phosphatase levels, deletion of *yodM* can reduce the frequency of suppressor mutants (Zhao *et al.*, 2016). Its role during CES, however, seems to be very limited. In **manuscript I**, we showed that there was no influence of YodM on bacitracin MIC in strains already lacking either *uppP* or *bcrC*, even in the absence of the main resistance determinant BceAB. Taken together,

YodM seems to have UPP phosphatase activity, but its role is very limited due to low expression levels.

3.3.4 RECYCLING AND *DE NOVO* SYNTHESIS OF UP: IS A FLIPPASE INVOLVED?

There are two details of UPP dephosphorylation which are not yet fully understood: (i) All known UPP phosphatases are active at the outer leaflet of the cytoplasmic membrane (Fan *et al.*, 2014; Manat *et al.*, 2015). It remains elusive, how *de novo* synthesized UPP, which is generated at the inner leaflet of the plasma membrane, is dephosphorylated. This raises the question, if there are novel UPP phosphatases yet to be found that are active in the cytosol. Alternatively, UPP could be flipped outside to be dephosphorylated. (ii) How is UP flipped from the outer to the cytosolic leaflet of the membrane? As spontaneous flipping rates are not sufficient to satisfy the high rates of PG synthesis, the existence of a flippase is assumed (McCloskey & Troy, 1980). It is speculated that UP could be shuttled by the same, substrate-specific flippases that mediate flipping of glycan-derivatives (Sanyal & Menon, 2010). UPP phosphatases might act as flippases themselves, or they might drive associated flippases (to be identified) with the energy released by dephosphorylation of UPP (Manat *et al.*, 2014).

These examples illustrate that many fundamental details of the lipid II cycle are still unknown. In case of UPP phosphatases, bacitracin resistance and lipid II cycle progression are closely interlinked processes in *B. subtilis*. We therefore shifted our focus to the central molecule of the lipid II cycle: UP.

3.4 UP AS CENTRAL MOLECULE FOR CELL ENVELOPE ASSEMBLY

UP, the carrier molecule for PG and WTA building blocks, is the central molecule of the lipid II cycle. It is generated by UPP dephosphorylation or by phosphorylation of undecaprenol. Despite its importance, the total fraction of UP-derivatives is estimated to be only about 1% of the phospholipid content in bacterial membranes (Hartley & Imperiali, 2012; Jones *et al.*, 1958; Mitchell & Moyle, 1954). In *E. coli*, this corresponds to ~ $2 * 10^7$ lipid molecules and ~ $1.5 * 10^5$ UP+UPP molecules per cell. A roughly equivalent number has been determines for a number of Gram-positive

and Gram-negative bacteria, e.g. *S. aureus*, *Micrococcus luteus*[8], *Micrococcus flavus* and *Listeria monocytogenes* (Barreteau *et al.*, 2009; Kramer *et al.*, 2004; Neidhardt & Umbarger, 1996; Storm & Strominger, 1974).

The amount of PG building blocks in the PG layer (and therefore the minimal amount of building blocks that need to be synthesized, shuttled and incorporated during one cell division cycle) is ~ 2.5-5 * 10^6 in *E. coli* (Mengin-Lecreulx & van Heijenoort, 1985; van Heijenoort *et al.*, 1992). Consequently, each carrier molecule is statistically used at least 20 times per division cycle, and during exponential growth at least about 5 * 10^3 molecules of lipid II are shuttled across the membrane per second (Mengin-Lecreulx & van Heijenoort, 1985; van Heijenoort *et al.*, 1992). In Gram-positive bacteria, this rate is elevated by a factor of ~ 5, depending on the amount of PG per cell and the growth rate (Barreteau *et al.*, 2009).

The lipid II cycle is a set of consecutive chemical reactions, in which the slowest step (bottleneck) determines the overall reaction rate. Throughout the growth phases of *E. coli*, lipid II generating enzymes appear to be constitutively active and all cytosolic adducts are readily available (Mengin-Lecreulx & van Heijenoort, 1985), so these factors seem not to be involved. The levels of lipid I and II are low (~ 7 * 10^2, and 1-2 * 10^3, respectively (van Heijenoort *et al.*, 1992)), compared to those of UP and UPP (~1.5 * 10^5, (Barreteau *et al.*, 2009)). It was shown that the availability of UP is rate-limiting for *in vitro* production of lipid II via membrane vesicles (Egan *et al.*, 2015), but there is no clear evidence that this is also the case *in vivo*. Why would the levels of lipid I and II be lower than those of UP, if the (missing) availability of UP is rate limiting? One explanation could be that the majority of UP molecules is localized at the outer leaflet of the plasma membrane (where dephosphorylation of UPP takes place), but for the formation of lipid I and lipid II, UP is required at the inner leaflet. In this case, the membrane orientation of UP might be critical and worth studying.

[8] Outdates species name was used: *Micrococcus lysodeikticus*

3.4.1 UP/UPP-LEVELS INCREASE UPON BACITRACIN ADDITION

As a small step toward a comprehensive dataset, Barreteau *et al.* determined the fraction of undecaprenol, UP and UPP in the Gram-positive organism *S. aureus* to be approximately 30% (undecaprenol), 20% (UP), and 50% (UPP) (Barreteau *et al.*, 2009). Addition of bacitracin lead to a shift (15% (undecaprenol), 15% (UP), and 70% (UPP)), and increased levels of UP-derivatives in total (+45% ,Barreteau *et al.*, 2009). These measurements showed that UPP indeed accumulated upon bacitracin addition while undecaprenol levels simultaneously decreased, which indicates its utilization for the generation of UP. It is not clear if UPP *de novo* synthesis is the sole source of the increased amount of carrier molecules. In *E. coli* no undecaprenol was detected. Here, the amount of UP-derivatives increased by 52% upon bacitracin addition, and the fraction of UP increased from 22 to 30% (UPP decreased from 78 to 70%). In this case, no accumulation of UPP occurred, its fraction rather decreased to a smaller degree (Barreteau *et al.*, 2009). This data suggests that both *E. coli* and *S. aureus* increase their carrier pools upon bacitracin addition. While *S. aureus* seems to mobilize its undecaprenol pool, resulting in UPP accumulation, *E. coli* might reduce the overall activity of the lipid II cycle, which leads to a slight accumulation of UP. An investigation of undecaprenol, UP and UPP levels in *B. subtilis* (wild type and *bceAB* mutant) would elucidate, if undecaprenol is present and if UPP-bacitracin accumulates, similar to the Gram-positive organism *S. aureus*.

3.4.2 DIFFERENTIAL RESPONSE OF THE LIA-SYSTEM TO BACITRACIN ADDITION AND UPP PHOSPHATASE DEPLETION

Figure 5 illustrates the flow of undecaprenol, UP and UPP in *B. subtilis* W168. In this organism, mobilization of undecaprenol to UP is possible via DgkA (**manuscript I**), UPP is dephosphorylated to UP by BcrC and UppP, and BceAB can release UPP from its complex with bacitracin (**publication I**). Unfortunately, no quantitative data is available for any of the intermediates in this organism. Wolf *et al.* found that the strong activation of the *liaI*-promoter in the presence of lipid II cycle targeting antibiotics (e.g. bacitracin, mersacidin, vancomycin, nisin, daptomycin) was absent in *murE*-depleted, cell wall deficient L-forms of *B. subtilis* (Wolf *et al.*, 2012). This suggested that instead of the antibiotics themselves (“drug-sensing”), downstream

effects on the lipid II cycle are the inducer for the Lia-system ("damage-sensing"). Along these lines, we tested if the depletion of UPP phosphatases leads to the activation of P_{lial}, but this was not the case (**manuscript I**). This result was independently obtained in UPP phosphatase knock-down mutants, using a CRISPR/dCas9-mediated approach (Zhao *et al.*, 2016).

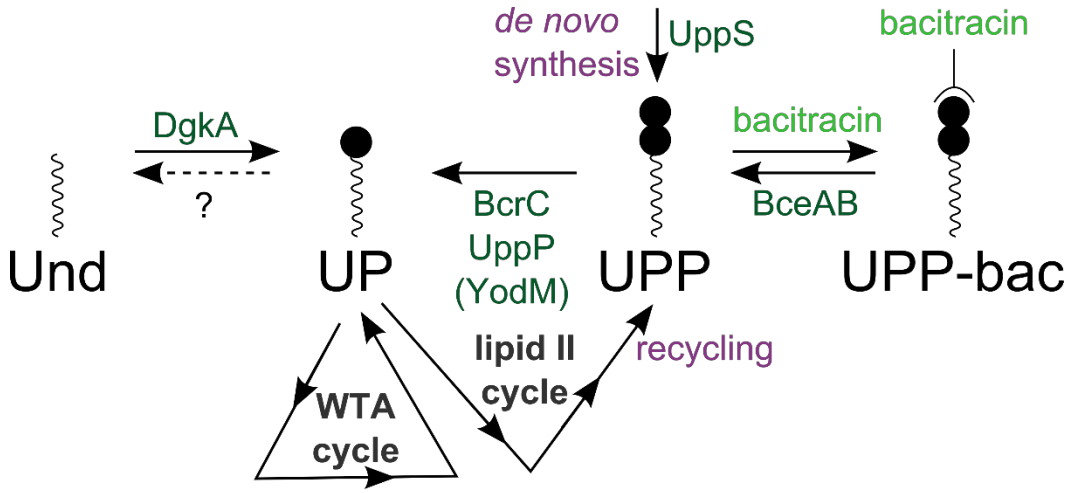

Figure 5. Schematic representation of the generation and use of UP in *B. subtilis*. Und, undecaprenol; UP, undecaprenyl phosphate; UPP, undecaprenyl pyrophosphate; UPP-bac, complex between UPP and bacitracin. UP is generated by phosphorylation of undecaprenol via DgkA, or dephosphorylation of UPP via BcrC or UppP. UP is utilized for the synthesis of lipid II and WTA. After the attachment of PG or WTA-building blocks to the cell wall, the carrier is released as UPP or UP, respectively. UPP is also generated by *de novo* synthesis, where UppS catalyzes the final step. Bacitracin binds to UPP, thereby blocking its dephosphorylation. The ABC-transporter BceAB efficiently removes bacitracin from its target. Some of these steps occur at different leaflets of the plasa membrane, which is not depicted, because it is not yet fully understood. See Figure 1 for more details. Modified from (Brown *et al.*, 2013).

Since downstream effects of bacitracin addition (which binds to UPP and blocks its dephosphorylation) lead to P_{lial}-activation, but depletion of UPP phosphatases does not (although the same reaction is affected), it can be assumed that the two alterations result in distinct types of cell envelope damage. In case of bacitracin addition, it was estimated that about 90% of all UP-derivatives are locked in the UPP-bac state at lethal concentrations of bacitracin (**publication I**). Here, the pools of UPP (without bacitracin), UP, lipid I, lipid II, and presumably undecaprenol are all reduced. Depleted UPP phosphatase activity, in contrast, primarily leads to increased levels of UPP, which might influence the activity of PBPs and lead to the accumulation of upstream precursors. While P_{lial} is only activated upon addition of bacitracin, P_{bcrC} is activated additionally by UPP phosphatase depletion, presumably via σ^M (Cao &

Helmann, 2002; Zhao *et al.*, 2016). This indicates that the molecular triggers of both "damage-sensing" systems are different.

We demonstrated that the depletion of UPP phosphatases has different effects on the lipid II cycle than the addition of bacitracin. Such comparisons can help to elucidate the molecular triggers of CESR systems. In this case, the CESR of two groups should be compared: (i) mutants in which enzymes are depleted that are involved in the lipid II cycle, and (ii) cells that were treated lipid II cycle-targeting antibiotics. Consequently, differences in the activation spectrum of both groups can be analyzed. Especially if combined with studies that measure the amount of carrier in various stages, as detailed in 3.4.1, new experimental-driven insights can be gained on the molecular cues of "damage-sensing" CESR systems.

3.4.3 PROMISCUOUS ACTIVITY OF SOME UPP PHOSPHATASES

Those steps of the lipid II cycle that take place at the inner leaflet of the plasma membrane are performed by single essential proteins, like *de novo* synthesis of UPP by UppS, or formation of lipid I and lipid II by MraY and MurG, respectively (Figure 1). The reactions that are localized at the outer leaflet, crosslinking of PG building blocks to the cell wall by PBPs and dephosphorylation of UPP by UPP phosphatases, are performed redundantly. In case of UPP phosphatases, two protein families are involved, as outlined in section 3.3.3. What could possibly be the reason(s) for this partial redundancy?[9] One answer might be that enzymes which are active at the outer leaflet of the cytoplasmic membrane are easier to target by antibiotics – a weakness that can be overcome by redundancy. Or, the redundant enzymes specialize in different physiological roles, as we have shown for *B. subtilis* (**manuscript I**), in which UPP phosphatases are involved during different growth stages (sporulation) or environmental conditions (bacitracin addition). Another example is the performance of additional (promiscuous) functions by the same protein, as described by Manat *et al.* for three PAP2-type UPP phosphatases (Manat *et al.*, 2014): (i) *E. coli* PgpB is additionally involved in the dephosphorylation of

[9] Genetic redundancy, in general, allows the evolution of new proteins while the essential function is still fulfilled (Nowak *et al.*, 1997).

phosphatidylglycerol phosphate to the essential lipid phosphatidylglycerol – a task that is also performed redundantly by PgpA, PgpB, and PgpC (Funk *et al.*, 1992; Lu *et al.*, 2011). (ii) YeiU=LpxT from *E. coli*, *Salmonella typhimurium* and *S. enterica* were found to catalyze the specific transfer of one phosphate group from UPP to lipopolysaccharides, thereby linking UP metabolism to the pathway of remodeling the lipid A group of lipopolysaccharides (Kato *et al.*, 2012; Touze *et al.*, 2008b). These are part of the outer membrane in Gram-negative bacteria and their modification is critical for resistance to some antibiotics or evasion of host immune defenses (Needham & Trent, 2013). (iii) PbrB of *Cupriavidus metallidurans* participates in lead resistance by precipitating lead (Pb^{2+}) in the periplasm with inorganic phosphate groups released from UPP dephosphorylation (Hynninen *et al.*, 2009). These examples demonstrate the diversity of functions exhibited by UPP phosphatases, which could explain their redundancy (Manat *et al.*, 2014). Future investigations need to reveal, if such systems are also present in *B. subtilis* and other Gram-positive bacteria.

3.4.4 THE UNDECAPRENOL KINASE DGKA CONTRIBUTES TO THE UP POOL DURING SPORULATION

In *B. subtilis, dgkA* encodes an UDPK that phosphorylates undecaprenol to UP (Higashi *et al.*, 1970; Jerga *et al.*, 2007) and is necessary for efficient sporulation (Amiteye *et al.*, 2003). In a *dgkA* mutant, fewer phase-bright endospores were generated and the cortex was drastically reduced in some spores (Amiteye *et al.*, 2003), which suggests a deficiency in cell wall biosynthesis, probably due to a lack of the lipid carrier UP. Additionally, we could demonstrate that the CESR was increased during the stationary phase, as indicated by the upregulation of the CES-responsive *bcrC*-promoter under low UPP phosphatase conditions (**manuscript I**). We therefore propose that a lack of UP carrier is the input signal for σ^M-dependent activation of P_{bcrC}. In this case, the activation of P_{bcrC} in a Δ*dgkA* mutant suggests a lack of UP, similar to that caused by a lack of UPP phosphatases or bacitracin addition. This implies a contribution to the UP pool, by DgkA-mediated phosphorylation of undecaprenol to UP. The identification of spores that lack PG structures (similar, but less prominent than the sporulation phenotype observed for a *uppP* mutant (Meeske

et al., 2016)) supports this theory (Amiteye *et al.*, 2003). The bacitracin sensitivity, which is severely increased in UPP phosphatase depletion mutants, was not altered if *dgkA* was additionally deleted (**manuscript I**), indicating that the contribution of DgkA might be limited to sporulation. In summary, this data is a first indicator that DgkA indeed contributes to the pool of UP in *B. subtilis*, especially during sporulation.

The contribution of undecaprenol to the UP pool is of paramount importance to understand the flow of carrier molecules in the lipid II cycle. Unfortunately, no data is available for *B. subtilis*. Therefore, data from Gram-positive relatives will be discussed below, to shed a light on the current status of knowledge on undecaprenol and the corresponding kinase DgkA.

Bacterial UDPKs are closely related to bacterial DAGKs, to the extent that the corresponding genes are sometimes both named *dgkA*. Bacterial DAGKs are structurally different from "eukaryotic" diacylglycerol kinases and their prokaryotic homologues (encoded by *dgkB*) (Van Horn & Sanders, 2012). In *B. subtilis*, DgkB performs DAGK-activity and DgkA UDPK-activity (Jerga *et al.*, 2007; Sandermann & Strominger, 1971). UDPK-activity is required for bacitracin resistance, growth at low pH, biofilm and smooth surface dental caries formation in *Streptococcus mutans* (Lis & Kuramitsu, 2003; Shibata *et al.*, 2009; Yamashita *et al.*, 1993; Yoshida & Kuramitsu, 2002), and for efficient sporulation in *B. subtilis* (Amiteye *et al.*, 2003). But despite its physiological relevance, little is mechanistic knowledge exists about this process so far.

While UP and UPP[10] are present in all bacteria with a cell wall (Manat *et al.*, 2014), undecaprenol, the substrate of UDPKs, was only found in Gram-positive bacteria to date (*S. aureus, E. faecalis*[11]*, Lactobacillus plantarum, L. monocytogenes*), but not in Gram-negative bacteria (*E. coli*)[12] (Barreteau *et al.*, 2009; Bohnenberger & Sandermann, 1976; Gough *et al.*, 1970; Higashi *et al.*, 1970; Umbreit *et al.*, 1972). In

[10] or rare derivatives with shorter prenyl chains
[11] Outdated species name was used: *Streptococcus faecalis*
[12]Bohnenberger. & Sandermann (1976) cite a personal communication from H. Kleinig that undecaprenol was found in *Myxococcus fulvus*, a Gram-negative bacterium, but no publication was found to support this.

these studies, the level of undecaprenol (if present) was higher or similar to that of UP (Barreteau *et al.*, 2009; Umbreit *et al.*, 1972). For *B. subtilis*, no data is available.

Little is known about the origin of undecaprenol. The *de novo* generation of UPP does not involve undecaprenol as an intermediate step. It is therefore either generated by an unknown pathway, or by dephosphorylation of UP. The presence of UP phosphatase activity has been reported for membranes of *S. aureus* , but not *B. subtilis*, *M. luteus*[13] , *E. faecalis*[14], or *E. coli* (Willoughby *et al.*, 1972). This data needs to be interpreted with a grain of salt: ficaprenol phosphate, which was used in the phosphorylation assay, shows a different conformation than UP, so it might be an unsuitable substrate for UP phosphatases. At least in *E. faecalis*, in which undecaprenol was detected (Umbreit *et al.*, 1972), the presence of a UP phosphatase activity is expected, if this is the source of undecaprenol.

Taken together, more data is needed to shed light on the source of undecaprenol and its regulation, which might be linked to the lipid II cycle and therefore cell wall biosynthesis. Toward this end, the amounts of undecaprenol, UP and UPP could be measured to test the hypothesis if undecaprenol is present in Gram-positive, but not in Gram-negative bacteria. Furthermore, the presence of UP phosphatase activity needs to be verified for *S. aureus* and further bacteria that contain undecaprenol to elucidate if this pathway is responsible of the generation of undecaprenol.

3.5 CONCLUSION AND OUTLOOK

In this thesis, we demonstrated that in the presence of bacitracin, BceAB of *B. subtilis* regulates its own expression by a flux-sensing mechanism. The CESR of *B. subtilis* towards bacitracin is organized in two layers, which are partially redundant. We showed that the expression of the secondary layer of resistance (consisting of BcrC and LiaIH) depends on the expression levels of the primary resistance layer (the ABC-transporter BceAB). Furthermore, we revealed that the contribution of LiaIH to the cell's resistance toward bacitracin is masked by the activity of BceAB in the wild type.

[13] Outdated species name was used: *M. lysodeikticus*
[14] Outdated species name was used: *S. faecalis*

The activation of P_{bcrC} in a *bcrC* mutant lead us to investigate the reaction of UPP dephosphorylation in the lipid II cycle from a different angle: UPP phosphatase depletion instead of bacitracin addition. Here, we found that *bcrC* and *uppP* are a synthetic lethal gene pair and that the main contributions of their gene products are at different growth stages. The observation of elevated CESR in a *dgkA* mutant is a hint that undecaprenol phosphorylation (in addition to UPP dephosphorylation) contributes to the UP pool in *B. subtilis*, especially during sporulation. Nevertheless, several unsolved questions remain to be addressed in the course of future investigations. They will be briefly discussed below.

3.5.1 WHAT ARE THE MOLECULAR CUES OF THE SYSTEMS INDUCED BY BACITRACIN?

For the Bce-system, we have elucidated that the transporter senses its own activity when removing bacitracin from its target UPP (**publication I**). LiaIH expression is regulated by LiaFSR and BcrC expression by σ^M. Both are supposed to respond to some aspect of cell envelope damage, triggered by the extracellular presence of bacitracin. Remarkeably, the depletion of UPP phosphatases, which targets the same reaction (UPP dephosphorylation) only activated σ^M, but not LiaFSR, (**manuscript I**; Zhao *et al.*, 2016). This observation indicates that the molecular stimuli of both systems differ. σ^M activation might be related to decreased levels of UP or increased levels of UPP, although not all inducing conditions can be explained with that model (Helmann, 2016; Meeske *et al.*, 2015). As a first step to challenge this hypothesis, the measurement of UP and UPP levels or availability need to be determined in *B. subtilis*.

Since LiaFSR activation by bacitracin depends on active cell wall synthesis (Wolf *et al.*, 2012), the involvement of the lipid II cycle in the generation of the molecular stimulus is conceivable. P_{lial} was not activated by UPP phosphatase depletion, so the accumulation of UPP alone does not seem to represent the molecular stimulus. The investigation of the stoichiometry of lipid II cycle intermediates in *B. subtilis* under different Lia- inducing and -non-inducing conditions might reveal if the lipid II cycle is involved at all, and maybe even what the trigger might be.

3.5.2 HOW DOES LIAIH MEDIATE RESISTANCE?

In **publication II**, we demonstrated for the first time that, LiaIH mediate resistance against bacitracin in *B. subtilis*. Studies from *E. coli* suggest that PspA-proteins prevent proton leakage across the membrane (Kobayashi *et al.*, 2007). LiaH, a PspA homolog, forms static, membrane associated foci upon bacitracin addition that are recruited by LiaI, similar to PspA and PspBC in *E. coli* (Dominguez-Escobar *et al.*, 2014). It has been postulated recently that the protection of the membrane integrity is achieved by dissociation of the large (LiaH or PspA) protein complexes, which results in the coverage of a stressed membrane area by mono- or oligomers (Thurotte *et al.*, 2017). However, it is not yet clear, which damages are caused by bacitracin addition – or other inducing conditions – and how they are prevented by LiaIH.

While the molecular mechanism is almost impossible to be studied directly, further data might be generated using a genetic approach. In **publication II**, we revealed that the contribution of LiaIH to bacitracin resistance only becomes detectable in the absence of the primary resistance determinant BceAB. If specialized resistance determinants for certain inducing conditions are known, the potential of LiaIH might be demonstrated in the respective deletion mutants.

3.5.3 HOW IS THE GENERATION AND UTILIZATION OF UP REGULATED?

UP is generated by UPP dephosphorylation or undecaprenol phosphorylation in *B. subtilis*. To unravel the influence of these reactions on the lipid II cycle, it is important to know the contribution of each reaction in different growth stages or stress conditions. For example, undecaprenol phosphorylation seems to be important especially during *B. subtilis* sporulation (**manuscript I**; Amiteye *et al.*, 2003).

In this study, we focused on UP as a carrier of PG building blocks in the lipid II cycle. But it is also used for other cell envelope-related structures, such as WTAs or – in Gram-negative bacteria – exopolysaccharides. A comprehensive understanding of the use and flow of the lipid carrier (in different organisms), similar to metabolic models, will be a great tool for basic science. Especially research in *B. subtilis* will be useful, because it is one of the main model organisms for cell wall biosynthesis. Such

a model might even be able to predict the effect of stress conditions or the addition of a combination of antibiotics (Ahmed *et al.*, 2014). A comprehensive knowledge about the metabolism and cell wall synthesis is the key to predict the impact of these treatments on a targeted organism (Schneider & Sahl, 2010).

4 REFERENCES

Abe, T., Lu, X., Jiang, Y., Boccone, C. E., Qian, S., Vattem, K. M., Wek, R. C. & Walsh, J. P. (2003). Site-directed mutagenesis of the active site of diacylglycerol kinase alpha: calcium and phosphatidylserine stimulate enzyme activity via distinct mechanisms. *Biochem J* **375**, 673-680.

Adams, H., Teertstra, W., Demmers, J., Boesten, R. & Tommassen, J. (2003). Interactions between phage-shock proteins in *Escherichia coli*. *J Bacteriol* **185**, 1174-1180.

Ahmed, A., Azim, A., Gurjar, M. & Baronia, A. K. (2014). Current concepts in combination antibiotic therapy for critically ill patients. *Indian Journal of Critical Care Medicine : Peer-reviewed, Official Publication of Indian Society of Critical Care Medicine* **18**, 310-314.

Amiteye, S., Kobayashi, K., Imamura, D., Hosoya, S., Ogasawara, N. & Sato, T. (2003). *Bacillus subtilis* Diacylglycerol Kinase (DgkA) Enhances Efficient Sporulation. *Journal of Bacteriology* **185**, 5306-5309.

Anderson, R. G., Hussey, H. & Baddiley, J. (1972). The mechanism of wall synthesis in bacteria. The organization of enzymes and isoprenoid phosphates in the membrane. *Biochem J* **127**, 11-25.

Aso, Y., Okuda, K., Nagao, J. & other authors (2005). A novel type of immunity protein, NukH, for the lantibiotic nukacin ISK-1 produced by Staphylococcus warneri ISK-1. *Biosci Biotechnol Biochem* **69**, 1403-1410.

Azevedo, E. C., Rios, E. M., Fukushima, K. & Campos-Takaki, G. M. (1993). Bacitracin production by a new strain of *Bacillus subtilis*. Extraction, purification, and characterization. *Appl Biochem Biotechnol* **42**, 1-7.

Barreteau, H., Magnet, S., El Ghachi, M., Touze, T., Arthur, M., Mengin-Lecreulx, D. & Blanot, D. (2009). Quantitative high-performance liquid chromatography analysis of the pool levels of undecaprenyl phosphate and its derivatives in bacterial membranes. *J Chromatogr B Analyt Technol Biomed Life Sci* **877**, 213-220.

Bernard, R., Joseph, P., Guiseppi, A., Chippaux, M. & Denizot, F. o. (2003). YtsCD and YwoA, two independent systems that confer bacitracin resistance to *Bacillus subtilis*. *FEMS Microbiology Letters* **228**, 93-97.

Bernard, R., El Ghachi, M., Mengin-Lecreulx, D., Chippaux, M. & Denizot, F. (2005). BcrC from *Bacillus subtilis* acts as an undecaprenyl pyrophosphate phosphatase in bacitracin resistance. *J Biol Chem* **280**, 28852-28857.

Bernard, R., Guiseppi, A., Chippaux, M., Foglino, M. & Denizot, F. (2007). Resistance to bacitracin in *Bacillus subtilis*: unexpected requirement of the BceAB ABC transporter in the control of expression of its own structural genes. *J Bacteriol* **189**, 8636-8642.

Bhavsar, A. P., Erdman, L. K., Schertzer, J. W. & Brown, E. D. (2004). Teichoic acid is an essential polymer in *Bacillus subtilis* that is functionally distinct from teichuronic acid. *J Bacteriol* **186**, 7865-7873.

Bohnenberger, E. & Sandermann, H., Jr. (1976). Dephosphorylation of C55-isoprenyl-monophosphate by non-specific phosphatases. *FEBS Lett* **67**, 85-89.

Botella, E., Devine, S. K., Hubner, S. & other authors (2014). PhoR autokinase activity is controlled by an intermediate in wall teichoic acid metabolism that is sensed by the intracellular PAS domain during the PhoPR-mediated phosphate limitation response of Bacillus subtilis. *Mol Microbiol* **94**, 1242-1259.

Bouhss, A., Trunkfield, A. E., Bugg, T. D. & Mengin-Lecreulx, D. (2008). The biosynthesis of peptidoglycan lipid-linked intermediates. *FEMS Microbiol Rev* **32**, 208-233.

Breukink, E. & de Kruijff, B. (2006). Lipid II as a target for antibiotics. *Nat Rev Drug Discov* **5**, 321-332.

Brissette, J. L., Russel, M., Weiner, L. & Model, P. (1990). Phage shock protein, a stress protein of *Escherichia coli*. *Proc Natl Acad Sci U S A* **87**, 862-866.

Brötz, H., Bierbaum, G., Leopold, K., Reynolds, P. E. & Sahl, H. G. (1998). The lantibiotic mersacidin inhibits peptidoglycan synthesis by targeting lipid II. *Antimicrob Agents Chemother* **42**, 154-160.

Brown, S., Santa Maria, J. P., Jr. & Walker, S. (2013). Wall teichoic acids of gram-positive bacteria. *Annu Rev Microbiol* **67**, 313-336.

Bugg, T. D., Braddick, D., Dowson, C. G. & Roper, D. I. (2011). Bacterial cell wall assembly: still an attractive antibacterial target. *Trends Biotechnol* **29**, 167-173.

Butcher, B. G., Lin, Y. P. & Helmann, J. D. (2007). The yydFGHIJ operon of *Bacillus subtilis* encodes a peptide that induces the LiaRS two-component system. *J Bacteriol* **189**, 8616-8625.

Cain, B. D., Norton, P. J., Eubanks, W., Nick, H. S. & Allen, C. M. (1993). Amplification of the *bacA* gene confers bacitracin resistance to *Escherichia coli*. *J Bacteriol* **175**, 3784-3789.

Cao, M. & Helmann, J. D. (2002). Regulation of the *Bacillus subtilis bcrC* bacitracin resistance gene by two extracytoplasmic function s factors. *J Bacteriol* **184**, 6123-6129.

Carballido-Lopez, R., Formstone, A., Li, Y., Ehrlich, S. D., Noirot, P. & Errington, J. (2006). Actin homolog MreBH governs cell morphogenesis by localization of the cell wall hydrolase LytE. *Dev Cell* **11**, 399-409.

Chalker, A. F., Ingraham, K. A., Lunsford, R. D., Bryant, A. P., Bryant, J., Wallis, N. G., Broskey, J. P., Pearson, S. C. & Holmes, D. J. (2000). The *bacA* gene, which determines bacitracin susceptibility in *Streptococcus pneumoniae* and *Staphylococcus aureus*, is also required for virulence. *Microbiology* **146**, 1547-1553.

Cudic, P., Kranz, J. K., Behenna, D. C., Kruger, R. G., Tadesse, H., Wand, A. J., Veklich, Y. I., Weisel, J. W. & McCafferty, D. G. (2002). Complexation of peptidoglycan intermediates by the lipoglycodepsipeptide antibiotic ramoplanin: minimal structural requirements for intermolecular complexation and fibril formation. *Proc Natl Acad Sci U S A* **99**, 7384-7389.

Darwin, A. J. (2005). The phage-shock-protein response. *Mol Microbiol* **57**, 621-628.

Darwin, A. J. (2007). Regulation of the phage-shock-protein stress response in *Yersinia enterocolitica*. *Adv Exp Med Biol* **603**, 167-177.

Dawson, R. J., Hollenstein, K. & Locher, K. P. (2007). Uptake or extrusion: crystal structures of full ABC transporters suggest a common mechanism. *Mol Microbiol* **65**, 250-257.

Deller, S., Sollner, S., Trenker-El-Toukhy, R., Jelesarov, I., Gübitz, G. M. & Macheroux, P. (2006). Characterization of a Thermostable NADPH:FMN Oxidoreductase from the Mesophilic Bacterium Bacillus subtilis. *Biochemistry* **45**, 7083-7091.

Dintner, S., Staron, A., Berchtold, E., Petri, T., Mascher, T. & Gebhard, S. (2011). Coevolution of ABC transporters and two-component regulatory systems as resistance modules against antimicrobial peptides in Firmicutes Bacteria. *J Bacteriol* **193**, 3851-3862.

Dintner, S., Heermann, R., Fang, C., Jung, K. & Gebhard, S. (2014). A sensory complex consisting of an ATP-binding cassette transporter and a two-component regulatory system controls bacitracin resistance in *Bacillus subtilis*. *J Biol Chem* **289**, 27899-27910.

Dominguez-Escobar, J., Wolf, D., Fritz, G., Hofler, C., Wedlich-Soldner, R. & Mascher, T. (2014). Subcellular localization, interactions and dynamics of the phage-shock protein-like Lia response in *Bacillus subtilis*. *Mol Microbiol* **92**, 716-732.

Dufresne, K. & Paradis-Bleau, C. (2015). Biology and Assembly of the Bacterial Envelope. In Prokaryotic Systems Biology, pp. 41-76. Edited by P. J. N. Krogan & P. M. Babu. Cham: Springer International Publishing.

Economou, N. J., Cocklin, S. & Loll, P. J. (2013). High-resolution crystal structure reveals molecular details of target recognition by bacitracin. *Proc Natl Acad Sci U S A* **110**, 14207-14212.

Egan, A. J., Biboy, J., van't Veer, I., Breukink, E. & Vollmer, W. (2015). Activities and regulation of peptidoglycan synthases. *Philos Trans R Soc Lond B Biol Sci* **370**.

Eiamphungporn, W. & Helmann, J. D. (2008). The Bacillus subtilis sigma(M) regulon and its contribution to cell envelope stress responses. *Mol Microbiol* **67**, 830-848.

Eijsink, V. G., Axelsson, L., Diep, D. B., Havarstein, L. S., Holo, H. & Nes, I. F. (2002). Production of class II bacteriocins by lactic acid bacteria; an example of biological warfare and communication. *Antonie Van Leeuwenhoek* **81**, 639-654.

El Ghachi, M., Bouhss, A., Blanot, D. & Mengin-Lecreulx, D. (2004). The *bacA* gene of *Escherichia coli* encodes an undecaprenyl pyrophosphate phosphatase activity. *J Biol Chem* **279**, 30106-30113.

Fan, J., Jiang, D., Zhao, Y., Liu, J. & Zhang, X. C. (2014). Crystal structure of lipid phosphatase *Escherichia coli* phosphatidylglycerophosphate phosphatase B. *Proc Natl Acad Sci U S A* **111**, 7636-7640.

Field, D., Cotter, P. D., Hill, C. & Ross, R. P. (2015). Bioengineering Lantibiotics for Therapeutic Success. *Front Microbiol* **6**, 1363.

Finn, R. D., Coggill, P., Eberhardt, R. Y. & other authors (2016). The Pfam protein families database: towards a more sustainable future. *Nucleic Acids Res* **44**, D279-285.

Flores-Cruz, Z. & Allen, C. (2009). *Ralstonia solanacearum* Encounters an Oxidative Environtmenr During Tomato Infection. *MPMI* **22**, 773-782.

Flores-Kim, J. & Darwin, A. J. (2016). The Phage Shock Protein Response. *Annu Rev Microbiol* **70**, 83-101.

Frøyshov, Ø. & Laland, S. G. (1974). On the Biosynthesis of Bacitracin by a Soluble Enzyme Complex from *Bacillus licheniformis*. *Eur J Biochem* **46**, 235-242.

Funk, C. R., Zimniak, L. & Dowhan, W. (1992). The pgpA and pgpB genes of *Escherichia coli* are not essential: evidence for a third phosphatidylglycerophosphate phosphatase. *Journal of Bacteriology* **174**, 205-213.

Gao, R., Mack, T. R. & Stock, A. M. (2007). Bacterial response regulators: versatile regulatory strategies from common domains. *Trends Biochem Sci* **32**, 225-234.

Gauntlett, J. C., Gebhard, S., Keis, S., Manson, J. M., Pos, K. M. & Cook, G. M. (2008). Molecular analysis of BcrR, a membrane-bound bacitracin sensor and DNA-binding protein from *Enterococcus faecalis*. *J Biol Chem* **283**, 8591-8600.

Gebhard, S., Gaballa, A., Helmann, J. D. & Cook, G. M. (2009). Direct stimulus perception and transcription activation by a membrane-bound DNA binding protein. *Mol Microbiol* **73**, 482-491.

Gebhard, S. & Mascher, T. (2011). Antimicrobial peptide sensing and detoxification modules: unraveling the regulatory circuitry of *Staphylococcus aureus*. *Mol Microbiol* **81**, 581-587.

Gebhard, S. (2012). ABC transporters of antimicrobial peptides in Firmicutes bacteria - phylogeny, function and regulation. *Mol Microbiol* **86**, 1295-1317.

Gebhard, S., Fang, C., Shaaly, A., Leslie, D. J., Weimar, M. R., Kalamorz, F., Carne, A. & Cook, G. M. (2014). Identification and characterization of a bacitracin resistance network in *Enterococcus faecalis*. *Antimicrob Agents Chemother* **58**, 1425-1433.

Goffin, C. & Ghuysen, J. M. (1998). Multimodular penicillin-binding proteins: an enigmatic family of orthologs and paralogs. *Microbiol Mol Biol Rev* **62**, 1079-1093.

Gonzalez-Pastor, J. E., Hobbs, E. C. & Losick, R. (2003). Cannibalism by sporulating bacteria. *Science* **301**, 510-513.

Gough, D. P., Kirby, A. L., Richards, J. B. & Hemming, F. W. (1970). The characterization of undecaprenol of *Lactobacillus plantarum*. *Biochemical Journal* **118**, 167-170.

Guariglia-Oropeza, V. & Helmann, J. D. (2011). *Bacillus subtilis* sigma(V) confers lysozyme resistance by activation of two cell wall modification pathways, peptidoglycan O-acetylation and D-alanylation of teichoic acids. *J Bacteriol* **193**, 6223-6232.

Guo, R. T., Ko, T. P., Chen, A. P., Kuo, C. J., Wang, A. H. & Liang, P. H. (2005). Crystal structures of undecaprenyl pyrophosphate synthase in complex with magnesium, isopentenyl pyrophosphate, and farnesyl thiopyrophosphate: roles of the metal ion and conserved residues in catalysis. *J Biol Chem* **280**, 20762-20774.

Hachmann, A.-B., Angert, E. R. & Helmann, J. D. (2009). Genetic analysis of factors affecting susceptibility of *Bacillus subtilis* to daptomycin. *Antimicrob Agents Chemother* **53**, 1598-1609.

Hahne, H., Wolff, S., Hecker, M. & Becher, D. (2008). From complementarity to comprehensiveness--targeting the membrane proteome of growing *Bacillus subtilis* by divergent approaches. *Proteomics* **8**, 4123-4136.

Hartley, M. D. & Imperiali, B. (2012). At the membrane frontier: a prospectus on the remarkable evolutionary conservation of polyprenols and polyprenyl-phosphates. *Arch Biochem Biophys* **517**, 83-97.

Hebrard, M., Viala, J. P., Meresse, S., Barras, F. & Aussel, L. (2009). Redundant hydrogen peroxide scavengers contribute to *Salmonella* virulence and oxidative stress resistance. *J Bacteriol* **191**, 4605-4614.

Helmann, J. D. (2016). *Bacillus subtilis* extracytoplasmic function (ECF) sigma factors and defense of the cell envelope. *Curr Opin Microbiol* **30**, 122-132.

Higashi, Y., Strominger, J. L. & Sweeley, C. C. (1970). Biosynthesis of the peptidoglycan of bacterial cell walls. XXI. Isolation of free C55-isoprenoid alcohol and of lipid intermediates in peptidoglycan synthesis from *Staphylococcus aureus*. *J Biol Chem* **245**, 3697-3702.

Hiron, A., Falord, M., Valle, J., Debarbouille, M. & Msadek, T. (2011). Bacitracin and nisin resistance in *Staphylococcus aureus*: a novel pathway involving the BraS/BraR two-component system (SA2417/SA2418) and both the BraD/BraE and VraD/VraE ABC transporters. *Mol Microbiol* **81**, 602-622.

Höfler, C., Heckmann, J., Fritsch, A., Popp, P., Gebhard, S., Fritz, G. & Mascher, T. (2016). Cannibalism stress response in *Bacillus subtilis*. *Microbiology* **162**, 164-176.

Horsburgh, M. J. & Moir, A. (1999). sigmaM, an ECF RNA polymerase sigma factor of *Bacillus subtilis* 168, is essential for growth and survival in high concentrations of salt. *Molecular Microbiology* **32**, 41-50.

Horstman, N. K. & Darwin, A. J. (2012). Phage shock proteins B and C prevent lethal cytoplasmic membrane permeability in *Yersinia enterocolitica*. *Molecular Microbiology* **85**, 445-460.

Hughes, K. T. & Mathee, K. (1998). The anti-sigma factors. *Annu Rev Microbiol* **52**, 231-286.

Hurdle, J. G., O'Neill, A. J., Chopra, I. & Lee, R. E. (2011). Targeting bacterial membrane function: an underexploited mechanism for treating persistent infections. *Nat Rev Microbiol* **9**, 62-75.

Huvet, M., Toni, T., Sheng, X., Thorne, T., Jovanovic, G., Engl, C., Buck, M., Pinney, J. W. & Stumpf, M. P. (2011). The evolution of the phage shock protein response system: interplay between protein function, genomic organization, and system function. *Mol Biol Evol* **28**, 1141-1155.

Hynninen, A., Touze, T., Pitkanen, L., Mengin-Lecreulx, D. & Virta, M. (2009). An efflux transporter PbrA and a phosphatase PbrB cooperate in a lead-resistance mechanism in bacteria. *Mol Microbiol* **74**, 384-394.

Inaoka, T. & Ochi, K. (2012). Undecaprenyl pyrophosphate involvement in susceptibility of *Bacillus subtilis* to rare earth elements. *J Bacteriol* **194**, 5632-5637.

Ishihara, H., Takoh, M., Nishibayashi, R. & Sato, A. (2002). Distribution and variation of bacitracin synthetase gene sequences in laboratory stock strains of *Bacillus licheniformis*. *Curr Microbiol* **45**, 18-23.

Jensen, S. O., Thompson, L. S. & Harry, E. J. (2005). Cell division in *Bacillus subtilis*: FtsZ and FtsA association is Z-ring independent, and FtsA is required for efficient midcell Z-Ring assembly. *J Bacteriol* **187**, 6536-6544.

Jerga, A., Lu, Y. J., Schujman, G. E., de Mendoza, D. & Rock, C. O. (2007). Identification of a soluble diacylglycerol kinase required for lipoteichoic acid production in *Bacillus subtilis*. *J Biol Chem* **282**, 21738-21745.

Jervis, A. J., Thackray, P. D., Houston, C. W., Horsburgh, M. J. & Moir, A. (2007). SigM-responsive genes of *Bacillus subtilis* and their promoters. *J Bacteriol* **189**, 4534-4538.

Joly, N., Engl, C., Jovanovic, G., Huvet, M., Toni, T., Sheng, X., Stumpf, M. P. & Buck, M. (2010). Managing membrane stress: the phage shock protein (Psp) response, from molecular mechanisms to physiology. *FEMS Microbiol Rev* **34**, 797-827.

Jones, A. S., Rizvi, S. B. & Stacey, M. (1958). The phosphorus-containing compounds of gram-positive and gram-negative organisms in relation to the gram staining reaction. *J Gen Microbiol* **18**, 597-606.

Jordan, S., Junker, A., Helmann, J. D. & Mascher, T. (2006). Regulation of LiaRS-dependent gene expression in *Bacillus subtilis*: identification of inhibitor proteins, regulator binding sites, and target genes of a conserved cell envelope stress-sensing two-component system. *J Bacteriol* **188**, 5153-5166.

Jordan, S., Hutchings, M. I. & Mascher, T. (2008). Cell envelope stress response in Gram-positive bacteria. *FEMS Microbiol Rev* **32**, 107-146.

Jovanovic, G., Weiner, L. & Model, P. (1996). Identification, nucleotide sequence, and characterization of PspF, the transcriptional activator of the *Escherichia coli* stress-induced psp operon. *J Bacteriol* **178**, 1936-1945.

Kallenberg, F., Dintner, S., Schmitz, R. & Gebhard, S. (2013). Identification of regions important for resistance and signalling within the antimicrobial peptide transporter BceAB of *Bacillus subtilis*. *J Bacteriol* **195**, 3287-3297.

Kato, A., Chen, H. D., Latifi, T. & Groisman, E. A. (2012). Reciprocal control between a bacterium's regulatory system and the modification status of its lipopolysaccharide. *Mol Cell* **47**, 897-908.

Kelley, L. A., Mezulis, S., Yates, C. M., Wass, M. N. & Sternberg, M. J. (2015). The Phyre2 web portal for protein modeling, prediction and analysis. *Nat Protoc* **10**, 845-858.

Khosa, S., Lagedroste, M. & Smits, S. H. (2016). Protein Defense Systems against the Lantibiotic Nisin: Function of the Immunity Protein NisI and the Resistance Protein NSR. *Front Microbiol* **7**, 504.

Kingston, A. W., Zhao, H., Cook, G. M. & Helmann, J. D. (2014). Accumulation of heptaprenyl diphosphate sensitizes *Bacillus subtilis* to bacitracin: implications for the mechanism of resistance mediated by the BceAB transporter. *Mol Microbiol* **93**, 37-49.

Kleerebezem, M. & Tommassen, J. (1993). Expression of the *pspA* gene stimulates efficient protein export in *Escherichia coli*. *Mol Microbiol* **7**, 947-956.

Kleerebezem, M., Crielaard, W. & Tommassen, J. (1996). Involvement of stress protein PspA (phage shock protein A) of *Escherichia coli* in maintenance of the protonmotive force under stress conditions. *Embo J* **15**, 162-171.

Kobayashi, R., Suzuki, T. & Yoshida, M. (2007). *Escherichia coli* phage-shock protein A (PspA) binds to membrane phospholipids and repairs proton leakage of the damaged membranes. *Mol Microbiol* **66**, 100-109.

Konz, D., Klens, A., Schorgendorfer, K. & Marahiel, M. A. (1997). The bacitracin biosynthesis operon of *Bacillus licheniformis* ATCC 10716: molecular characterization of three multi-modular peptide synthetases. *Chem Biol* **4**, 927-937.

Kramer, N. E., Smid, E. J., Kok, J., De Kruijff, B., Kuipers, O. P. & Breukink, E. (2004). Resistance of Gram-positive bacteria to nisin is not determined by Lipid II levels. *FEMS Microbiol Lett* **239**, 157-161.

Kwun, M. J. & Hong, H. J. (2014). The activity of glycopeptide antibiotics against resistant bacteria correlates with their ability to induce the resistance system. *Antimicrob Agents Chemother* **58**, 6306-6310.

Laddomada, F., Miyachiro, M. M. & Dessen, A. (2016). Structural Insights into Protein-Protein Interactions Involved in Bacterial Cell Wall Biogenesis. *Antibiotics (Basel)* **5**.

Lis, M. & Kuramitsu, H. K. (2003). The stress-responsive dgk gene from *Streptococcus mutans* encodes a putative undecaprenol kinase activity. *Infection and immunity* **71**, 1938-1943.

Liu, Y., Qin, W., Liu, Q., Zhang, J., Li, H., Xu, S., Ren, P., Tian, L. & Li, W. (2016). Genome-wide identification and characterization of macrolide glycosyltransferases from a marine-derived *Bacillus* strain and their phylogenetic distribution. *Environ Microbiol* **18**, 4770-4781.

Lu, Y. H., Guan, Z., Zhao, J. & Raetz, C. R. (2011). Three phosphatidylglycerol-phosphate phosphatases in the inner membrane of *Escherichia coli*. *J Biol Chem* **286**, 5506-5518.

Manat, G., Roure, S., Auger, R., Bouhss, A., Barreteau, H., Mengin-Lecreulx, D. & Touze, T. (2014). Deciphering the metabolism of undecaprenyl-phosphate: the bacterial cell-wall unit carrier at the membrane frontier. *Microb Drug Resist* **20**, 199-214.

Manat, G., El Ghachi, M., Auger, R., Baouche, K., Olatunji, S., Kerff, F., Touze, T., Mengin-Lecreulx, D. & Bouhss, A. (2015). Membrane Topology and Biochemical Characterization of the *Escherichia coli* BacA Undecaprenyl-Pyrophosphate Phosphatase. *PLoS One* **10**, e0142870.

Manson, J. M., Keis, S., Smith, J. M. B. & Cook, G. M. (2004). Acquired bacitracin resistance in *Enterococcus faecalis* is mediated by an ABC transporter and a novel regulatory protein, BcrR. *Antimicrob Agents Chemother* **48**, 3743-3748.

Mascher, T., Margulis, N. G., Wang, T., Ye, R. W. & Helmann, J. D. (2003). Cell wall stress responses in *Bacillus subtilis*: the regulatory network of the bacitracin stimulon. *Mol Microbiol* **50**, 1591-1604.

Mascher, T., Zimmer, S. L., Smith, T. A. & Helmann, J. D. (2004). Antibiotic-inducible promoter regulated by the cell envelope stress-sensing two-component system LiaRS of *Bacillus subtilis*. *Antimicrob Agents Chemother* **48**, 2888-2896.

Mascher, T., Helmann, J. D. & Unden, G. (2006). Stimulus perception in bacterial signal-transducing histidine kinases. *Microbiol Mol Biol Rev* **70**, 910-938.

Mascher, T. (2013). Signaling diversity and evolution of extracytoplasmic function (ECF) s factors. *Curr Opin Microbiol* **16**, 148-155.

Mascher, T. (2014). Bacterial (intramembrane-sensing) histidine kinases: signal transfer rather than stimulus perception. *Trends Microbiol* **22**, 559-565.

McCloskey, M. A. & Troy, F. A. (1980). Paramagnetic isoprenoid carrier lipids. 2. Dispersion and dynamics in lipid membranes. *Biochemistry* **19**, 2061-2066.

Meehl, M., Herbert, S., Götz, F. & Cheung, A. (2007). Interaction of the GraRS two-component system with the VraFG ABC transporter to support vancomycin-intermediate resistance in *Staphylococcus aureus*. *Antimicrob Agents Chemother* **51**, 2679-2689.

Meeske, A. J., Sham, L. T., Kimsey, H., Koo, B. M., Gross, C. A., Bernhardt, T. G. & Rudner, D. Z. (2015). MurJ and a novel lipid II flippase are required for cell wall biogenesis in *Bacillus subtilis*. *Proc Natl Acad Sci U S A* **112**, 6437-6442.

Meeske, A. J., Rodrigues, C. D., Brady, J., Lim, H. C., Bernhardt, T. G. & Rudner, D. Z. (2016). High-Throughput Genetic Screens Identify a Large and Diverse Collection of New Sporulation Genes in *Bacillus subtilis*. *PLoS Biol* **14**, e1002341.

Melnyk, A. H., Wong, A. & Kassen, R. (2015). The fitness costs of antibiotic resistance mutations. *Evol Appl* **8**, 273-283.

Mengin-Lecreulx, D. & van Heijenoort, J. (1985). Effect of growth conditions on peptidoglycan content and cytoplasmic steps of its biosynthesis in Escherichia coli. *Journal of Bacteriology* **163**, 208-212.

Mitchell, P. & Moyle, J. (1954). The Gram reaction and cell composition: nucleic acids and other phosphate fractions. *J Gen Microbiol* **10**, 533-540.

Model, P., Jovanovic, G. & Dworkin, J. (1997). The *Escherichia coli* phage-shock-protein (*psp*) operon. *Mol Microbiol* **24**, 255-261.

Muchova, K., Chromikova, Z. & Barak, I. (2013). Control of *Bacillus subtilis* cell shape by RodZ. *Environ Microbiol* **15**, 3259-3271.

Needham, B. D. & Trent, M. S. (2013). Fortifying the barrier: the impact of lipid A remodelling on bacterial pathogenesis. *Nat Rev Microbiol* **11**, 467-481.

Neidhardt, F. C. & Umbarger, H. E. (1996). Chemical Composition of *Escherichia coli*. In *Escherichia coli* and *Salmonella*: Cellular and Molecular Biology. Edited by F. C. Neidhardt, R. Curtis III, J. L. Ingraham & other authors. Washington, D.C.: ASM Press

Nowak, M. A., Boerlijst, M. C., Cooke, J. & Smith, J. M. (1997). Evolution of genetic redundancy. *Nature* **388**, 167-171.

Ohki, R., Giyanto, Tateno, K., Masuyama, W., Moriya, S., Kobayashi, K. & Ogasawara, N. (2003a). The BceRS two-component regulatory system induces expression of the bacitracin transporter, BceAB, in *Bacillus subtilis*. *Molecular Microbiology* **49**, 1135-1144.

Ohki, R., Tateno, K., Okada, Y., Okajima, H., Asai, K., Sadaie, Y., Murata, M. & Aiso, T. (2003b). A bacitracin-resistant *Bacillus subtilis* gene encodes a homologue of the membrane-spanning subunit of the *Bacillus licheniformis* ABC transporter. *J Bacteriol* **185**, 51-59.

Ouyang, J., Tian, X. L., Versey, J., Wishart, A. & Li, Y. H. (2010). The BceABRS four-component system regulates the bacitracin-induced cell envelope stress response in *Streptococcus mutans*. *Antimicrob Agents Chemother* **54**, 3895-3906.

Pahl, G., Beitz, W., Feldhusen, J. & Grote, K. H. (2007). Engineering Design. A Systematic Approach, 3rd edn. London: Springer.

Pietiäinen, M., Francois, P., Hyyryläinen, H. L., Tangomo, M., Sass, V., Sahl, H. G., Schrenzel, J. & Kontinen, V. P. (2009). Transcriptome analysis of the responses of Staphylococcus aureus to antimicrobial peptides and characterization of the roles of vraDE and vraSR in antimicrobial resistance. *BMC Genomics* **10**, 429.

Podlesek, Z., Comino, A., Herzog-Velikonja, B., Zgur-Bertok, D., Komel, R. & Grabnar, M. (1995). *Bacillus licheniformis* bacitracin-resistance ABC transporter: relationship to mammalian multidrug resistance. *Mol Microbiol* **16**, 969-976.

Pollock, T. J., Thorne, L., Yamazaki, M., Mikolajczak, M. J. & Armentrout, R. W. (1994). Mechanism of bacitracin resistance in gram-negative bacteria that synthesize exopolysaccharides. *J Bacteriol* **176**, 6229-6237.

Radeck, J., Kraft, K., Bartels, J. & other authors (2013). The *Bacillus* BioBrick Box: generation and evaluation of essential genetic building blocks for standardized work with *Bacillus subtilis*. *Journal of biological engineering* **7**, 29.

Revilla-Guarinos, A., Gebhard, S., Alcantara, C., Staron, A., Mascher, T. & Zuniga, M. (2013). Characterization of a regulatory network of peptide antibiotic detoxification modules in *Lactobacillus casei* BL23. *Appl Environ Microbiol* **79**, 3160-3170.

Revilla-Guarinos, A., Gebhard, S., Mascher, T. & Zuniga, M. (2014). Defence against antimicrobial peptides: different strategies in Firmicutes. *Environ Microbiol*.

Rietkötter, E., Hoyer, D. & Mascher, T. (2008). Bacitracin sensing in *Bacillus subtilis*. *Mol Microbiol* **68**, 768-785.

Röse, L., Kaufmann, S. H. E. & Daugelat, S. (2004). Involvement of Mycobacterium smegmatis undecaprenyl phosphokinase in biofilm and smegma formation. *Microbes and Infection* **6**, 965-971.

Sandermann, H., Jr. & Strominger, J. L. (1971). C 55 -isoprenoid alcohol phosphokinase: an extremely hydrophobic protein from the bacterial membrane. *Proc Natl Acad Sci U S A* **68**, 2441-2443.

Sanyal, S. & Menon, A. K. (2010). Stereoselective transbilayer translocation of mannosyl phosphoryl dolichol by an endoplasmic reticulum flippase. *Proc Natl Acad Sci U S A* **107**, 11289-11294.

Scheffers, D. J. & Tol, M. B. (2015). LipidII: Just Another Brick in the Wall? *PLoS pathogens* **11**, e1005213.

Schneider, T. & Sahl, H.-G. (2010). An oldie but a goodie - cell wall biosynthesis as antibiotic target pathway. *Int J Med Microbiol* **300**, 161-169.

Schrecke, K., Staroń, A. & Mascher, T. (2012). Two-component signaling in the Gram-positive envelope stress response: intramembrane-sensing histidine kinases and accessory membrane proteins. In Two component systems in bacteria, pp. 199-229. Edited by R. Gross & D. Beier. Hethersett, Norwich, UK: Horizon Scientific Press.

Schrecke, K., Jordan, S. & Mascher, T. (2013). Stoichiometry and perturbation studies of the LiaFSR system of *Bacillus subtilis*. *Mol Microbiol* **87**, 769-788.

Shibata, Y., van der Ploeg, J. R., Kozuki, T., Shirai, Y., Saito, N., Kawada-Matsuo, M., Takeshita, T. & Yamashita, Y. (2009). Kinase activity of the dgk gene product is involved in the virulence of *Streptococcus mutans*. *Microbiology* **155**, 557-565.

Siewert, G. & Strominger, J. L. (1967). Bacitracin: an inhibitor of the dephosphorylation of lipid pyrophosphate, an intermediate in the biosynthesis of the peptidoglycan of bacterial cell walls. *Proc Natl Acad Sci U S A* **57**, 767-773.

Silhavy, T. J., Kahne, D. & Walker, S. (2010). The Bacterial Cell Envelope. *Cold Spring Harbor perspectives in biology* **2**, a000414.

Staroń, A., Finkeisen, D. E. & Mascher, T. (2011). Peptide antibiotic sensing and detoxification modules of *Bacillus subtilis*. *Antimicrob Agents Chemother* **55**, 515-525.

Storm, D. R. & Strominger, J. L. (1973). Complex formation between bacitracin peptides and isoprenyl pyrophosphates. The specificity of lipid-peptide interactions. *J Biol Chem* **248**, 3940-3945.

Storm, D. R. & Strominger, J. L. (1974). Binding of Bacitracin to Cells and Protoplasts of *Micrococcus lysodeikticus*. *Journal of Biological Chemistry* **249**, 1823-1827.

Storz, G., Hengge, R. & American Society for, M. (2011). Bacterial stress responses. Washington, DC: ASM Press.

Thurotte, A., Brüser, T., Mascher, T. & Schneider, D. (2017). Membrane chaperoning by members of the PspA/IM30 protein family. *Communicative & integrative biology* **10**, e1264546.

Touze, T., Blanot, D. & Mengin-Lecreulx, D. (2008a). Substrate specificity and membrane topology of *Escherichia coli* PgpB, an undecaprenyl pyrophosphate phosphatase. *J Biol Chem* **283**, 16573-16583.

Touze, T., Tran, A. X., Hankins, J. V., Mengin-Lecreulx, D. & Trent, M. S. (2008b). Periplasmic phosphorylation of lipid A is linked to the synthesis of undecaprenyl phosphate. *Mol Microbiol* **67**, 264-277.

Trookman, N. S., Rizer, R. L. & Weber, T. (2011). Treatment of minor wounds from dermatologic procedures: a comparison of three topical wound care ointments using a laser wound model. *J Am Acad Dermatol* **64**, S8-15.

Tseng, C. L. & Shaw, G. C. (2008). Genetic evidence for the actin homolog gene *mreBH* and the bacitracin resistance gene *bcrC* as targets of the alternative sigma factor SigI of *Bacillus subtilis*. *J Bacteriol* **190**, 1561-1567.

Tsuda, H., Yamashita, Y., Shibata, Y., Nakano, Y. & Koga, T. (2002). Genes involved in bacitracin resistance in *Streptococcus mutans*. *Antimicrob Agents Chemother* **46**, 3756-3764.

Typas, A., Banzhaf, M., Gross, C. A. & Vollmer, W. (2012). From the regulation of peptidoglycan synthesis to bacterial growth and morphology. *Nat Rev Microbiol* **10**, 123-136.

Ulrich, L. E., Koonin, E. V. & Zhulin, I. B. (2005). One-component systems dominate signal transduction in prokaryotes. *Trends Microbiol* **13**, 52-56.

Umbreit, J. N., Stone, K. J. & Strominger, J. L. (1972). Isolation of Polyisoprenyl Alcohols from Streptococcus faecalis. *Journal of Bacteriology* **112**, 1302-1305.

van Gestel, J., Vlamakis, H. & Kolter, R. (2015). From cell differentiation to cell collectives: Bacillus subtilis uses division of labor to migrate. *PLoS Biol* **13**, e1002141.

van Heijenoort, Y., Gómez, M., Derrien, M., Ayala, J. & van Heijenoort, J. (1992). Membrane intermediates in the peptidoglycan metabolism of *Escherichia coli*: possible roles of PBP 1b and PBP 3. *Journal of Bacteriology* **174**, 3549-3557.

Van Horn, W. D. & Sanders, C. R. (2012). Prokaryotic diacylglycerol kinase and undecaprenol kinase. *Annu Rev Biophys* **41**, 81-101.

Vollmer, W. & Höltje, J. V. (2004). The architecture of the murein (peptidoglycan) in gram-negative bacteria: vertical scaffold or horizontal layer(s)? *J Bacteriol* **186**, 5978-5987.

Weiner, L. & Model, P. (1994). Role of an *Escherichia coli* stress-response operon in stationary-phase survival. *Proc Natl Acad Sci U S A* **91**, 2191-2195.

Willoughby, E., Higashi, Y. & Strominger, J. L. (1972). Enzymatic Dephosphorylation of C55-Isoprenylphosphate. *J Biol Chem* **247**, 5113-5115.

Wolf, D., Kalamorz, F., Wecke, T. & other authors (2010). In-depth profiling of the LiaR response of *Bacillus subtilis*. *J Bacteriol* **192**, 4680-4693.

Wolf, D., Dominguez-Cuevas, P., Daniel, R. A. & Mascher, T. (2012). Cell envelope stress response in cell wall-deficient L-forms of *Bacillus subtilis*. *Antimicrob Agents Chemother* **56**, 5907-5915.

Yamashita, Y., Takehara, T. & Kuramitsu, H. K. (1993). Molecular characterization of a *Streptococcus mutans* mutant altered in environmental stress responses. *Journal of Bacteriology* **175**, 6220-6228.

Yoshida, A. & Kuramitsu, H. K. (2002). Multiple *Streptococcus mutans* Genes Are Involved in Biofilm Formation. *Applied and environmental microbiology* **68**, 6283-6291.

Yoshimura, M., Asai, K., Sadaie, Y. & Yoshikawa, H. (2004). Interaction of *Bacillus subtilis* extracytoplasmic function (ECF) sigma factors with the N-terminal regions of their potential anti-sigma factors. *Microbiology* **150**, 591-599.

Zhao, H., Sun, Y., Peters, J. M., Gross, C. A., Garner, E. C. & Helmann, J. D. (2016). Depletion of undecaprenyl pyrophosphate phosphatases (UPP-Pases) disrupts cell envelope biogenesis in *Bacillus subtilis*. *J Bacteriol*.

Zweers, J. C., Nicolas, P., Wiegert, T., van Dijl, J. M. & Denham, E. L. (2012). Definition of the sigma(W) regulon of *Bacillus subtilis* in the absence of stress. *PLoS One* **7**, e48471.

5 OVERVIEW OF FIGURES

6 OVERVIEW OF TABLES

7 APPENDICES

7.1 PUBLICATION I: A NEW WAY OF SENSING: NEED-BASED ACTIVATION OF ANTIBIOTIC RESISTANCE BY A FLUX-SENSING MECHANISM

Publication I:

Fritz G, Dintner S, Treichel N S, **Radeck J**, Gerland U, Mascher T, Gebhard S (2015) A new way of sensing: need-based activation of antibiotic resistance by a flux-sensing mechanism. **mBio**. 6(4):e00975. doi: 10.1128/mBio.00975-15.

A New Way of Sensing: Need-Based Activation of Antibiotic Resistance by a Flux-Sensing Mechanism

Georg Fritz,[a,b]* Sebastian Dintner,[a] Nicole Simone Treichel,[a] Jara Radeck,[a] Ulrich Gerland,[b]* Thorsten Mascher,[a]* Susanne Gebhard[a]*

Department Biology I, Ludwig-Maximilians-Universität München, Planegg-Martinsried, Germany[a]; Arnold Sommerfeld Center for Theoretical Physics, Ludwig-Maximilians-Universität München, Munich, Germany[b]

* Present address: Georg Fritz, LOEWE-Center for Synthetic Microbiology, Philipps-Universität Marburg, Marburg, Germany; Ulrich Gerland, Technische Universität München, Garching, Germany; Thorsten Mascher, Technische Universität Dresden, Institute of Microbiology, Dresden, Germany; Susanne Gebhard, Department of Biology and Biochemistry, University of Bath, Claverton Down, United Kingdom.

ABSTRACT **Sensing of and responding to environmental changes are of vital importance for microbial cells. Consequently, bacteria have evolved a plethora of signaling systems that usually sense biochemical cues either via direct ligand binding, thereby acting as "concentration sensors," or by responding to downstream effects on bacterial physiology, such as structural damage to the cell. Here, we describe a novel, alternative signaling mechanism that effectively implements a "flux sensor" to regulate antibiotic resistance. It relies on a sensory complex consisting of a histidine kinase and an ABC transporter, in which the transporter fulfills the dual role of both the sensor of the antibiotic and the mediator of resistance against it. Combining systems biological modeling with *in vivo* experimentation, we show that these systems in fact respond to changes in activity of individual resistance transporters rather than to changes in the antibiotic concentration. Our model shows that the cell thereby adjusts the rate of *de novo* transporter synthesis to precisely the level needed for protection. Such a flux-sensing mechanism may serve as a cost-efficient produce-to-demand strategy, controlling a widely conserved class of antibiotic resistance systems.**

IMPORTANCE **Bacteria have to be able to accurately perceive their environment to allow adaptation to changing conditions. This is usually accomplished by sensing the concentrations of beneficial or harmful substances or by measuring the effect of the prevailing conditions on the cell. Here we show the existence of a new way of sensing the environment, where the bacteria monitor the activity of an antibiotic resistance transporter. Such a "flux-sensing" mechanism allows the cell to detect its current capacity to deal with the antibiotic challenge and thus precisely respond to the need for more transporters. We propose that this is a cost-efficient way of regulating antibiotic resistance on demand.**

Received 11 June 2015 **Accepted** 22 June 2015 **Published** 21 July 2015

Citation Fritz G, Dintner S, Treichel NS, Radeck J, Gerland U, Mascher T, Gebhard S. 2015. A new way of sensing: need-based activation of antibiotic resistance by a flux-sensing mechanism. mBio 6(4):e00975-15. doi:10.1128/mBio.00975-15.

Editor George L. Drusano, University of Florida

Address correspondence to Thorsten Mascher, thorsten.mascher@tu-dresden.de.

Sensing of and responding to environmental changes are of vital importance for microbial cells, as they facilitate their fine-tuned adaptation to prevailing conditions. The range of parameters a single cell can monitor is immense, including conditions as diverse as nutrient supply, oxygen levels, temperature, pH, cell densities, and presence of toxic compounds. It is therefore hardly surprising that bacteria have developed a plethora of sensory and regulatory strategies to accomplish this feat. In the specific context of antibiotic resistance, bacteria have to be able to accurately determine the severity of the attack in order to decide on an adequate response. The precision of this response is key to both survival of antimicrobial action and minimizing the metabolic cost of resistance (1, 2).

One common feature of controlling a cellular response is to monitor the ambient concentration of a specific substance. In the case of antibiotic resistance, this can be achieved, e.g., via direct binding to a sensory protein, such as the vancomycin-responsive histidine kinase (HK) VanSsc of *Streptomyces coelicolor* (3). An alternative approach is to monitor the cellular damage caused by the antibiotic, as is the case, e.g., for the LiaRS cell envelope damage-sensing system of *Bacillus subtilis* (4). Such an indirect sensing strategy allows the cell to integrate into its response its current physiological state, which can significantly influence the potency of a given concentration of antibiotic. For instance, fast-growing cells are usually much more susceptible to antibiotic action than slow-growing cells. While a damage-sensing strategy undoubtedly provides a more context-dependent response, it requires the accumulation of a certain degree of cellular damage. Here, we present evidence for a third, previously undescribed regulatory strategy, allowing the bacterium to directly monitor its current capacity to deal with the antibiotic threat by measuring the activity of a drug efflux pump (referred to as "flux sensing").

We recently showed that a unique type of ATP-binding cassette (ABC) transporters is actively involved in a signaling pathway controlling its own production (5–7). These transporters mediate resistance against a wide range of antimicrobial peptides in many Gram-positive species, including important pathogens, such as *Staphylococcus aureus* and *Enterococcus faecalis* (8). Their expres-

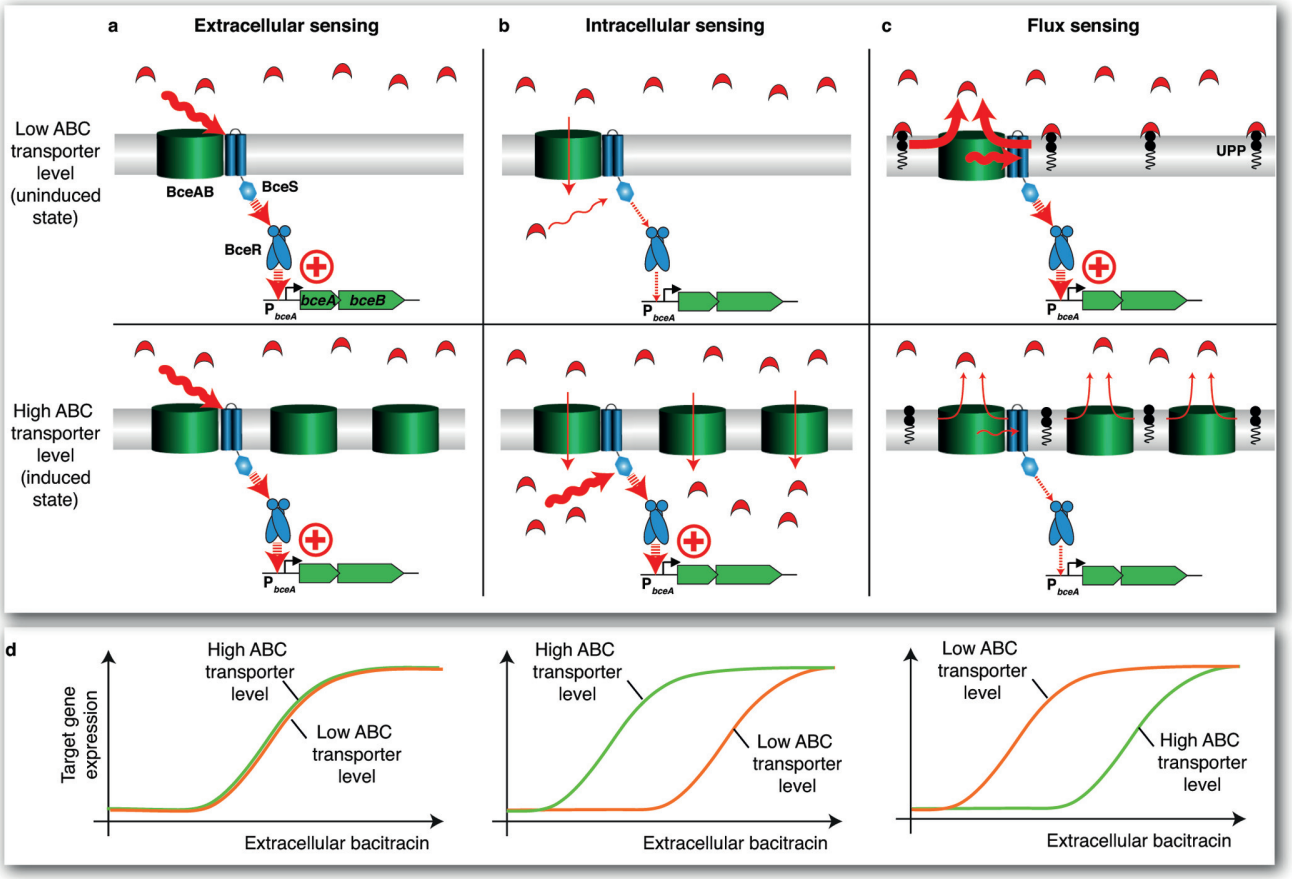

FIG 1 Schematic of conceivable sensory scenarios employed by the BceRS-BceAB system. In an external sensing scenario (a), the ABC transporter BceAB might act as a scaffold that keeps the histidine kinase BceS in an active conformation, which would allow BceS to perceive the extracellular concentration of bacitracin (red symbols). Since up-regulation of BceAB is not expected to change the extracellular concentration of bacitracin, the rate of gene expression should be independent of the BceAB level in this scenario (no feedback). In an internal sensing scenario (b), BceAB might be required to translocate bacitracin into the cytoplasm where BceS could sense its abundance. Here, up-regulation of BceAB should lead to an increased rate of bacitracin influx, which would in turn lead to further up-regulation of BceAB expression (positive feedback). In a flux-sensing scenario (c), BceAB itself is the true sensor, which directly signals its transport activity to BceS. In such a scenario, up-regulation of BceAB would reduce the load experienced by each individual transporter and thereby reduce signaling via BceS (negative feedback). (d) Schematic depiction of the expected impact of different levels of the BceAB transporter (low, red curves; high, green curves) on dose-dependent P_{bceA} activity.

sion is regulated by two-component systems whose HKs lack discernible ligand-binding domains and instead form a sensory complex with the transporter (9, 10). The signaling process is best understood in *Bacillus subtilis*, where the two-component system BceRS and its associated ABC-transporter BceAB together sense and counteract the deleterious effects of bacitracin and several other antimicrobial peptides interfering with the lipid II cycle of cell wall biosynthesis, by triggering a 500-fold increase in the expression of the *bceAB* transporter operon (5, 9, 11) (Fig. 1a).

To characterize the regulatory role of the transporter, here we took a systems approach, combining mathematical modeling with experiments probing the time-resolved, dose-dependent response of the Bce system to its substrate bacitracin. We show that signaling within the Bce system operates by a flux-sensing mechanism, monitoring the activity of individual transporters. Our model allowed us to derive a unique response signature for a flux sensor, which was experimentally validated. Moreover, the model was able to predict the antibiotic sensitivity of cells depending on transporter expression, leading us to propose that flux sensing serves as a novel produce-to-demand strategy to control antibiotic resistance in changing environments.

RESULTS

ABC transporter production rapidly adapts to a wide range of bacitracin inputs. To obtain detailed quantitative information on the regulatory dynamics of the Bce system, we first studied the relationship between the external antibiotic concentration and the transcriptional response of the target promoter P_{bceA}. To this end, exponentially growing SGB073 cells (wild-type *B. subtilis* carrying a chromosomally integrated P_{bceA}-*luxABCDE* reporter) were exposed to sublethal concentrations of bacitracin. At virtually all bacitracin concentrations tested, luciferase activity initially rose rapidly upon antibiotic addition, before leveling off to reach a plateau 20 to 30 min after induction (Fig. 2A). A plot of the plateau level against antibiotic concentration revealed that the system's response quickly adapted to a wide dynamic range of antibiotic

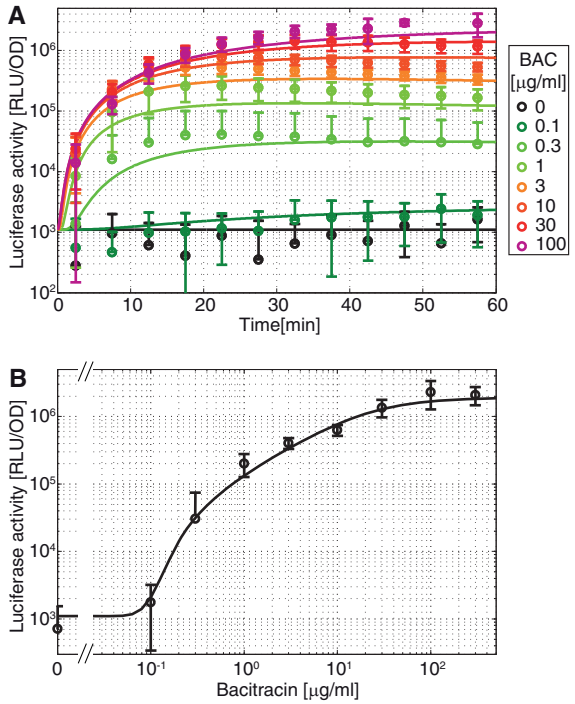

FIG 2 Gene expression driven by the P_{bceA} promoter rapidly adapts to a wide range of antibiotic concentrations. (A) Exponentially growing cells of strain SGB073 were exposed to sublethal concentrations of bacitracin at 0 min, and luciferase activity from a P_{bceA}-*luxABCDE* reporter construct was monitored over time. Data are means and standard deviations for at least three independent biological replicates (lower error bars are not depicted if negative values were reached). Lines show the dynamics predicted by the quantitative mathematical model described in the main text. (B) Experimental dose-response curve of the P_{bceA} promoter at a fixed time (42.5 min) after induction (symbols) and the fit to the mathematical model (lines). For details, see the text.

input (0.1 to 100 μg/ml bacitracin) (Fig. 2B). Such gradual, homeostatic control of target gene expression is often found in regulatory systems that exploit negative-feedback mechanisms, while positive-feedback regulation frequently enables switch-like or even hysteretic responses (12). The presence of a negative feedback mechanism was also suggested by our observation that the P_{bceA} promoter activity reached its steady-state value within a short time (20 to 30 min) (Fig. 2A) relative to the cell doubling time of ~70 min (see Fig. S1 in the supplemental material), as negative-feedback control is known to reduce the response time of genetic circuits (13).

To elucidate the source of this apparent feedback effect, we considered three plausible roles of the transporter in the regulatory pathway. (i) In the simplest scenario, the transporter acts as a mere ligand-binding component in a sensory complex with the HK, as is the case in regulation of sugar phosphate uptake by the Uhp system in *Escherichia coli* (14, 15). The input signal for such a system is the ambient concentration of the cognate substrate (Fig. 1a). This signal will not change if the number of transporters inserted in the membrane increases, since the amount of HK, and hence the number of sensory complexes, remains constant. Thus, there will be no feedback on regulation. (ii) Alternatively, the transporter might be required to translocate the substrate to a cytoplasmic recognition site (Fig. 1b). Such a strategy is realized, e.g., in the regulation of arabinose utilization by *E. coli* (16), where the level of intracellular substrate serves as the input signal. While the polarity of BceAB-mediated transport is not known, it has been suggested that BceAB may act as an importer of bacitracin, releasing it into the cytoplasm for degradation (5, 8). Here, the strength of the stimulus should increase during the induction process, because the amount of bacitracin transported into the cell will rise with the supply of transporters, thus creating a positive feedback on the response. (iii) The third conceivable scenario is that the HK activity is determined by the rate of flux through individual transporters (Fig. 1c). BceAB has also been proposed to act as a "hydrophobic vacuum cleaner" (17), conferring resistance by clearing the target from the inhibitory grip of the antibiotic (Fig. 1c) (7, 18). In such a scenario, increasing BceAB copy numbers should alleviate the load experienced by individual transporters (Fig. 1c), resulting in a negative feedback of BceAB on its own expression. Thus, qualitatively, a flux-sensing scenario best reflects the observed dynamics of P_{bceA} activation.

The behavior of the wild-type system is compatible with a mathematical model for relative flux sensing. To test if the proposed flux-sensing mechanism can quantitatively explain the regulatory dynamics in the Bce system, we developed a mathematical model, incorporating signal transduction via such a mechanism. Bacitracin is known to bind to its membrane-associated target molecule undecaprenol-pyrophosphate (UPP), thus blocking the dephosphorylation and recycling of UPP in the lipid II cycle of cell wall biosynthesis (19). If we suppose that the ABC transporter BceAB catalyzes the release of bacitracin from UPP with Michaelis-Menten enzyme kinetics, the time-dependent concentration of the bacitracin-bound form of UPP, UPP-bac, can be described by a differential equation of the form

$$\frac{d}{dt}[\text{UPP-bac}] = k^{\text{on}}[\text{bac}](\text{UPP}_{\text{tot}} - [\text{UPP-bac}]) - k^{\text{off}}[\text{UPP-bac}] - v_{\max}J_{\text{bac}}[\text{BceAB}] \quad (1)$$

Here, [bac] is the externally applied bacitracin concentration, k^{on} and k^{off} are the spontaneous on and off rates for the binding of bacitracin to UPP, UPP_{tot} is the total UPP level in the cell, $J_{\text{bac}} = [\text{UPP-bac}]/(K_m + [\text{UPP-bac}])$ is the relative bacitracin load per BceAB transporter, and $v_{\max}$ and K_m are the maximal transport rate and Michaelis-Menten constant of BceAB, respectively (see Tables S1 and S2 in the supplemental material).

To implement the proposed flux-sensing mechanism in our model, we took into account that the expression of the two-component system operon *bceRS* is constitutive (see Fig. S2 in the supplemental material) and also that the interaction between the histidine kinase BceS and the BceAB transporter is bacitracin independent (9). Moreover, we verified that the overproduction of BceS did not significantly affect the MIC of a strain with constitutive BceAB expression (see Fig. S3 in the supplemental material), indicating that the transport activity of BceAB is not affected by the formation of the sensory complex with BceS *in vivo*. Thus, as long as BceAB molecules outnumber BceS molecules, so that BceS is the limiting component in complex formation, there should be a constant number of functional BceS-BceAB sensory complexes in the cell, while the number of free BceAB transporters should change with increasing total transporter levels. Under inducing conditions this is a safe assumption, because we can readily detect the presence of BceAB, but not of BceS, using Western blotting or

fluorescent protein fusions (our unpublished observations). Under noninducing conditions, both proteins are below our current detection limit and therefore not accessible to quantification. Based on the relative promoter strengths of P_{bceR} (see Fig. S2 in the supplemental material) and P_{bceA} (Fig. 2A), it could well be that uninduced cells possess more kinases than transporters. Nevertheless, within our mathematical model we assume that the number of sensory complexes does not change over time and thus that BceS always monitors the activity of a fixed number of transporters. While this assumption might be inaccurate in the early phase of induction, BceAB levels are expected to quickly exceed those of BceS such that the model should well reflect the experimental conditions shortly after induction.

Based on these considerations, we assume within our model that BceS signals the load of individual transporters to the response regulator BceR, such that the level of the active (phosphorylated) form of BceR is proportional to the bacitracin load per transporter, J_{bac}. Following a thermodynamic model for transcriptional regulation (20), activation of gene expression from the P_{bceA} promoter by phosphorylated BceR can then be formulated in terms of J_{bac}, such that the dynamic equations for *bceAB* mRNA concentration, $[m]$, and BceAB protein level, [BceAB], read

$$\frac{d}{dt}[m] = \alpha\frac{1+\omega(J_{\mathrm{bac}}/\kappa)^n}{1+(J_{\mathrm{bac}}/\kappa)^n} - \lambda[m] \qquad (2)$$

$$\frac{d}{dt}[\mathrm{BceAB}] = \beta[m] - \delta[\mathrm{BceAB}] \qquad (3)$$

Here, α is the basal transcription rate, ω is the ratio of maximal to basal promoter activity, λ is the mRNA degradation rate, and κ is a measure of the relative flux at which P_{bceA} is activated. The Hill exponent (n) in turn reflects all forms of cooperativity in stimulus perception and signal transduction, as well as in BceR-DNA binding and recruitment of RNA polymerase. Finally, β is the translation rate and δ is the protein dilution rate due to cell doubling. The dynamic equations for luciferase reporter expression were formulated analogously to equations 2 and 3 and are given in Materials and Methods.

We then asked whether the data in Fig. 2 were in quantitative agreement with our mathematical model. To this end, all known and measured model parameters were fixed to their physiological values (see Table S1 in the supplemental material), the remaining ones were confined to physiological intervals (see Table S2 in the supplemental material), and then the model was fitted to the experimental dose-response in Fig. 2B (see Materials and Methods for details of the fitting procedure). Overall, we found that the dynamic behavior of the model closely resembled the rapid adaptation kinetics observed in the experimental time series (Fig. 2A). Likewise, the model adequately captured the gradual increase of the experimental dose-response characteristics over a wide range of input levels (Fig. 2B). These findings provided the first quantitative indication that the Bce system does in fact implement a flux-sensing mechanism that monitors the bacitracin load per BceAB transporter. The agreement between theory and experiment in the early phase (0 to 15 min) after induction further demonstrates that the model assumption of a constant number of sensory complexes per cell was reasonable: if BceAB were initially less abundant than BceS, the number of sensory complexes should increase upon induction of BceAB production, which should result in a positive feedback on signaling. Such a positive feedback should cause a lag in the response while the number of sensory complexes is still very low, followed by a rapid increase in signaling as more and more complexes are formed. Such an effect is not visible in our data (Fig. 2A), showing that the window in which the number of sensory complexes is not constant is short and cannot be resolved by the luciferase reporter.

Predicting the signature of a relative flux sensor. One key feature of the proposed flux sensor model is that up-regulation of BceAB leads to a reduction of the bacitracin load per transporter, which ultimately down-regulates transcription of *bceAB*. Hence, if the model was correct, disabling this negative autoregulation of BceAB should abolish the graded response to bacitracin. Consequently, constitutively supplying the cell with a fixed number of transporter molecules should provide an alternative means of distinguishing between the three different signaling scenarios detailed above. For a relative flux-sensing mechanism, in cells with few transporters, the load per transporter should be saturated at low bacitracin concentrations, leading to a highly sensitive response (Fig. 1d, right). Conversely, cells with many transporters should respond more sluggishly (Fig. 1d, right), because more bacitracin is required to produce a high load per transporter. For an intracellular sensing mechanism, the opposite behavior is expected: cells with a high level of BceAB should respond more sensitively than those with few transporters, as the total amount of bacitracin translocated increases with the number of transporters present (Fig. 1d, center). Last, for an extracellular-concentration-sensing mechanism, the dose-response behavior should not be affected by alterations in the level of the transporter (Fig. 1d, left). In fact, this last situation was recently reported for the DctA/DcuS sensor complex of *E. coli* (21), in which the transporter DctA merely acts as an activity switch for the HK DcuS.

When we modified our mathematical model to accommodate constitutive production of the transporter, the predicted dose-response behavior was altered in two respects. First, the elimination of autoregulation of the level of BceAB results in a more switch-like response of the P_{bceA} promoter to increasing bacitracin concentrations (Fig. 3a). This sharp response is due to the fact that the fit to the data for the wild type in Fig. 2 yielded a Hill exponent (n) of 7.5 ± 0.2, suggesting that signal transduction and regulation of P_{bceA} exhibit a high degree of cooperativity. Second, when the copy number of the transporter is changed, the model predicts a shift in the dose-response curves consistent with the signature of a flux sensor: in cells that constitutively express low levels of BceAB, the promoter is triggered by low bacitracin concentrations (Fig. 3a), while much higher concentrations of the antibiotic are required to activate P_{bceA} in cells that synthesize large amounts of BceAB (Fig. 3a).

In order to test these predictions experimentally, we constructed a strain (SGB218) in which the endogenous *bceAB* locus had been deleted, and replaced by a chromosomally integrated construct driven by the xylose-inducible promoter P_{xylA}. In addition, this strain carries the P_{bceA}-*luxABCDE* reporter used above. We previously quantified the dose-response characteristics of P_{xylA} (22). It showed a basal transcription level ~30-fold higher than that driven by P_{bceA} and could be activated up to ~100-fold by increasing the xylose concentration in the medium (Fig. 3b). Based on these data, we selected five xylose concentrations (0%, 0.005%, 0.01%, 0.03%, and 0.2%) that resulted in markedly different P_{xylA} activities. Incorporation of these promoter activities into our mathematical model led to distinct BceAB protein levels

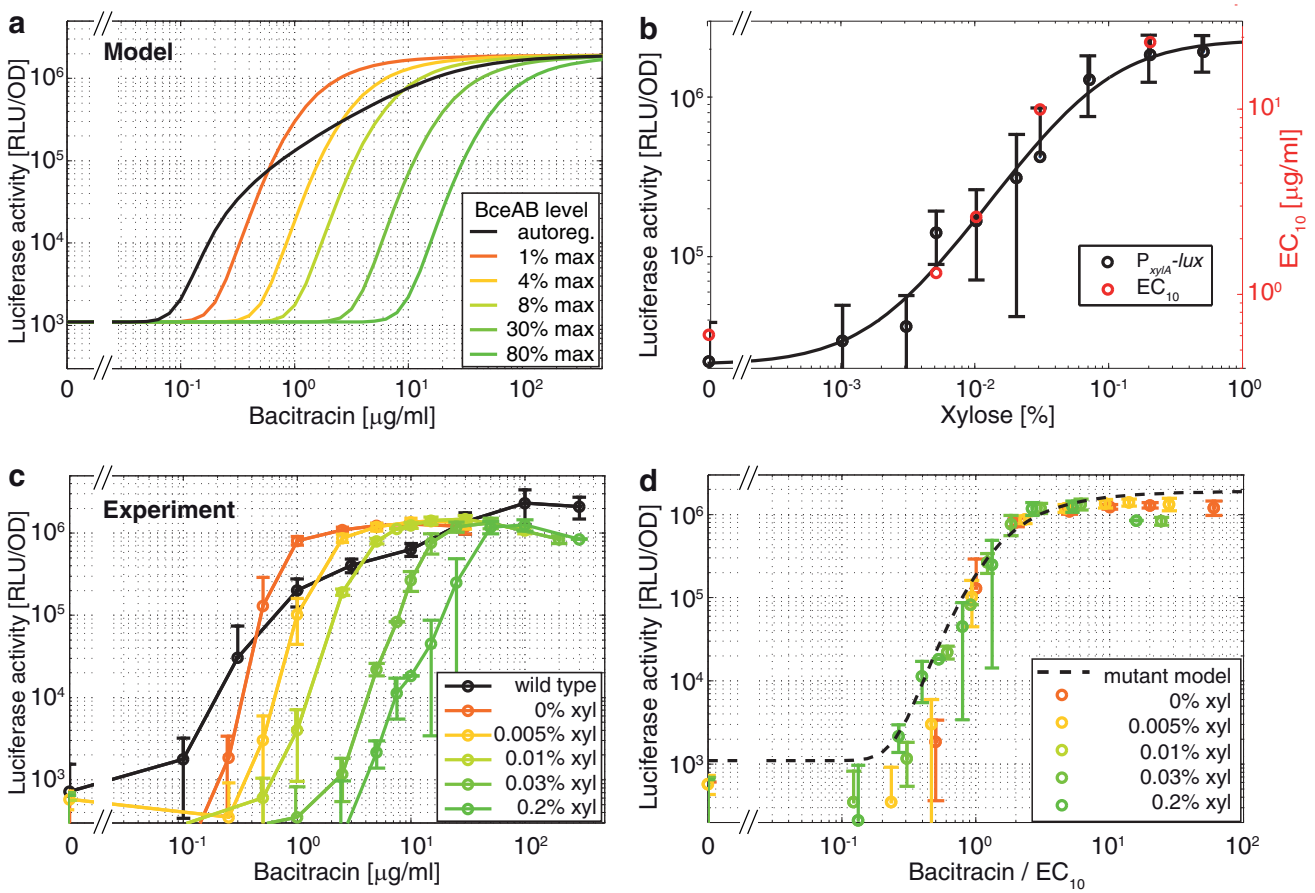

FIG 3 Signature of a relative flux sensor. (a) Theoretical prediction of P_{bceA}-*luxABCDE* dose-response curves for various levels of constitutive BceAB transporter production (colored curves), compared to the wild type with autoregulated *bceAB* expression (black curve). The expression levels of *bceAB* in the legend are percentages of the maximal P_{bceA} expression level in the wild type. These expression levels were derived from the experimental dose-response curve of the P_{xylA} promoter in panel b, which drives expression of *bceAB* in the experimental system in panel c. (b) Xylose-dependent dose-response curve of a P_{xylA}-*luxABCDE* reporter strain (black symbols) published previously (22) and fitted by a Hill function (black curve). In addition, the EC_{10} values , i.e., concentrations at which the dose-response curves in panel c reach 10% of their maximal activity, are shown as a function of xylose concentration (red symbols). (c) Experimental P_{bceA}-*luxABCDE* dose-response curves in strain SGB218, in which the endogenous chromosomal *bceAB* locus has been deleted and transporter expression is constitutively driven from a chromosomally integrated xylose-dependent P_{xylA}-*bceAB* construct (colored symbols). The wild-type dose-response curve (black symbols) was derived from strain SGB073. (d) Data from panels a and c with the *x* axis rescaled by the respective EC_{10} values. For details, see the text.

for each xylose concentration and thus also to the parameter-free predictions for the shifts in the activation threshold of P_{bceA} discussed above (Fig. 3a).

Figure 3c shows the bacitracin-dependent P_{bceA} activity of SGB218 cells grown in the presence of the selected xylose concentrations. Strikingly, we found that both the theoretically predicted abrupt onset of activation and the shift in induction threshold with increasing xylose concentration were quantitatively reflected in our experimental results. The latter becomes manifest, for instance, when EC_{10} values (the bacitracin concentration at which the dose-response reached 10% of its maximum) are plotted as a function of xylose concentration. Theoretically, the EC_{10} is expected to be proportional to the concentration of BceAB in the cell and, accordingly, to reflect the level of P_{xylA} promoter activity (Fig. 3b). Indeed, the experimental EC_{10} values all fell along this curve (Fig. 3b), suggesting (i) that P_{xylA} activity is in fact proportional to BceAB protein levels and (ii) that the number of BceAB transporters per cell determines how much bacitracin the cell will tolerate before signaling is activated. To inspect the shape of the dose-response curves in Fig. 3c more closely, we rescaled all *x* axes to the EC_{10} values. When this was done, all dose-response curves collapsed onto a single master curve (Fig. 3d). Remarkably, the experimental data points showed an even steeper increase than predicted by our model (Fig. 3d), highlighting the strong cooperativity involved in signal perception, transduction, and gene regulation at P_{bceA}. Considering that sensory perception and signaling by the Bce system involve a multiprotein complex (9), it is not difficult to envisage such strongly cooperative effects arising. Moreover, it was previously shown that many promoters of *bceAB*-like operons contain binding sites for two dimers of the response regulator (23). Indeed, P_{bceA} also possesses two BceR binding sites, spaced 13 bp apart and located directly upstream of the −10/−35 promoter elements. We recently showed that both binding sites are required for bacitracin-dependent induction of P_{bceA} (C. Fang and T. Mascher, unpublished data). Since each binding site consists of a repeat sequence, each site will likely be

occupied by a dimer of BceR, indicating that a total of four BceR molecules are required for promoter induction, which could further enhance cooperativity in signaling.

The model successfully predicts inhibitory concentrations of bacitracin. Bacitracin acts by binding to the lipid carrier UPP and preventing its dephosphorylation (19). Due to its essentiality for cell growth, a certain minimal fraction of free lipid carrier is needed to maintain cell wall biosynthesis at a given growth rate, and blocking a larger fraction of UPP is thus lethal. Intuitively, expression of the BceAB transporter is expected to release UPP from the inhibitory grip of bacitracin and thereby keep a significant fraction of UPP bacitracin free. Hence, BceAB expression should directly affect the bacitracin-bound UPP levels in the cell and, with that, the cellular sensitivity to inhibition by bacitracin.

To analyze the physiological implications of the flux-sensing mechanism, we first calculated the fraction of bacitracin-bound UPP in the cell using our mathematical model. For the wild-type strain employing bacitracin-dependent feedback regulation of *bceAB* expression, the fraction of bacitracin-bound UPP first increases rapidly with the applied concentration of the antibiotic (Fig. 4a). As soon as BceS detects a significant bacitracin flux via the BceAB transporter (at ca. 0.3 μg/ml bacitracin), transporter production is up-regulated and the rate of accumulation of bacitracin-bound UPP is slowed. Based on the bacitracin concentration needed to inhibit the growth of the wild type (ca. 200 μg/ml), we calculated the lethal fraction of bacitracin-bound UPP to be 90% (Fig. 4a). In the absence of BceAB transporters, our model predicted that the fraction of bacitracin-bound UPP increases rapidly with the applied bacitracin concentration and reaches the lethal 90% threshold at 2 μg/ml bacitracin (Fig. 4a). This is slightly below the experimentally determined MIC of 8 to 16 μg/ml for a strain with *bceAB* deleted. However, the difference is not surprising given that the model does not take into account residual bacitracin resistance caused, e.g., by the UPP phosphatase BcrC and other members of the σ^M, σ^X, and σ^W regulons involved in the response of *B. subtilis* to cell envelope stress (24–26). In contrast to the homeostatic control seen in the wild type, for the strain with constitutive *bceAB* expression, the model predicted the binding curve to be of the same shape as in the absence of BceAB. However, the curves were shifted to ever-higher bacitracin concentrations the more transporter was present in the cell (Fig. 4a). Hence, the model also predicted that the higher the level of BceAB, the greater the antibiotic concentration required for killing (Fig. 4a).

To confront these predictions with experimental data, we assayed the reporter strains for growth inhibition by bacitracin. For this, growth rates were determined after addition of a range of bacitracin concentrations to exponentially growing cultures producing different levels of transporter. For each culture, increasing the added concentration of bacitracin first led to a significant decrease in growth rate (Fig. 4b) and eventually to complete cessation of growth or cell lysis, with higher concentrations being required to inhibit cells expressing *bceAB* at higher levels. Prediction of the lethal threshold concentration by the model approximately reproduced the observed relationship between growth inhibition and *bceAB* expression (dashed line in Fig. 4b). The steeper decline of the theoretical curve compared to the experimental data at low levels of BceAB can again be explained by the presence of alternative resistance determinants in *B. subtilis*, as discussed above. When we adjusted the model to the background resistance of a *bceAB* deletion-containing strain (here, 15 μg/ml), it accurately described the correlation between BceAB expression levels and inhibitory bacitracin concentration (solid line in Fig. 4b).

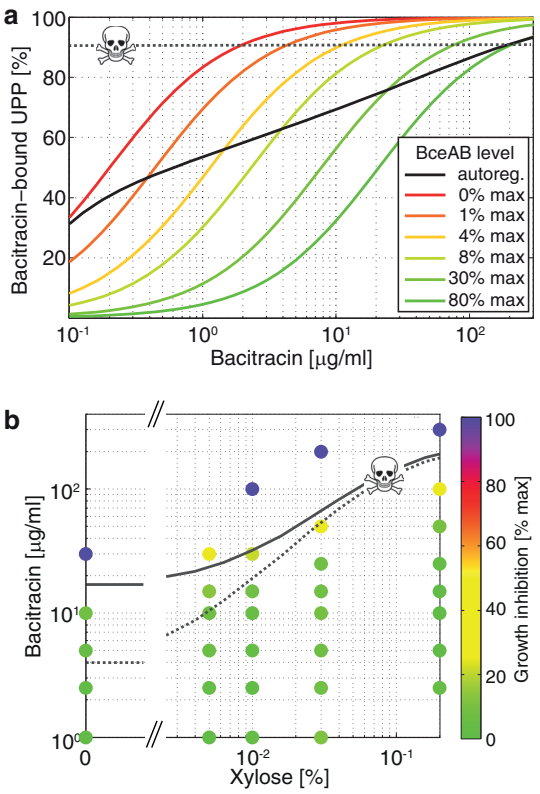

FIG 4 Inhibition of cell wall biosynthesis by blocking UPP recycling. (a) Change in the fraction of bacitracin-bound UPP as a function of external bacitracin, predicted by a model with feedback regulation (black curve) and a model with the indicated levels of constitutive *bceAB* expression (colored curves). In addition to the *bceAB* expression levels used in Fig. 3, the red curve shows the percentage of bacitracin-bound UPP in the absence of the BceAB transporter. Assuming that cell wall biosynthesis can be maintained as long as the percentage of blocked UPP carrier molecules remains below a given limit (dashed grey line), the intersection with the solid lines leads to a prediction of how the bacitracin MIC should scale with increasing BceAB expression level (dashed grey line in panel b). (b) Growth inhibition of strain SGB218 with constitutive transporter expression from a xylose-dependent P_{xylA}-*bceAB* construct (colored symbols). Cultures with a low *bceAB* expression level (0% xylose) are more susceptible to bacitracin than cultures with a high *bceAB* expression level (0.2% xylose). The model quantitatively captures the scaling of this growth inhibition line (solid grey line), when background resistance mechanisms, which are reflected in an additive offset for low *bceAB* expression level, are taken into account.

Our model does not distinguish between the cellular concentration of UPP-bacitracin complexes (i.e., the assumed transport substrate) and the true transport flux as input parameters, because binding kinetics and transport activity are mathematically equivalent in the Michaelis-Menten equation employed. This consideration becomes important in light of the possibility that BceAB might serve as a sensor without actually translocating any of its substrate. However, if BceAB were transport deficient, the concentration of UPP-associated bacitracin should always be proportional to the extracellular antibiotic concentration, regardless of the number of functional transporters in the cell. This is entirely inconsistent with the shifts in dose-response curves observed in cells expressing different amounts of BceAB (Fig. 3). Furthermore,

the good fit between observed growth inhibition by bacitracin and predicted lethal threshold at different transporter expression levels (Fig. 4) showed that the transporter indeed had an impact on the fraction of bacitracin-bound UPP and thus must be able to translocate its substrate.

Taken together, our theoretical and experimental data clearly indicate that a combination of relative flux sensing and concomitant negative feedback provides efficient homeostatic control over the level of bacitracin-bound UPP, allowing it to be maintained below the lethal concentration threshold over a range of antibiotic concentrations covering at least two orders of magnitude.

DISCUSSION

Bacteria can perceive their environment either directly, by monitoring the concentration of a relevant substance, or indirectly, by monitoring the effects on cellular physiology caused by a particular condition. We show here that sensing of transport flux of antimicrobial substances through a resistance pump presents a third and novel sensing strategy, by which the cell can directly monitor and respond to its current detoxification capacity. Through quantitative, time-resolved analysis of the dose-response dynamics, combined with mathematical modeling of the regulatory pathway, we obtained evidence that the Bce system of *B. subtilis* implements such a flux sensor, where the parameter monitored by the signaling system is the activity of individual BceAB transporters. This elegant mechanism permits continual assessment of the most critical parameter of antibiotic resistance, i.e., the cell's current capacity to deal with the inhibitory effects of the applied drug. From a systems perspective, this parameter is far more relevant to the cell than the present concentration of the antibiotic: as long as the cell's transport capacity is sufficient to detoxify the drug, there is no need for a further response even at high antibiotic concentrations. We therefore propose that flux sensing is a very cost-efficient regulatory strategy to control antibiotic resistance. To our knowledge, this is the first report of such a regulatory mechanism in any physiological context.

Over 200 Bce-like systems can currently be found in protein databases, and their components were shown to have coevolved (23). Combined with experimental confirmation of the transporter's sensory role in all systems studied to date (8, 11, 27–29), this tight evolutionary correlation suggests conservation of the signaling mechanism. Flux sensing may therefore be a widespread regulatory principle in antimicrobial peptide resistance. Because this mechanism relies on the intricate process of communicating transport flux between proteins, it should, conceivably, be easy to disrupt and thus might constitute a prime drug target to counteract resistance in pathogenic bacteria possessing Bce-like systems, such as *S. aureus*, *E. faecalis*, *Listeria monocytogenes*, and *Clostridium difficile* (8, 23, 27, 30).

Our modeling approach not only has provided evidence for a flux-sensing mechanism but also has given access to important system variables that are difficult to quantify experimentally, most notably the fraction of bacitracin-bound UPP. Analysis of such "hidden" parameters can lead to highly relevant predictions for bacterial physiology, such as our calculation of the dependence between the bacitracin concentration required to inhibit growth and the expression level of the resistance determinant. Ultimately, such an approach may have important implications for the treatment of infectious disease caused by drug-resistant bacteria. Importantly, Bce-like systems have been shown to respond to a large variety of peptide antibiotics that interfere with different stages of cell wall synthesis, including lantibiotics such as nisin, but also the clinically relevant glycopeptides vancomycin and teicoplanin (6, 31, 32).

In summary, we report the first observation of transport flux sensing as an elegant way of implementing adaptation via negative feedback regulation. We propose that this represents a highly cost-efficient mode of gene regulation, finely adjusted to the current physiological needs of the cell. In the case of antibiotic resistance mediated by Bce-like systems, this need is an increased demand for detoxification. Future exploration of further systems employing transporters to control a signaling pathway will show if this mechanism can also be found in other physiological contexts.

MATERIALS AND METHODS

Bacterial strains and growth conditions. All strains used in this study are listed in Table S3 in the supplemental material. Strains were routinely propagated in Luria-Bertani (LB) medium. For all functional assays, *B. subtilis* was grown in chemically defined CSE medium (33), in which the carbon source was modified to provide constant growth rates over an extended period of time [3.3 g/liter $(NH_4)_2SO_4$, 29 mM KH_2PO_4, 70 mM K_2HPO_4, 1× III′ salts (100× III′ salts is 0.232 g/liter $MnSO_4{\cdot}4H_2O$, 12.3 g/liter $MgSO_4{\cdot}7H_2O$), 50 mg/liter tryptophan, 22 mg/liter ammonium ferric citrate, 0.8% (wt/vol) potassium glutamate, 0.6% (wt/vol) sodium succinate, 2.5% (wt/vol) fructose]. Selective medium for *B. subtilis* contained kanamycin (10 mg/liter), chloramphenicol (5 mg/liter) or erythromycin (1 mg/liter) in combination with lincomycin (25 mg/liter) for macrolide-lincosamide-streptogramin B resistance (MLS^r). Selective medium for *E. coli* contained ampicillin (100 mg/liter). Solid medium additionally contained 1.5% (wt/vol) agar.

Construction of plasmids and strains. All cloning was performed according to BioBrick standard RFC10 (http://hdl.handle.net/1721.1/45138) or RFC25 (http://hdl.handle.net/1721.1/45140). Plasmids, strains, and primer sequences are listed in Table S3 in the supplemental material. The *bceAB* operon of *B. subtilis* was adapted to the BioBrick standard by addition of prefix and suffix sequences according to a modified RFC25 standard (22) using PCR (primers TM2577 and TM2578). All internal PstI sites were changed from CTGCAG to CTCCAG and EcoRI sites from GAATTC to GAGTTC by PCR overlap extension mutagenesis (34). Point mutations were chosen so to avoid any change in the encoded protein sequence. Cloning of the resulting fragment into the EcoRI and SpeI sites of pSB1A3 resulted in pNTSB103. The P_{xylA} region of pXT was adapted for BioBrick cloning by the addition of RFC10 prefix and suffix sequences via PCR (primers iGEM134 and iGEM135) and cloning into the EcoRI and SpeI sites of pSB1A3, to generate pNTSB104. Subsequently, the *bceAB* operon was placed under the transcriptional control of P_{xylA} by BioBrick assembly of the pNTSB103 and pNTSB104 inserts into the vector pBS2E (22), resulting in pNT2E01. To quantify target promoter activities, wild-type *B. subtilis* W168 was transformed with a transcriptional P_{bceA}-*luxABCDE* reporter construct, pSDlux101 (35), producing strain SGB073. Introduction of the same reporter together with pNT2E01 into the *bceAB*::Kan deletion strain TMB035 produced strain SGB218.

Luciferase assays. Luciferase activities were assayed using a Synergy2 multimode microplate reader from BioTek (Winooski, VT) controlled by the software Gen5. Aliquots of culture (100 μl) were added to 96-well plates (black walls, clear bottoms; Greiner Bio-One, Frickenhausen, Germany), which were incubated at 37°C with medium-intensity agitation. Cell growth was monitored by measuring optical density at 600 nm (OD_{600}). For each individual sample, the OD_{600} and relative luminescence units (RLU) (endpoint reads; 1-s integration time; sensitivity, 200) were background corrected by subtracting the respective values measured for wells containing 100 μl of CSE medium. RLU/OD_{600} values were calculated for individual measurements. Means and standard deviations

of RLU/OD_{600} values were determined from at least three biological replicates.

To synchronize cultures, 10 ml of CSE medium in a 125-ml flask was inoculated with 0.2 ml of an overnight culture and incubated at 37°C with agitation (200 rpm) to an OD_{600} of 0.2 to 0.5. Cultures were then diluted in fresh CSE medium to an OD_{600} of 0.05 and transferred to 96-well plates. OD_{600} and luminescence were monitored every 10 min, and at an OD_{600} of ~0.1 (corresponding to an OD_{600} of ~0.4 in cuvettes with a 1-cm light path length), 5 μl of Zn^{2+} bacitracin was added to give the final concentrations indicated in the figure legends. Incubation was continued, and OD_{600} and luminescence were monitored every 5 min for 1 h. For controlled expression of *bceAB* in strain SGB218, xylose was added to all growth media at the final concentrations indicated in the figure legends.

Bacitracin sensitivity assays. The MIC of bacitracin for *B. subtilis* grown in CSE medium was determined by a broth dilution technique. Cultures were grown to stationary phase in CSE medium and then diluted (1:500) into fresh CSE medium containing different concentrations of Zn^{2+} bacitracin. Following 20 to 24 h of incubation at 37°C with agitation, the MIC was scored as the lowest concentration at which no growth was observed. Inhibition of growing cultures (Fig. 4b) was determined as follows. Cells of strain SGB218 were cultured with the indicated xylose concentrations and challenged with the final concentrations of Zn^{2+} bacitracin indicated in the figure legends as described for the luciferase assays above. Average growth rates (γ) were estimated from an exponential fit to the growth curve (OD_{600}) from 0 h (bacitracin addition) to 1 h for each experimental condition. Growth inhibition was calculated as $1 - (\gamma/\gamma_{max})$, where γ_{max} is the maximal growth rate at a given xylose concentration.

Mathematical model and parameter estimation. The minimal model for the dynamics of the *bceAB* operon in the wild-type strain SGB073 is described by equations 1 to 3. In constructing this model we made the simplifying assumption that the maximal amount of UPP in a cell, UPP_{tot}, is given by the sum of all intermediate forms of the lipid carrier molecule present in the cell (see Table S1 in the supplemental material for parameter values). Binding of bacitracin to UPP then leads to the accumulation of the bacitracin-bound form of UPP, UPP-bac, to the maximal amount (UPP_{tot}). To model the constitutive expression of *bceAB* in strain SGB218, the flux-dependent transcription rate in equation 2 was replaced by a temporally constant transcription rate, which is determined solely by the concentration of externally supplied xylose:

$$\frac{d}{dt}[m] = \alpha_{xyl} - \lambda[m] \tag{4}$$

The xylose-dependent rate of *bceAB* transcription driven by P_{xylA} was modeled as $\alpha_{xyl} = \alpha \times f(xyl)/g(\mathrm{bac}=0)$, where α is the rate of P_{bceA}-controlled transcription in the absence of bacitracin and $f(xyl)$ and $g(\mathrm{bac})$ are the experimental dose-response curves for P_{xylA} (Fig. 3b) and P_{bceA} (Fig. 2B), respectively. In addition, expression of the *luxABCDE* reporter genes in all strains is under the control of an ectopically integrated P_{bceA} promoter, which is assumed to follow the same transcriptional kinetics as the promoter at its native genomic locus (cf. equation 2):

$$\frac{d}{dt}[m_{lux}] = \alpha \frac{1 + \omega\left(J_{\mathrm{bac}}/\kappa\right)^n}{1 + \left(J_{\mathrm{bac}}/\kappa\right)^n} - \lambda_{lux}[m_{lux}] \tag{5}$$

Here, m_{lux} is the *luxABCDE* mRNA, λ_{lux} is the associated degradation rate, and all other parameters are the same as in equation 2. Assuming that one of the proteins in the *lux* operon is rate limiting for light production, its dynamics is modeled by

$$\frac{d}{dt}[\mathrm{Lux}] = \beta[m_{lux}] - \delta_{lux}[\mathrm{Lux}] \tag{6}$$

where β is the translation rate and δ_{lux} is the corresponding protein half-life. In addition, a multiplicative scaling factor, σ, was introduced to relate the Lux protein level to the experimentally measured luminescence output.

To fit the model to our experimental data, the parameters were fixed to physiological values whenever possible (see Table S1 in the supplemental material) and constrained to physiologically reasonable intervals in all other cases (see Table S2 in the supplemental material). Then, a trust region-reflective Newton method (MatLab; The MathWorks, Inc.) was used to minimize the value of χ^2 between the dose-response curve in Fig. 2B and the model. To account for the presence of local optima and to quantify the uncertainty in the estimated parameters, 100 independent fits were performed with randomly chosen initial parameter sets (see Fig. S4 and S5 in the supplemental material for correlation graphs between χ^2 and estimated parameters). Confidence intervals for the fitted parameters (see Table S2) were obtained as previously described (36). The prediction of the dose-response curves for strain SGB218 was based on the parameter set from strain SGB073, but calculated using equation 4 instead of equation 2.

SUPPLEMENTAL MATERIAL

Supplemental material for this article may be found at http://mbio.asm.org/lookup/suppl/doi:10.1128/mBio.00975-15/-/DCSupplemental.

Figure S1, EPS file, 0.5 MB.
Figure S2, EPS file, 0.1 MB.
Figure S3, TIF file, 2.3 MB.
Figure S4, EPS file, 0.8 MB.
Figure S5, EPS file, 2 MB.
Table S1, DOCX file, 0.1 MB.
Table S2, DOCX file, 0.1 MB.
Table S3, DOCX file, 0.02 MB.

ACKNOWLEDGMENTS

Work in the labs of U.G., T.M., and G.F. was funded through the Deutsche Forschungsgemeinschaft (DFG) in the context of the Priority Program SPP 1617 "Phenotypic Heterogeneity and Sociobiology of Bacterial Populations" (GE1098/6-1 to U.G., MA2837/3-1 to T.M., and a start-up grant to G.F.). Work in S.G.'s lab was funded by a DFG research grant (GE2164/3-1).

We thank Ina Lackerbauer for technical assistance in strain construction and Ulrike Mäder for determination of the *bceAB* mRNA half-life. We are also grateful to Laurence Hurst for valuable suggestions during the writing process and to Jim Caunt for critical reading of the manuscript.

G.F. performed all mathematical modeling; S.D., N.S.T., and J.R. performed the experiments; S.G. coordinated experimental work; T.M., U.G., G.F., and S.G. designed the study; G.F. and S.G. wrote the manuscript; all authors approved the manuscript.

REFERENCES

1. **Kwun MJ, Hong H-J.** 2014. The activity of glycopeptide antibiotics against resistant bacteria correlates with their ability to induce the resistance system. Antimicrob Agents Chemother **58:**6306–6310. http://dx.doi.org/10.1128/AAC.03668-14.
2. **Andersson DI, Hughes D.** 2010. Antibiotic resistance and its cost: is it possible to reverse resistance? Nat Rev Microbiol **8:**260–271. http://dx.doi.org/10.1038/nrmicro2319.
3. **Koteva K, Hong HJ, Wang XD, Nazi I, Hughes D, Naldrett MJ, Buttner MJ.** 2010. A vancomycin photoprobe identifies the histidine kinase VanSsc as a vancomycin receptor. Nat Chem Biol **6:**327–329.
4. **Wolf D, Domínguez-Cuevas P, Daniel RA, Mascher T.** 2012. Cell envelope stress response in cell wall-deficient L-forms of *Bacillus subtilis*. Antimicrob Agents Chemother **56:**5907–5915. http://dx.doi.org/10.1128/AAC.00770-12.
5. **Rietkötter E, Hoyer D, Mascher T.** 2008. Bacitracin sensing in *Bacillus subtilis*. Mol Microbiol **68:**768–785. http://dx.doi.org/10.1111/j.1365-2958.2008.06194.x.
6. **Gebhard S, Mascher T.** 2011. Antimicrobial peptide sensing and detoxification modules: unravelling the regulatory circuitry of *Staphylococcus aureus*. Mol Microbiol **81:**581–587. http://dx.doi.org/10.1111/j.1365-2958.2011.07747.x.
7. **Gebhard S.** 2012. ABC transporters of antimicrobial peptides in Firmic-

utes bacteria—phylogeny, function and regulation. Mol Microbiol **86:** 1295–1317. http://dx.doi.org/10.1111/mmi.12078.

8. **Hiron A, Falord M, Valle J, Débarbouillé M, Msadek T.** 2011. Bacitracin and nisin resistance in *Staphylococcus aureus*: a novel pathway involving the BraS/BraR two-component system (SA2417/SA2418) and both the BraD/BraE and VraD/VraE ABC transporters. Mol Microbiol **81:** 602–622. http://dx.doi.org/10.1111/j.1365-2958.2011.07735.x.
9. **Dintner S, Heermann R, Fang C, Jung K, Gebhard S.** 2014. A sensory complex consisting of an ATP-binding cassette transporter and a two-component regulatory system controls bacitracin resistance in *Bacillus subtilis*. J Biol Chem **289:**27899–27910. http://dx.doi.org/10.1074/jbc.M114.596221.
10. **Mascher T.** 2014. Bacterial (intramembrane-sensing) histidine kinases: signal transfer rather than stimulus perception. Trends Microbiol **22:** 559–565. http://dx.doi.org/10.1016/j.tim.2014.05.006.
11. **Staroń A, Finkeisen DE, Mascher T.** 2011. Peptide antibiotic sensing and detoxification modules of *Bacillus subtilis*. Antimicrob Agents Chemother **55:**515–525. http://dx.doi.org/10.1128/AAC.00352-10.
12. **Hasty J, McMillen D, Isaacs F, Collins JJ.** 2001. Computational studies of gene regulatory networks: *in numero* molecular biology. Nat Rev Genet **2:**268–279. http://dx.doi.org/10.1038/35066056.
13. **Rosenfeld N, Elowitz MB, Alon U.** 2002. Negative autoregulation speeds the response times of transcription networks. J Mol Biol **323:**785–793. http://dx.doi.org/10.1016/S0022-2836(02)00994-4.
14. **Island MD, Kadner RJ.** 1993. Interplay between the membrane-associated UhpB and UhpC regulatory proteins. J Bacteriol **175:** 5028–5034.
15. **Schwöppe C, Winkler HH, Neuhaus HE.** 2003. Connection of transport and sensing by UhpC, the sensor for external glucose-6-phosphate in *Escherichia coli*. Eur J Biochem **270:**1450–1457. http://dx.doi.org/10.1046/j.1432-1033.2003.03507.x.
16. **Schleif R.** 2000. Regulation of the L-arabinose operon of *Escherichia coli*. Trends Genet **16:**559–565. http://dx.doi.org/10.1016/S0168-9525(00)02153-3.
17. **Chang G.** 2003. Multidrug resistance ABC transporters. FEBS Lett **555:** 102–105. http://dx.doi.org/10.1016/S0014-5793(03)01085-8.
18. **Ohki R, Giyanto, Tateno K, Masuyama W, Moriya S, Kobayashi K, Ogasawara N.** 2003. The BceRS two-component regulatory system induces expression of the bacitracin transporter, BceAB, in *Bacillus subtilis*. Mol Microbiol **49:**1135–1144. http://dx.doi.org/10.1046/j.1365-2958.2003.03653.x.
19. **Storm DR, Strominger JL.** 1973. Complex formation between bacitracin peptides and isoprenyl pyrophosphates. The specificity of lipid-peptide interactions. J Biol Chem **248:**3940–3945.
20. **Bintu L, Buchler NE, Garcia HG, Gerland U, Hwa T, Kondev J, Phillips R.** 2005. Transcriptional regulation by the numbers: models. Curr Opin Genet Dev **15:**116–124. http://dx.doi.org/10.1016/j.gde.2005.02.007.
21. **Steinmetz PA, Wörner S, Unden G.** 2014. Differentiation of DctA and DcuS function in the DctA/DcuS sensor complex of *Escherichia coli*: function of DctA as an activity switch and of DcuS as the C4-dicarboxylate sensor. Mol Microbiol **94:**218–229. http://dx.doi.org/10.1111/mmi.12759.
22. **Radeck J, Kraft K, Bartels J, Cikovic T, Dürr F, Emenegger J, Kelterborn S, Sauer C, Fritz G, Gebhard S, Mascher T.** 2013. The *Bacillus* BioBrick box: generation and evaluation of essential genetic building blocks for standardized work with *Bacillus subtilis*. J Biol Eng **7:**29. http://dx.doi.org/10.1186/1754-1611-7-29.
23. **Dintner S, Staroń A, Berchtold E, Petri T, Mascher T, Gebhard S.** 2011. Coevolution of ABC transporters and two-component regulatory systems as resistance modules against antimicrobial peptides in Firmicutes bacteria. J Bacteriol **193:**3851–3862. http://dx.doi.org/10.1128/JB.05175-11.
24. **Cao M, Helmann JD.** 2002. Regulation of the *Bacillus subtilis bcrC* bacitracin resistance gene by two extracytoplasmic function σ factors. J Bacteriol **184:**6123–6129. http://dx.doi.org/10.1128/JB.184.22.6123-6129.2002.
25. **Cao M, Helmann JD.** 2004. The *Bacillus subtilis* extracytoplasmic-function σ^X factor regulates modification of the cell envelope and resistance to cationic antimicrobial peptides. J Bacteriol **186:**1136–1146. http://dx.doi.org/10.1128/JB.186.4.1136-1146.2004.
26. **Eiamphungporn W, Helmann JD.** 2008. The *Bacillus subtilis* σ^M regulon and its contribution to cell envelope stress responses. Mol Microbiol **67:** 830–848. http://dx.doi.org/10.1111/j.1365-2958.2007.06090.x.
27. **Gebhard S, Fang C, Shaaly A, Leslie DJ, Weimar MR, Kalamorz F, Carne A, Cook GM.** 2014. Identification and characterization of a bacitracin resistance network in *Enterococcus faecalis*. Antimicrob Agents Chemother **58:**1425–1433. http://dx.doi.org/10.1128/AAC.02111-13.
28. **Revilla-Guarinos A, Gebhard S, Alcántara C, Staron A, Mascher T, Zúñiga M.** 2013. Characterization of a regulatory network of peptide antibiotic detoxification modules in *Lactobacillus casei* BL23. Appl Environ Microbiol **79:**3160–3170. http://dx.doi.org/10.1128/AEM.00178-13.
29. **Ouyang J, Tian X-L, Versey J, Wishart A, Li Y-H.** 2010. The BceABRS four-component system regulates the bacitracin-induced cell envelope stress response in *Streptococcus mutans*. Antimicrob Agents Chemother **54:**3895–3906. http://dx.doi.org/10.1128/AAC.01802-09.
30. **Collins B, Curtis N, Cotter PD, Hill C, Ross RP.** 2010. The ABC transporter AnrAB contributes to the innate resistance of *Listeria monocytogenes* to nisin, bacitracin, and various beta-lactam antibiotics. Antimicrob Agents Chemother **54:**4416–4423. http://dx.doi.org/10.1128/AAC.00503-10.
31. **Meehl M, Herbert S, Götz F, Cheung A.** 2007. Interaction of the GraRS two-component system with the VraFG ABC transporter to support vancomycin-intermediate resistance in *Staphylococcus aureus*. Antimicrob Agents Chemother **51:**2679–2689. http://dx.doi.org/10.1128/AAC.00209-07.
32. **Pietiäinen M, François P, Hyyryläinen H-L, Tangomo M, Sass V, Sahl H-G, Schrenzel J, Kontinen VP.** 2009. Transcriptome analysis of the responses of *Staphylococcus aureus* to antimicrobial peptides and characterization of the roles of *vraDE* and *vraSR* in antimicrobial resistance. BMC Genomics **10:**429. http://dx.doi.org/10.1186/1471-2164-10-429.
33. **Stülke J, Hanschke R, Hecker M.** 1993. Temporal activation of beta-glucanase synthesis in *Bacillus subtilis* is mediated by the GTP pool. J Gen Microbiol **139:**2041–2045. http://dx.doi.org/10.1099/00221287-139-9-2041.
34. **Ho SN, Hunt HD, Horton RM, Pullen JK, Pease LR.** 1989. Site-directed mutagenesis by overlap extension using the polymerase chain reaction. Gene **77:**51–59. http://dx.doi.org/10.1016/0378-1119(89)90358-2.
35. **Kallenberg F, Dintner S, Schmitz R, Gebhard S.** 2013. Identification of regions important for resistance and signalling within the antimicrobial peptide transporter BceAB of *Bacillus subtilis*. J Bacteriol **195:**3287–3297. http://dx.doi.org/10.1128/JB.00419-13.
36. **Wall ME, Markowitz DA, Rosner JL, Martin RG.** 2009. Model of transcriptional activation by MarA in *Escherichia coli*. PLoS Comput Biol **5:**e1000614. http://dx.doi.org/10.1371/journal.pcbi.1000614.

Supplement Fritz 2015:

Table S1. Fixed parameters used in the mathematical model.

Parameter	Notation	Value	Source
Binding constant for bacitracin – UPP interaction	$K_{d,BAC\text{-}UPP}$	1 μM	*In vitro* equilibrium dissociation constant for bacitracin A – C_{55}-isoprenyl-pyrophosphate interaction (Storm & Strominger, 1973)
Dissociation rate for bacitracin – UPP interaction	$k_{d,BAC\text{-}UPP}$	0.75 min^{-1}	Estimated from Fig. 2B in (Economou et al., 2013)
Association rate for bacitracin – UPP interaction	$k_{a,BAC\text{-}UPP}$	0.75 μM^{-1} min^{-1}	Adjusted to match $K_{d,BAC\text{-}UPP}$
Total number of UPP molecules per cell	UPP_{tot}	10^4 molecules/cell	We made the simplifying assumption that the maximal amount of UPP, UPP_{tot} , is given by the total sum over all intermediate forms of the lipid carrier molecule; Pool levels of uridine nucleotides range from 10^4-10^5 molecules per cell (Mengin-Lecreulx et al., 1982)
Fold-change of P_{bceAB} promoter	ω	5000	Suggested by data in Fig. 2B in the main text; within physiological range of 1-10^4 (see e.g. (Lutz & Bujard, 1997) for promoters with high dynamic range)
bceAB mRNA degradation rate	λ_{bceAB}	0.462 min^{-1}	Corresponds to a *bceAB* mRNA half-life of 1.5 min (this study; data not shown)
luxABCDE mRNA degradation rate	λ_{lux}	0.138 min^{-1}	Corresponds to a *lux* mRNA half-life of 5 min; upper limit for mRNA half-life inferred in (Radeck et al., 2013)
BceAB protein decay rate	δ□□□□□	0.01 min^{-1}	Corresponds to a cell doubling time of 70 min (this study)
LuxABCDE protein decay rate	δ□□□	0.023 min^{-1}	Corresponds to a protein half-life of 30 min
Translation rate	ν	10 proteins/mRNA/min	
Scaling factor between protein level and luminescence	σ	83 RLU/OD/protein	Arbitrary choice

Table S2. Estimated model parameters.

Parameter	Notation	LB[a]	UB[a]	Estimated Value	Comment
Maximal bacitracin transport rate via BceAB	v_{max}	1	10^4	(1.0±0.8) x 10^4 molecules/protein/min	Unknown parameter with wide range
Michaelis-Menten constant for bacitracin transport via BceAB	K_m	10^{-3}	10	(2.9±2.4) mM	Unknown parameter with wide range
Basal transcription rate of P_{bceAB} promoter	α	10^{-3}	1	(4.2±0.1) x 10^{-3} mRNA/min	Physiological range (see e.g. (Fritz et al., 2014))
P_{bceAB} activation threshold	κ	10^{-4}	1	(0.3±4.1) x 10^{-3}	Relative bacitracin flux per transporter at which P_{bceAB} promoter is activated
Hill coefficient	n	1	10	7.5±0.2	Effective parameter with wide range

[a]LB, UB: lower and upper boundary, respectively, for constrained optimization of parameters

Table S3. Plasmids, strains and primers used in this study

Name	Description[a]	Source[b]
Plasmids		
pAH328	Vector for transcriptional promoter fusions to *luxABCDE* (luciferase); integrates in *B. subtilis sacA*; Amp^r, Cm^r	(Schmalisch et al., 2010)
pBS2E	Empty vector; integrates in *B. subtilis lacA*; Amp^r, Mls^r	(Radeck et al., 2013)
pBS1C	Empty vector; integrates in *B. subtilis amyE*; Amp^r, Cm^r	(Radeck et al., 2013)
pSB1A3	Empty *E. coli* vector, MCS features *rfp* cassette; Amp^r	RSBP
pNTSB103	pSB1A3 harboring *B. subtilis bceAB* adapted to the BioBrick RFC25 cloning standard	This study
pNTSB101	pSB1A3 harboring *bceS* adapted to the BioBrick RFC25 cloning standard, using same strategy as for pNTSB103	This study
pNTSB104	pSB1A3 harboring P_{xylA} from pXT (Derré et al., 2000) adapted to the BioBrick RFC10 cloning standard	This study
pNT2E01	pBS2E harboring P_{xylA}-*bceAB* assembled according to the BioBrick RFC10 cloning standard	This study
pSDlux101	pAH328 harboring a transcriptional P_{bceA}-*luxABCDE* fusion	(Kallenberg et al., 2013)
pNT2E07	pBS2E harboring P_{xylA}-*bceS* assembled according to the BioBrick RFC10 cloning standard	This study
pJR1C02	pBS1C harboring P_{bceR}-*bceAB* assembled according to the BioBrick RFC10 cloning standard	This study
E. coli strains		
XL1-Blue	*recA1 endA1 gyrA96 thi-1 hsdR17 supE44 relA1 lac F'*::Tn*10 proAB lacI*^{q} Δ(*lacZ*)M15]	Stratagene
B. subtilis strains		
W168	Wild-type, *trpC2*	Laboratory stock
SGB073	W168 *sacA*::pSDlux101	This study
SGB218	W168 *bceAB*::kan *sacA*::pSDlux101 *lacA*::pNT2E01	This study
TMB035	W168 *bceAB*::kan; Kan^r	(Rietkötter et al., 2008)
TMB1461	W168 Δ*bceRSAB*	This study
TMB3095	W168 Δ*bceRSAB amyE*::pJR1C02 lacA::pNT2E07	This study
TMB3097	W168 Δ*bceRSAB amyE*::pJR1C02	This study
Primer sequences (5'-3' direction)		
TM2577	GATCGAATTCGCGGCCGCTTCTAGA***AAGGAGG***TGGCCGGC**A TG**GTGATTTTAGAAGCGAA	This study
TM2578	GATCACTAGTA*TTA*ACCGGTCAACGACGATTTAATGACC	This study
iGEM134	GATCGAATTCGCGGCCGCTTCTAGAGAAGGCCAAAAAACTGC TGCC	This study
iGEM135	GATCACTAGTATTCGATAAGCTTGGGATCCC	This study

[a]Amp^r, ampicillin resistance; Cm^r, chloramphenicol resistance; Kan^r, kanamycin resistance; Mls^r, erythromycin-induced resistance to macrolide, lincosamide and streptogramin B antibiotics (MLS). Restriction sites in primer sequences are underlined; start codons are in bold; stop codons in italics; the optimal Shine-Dalgarno sequence in bold italics.

[b]RSBP, Registry of Standard Biological parts (http://partsregistry.org)

Figure S1

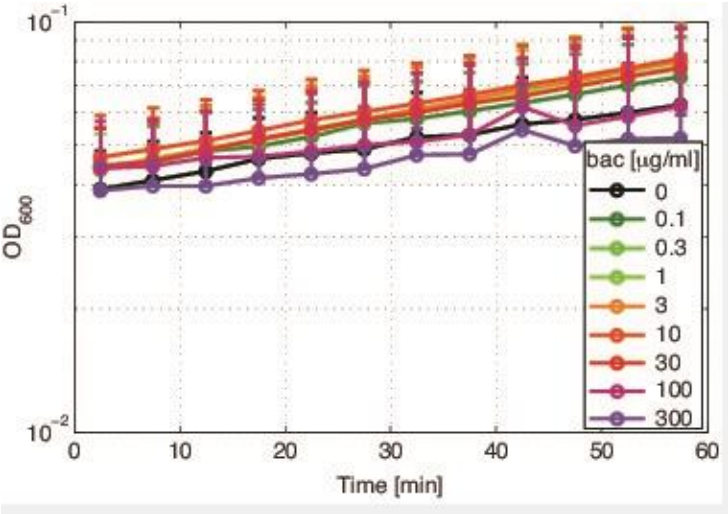

Figure S2:

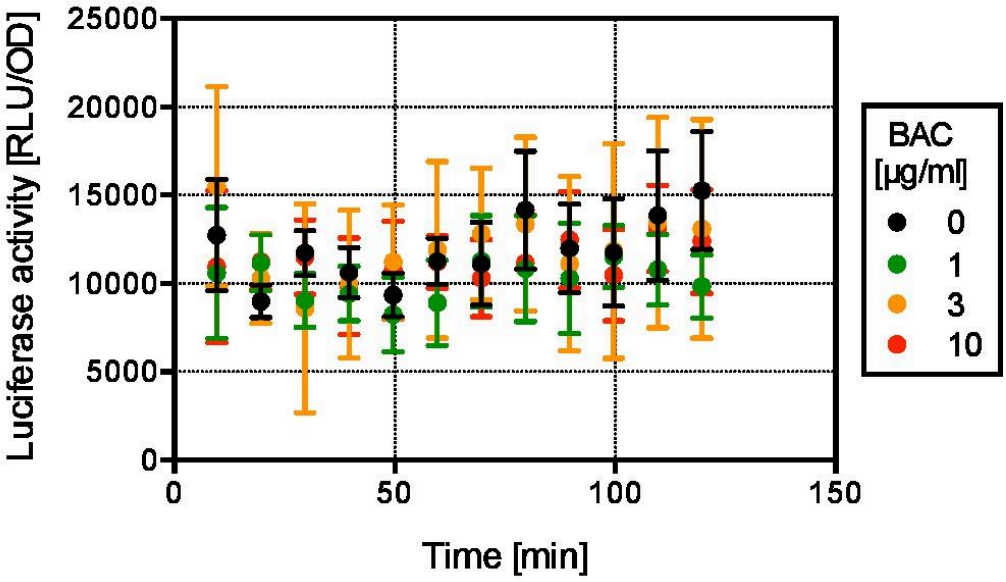

Figure S3:

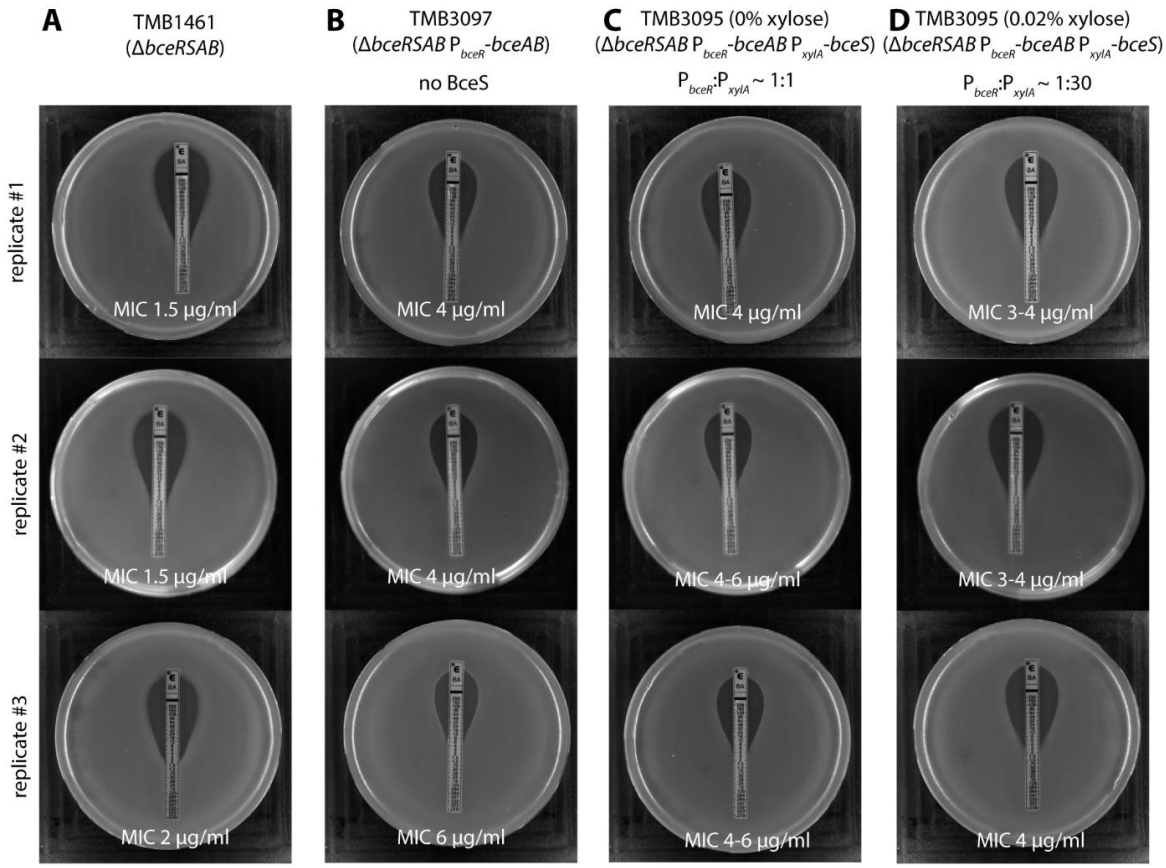
A
TMB1461
(ΔbceRSAB)
B
TMB3097
(ΔbceRSAB P bceR -bceAB)
no BceS
C
TMB3095 (0% xylose)
(ΔbceRSAB P bceR -bceAB P xylA -bceS)
P bceR :P xylA ~ 1:1
D
TMB3095 (0.02% xylose)
(ΔbceRSAB P bceR -bceAB P xylA -bceS)
P bceR :P xylA ~ 1:30
replicate #1
replicate #2
replicate #3
MIC 1.5 µg/ml
MIC 4 µg/ml
MIC 4 µg/ml
MIC 3-4 µg/ml
MIC 1.5 µg/ml
MIC 4 µg/ml
MIC 4-6 µg/ml
MIC 3-4 µg/ml
MIC 2 µg/ml
MIC 6 µg/ml
MIC 4-6 µg/ml
MIC 4 µg/ml

Figure S4:

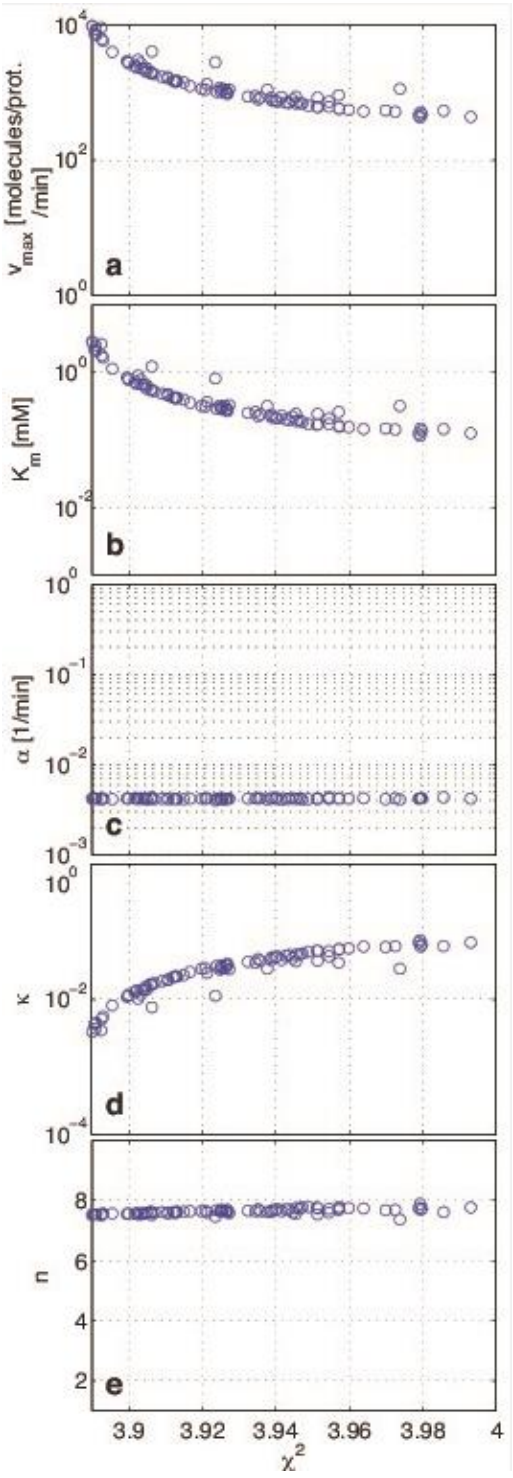
v_{max} [molecules/prot. /min]
10^4
10^2
10^0
a
K_m [mM]
10^0
10^{-2}
b
α [1/min]
10^0
10^{-1}
10^{-2}
10^{-3}
c
κ
10^0
10^{-2}
10^{-4}
d
n
8
6
4
2
e
3.9
3.92
3.94
3.96
3.98
4
χ^2

Figure S5:

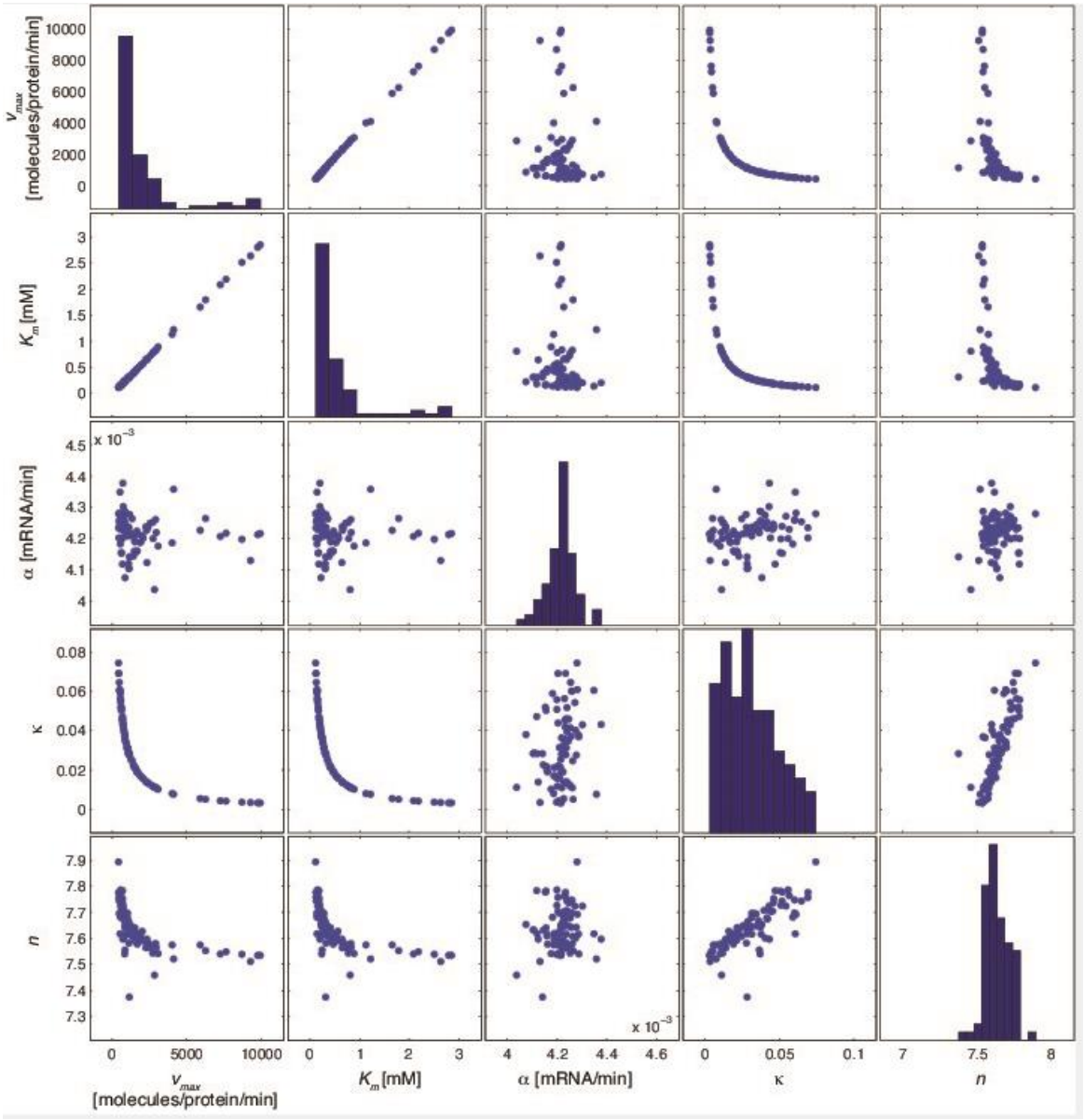
v_{max} [molecules/protein/min]
K_m [mM]
α [mRNA/min]
κ
n
x 10^-3
0 5000 10000
0 1 2 3
4 4.2 4.4 4.6
0 0.05 0.1
7 7.5 8

SUPPORTING REFERENCES

Fritz G et al. (2014) Single cell kinetics of phenotypic switching in the arabinose utilization system of *E. coli*. *PLoS ONE* 9:e89532.

Radeck J et al. (2013) The *Bacillus* BioBrick Box: generation and evaluation of essential genetic building blocks for standardized work with *Bacillus subtilis*. *J Biol Eng* 7:29.

Schmalisch M et al. (2010) Small genes under sporulation control in the *Bacillus subtilis* genome. *J Bacteriol* 192:5402–5412.

Derré I, Rapoport G, Msadek T (2000) The CtsR regulator of stress response is active as a dimer and specifically degraded *in vivo* at 37 degrees C. *Mol Microbiol* 38:335–347.

Kallenberg F, Dintner S, Schmitz R, Gebhard S (2013) Identification of regions important for resistance and signalling within the antimicrobial peptide transporter BceAB of *Bacillus subtilis*. *J Bacteriol* 195:3287–3297.

Rietkötter E, Hoyer D, Mascher T (2008) Bacitracin sensing in *Bacillus subtilis*. *Mol Microbiol* 68:768–785.

Storm DR, Strominger JL (1973) Complex formation between bacitracin peptides and isoprenyl pyrophosphates. The specificity of lipid-peptide interactions. *J Biol Chem* 248:3940–3945.

Economou NJ, Cocklin S, Loll PJ (2013) High-resolution crystal structure reveals molecular details of target recognition by bacitracin. *Proc Natl Acad Sci USA* 110:14207–14212.

Mengin-Lecreulx D, Flouret B, van Heijenoort J (1982) Cytoplasmic steps of peptidoglycan synthesis in *Escherichia coli*. *J Bacteriol* 151:1109–1117.

Lutz R, Bujard H (1997) Independent and tight regulation of transcriptional units in *Escherichia coli* via the LacR/O, the TetR/O and AraC/I1-I2 regulatory elements. *Nucl Acids Res* 25:1203–1210.

Radeck J et al. (2013) The *Bacillus* BioBrick Box: generation and evaluation of essential genetic building blocks for standardized work with *Bacillus subtilis*. *J Biol Eng* 7:29.

7.2 PUBLICATION II: ANATOMY OF THE BACITRACIN RESISTANCE NETWORK IN *BACILLUS SUBTILIS*

Publication II:

Radeck J, Gebhard S, Orchard P, Kirchner M, Bauer S, Mascher T, Fritz G (2016) Anatomy of the bacitracin resistance network in *Bacillus subtilis*. **Mol Micro**.100(4):607-20. doi: 10.1111/mmi.13336

Molecular Microbiology (2016) 100(4), 607–620 ■
doi:10.1111/mmi.13336
First published online 10 March 2016

Anatomy of the bacitracin resistance network in *Bacillus subtilis*

Jara Radeck,[1,2] Susanne Gebhard,[3] Peter Shevlin Orchard,[2] Marion Kirchner,[2†] Stephanie Bauer,[2] Thorsten Mascher[1*] and Georg Fritz[4]

[1] *Technische Universität Dresden, Institute of Microbiology, Dresden, Germany.*
[2] *Ludwig-Maximilians-Universität München, Department Biology I, München, Germany.*
[3] *University of Bath, Department of Biology and Biochemistry, Milner Centre for Evolution, Bath, United Kingdom.*
[4] *Philipps-Universität Marburg, LOEWE-Center for Synthetic Microbiology (SYNMIKRO), Marburg, Germany.*

Summary

Protection against antimicrobial peptides (AMPs) often involves the parallel production of multiple, well-characterized resistance determinants. So far, little is known about how these resistance modules interact and how they jointly protect the cell. Here, we studied the interdependence between different layers of the envelope stress response of *Bacillus subtilis* when challenged with the lipid II cycle-inhibiting AMP bacitracin. The underlying regulatory network orchestrates the production of the ABC transporter BceAB, the UPP phosphatase BcrC and the phage-shock proteins LialH. Our systems-level analysis reveals a clear hierarchy, allowing us to discriminate between primary (BceAB) and secondary (BcrC and LialH) layers of bacitracin resistance. Deleting the primary layer provokes an enhanced induction of the secondary layer to partially compensate for this loss. This study reveals a direct role of LialH in bacitracin resistance, provides novel insights into the feedback regulation of the Lia system, and demonstrates a pivotal role of BcrC in maintaining cell wall homeostasis. The compensatory regulation within the bacitracin network can also explain how gene expression noise propagates between resistance layers. We suggest that this active redundancy in the bacitracin resistance network of *B. subtilis* is a general principle to be found in many bacterial antibiotic resistance networks.

Accepted 24 January, 2016. *For correspondence E-mail thorsten.mascher@tu-dresden.de; Tel. (+49) 351 463–40420; Fax (+49) 351 463–37715. †Present address: Technische Universität München, Department of Chemistry, Garching, Germany.

Introduction

In their natural environment many microbes are in fierce competition for a limited supply of resources. This frequently involves the production of antimicrobial peptides (AMPs) that suppress the proliferation of competitors (Eijsink *et al.*, 2002). In this biochemical warfare, the cell envelope serves as a prime target, and many AMPs interfere with its biosynthesis and integrity (Breukink and de Kruijff, 2006). To defend against antimicrobial attacks by rival species, it is thus of vital importance for cells to accurately sense these cues and to swiftly mount protective countermeasures, collectively referred to as cell envelope stress response (CESR) (Jordan *et al.*, 2008; Schrecke *et al.*, 2012). In many bacteria the defense against AMPs involves the simultaneous expression of a number of resistance systems that protect cells at various levels. Those include on the one hand specific resistance determinants, such as ABC transporters (Gebhard, 2012) and immunity lipoproteins (Stein *et al.*, 2003; Aso *et al.*, 2005) that transport and/or sequester AMPs from their molecular targets. On the other hand, bacteria induce the production of more nonspecific resistance determinants that alter the charge and composition of the cell envelope to reduce access of AMPs to their sites of action (Revilla-Guarinos *et al.*, 2014) and allow cells to cope with deleterious effects on downstream cell physiology (Joly *et al.*, 2010). While many of the AMP resistance modules have been individually characterized in great detail, our present knowledge about how these modules interact, and how they jointly contribute to the overall AMP resistance of a cell, is still limited. Thus, as for many other bacterial stress responses, the daunting task is to decipher how the cell

orchestrates the activity of individual resistance modules into a complex and multi-layered CESR network.

In the present work we approached this question by focusing on the resistance mechanisms of *Bacillus subtilis* against the peptide antibiotic bacitracin, which is produced by some strains of *Bacillus licheniformis* and *B. subtilis* (Azevedo *et al*., 1993; Ishihara *et al*., 2002) and is clinically used as broad spectrum antibiotic against Gram-positive bacteria causing skin infections. Bacitracin acts by inhibiting the lipid II cycle of cell wall biosynthesis, which is essential for the translocation of peptidoglycan precursors from the cytosol to the extracytoplasmic space (Fig. 1A). The tight complex formation between bacitracin and the diphosphate lipid carrier undecaprenyl pyrophosphate (UPP) prevents dephosphorylation of UPP to undecaprenyl phosphate (UP) and thereby efficiently blocks recycling of the lipid carrier (Storm and Strominger, 1973; Economou *et al*., 2013).

To perpetuate progression of the lipid II cycle under bacitracin attack and to protect against cell envelope damage, *B. subtilis* up-regulates the expression of three major resistance modules (Mascher *et al*., 2003; Rietkötter *et al*., 2008): The ABC transporter BceAB (Ohki *et al*., 2003; Mascher *et al*., 2003), the UPP phosphatase BcrC (Cao and Helmann, 2002; Ohki *et al*., 2003; Bernard *et al*., 2005) and the phage shock protein (Psp)-like LiaI and LiaH proteins (Mascher *et al*., 2004; Jordan *et al*., 2006) (Fig. 1A and B). Recent evidence suggests that BceAB confers resistance by clearing UPP from the inhibitory grip of bacitracin (Fritz *et al*., 2015), but it remains elusive whether bacitracin is transported into the cytoplasm for degradation or whether it is released into the extracytoplasmic space, as suggested previously (Ohki *et al*., 2003; Rietkötter *et al*., 2008). Simultaneously, the phosphatase BcrC catalyzes the dephosphorylation of UPP to UP (Fig. 1A) and thereby promotes the progression of the Lipid II cycle. Finally, under cell-envelope perturbing conditions the *liaIH* operon is induced, and the small membrane anchor protein LiaI recruits the cytosolic PspA/IM30 protein family member LiaH into static, membrane-associated patches (Domínguez-Escobar *et al*., 2014). While the homologous Psp system encoded by the *pspABCDE* operon of *Escherichia coli* has been linked to maintenance of the proton motive force under envelope-perturbing conditions (Kleerebezem *et al*., 1996; Kobayashi *et al*., 2007), the physiological role of the Lia system in *B. subtilis* remained elusive: despite its more than ~100-fold induction under bacitracin stress, no increase in bacitracin sensitivity was detected in a *liaIH* deletion strain (Wolf *et al*., 2010). While this might suggest that there is no contribution of the Lia system to bacitracin resistance, we reasoned that the presence of the two other bacitracin resistance layers, BceAB and BcrC, could potentially compensate for the lack of LiaIH. However, to date it is not known whether these systems act in fact redundantly, or whether they contribute independently or even cooperatively to bacitracin resistance.

To gain deeper insight into how these modules interact and form an efficient bacitracin stress response network, we here systematically studied their functional and regulatory interactions in a comprehensive set of mutants deficient in the three resistance determinants. Our analysis reveals a hierarchy among resistance modules, which we find reflected in marked anti-correlations between the expression of primary (drug-sensing) and secondary (mostly damage-sensing) layers of bacitracin resistance. This means that the increased expression of the primary resistance layer reduced the expression of the secondary layer and *vice versa*. Strikingly, these anti-correlations can also explain how gene expression noise propagates between the different resistance modules at the single cell level, as revealed by flow cytometry analyses. Moreover, our study underpins the importance of the UPP phosphatase BcrC for cell wall homeostasis in the absence of bacitracin stress and provides novel clues about the physiological stimuli triggering the induction of the modules in the bacitracin resistance network.

Results

Contributions of CESR modules to antibiotic resistance

First, we studied whether the three CESR modules protect the cell in a redundant, independent or even in a cooperative manner. To this end we constructed mutants deficient in one, two or in all three resistance determinants and determined their sensitivity towards bacitracin using the E-test® agar gradient diffusion method (Fig. 2A). Compared to the minimal inhibitory concentration (MIC) of bacitracin for wild type cells (256 μg ml^{-1}), mutants deficient in only one of the resistance modules displayed a clear hierarchy in their sensitivity towards bacitracin: While the MIC of the Δ*liaIH* mutant was identical to that of the wild type, the Δ*bcrC* mutant displayed a 5-fold and the Δ*bceAB* mutant an 85-fold increase in bacitracin susceptibility, suggesting that BceAB acts as the primary resistance determinant under these growth conditions. Interestingly, in a mutant background devoid of *bceAB*, the additional deletion of either of the other two resistance modules had a significantly stronger impact on the MIC than observed in the single mutants. Here, the Δ*bceAB* Δ*liaIH* double mutant had a 6-fold lower MIC than the Δ*bceAB* mutant, thereby revealing the first phenotype of LiaIH in the bacitracin stress

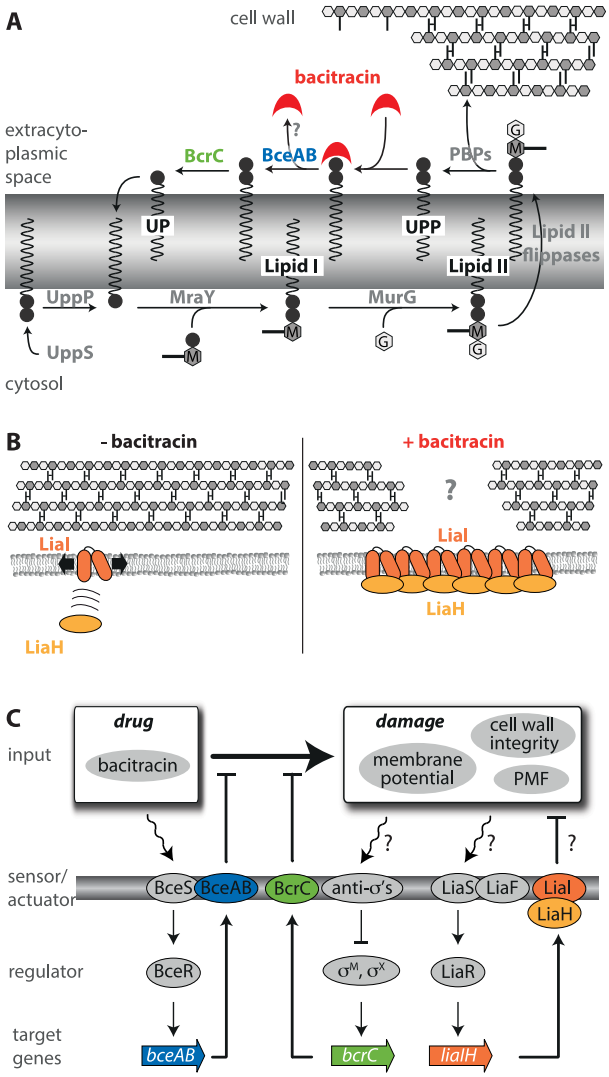

Fig. 1. Schematic overview of bacitracin resistance determinants and their regulation in *B. subtilis*.
A. In the absence of bacitracin, the membrane-associated steps of cell wall biosynthesis in *B. subtilis* involve the cytosolic attachment of peptidoglycan precursors to the lipid carrier undecaprenyl-phosphate (UP) via MraY and MurG, followed by transport of the resulting lipid II molecule to the extracytoplasmic leaflet of the cytoplasmic membrane via at least two redundant flippases MraY and Amj. After incorporating peptidoglycan precursors into the cell wall by penicillin binding proteins (PBPs), the remaining phosphorylated form of the lipid carrier, undecaprenyl-pyrophosphate (UPP), is converted to UP via the phosphatase BcrC, before it can enter the next transport cycle. Bacitracin blocks this essential lipid II cycle by tightly binding to UPP and thereby preventing the recycling of the lipid carrier. Bacitracin resistance is conferred by the increased production of the ABC-transporter BceAB, which removes bacitracin from UPP by a so far unknown transport mechanism, and the increased production of BcrC, which allows the lipid II cycle to progress in the presence of bacitracin.
B. The third player in the bacitracin stress response network is the phage-shock protein-like Lia response. Upon bacitracin challenge, the small membrane anchor LiaI recruits the cytosolic PspA/IM30 protein family member LiaH into membrane-associated patches of unknown physiological function. Potentially, these structures stabilize the membrane underneath damaged areas of the cell wall.
C. Regulation scheme of the bacitracin stress response network in *B. subtilis*. Expression of *bceAB* is activated via a flux-sensing mechanism, monitoring the detoxification flux of the ABC transporter BceAB via complex formation between BceAB and the histidine kinase BceS (Dintner *et al.*, 2014; Fritz *et al.*, 2015), which in turn activates transcription via phosphorylation of the response regulator BceR. Expression of *bcrC* is regulated by the ECF σ-factors σ^M and σ^X and their cognate anti σ-factors, which together are considered to be sensors for cell wall integrity (Inoue *et al.*, 2013; Lee and Helmann, 2013). Likewise, expression of *liaIH* is regulated by the LiaFSR three-component system (Jordan *et al.*, 2006; Mascher, 2006; Schrecke *et al.*, 2013), which has also been shown to be a sensor of cell envelope damage (Wolf *et al.*, 2012).

 Molecular Microbiology, **100**, 607–620

response. Hence, we suggest that the previously reported lack of a Δ*liaIH* phenotype upon bacitracin stress (Rietkötter *et al.*, 2008) might be explained by a redundant organization of the bacitracin stress response network, in which resistance conferred by BceAB masks the weaker contribution of the LiaIH module. Moreover, the Δ*bceAB* Δ*bcrC* double mutant was 24-fold more sensitive than the Δ*bceAB* reference strain, suggesting that BceAB also partially masks the contribution of BcrC. Please note that we did not observe a similar "masking effect" between the secondary resistance modules, as the MIC of a Δ*bcrC* mutant (48 μg ml^{-1}) was identical to that of a Δ*bcrC* Δ*liaIH* mutant (Fig. 2A). Only when compared to a Δ*bceAB* Δ*bcrC* double mutant, we found that a Δ*bceAB* Δ*bcrC* Δ*liaIH* triple mutant showed an ~3-fold increased bacitracin sensitivity (Fig. 2A). In summary, these results show that the secondary resistance modules do in fact protect the cell against bacitracin, but also reveal that the contributions of the secondary resistance modules are masked by the much stronger resistance conferred by the Bce system.

Next, we asked whether the increased bacitracin susceptibility of the mutants above was in fact due to the lack of the respective resistance modules, or whether those mutants exhibited a general growth defect that might result in increased bacitracin susceptibility. For instance, it is known that the BcrC phosphatase is also involved in Lipid II cycle progression under normal growth conditions (Bernard *et al.*, 2005), but the extent to which the cytosolic UPP phosphatase UppP (formerly YubB) could compensate for the deletion of BcrC was controversial (Cao and Helmann, 2002; Bernard *et al.*, 2005). To quantitatively test the fitness of the different mutants, we measured their doubling times in LB medium at 37°C in a microplate reader (Fig. 2B). In the absence of bacitracin, the wild type and Δ*liaIH* mutant grew at similar doubling times of $t_d = 23.0 \pm 2.2$ min, and $t_d = 24.7 \pm 2.1$ min, respectively, while the Δ*bceAB* mutant grew slightly faster ($t_d = 20.0 \pm 0.3$ min) and the Δ*bcrC* mutant significantly slower ($t_d = 28.7 \pm 1.7$ min) than wild type (P value of unpaired Student's *t*-test = 0.024). Moreover, we observed that under these conditions of rapid growth, the Δ*bcrC* mutant was about as sensitive as the Δ*bceAB* mutant, which displayed killing at 10 μg ml^{-1} bacitracin and higher (Fig. 2B). This suggests that at high growth rates the deletion of *bcrC* can only be partially compensated for by the activity of the second UPP phosphatase UppP, implying that UPP dephosphorylation might become the bottleneck for cell wall biosynthesis and hence for cell growth. Thus, we conclude that the increased bacitracin sensitivity of the Δ*bcrC* mutant can—at least partially—be attributed to a general growth defect incurred by reduced rates of UPP dephosphorylation.

Regulatory interactions between the CESR modules

The redundant contributions of the CESR modules to bacitracin resistance described above provoked the question of the extent to which deletion of one resistance module would affect the expression of the other resistance modules. To study these regulatory interactions, we fused the target promoter of each module to the *luxABCDE* cassette derived from *Photorhabdus luminescens* (Schmalisch *et al.*, 2010; Radeck *et al.*, 2013) and integrated the resulting reporter plasmids into the chromosome of wild type and mutants deficient in one of the three resistance modules (Supporting Information Table S1). Subsequently, exponentially growing cultures ($OD_{600} \approx 0.1$) were challenged with different bacitracin concentrations and the dose-dependent luciferase activity (one hour post-addition) was recorded as a proxy for promoter activity (Fig. 3).

Quantitative behavior of the unperturbed CESR network

In the wild type strain (Fig. 3, *black data*), P_{bceA} (Fig. 3A) displayed low activity (10^4 RLU/OD) in the absence of bacitracin and responded already at low bacitracin concentrations of ≥0.01 μg ml^{-1}. This response gradually increased with rising bacitracin levels and reached its maximum about 300-fold over background at 30 μg ml^{-1} bacitracin. Recently, we showed that this gradual response over a high input-dynamic range is the result of negative feedback regulation in the Bce system, in which a flux-sensing mechanism homeostatically adjusts the rate of *de novo* transporter synthesis to the level needed for cell protection (Fritz *et al.*, 2015). In contrast to P_{bceA}, P_{bcrC} (Fig. 3B) already had a high basal activity (7×10^5 RLU/OD) and only responded at much higher bacitracin concentrations (1 μg ml^{-1}) with a maximum 3-fold induction over background at 30 μg ml^{-1}. The strong P_{bcrC} activity in the absence of antibiotic treatment is consistent with the notion that BcrC is an important player in lipid II cycle progression under exponential growth conditions, as noted above. Similar to P_{bceA}, P_{lial} (Fig. 3C) displayed a low basal activity and a strong (400-fold) induction at high bacitracin levels, but its input-dynamic range was much narrower (0.1 to 10 μg ml^{-1} bacitracin) than seen for P_{bceA} (0.01 to 30 μg ml^{-1} bacitracin). Hence, production of the primary resistance determinant BceAB is induced already at lower antibiotic concentrations than expression of the secondary resistance modules. This suggests that the primary layer might "buffer" against cell envelope stress at low bacitracin levels, while the demand for further protective measures only occurs at higher antibiotic concentrations.

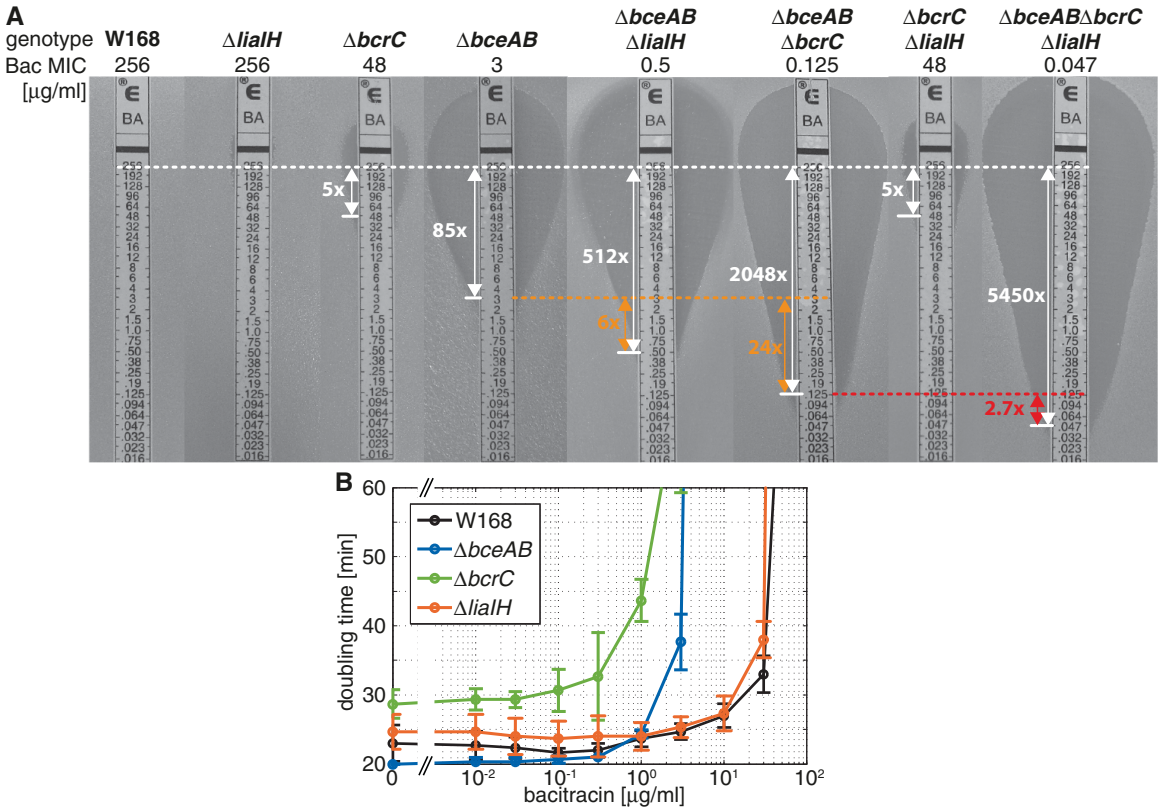

Fig. 2. Contributions of CESR modules to bacitracin resistance.
A. MIC of indicated *B. subtilis* strains as determined by the E-test® agar gradient diffusion method on Müller-Hinton medium. Strains tested were W168, TMB35 (Δ*bceAB*), TMB297 (Δ*bcrC*), TMB1151 (Δ*lialH*), TMB713 (Δ*bceAB* Δ*bcrC*), TMB2127 (Δ*bceAB* Δ*lialH*), TMB2128 (Δ*bcrC* Δ*lialH*) and TMB1829 (Δ*bceAB* Δ*bcrC* Δ*lialH*). Pictures are representative for three biological replicates with a maximal sample deviation of one concentration step; arrows indicate the fold-change of sensitivity.
B. Doubling times of exponentially growing cells one hour after treatment with indicated bacitracin concentration. Graphs show data for single mutant strains containing the *lux*-reporter, see caption of Fig. 3. Standard deviation was obtained from at least nine biological replicates.

BceAB is the pacemaker of the CESR network

If this buffering hypothesis was accurate, the secondary layer should become more sensitive and also more active in the absence of the primary resistance. Indeed, we found that in a Δ*bceAB* mutant the P_{bcrC} and P_{lialH} promoters were activated already at lower bacitracin concentrations and displayed a steeper dose-response behavior than in the wild type (Fig. 3B and C, *blue data*). Note that the activity of P_{bceA} itself remained at a basal level in the Δ*bceAB* mutant (Fig. 3A), again highlighting that the transport activity of BceAB is strictly required for activation of the P_{bceA} promoter (Rietkötter *et al.*, 2008; Fritz *et al.*, 2015). To further corroborate the buffering hypothesis, we next tested the effect of different constitutive BceAB levels on the expression of the secondary resistance layer. To this end, we complemented the Δ*bceAB* mutant with a xylose-inducible copy of *bceAB*. Strikingly, compared to the highly sensitive P_{lial} response in the Δ*bceAB* mutant (Fig. 4A (ii); *red data*), constitutive expression of *bceAB* at low levels was already sufficient to shift the induction threshold of the P_{lial} promoter to 3-fold higher bacitracin levels [Fig. 4A (ii); *orange data*]. A high constitutive expression level of *bceAB* resulted in a further 10-fold increase of the P_{lial} induction threshold [Fig. 4A (ii); *light green data*], which could be even further increased by overexpression of *bceAB* in the wild type [Fig. 4A (ii); *dark green data*]. Importantly, varying the *bceAB* expression level caused similar shifts in the induction threshold of the P_{bcrC} promoter (Supporting Information Fig. S1). Hence these data show that whenever the production level of BceAB is high, the expression of the two secondary resistance modules is low and *vice versa*. These clear-cut anti-correlations suggest that the ABC transporter actively prevents cell envelope stress and thereby

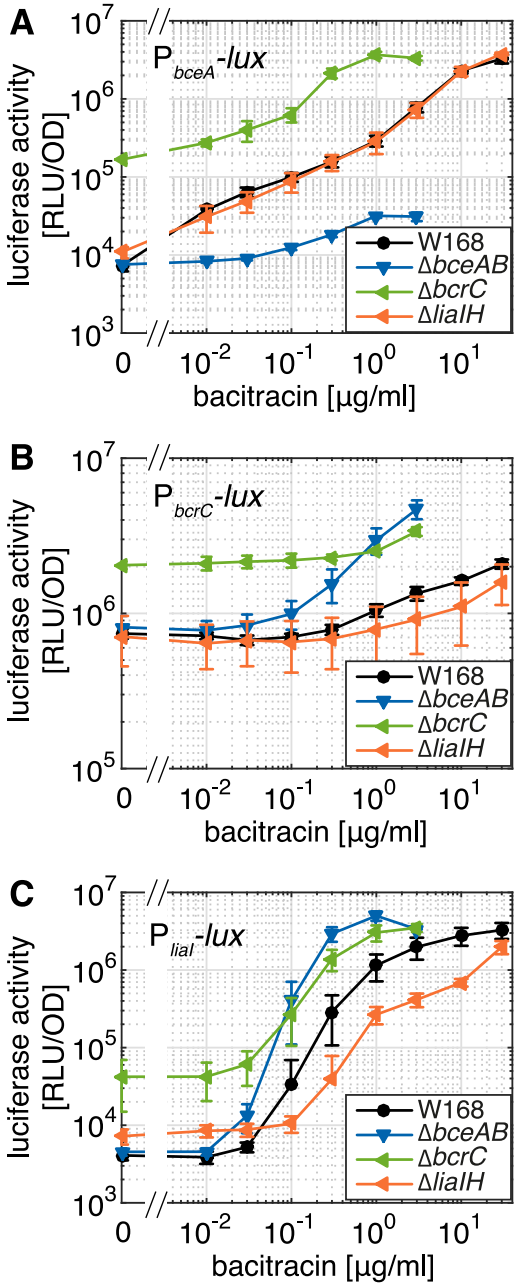

Fig. 3. Dose-dependent activation of resistance modules in perturbed and unperturbed CESR networks. Target promoter activities of (A) P_{bce}-*lux*, (B) P_{bcrC}-*lux* and (C) P_{liaI}-*lux* in strains carrying indicated deletions of CESR modules, as given by specific luciferase activity (RLU/OD_{600}) one hour after addition of indicated amounts of bacitracin. Measurements were performed during exponential growth phase in LB medium at 37°C in a microtiter plate reader. Data are shown for strains TMB1619, TMB1620, TMB1617 (W168); TMB1623, TMB1624, TMB1621 (Δ*bceAB*); TMB1627, TMB1628, TMB1625 (Δ*bcrC*) and TMB1661, TMB1662, TMB1659 (Δ*liaIH*) containing P_{bceA}-*lux*, P_{bcrC}-*lux* or P_{liaI}-*lux*, respectively, see Supporting Information Table S1. Data points and error bars indicate means and standard deviations derived from at least three biological replicates.

reduces the demand for expression of the secondary layers of the CESR network.

Note that the variation of the *bceAB* expression levels also triggered shifts in the response of the P_{bceA} promoter itself [Fig. 4A (i)]. Previously, we showed that this behavior can be rationalized by a flux-sensing mechanism, in which a sensory complex between the ABC transporter BceAB and the histidine kinase BceS detects the rate of bacitracin flux by individual transporters, which in turn activates the P_{bceA} promoter via the response regulator BceR (Fritz *et al.*, 2015). Accordingly, in cells with low BceAB levels the load per transporter saturates already at low bacitracin levels and triggers full induction of P_{bceA} [Fig. 4A (i); *orange curve*]. Conversely, in cells with higher BceAB levels the load per transporter saturates at significantly higher bacitracin levels, which in turn leads to proportional shifts of the P_{bceA} dose-response characteristic to the right [Fig. 4A (i); *green curves*] (Fritz *et al.*, 2015).

BcrC has pleiotropic effects on CESR modules

The deletion of *bcrC* triggered a 2- to 3-fold increased activity of its own promoter, P_{bcrC}, compared to the wild type (Fig. 3B, *green data*)—even in the absence of bacitracin stress. Given that the deletion of *bcrC* slowed down growth by impairing cell wall biosynthesis (Fig. 2B), the elevated P_{bcrC} activity seemed reasonable, because this promoter belongs to the regulon of the alternative sigma factor σ^M (Cao and Helmann, 2002). σ^M itself responds to a broad spectrum of cell envelope-perturbing agents (Eiamphungporn and Helmann, 2008) and was therefore considered to be a sensor for cell wall integrity (Inoue *et al.*, 2013; Lee and Helmann, 2013). Likewise, the P_{liaI} promoter activity was elevated 3-fold in the Δ*bcrC* mutant (Fig. 3C), consistent with the role of the Lia system as a general sensor of cell envelope stress (Wolf *et al.*, 2012). However, it was surprising that the P_{bceA} promoter was also up-regulated 10-fold in the Δ*bcrC* mutant (Fig. 3A), since previous reports were consistent with a model in which the Bce system responds to the detoxification flux of the *drug* and not to downstream *damage* on cell physiology (cf. Fig. 1C). This curious effect is discussed in more detail below.

To further substantiate that the observed phenotypes specifically arose from the deletion of *bcrC*, we complemented the Δ*bcrC* mutant with a xylose-inducible copy of *bcrC*. This complementation indeed returned the elevated activities of P_{bceA} and P_{liaI} back to wild-type levels (Fig. 4B; *light green data*). Interestingly, the overexpression of *bcrC* in a wild type background lead to a further decrease of both the P_{liaI} and P_{bceA} activities (Fig. 4B; *dark green data*), suggesting that an elevated rate of UPP dephosphorylation reduced the cellular susceptibility to bacitracin.

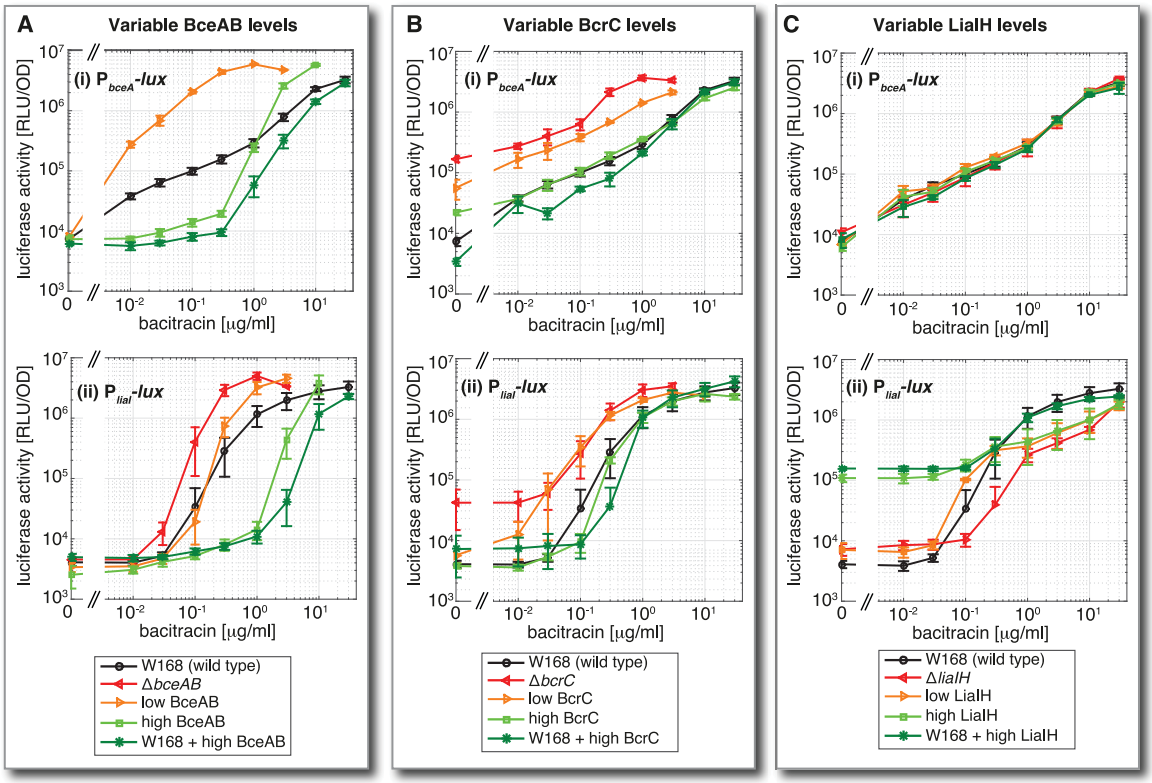

Fig. 4. Regulatory crosstalk between primary and secondary resistance modules. Target promoter activities of P_{bceA}-*lux* and P_{liaI}-*lux* in strains expressing different levels of (A) BceAB, (B) BcrC and (C) LiaIH, as given by specific luciferase activity (RLU/OD_{600}) one hour after addition of indicated amounts of bacitracin. Measurements were performed as described in Fig. 3. Colors code for different expression levels of resistance module *X* (*X* = *bceAB*, *bcrC* or *liaIH*), as driven by the xylose-inducible promoter P_{xylA}: (*red*) No expression, via deletion of module *X*; (*orange*) Low constitutive expression, via complementation of the deletion mutant with P_{xylA}-*X* in the absence of xylose; (*light green*) High constitutive expression, via complementation of the deletion mutant with P_{xylA}-*X* in the presence of 0.2% xylose; (*dark green*) Overexpression in W168 wild type background, via expression of P_{xylA}-*X* in the presence of 0.2% xylose. The corresponding strains are A. TMB1619, TMB1623, TMB2590, TMB2594 (P_{bceA}-*lux*) and TMB1617, TMB1621, TMB2589, TMB2593 (P_{liaI}-*lux*) (B) TMB1619, TMB1627, TMB2592, TMB2430 (P_{bceA}-*lux*) and TMB1617, TMB1625, TMB2591, TMB2429 (P_{liaI}-*lux*) (C) TMB1619, TMB1661, TMB2693, TMB2691 (P_{bceA}-*lux*) and TMB1617, TMB1659, TMB2692, TMB2690 (P_{liaI}-*lux*), as listed in Supporting Information Table S1. Error bars indicate the standard deviation between at least three biological replicates.

Taken together, these data show that the level of BcrC sets the rate of UPP dephosphorylation, which in turn determines how many UPP target molecules the cell displays for binding by bacitracin. Accordingly, low levels of BcrC lead to the accumulation of UPP and make cells vulnerable to bacitracin attack, whereas high BcrC levels keep UPP levels low and make cells more resistant. This pattern is reflected both in the responses of the Lia and BcrC systems, which measure bacitracin-dependent damage of the cell envelope, as well as in the response of the Bce system, which presumably senses the UPP-bound form of bacitracin (see Discussion for more details).

LiaIH plays a positive autoregulatory role

In contrast to the marked effects the deletions of *bceAB* and *bcrC* had on the expression of all resistance modules, the deletion of *liaIH* (Fig. 3, *orange data*) did not significantly influence the regulation of P_{bceA} and P_{bcrC} (Fig. 3A and B). However, the Δ*liaIH* mutant displayed up to 7-fold reduced activity of its own promoter (Fig. 3C). This is the first report showing that the expression of the *lia* operon is not only regulated via the LiaFSR three-component system (Schrecke *et al.*, 2013), but that also the target proteins LiaIH play a positive autoregulatory role required for the full Lia response. In fact, when scrutinizing the temporal dynamics of promoter activities, it became evident that the Δ*liaIH* mutant displayed only a transient P_{liaI} induction that reached a peak between 10 and 20 min after bacitracin addition and declined afterwards, whereas the wild type displayed prolonged P_{liaI} activity with a peak at ~40 min after bacitracin addition (Supporting Information Fig. S2).

In line with these observations, in a *liaIH* complementation strain variations of the LiaIH production level did not

affect the dose-response behavior of the P_{bceA} promoter, but had significant effects on P_{liaI} activity itself (Fig. 4C). In the absence of bacitracin, the constitutive expression of *liaIH* triggered a 20-fold increased P_{liaI} activity compared to the wild type [Fig. 4C (ii); *light green data*]. At bacitracin concentrations higher than 0.3 μg ml^{-1}, however, P_{liaI} displayed a weaker activity than in wild type. These data show on the one hand that LiaIH has a positive regulatory effect on the P_{liaI} promoter even in the absence of externally added antibiotics. On the other hand they show that the inability to up-regulate *liaIH* lead to reduced P_{liaI} activity, suggesting that a positive feedback via LiaIH might be needed for the full activation of the Lia system in wild type. To rule out that the markerless deletion of *liaIH* had polar effects on the expression of the signaling system LiaFSR, we complemented the Δ*liaIH* mutant with a copy of *liaIH* under the control of its native promoter (P_{liaI}), and found that wild type behavior of P_{liaI} induction could be restored (data not shown). Moreover, the overproduction of LiaIH in a wild type background [Fig. 4C (ii); *dark green data*] lead to an elevated P_{liaI} activity in the absence of bacitracin, while at high bacitracin levels the Lia system was as active as in the wild type. Taken together, these results show that LiaIH has no influence on the primary resistance BceAB, but is instead involved in fully activating and perpetuating its own expression by a so far unknown mechanism. In the future, it remains to be clarified whether LiaIH is involved in the *perception* of cell envelope stress, or whether LiaIH *generates* some degree of envelope stress itself.

Single cell induction of CESR modules

The compensatory regulation between the different CESR modules observed at the bulk-level (see above), raises the question of how the bacterial population implements this response at the individual cell level. Do all cells within the population behave uniformly, or is there significant phenotypic heterogeneity within the population? Given that the excess expression of resistance determinants is often associated with a fitness cost (Andersson and Hughes, 2010), it is in fact intriguing to ask whether bacteria evolved to *minimize* "noise" in resistance gene expression (adjusting resistance as close as possible to its optimal level), or whether they actively *use* heterogeneous gene expression as a means to diversify resistance levels within the population – a strategy that can be beneficial in fluctuating environments (Fraser and Kaern, 2009).

To scrutinize the expression behavior of the three CESR modules at the single cell level, we fused their promoters to a plasmid-borne copy of *gfp* and introduced them into wild type *B. subtilis* W168. We then challenged exponentially growing cells with various levels of bacitracin and quantified GFP fluorescence by flow cytometry one hour after bacitracin addition (Fig. 5). In the absence of bacitracin the fluorescence distributions of the P_{bceA}-*gfp* (Fig. 5A) and the P_{liaI}-*gfp* (Fig. 5C) reporters were identical to the autofluorescence distribution of *B. subtilis* W168 (data not shown), while the P_{bcrC}-*gfp* reporter activity was ∼5-fold higher than background (Fig. 5B), consistent with the high basal activity of the P_{bcrC} promoter quantified with the luciferase reporter above (cf. Fig. 3). This suggests that the *gfp* reporter is less sensitive than the luciferase reporter, such that promoter activities below $\sim 10^5$ RLU/OD in Fig. 3 are hidden by the autofluorescence of *B. subtilis*. However, apart from this difference in reporter sensitivity, the mean fluorescence values for all promoter-*gfp* fusions were consistent with the results obtained for the promoter-*lux* fusions in Fig. 3.

Next, we compared gene expression noise in the response of the three resistance modules. As mentioned before, in the absence of bacitracin the fluorescence distributions of P_{bceA}-*gfp* (Fig. 5A) and P_{liaI}-*gfp* (Fig. 5C) reporters were identical to the broad autofluorescence distribution of *B. subtilis*. In contrast, P_{bcrC}-*gfp* reporter displayed a narrow fluorescence distribution, and also showed low noise levels at all bacitracin levels tested. In the presence of bacitracin the response of the P_{bceA}-*gfp* reporter became almost as homogeneous as the P_{bcrC}-*gfp* reporter. Only the P_{liaI}-*gfp* reporter was expressed broadly heterogeneously across the population when challenged with intermediate concentrations (1–3 μg ml^{-1}) of bacitracin (Fig. 5C), as reported before (Kesel *et al*., 2013). Indeed, when quantifying gene expression noise by the coefficient of variation η, we found that at similar mean GFP expression levels the P_{liaI} promoter was significantly noisier than the other promoters (Supporting Information Fig. S3A). This broadly heterogeneous production of LiaIH argues for significant cell-to-cell variability in the downstream damage perceived by the Lia system in the presence of bacitracin. In contrast, the low noise levels in the expression of *bceAB* and *bcrC* suggest that their expression is subject to a more stringent control, which might be the result of negative feedback regulation within these systems (see Discussion).

To test whether the noisy Lia response is influenced by the expression of the other two resistance modules, we introduced the P_{liaI}-*gfp* reporter plasmid into Δ*bceAB* and Δ*bcrC* mutants and determined their single cell response towards bacitracin as above. Strikingly, the Lia response displayed notably less cell-to-cell variability in the Δ*bceAB* mutant than in the wild type (Fig. 5D). Also, when comparing their coefficients of variation at similar mean expression levels (Supporting Information Fig. S3B), we found that P_{liaI} is less noisy in the Δ*bceAB* mutant than in the wild type, thereby showing that the

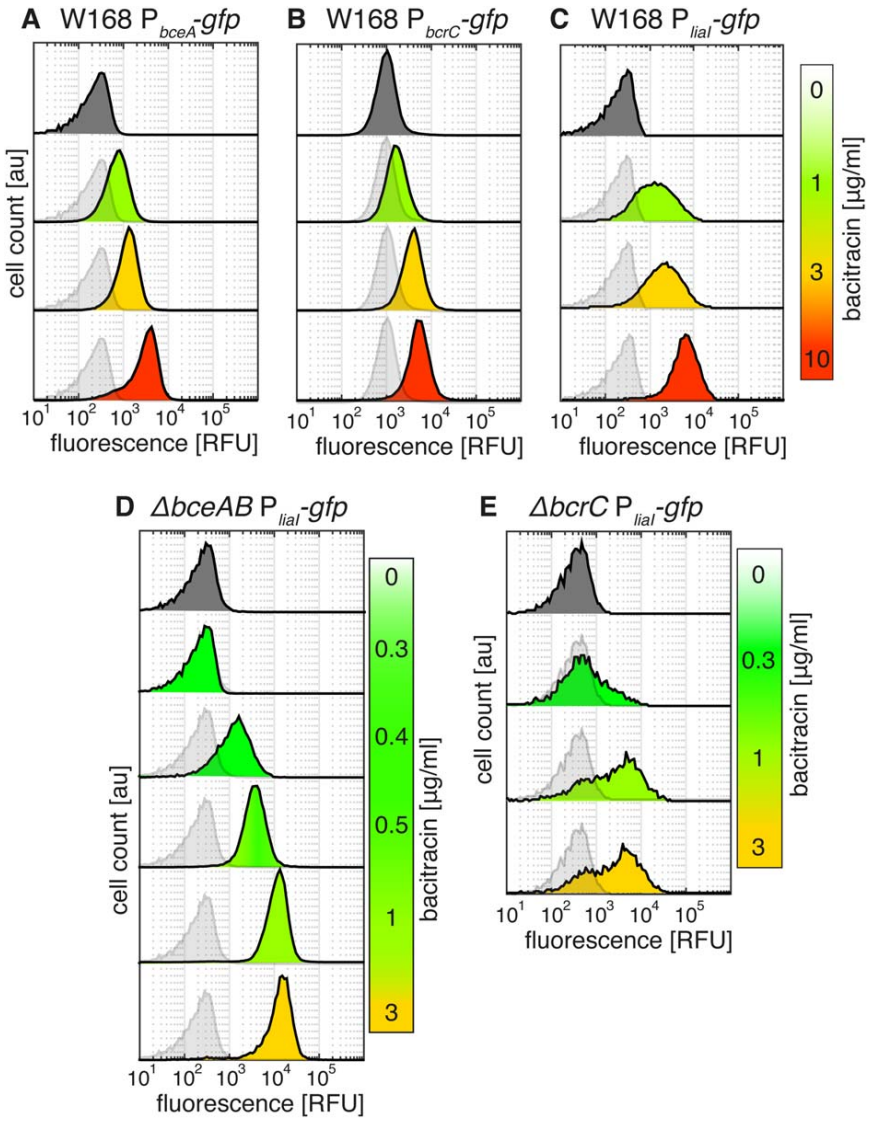

Fig. 5. Noise in the response of bacitracin resistance modules. Single cell bacitracin response of wild type strains carrying (A) P_{bceA}-*gfp*, (B) P_{bcrC}-*gfp*, and (C) P_{liaIH}-*gfp* reporter plasmids (strains TMB2174, TMB2173 and TMB1176, see Supporting Information Table S1), as well as in (D) Δ*bceAB* and (E) Δ*bcrC* mutant backgrounds carrying a P_{liaI}-*gfp* reporter plasmid (strains TMB2056 and TMB2057, see Supporting Information Table S1). Fluorescence distributions were quantified using flow cytometry, one hour after treatment of exponentially growing cells (37°C, LB medium) with bacitracin.
Fluorescence distributions (*colored*) were obtained under bacitracin treatment indicated on the right, while transparent overlays (*gray*) are reference distributions obtained in the absence of bacitracin treatment. In every case one representative dataset of at least two independent biological replicates is shown.

reduced noise level is not only caused by the stronger and more sensitive P_{liaI} response in this mutant. This suggests that in the unperturbed (wild type) CESR network, the broadly heterogeneous Lia response is directly triggered by heterogeneity in *bceAB* expression: At the time of antibiotic treatment there exists a narrow, yet stochastic distribution of BceAB protein levels across the population, such that cells with higher levels of BceAB have sufficient ability to cope with bacitracin, whereas cells with lower levels of BceAB experience more cell envelope damage, which in turn triggers higher LiaIH production levels. Consequently, in the absence of BceAB this model predicts that all cells in the population would experience a similar envelope stress level, consistent with the homogeneous Lia response in the Δ*bceAB* mutant.

In contrast, our data showed that in a Δ*bcrC* mutant noise in the Lia response was markedly increased (Fig. 5D). We suggest that the increased noise in the expression of *bceAB* in this mutant (Supporting Information Fig. S4) leads to a significant heterogeneity in the downstream damage perceived by the Lia system. However, we cannot exclude that population heterogeneity in other lipid II cycle-associated players factors into the noise properties of P_{liaI} in this highly impaired mutant strain. For instance, stochastic expression of *uppP*, encoding the second, BacA-like UPP phosphatase in *B. subtilis* (Cao and Helmann, 2002; Bernard *et al.*, 2005; Inaoka and Ochi, 2012), could result in largely variable rates of cell wall biogenesis, which would in turn lead to phenotypic heterogeneity in the susceptibility towards cell wall antibiotics.

 Molecular Microbiology, **100**, 607–620

Discussion

After the discovery of the bacitracin stimulon in *Bacillus subtilis* (Mascher *et al*., 2003) and the quantitative characterization of its individual modules (Rietkötter *et al*., 2008), we here present the first description of the full anatomy of the bacitracin resistance network in *B. subtilis*. Using a systems-level approach we showed that a clear hierarchy exists between resistance modules, allowing us to discriminate between primary (BceAB) and secondary layers (BcrC and LiaIH) of bacitracin resistance. Strikingly, in mutants devoid of the primary resistance layer, the secondary layer was more strongly induced, revealing a high level of redundancy between resistance modules. Accordingly, our data now show for the first time that in the absence of the primary bacitracin resistance module, the deletion of *liaIH* displays a clear-cut phenotype with a 6-fold reduction of bacitracin resistance. Hence, we argue that the high level of resistance conferred by BceAB masks the weaker contribution from the Lia system. This explains previous reports that noted surprisingly weak phenotypes of a *liaIH* deletion alone, despite the strong Lia expression under a variety of cell envelope-perturbing conditions, including lipid II cycle-interfering antibiotics as well as oxidative stress reagents (Jordan *et al*., 2006; Rietkötter *et al*., 2008; Suntharalingam *et al*., 2009; Wolf *et al*., 2010). So far, one of the strongest phenotypes was found during treatment with the membrane pore-forming lipopeptide daptomycin, where a *liaIH* deletion caused a 3-fold reduction of resistance (Hachmann *et al*., 2009; Wecke *et al*., 2009). Notably, *B. subtilis* features no primary resistance mechanism against daptomycin, again highlighting that the contribution of the Lia system to antibiotic resistance is strongest if other resistance layers are lacking. Based on these observations, and in conjunction with the wide distribution of the PspA/IM30 protein family (of which LiaH is a member) across various bacterial phyla and even in archaea and eukaryotes (Joly *et al*., 2010), we speculate that the Lia system constitutes an ancient resistance module that provides a low level of resistance against a broad range of cell envelope-perturbing agents. In contrast, the Bce-like resistance modules confer high levels of protection against a rather narrow range of antimicrobial peptides (Gebhard, 2012) and are almost exclusively found in Firmicutes bacteria (Joseph *et al*., 2002; Mascher, 2006; Dintner *et al*., 2011), suggesting that these specialized resistance layers were acquired later during evolution.

The results presented here also shed new light on the role of the UPP phosphatase BcrC in lipid II cycle homeostasis under antimicrobial peptide attack. First, we showed that the deletion of *bcrC* lead to a significant decrease in growth rate - even in the absence of antibiotic treatment. It appears likely that the second BacA-like UPP phosphatase, UppP, partially compensates for the loss of BcrC, but that its activity is insufficient to maintain adequate cell wall synthesis under the rapid growth conditions in LB media. The precise extent to which the *uppP* promoter is up-regulated in such a mutant, and how it responds to lipid II cycle-inhibiting antimicrobial peptides, remains to be elucidated. Second, our data revealed that *bcrC* deletion had pleiotropic effects on the expression of all resistance modules and, most notably, triggered their up-regulation also in the absence of externally added bacitracin. In these highly perturbed cells, the induction of the Lia system was consistent with its role as a general sensor of cell envelope stress (Wolf *et al*., 2010). Likewise, the up-regulation of the σ^M- and σ^X-dependent P_{bcrC} promoter was not unexpected, because these alternative σ factors were also shown to be sensors for cell wall integrity (Inoue *et al*., 2013; Lee and Helmann, 2013). However, it was surprising to find the P_{bceA} promoter affected in the *bcrC* mutant, because all previous reports were consistent with a model in which the Bce system responds to the detoxification flux of the *drug* and not to downstream *damage* on cell physiology (Wolf *et al*., 2012; Fritz *et al*., 2015).

One possible explanation for the elevated P_{bceA} activity might be that the lack of the phosphatase BcrC causes the accumulation of UPP in the membrane, and thereby provides a surplus of targets for bacitracin. In turn, increased levels of UPP-bacitracin complexes would increase the detoxification flux per BceAB transporter, which then serves as the signal for P_{bceA} activation. While this model can explain the increased P_{bceA} activity in the presence of bacitracin, it is less intuitive why there was also a ~10-fold activation in the absence of bacitracin (cf. Fig. 3A). One possibility is that the accumulation of UPP itself somehow triggers BceAB activity. Interestingly, Kingston and colleagues suggested that BceAB may recognize UPP directly and flip it to the inner face of the membrane, where it may be protected from bacitracin and dephosphorylated by a cytosolically acting UppP (Kingston *et al*., 2014). Although it is known that BceB directly binds free bacitracin *in vitro* with high affinity (Dintner *et al*., 2014), it is conceivable that the physiological substrate of the transporter is the UPP-bacitracin complex in the cell, as suggested previously (Fritz *et al*., 2015). In this case, the transporter may also be able to interact with both components of the complex separately, i.e., free bacitracin and free UPP, especially when increased amounts of these are present. The increased basal activity of P_{bceA} in the *bcrC* mutant may then be due to accumulation of UPP. A third alternative explanation might be that one or more of the endogeneously produced antimicrobial peptides activate the Bce system under these conditions. For instance, we recently showed that the endogeneous

production of the sporulation delay protein C (SdpC) and the sporulation killing factor A (SkfA) in early stationary phase up-regulate production of BceAB and the paralogous PsdAB transporter in *B. subtilis* more than 100-fold (Höfler *et al.*, 2016).

Taken together, the work from us and earlier work support the following, multi-layered model of the bacitracin resistance network in *B. subtilis*: In the presence of bacitracin (Bac) the accumulation of UPP-bacitracin (UPP-Bac) complexes blocks the lipid II cycle of cell wall biosynthesis and, as a consequence, leads to cell envelope damage. UPP-Bac is recognized by the ABC transporter BceAB, which releases UPP from the inhibitory grip of bacitracin by a so far unknown transport mechanism and thereby shifts the binding equilibrium towards the free form of UPP. Expression of *bceAB* is controlled by a flux-sensing mechanism (Fig. 1C), which homeostatically adjusts the BceAB level such that the transport activity of individual ABC transporters does not exceed a critical threshold (Fritz *et al.*, 2015). At the same time such homeostatic, negative feedback systems are known to reduce gene expression noise (Alon, 2007), fully consistent with the homogeneous response of the Bce system observed at the single cell level. Simultaneously to the action of BceAB, BcrC reduces the concentration of the bacitracin-target UPP by dephosphorylation to UP, thereby further promoting progression of the lipid II cycle. Under bacitracin stress, transcription of *bcrC* is controlled by the alternative ECF σ factor σ^M, which is regulated by the membrane-bound anti-σ factors YhdK/L (Fig. 1C). Previous data showed that either the depletion of UP and/or the depletion of lipid II could be the cues for anti-σ factors YhdK/L (Inoue *et al.*, 2013; Lee and Helmann, 2013; Meeske *et al.*, 2015). This suggests that the end product of the reaction catalyzed by BcrC (UPP → UP) could negatively regulate the expression of *bcrC*, which would in turn close a negative feedback loop that asserts homeostatic UP level control in the cell. This model is also consistent with all our data, most importantly the elevated P_{bcrC} activity in the *bcrC* mutant (which we expect to display low UP levels), as well as the low noise level of the P_{bcrC} promoter, which is again characteristic of negative feedback systems. Within our model, the Lia system constitutes the last line of defense that directly responds to and combats cell envelope damage, thereby explaining why the expression of the Lia system did not affect the expression of the other resistance modules in our data.

More generally, we propose that the redundant organization of the bacitracin resistance network of *B. subtilis* described here is a universal principle of many stress response networks within the microbial world, as demonstrated for instance in the oxidative stress responses of *Salmonella enterica* (Hébrard *et al.*, 2009) and *Ralstonia solanacearum* (Flores-Cruz and Allen, 2009) or in the regulation of drug efflux systems in various bacterial species (Grkovic *et al.*, 2002). Here the induction of individual stress response modules typically relieves stress perceived by other modules, which can be interpreted as a coupling between stress response modules via a global negative feedback mechanism. Failure of one of the "nodes" in such a network then triggers compensatory up-regulation of other nodes, which then jointly protect the cell. Interestingly, in the engineering disciplines this concept is known as "active redundancy," during which the performance of individual devices is automatically monitored and dynamically reconfigured to eliminate performance declines of the system (Pahl and Beitz, 1996). In contrast, "passive redundancy" uses excess capacity to reduce the impact of component failures (Pahl and Beitz, 1996), which would be akin to the constitutive expression of all resistance determinants. In biological stress response networks, we propose that the use of active redundancy serves as an optimal regulation strategy to maximize cellular protection while preventing the direct or indirect costs of excess resistance gene expression.

Experimental procedures

Bacterial strains and growth conditions

Bacillus subtilis and *Escherichia coli* were routinely grown in Luria-Bertani (LB) medium at 37°C with agitation (200 rpm). Transformations of *B. subtilis* were carried out as described previously (Harwood and Cutting, 1990). All strains used in this study are derivatives of the wild-type strain W168 and are listed in Supporting Information Table S1. Kanamycin (10 mg ml^{-1}), chloramphenicol (5 mg ml^{-1}), spectinomycin (100 mg ml^{-1}), tetracycline (10 mg ml^{-1}) and erythromycin (1 mg ml^{-1}) plus lincomycin (25 mg ml^{-1}) for macrolide-lincosamide-streptogramin B ("MLS") resistance were used for the selection of the *B. subtilis* mutants used in this study. Solid media contained 1.5% (w/v) agar. For complementation studies, full induction of the promoter P_{xylA} was achieved by adding xylose to a final concentration of 0.2% (w/v).

DNA manipulation

Plasmids were generated by using standard cloning techniques (Sambrook, Russell 2001) with enzymes and buffers from New England Biolabs (NEB; Ipswich, MA, USA) according to the respective protocols. PCR-DNA amplification for cloning purposes occurred with Phusion® or Q5® polymerase. Primers used in this study are listed in Supporting Information Table S2 and plasmid descriptions as well as details on their construction are given in Supporting Information Table S3. All plasmids were verified by sequencing of the insert. The integration of plasmids or DNA fragments into the genome, or the presence of a replicative vector, was confirmed by colony PCR. Integration into the *thrC*-locus was checked by threonine-auxotrophy in minimal medium.

Determination of minimal inhibitory concentration

Bacitracin resistance of *B. subtilis* strains was determined using Etest® strips on bacterial lawn (bioMérieux, Marcy l'Etoile, France), providing a concentration range from 256 to 0.016 μg ml^{-1} bacitracin. Briefly, 3 ml of Müller-Hinton (MH) medium (2.1% (w/v) Müller-Hinton broth) were inoculated 1:100 from fresh overnight culture and cells were grown at 37°C with agitation to $OD_{600} = 0.6–0.8$. Subsequently, 30 μl of the cell suspension were added to 3 ml molten MH soft agar (60°C, 0.75% (w/v) agar), mixed and distributed on MH agar plates. After 20 min of solidification, one Etest® strip was applied per agar plate. Results were documented after 24 h of incubation at 37°C.

Luciferase assays

Luciferase activities of *B. subtilis* strains harboring pBS3C*lux*-derivates were assayed using a Synergy™ NEOALPHAB multi-mode microplate reader from BioTek® (Winooski, VT, USA). The reader was controlled using the software Gen5™ (version 2.06). Cells were inoculated 1:1000 from fresh overnight cultures and grown to $OD_{600} = 0.1–0.5$. Subsequently, cultures were diluted to $OD_{600} = 0.01$ and split into 100 μl per well in 96-well plates (black walls, clear bottom; Greiner Bio-One, Frickenhausen, Germany). Cultures were incubated at 37°C with linear agitation (intensity, 567 cpm) and the optical density at 600 nm (OD_{600}) as well as luminescence was monitored every 5 min. After one hour, freshly diluted Zn^{2+}-bacitracin was added to the indicated final concentrations and incubation and monitoring was resumed for 2 h. Specific luminescence activity is given by the raw luminescence output (relative luminescence units, RLU) normalized by cell density (RLU/OD).

Flow cytometry assays

Single-cell fluorescence of *B. subtilis* strains carrying GFP-reporter plasmids was measured using a BD Accuri™ C6 flow cytometer (BD Biosciences, Becton, Dickinson and Company, New Jersey, USA). Cells were inoculated 1:1000 from overnight cultures and grown at 37°C to $OD_{600} \sim 0.1$. Subsequently the culture was split into test tubes, stained with FM® 4-64 (Life Technologies GmbH, USA) to a final concentration of 2 ng ml^{-1} and incubated at 37°C with agitation. After 30 min cells were induced with indicated final concentrations of Zn^{2+}-bacitracin and 1 hour after further incubation, culture samples were assayed by flow cytometry. It was controlled by the BD Accuri™ C6 software using the following settings: sample threshold = 11,000 on FSC-H, core size = 5μm, flow rate = 10 μl min^{-1}. Noise in the resulting fluorescence distributions (cf. Supporting Information Fig. S3) was quantified by the coefficient of variation η, defined as the ratio of the standard deviation σ to the mean μ. In doing so, we used the geometric mean and variance, because those measures are known to yield more accurate statistics for log-normal distributed values than the arithmetic mean and standard deviation.

Acknowledgement

This project was funded by the DFG priority program SPP1617 'Phenotypic Heterogeneity and Sociobiology of Bacterial Populations' (grants FR 3673/1-2 to GF and MA 2837/3-2 to TM).

References

Alon, U. (2007) Network motifs: theory and experimental approaches. *Nat Rev Genet* **8**: 450–461.

Andersson, D.I., Hughes, D. (2010) Antibiotic resistance and its cost: is it possible to reverse resistance? *Nat Rev Microbiol* **8**: 260–271.

Aso, Y., Okuda, K.-I., Nagao, J.-I., Kanemasa, Y., Thi Bich Phuong, N., Koga, H., *et al.* (2005) A novel type of immunity protein, NukH, for the lantibiotic nukacin ISK-1 produced by *Staphylococcus warneri ISK-1*. *Biosci Biotechnol Biochem* **69**: 1403–1410.

Azevedo, E.C., Rios, E.M., Fukushima, K., and Campos-Takaki, G.M. (1993) Bacitracin production by a new strain of *Bacillus subtilis*. *Appl Biochem Biotechnol* **42**: 1–7.

Bernard, R., Ghachi, El, M., Mengin-Lecreulx, D., Chippaux, M., and Denizot, F. (2005) BcrC from *Bacillus subtilis* acts as an undecaprenyl pyrophosphate phosphatase in bacitracin resistance. *J Biol Chem* **280**: 28852–28857.

Breukink, E., and de Kruijff, B. (2006) Lipid II as a target for antibiotics. *Nat Rev Drug Discov* **5**: 321–332.

Cao, M., and Helmann, J.D. (2002) Regulation of the *Bacillus subtilis bcrC* bacitracin resistance gene by two extracytoplasmic function sigma factors. *J Bacteriol* **184**: 6123–6129.

Dintner, S., Staroń, A., Berchtold, E., Petri, T., Mascher, T., and Gebhard, S. (2011) Coevolution of ABC transporters and two-component regulatory systems as resistance modules against antimicrobial peptides in Firmicutes bacteria. *J Bacteriol* **193**: 3851–3862.

Dintner, S., Heermann, R., Fang, C., Jung, K., and Gebhard, S. (2014) A sensory complex consisting of an ATP-binding cassette transporter and a two-component regulatory system controls bacitracin resistance in *Bacillus subtilis*. *J Biol Chem* **289**: 27899–27910.

Domínguez-Escobar, J., Wolf, D., Fritz, G., Höfler, C., Wedlich-Söldner, R., and Mascher, T. (2014) Subcellular localization, interactions and dynamics of the phage-shock protein-like Lia response in *Bacillus subtilis*. *Mol Microbiol* **92**: 716–732

Economou, N.J., Cocklin, S., and Loll, P.J. (2013) High-resolution crystal structure reveals molecular details of target recognition by bacitracin. *Proc Natl Acad Sci USA* **110**: 14207–14212.

Eiamphungporn, W., and Helmann, J.D. (2008) The *Bacillus subtilis* σ^M regulon and its contribution to cell envelope stress responses. *Mol Microbiol* **67**: 830–848.

Eijsink, V.G.H., Axelsson, L., Diep, D.B., Håvarstein, L.S., Holo, H., and Nes, I.F. (2002) Production of class II bacteriocins by lactic acid bacteria; an example of biological warfare and communication. *Antonie Van Leeuwenhoek* **81**: 639–654.

Flores-Cruz, Z., Allen, C. (2009) *Ralstonia solanacearum* encounters an oxidative environment during tomato infection. *Mol Plant Microbe Interact* **22**: 773–782.

Fraser, D., Kaern, M. (2009) A chance at survival: gene expression noise and phenotypic diversification strategies. *Mol Microbiol* **71**:1333–1340.

Fritz, G., Dintner, S., Treichel, N.S., Radeck, J., Gerland, U., Mascher, T., and Gebhard, S. (2015) A new way of sensing: Need-based activation of antibiotic resistance by a flux-sensing mechanism. *mBio* **6**: e00975.

Gebhard, S. (2012) ABC transporters of antimicrobial peptides in Firmicutes bacteria - phylogeny, function and regulation. *Mol Microbiol* **86**: 1295–1317.

Grkovic, S., Brown, M.H., and Skurray, R.A. (2002) Regulation of bacterial drug export systems. *Microbiol Mol Biol Rev* **66**: 671–701.

Hachmann, A.-B., Angert, E.R., and Helmann, J.D. (2009) Genetic analysis of factors affecting susceptibility of *Bacillus subtilis* to daptomycin. *Antimicrob Agents Chemother* **53**: 1598–1609.

Hébrard, M., Viala, J.P.M., Méresse, S., Barras, F., Aussel, L. (2009) Redundant hydrogen peroxide scavengers contribute to *Salmonella* virulence and oxidative stress resistance. *J Bacteriol* **191**: 4605–4614.

Höfler, C., Heckmann, J., Fritsch, A., Popp, P., Gebhard, S., Fritz, G., and Mascher, T. (2016) Cannibalism Stress Response in *Bacillus subtilis*. *Microbiology* **162**: 164–176.

Inaoka, T., and Ochi, K. (2012) Undecaprenyl Pyrophosphate involvement in susceptibility of *Bacillus subtilis* to rare earth elements. *J Bacteriol* **194**: 5632–5637.

Inoue, H., Suzuki, D., and Asai, K. (2013) A putative bactoprenol glycosyltransferase, CsbB, in *Bacillus subtilis* activates SigM in the absence of co-transcribed YfhO. *Biochem Biophys Res Commun* **436**: 6–11.

Ishihara, H., Takoh, M., Nishibayashi, R., and Sato, A. (2002) Distribution and variation of bacitracin synthetase gene sequences in laboratory stock strains of *Bacillus licheniformis*. *Curr Microbiol* **45**: 18–23.

Joly, N., Engl, C., Jovanovic, G., Huvet, M., Toni, T., Sheng, X., *et al*. (2010) Managing membrane stress: the phage shock protein (Psp) response, from molecular mechanisms to physiology. *FEMS Microbiol Rev* **34**: 797–827.

Jordan, S., Junker, A., Helmann, J.D., and Mascher, T. (2006) Regulation of LiaRS-dependent gene expression in *Bacillus subtilis*: identification of inhibitor proteins, regulator binding sites, and target genes of a conserved cell envelope stress-sensing two-component system. *J Bacteriol* **188**: 5153–5166.

Jordan, S., Rietkötter, E., Strauch, M.A., Kalamorz, F., Butcher, B.G., Helmann, J.D., and Mascher, T. (2007) LiaRS-dependent gene expression is embedded in transition state regulation in *Bacillus subtilis*. *Microbiology* **153**: 2530–2540.

Jordan, S., Hutchings, M.I., and Mascher, T. (2008) Cell envelope stress response in Gram-positive bacteria. *FEMS Microbiol Rev* **32**: 107–146.

Joseph, P., Fichant, G., Quentin, Y., Denizot, F. (2002) Regulatory relationship of two-component and ABC transport systems and clustering of their genes in the *Bacillus/Clostridium* group, suggest a functional link between them. *J Mol Microbiol Biotechnol* **4**: 503–513.

Kesel, S., Mader, A., Höfler, C., Mascher, T., and Leisner, M. (2013) Immediate and heterogeneous response of the LiaFSR two-component system of *Bacillus subtilis* to the peptide antibiotic bacitracin. *PLoS One* **8**: e53457.

Kingston, A.W., Zhao, H., Cook, G.M., and Helmann, J.D. (2014) Accumulation of heptaprenyl diphosphate sensitizes *Bacillus subtilis* to bacitracin: implications for the mechanism of resistance mediated by the BceAB transporter. *Mol Microbiol* **93**: 37–49.

Kleerebezem, M., Crielaard, W., and Tommassen, J. (1996) Involvement of stress protein PspA (phage shock protein A) of *Escherichia coli* in maintenance of the protonmotive force under stress conditions. *EMBO J* **15**: 162–171.

Kobayashi, R., Suzuki, T., and Yoshida, M. (2007) *Escherichia coli* phage-shock protein A (PspA) binds to membrane phospholipids and repairs proton leakage of the damaged membranes. *Mol Microbiol* **66**: 100–109.

Lee, Y.H., and Helmann, J.D. (2013) Reducing the level of undecaprenyl pyrophosphate synthase has complex effects on susceptibility to cell wall antibiotics. *Antimicrob Agents Chemother* **57**: 4267–4275.

Mascher, T. (2006) Intramembrane-sensing histidine kinases: a new family of cell envelope stress sensors in Firmicutes bacteria. *FEMS Microbiol Lett* **264**: 133–144.

Mascher, T., Margulis, N.G., Wang, T., Ye, R.W., and Helmann, J.D. (2003) Cell wall stress responses in *Bacillus subtilis*: the regulatory network of the bacitracin stimulon. *Mol Microbiol* **50**: 1591–1604.

Mascher, T., Zimmer, S.L., Smith, T.-A., and Helmann, J.D. (2004) Antibiotic-inducible promoter regulated by the cell envelope stress-sensing two-component system LiaRS of *Bacillus subtilis*. *Antimicrob Agents Chemother* **48**: 2888–2896.

Meeske, A.J., Sham, L.-T., Kimsey, H., Koo, B.-M., Gross, C.A., Bernhardt, T.G., and Rudner, D.Z. (2015) MurJ and a novel lipid II flippase are required for cell wall biogenesis in *Bacillus subtilis*. *P Natl Acad Sci USA* **112**: 6437–6442.

Ohki, R., Giyanto, Tateno, K., Masuyama, W., Moriya, S., Kobayashi, K., and Ogasawara, N. (2003) The BceRS two-component regulatory system induces expression of the bacitracin transporter, BceAB, in *Bacillus subtilis*. *Mol Microbiol* **49**: 1135–1144.

Pahl, G., and Beitz, W. (1996). *Engineering Design*, Springer.

Radeck, J., Kraft, K., Bartels, J., Cikovic, T., Dürr, F., Emenegger, J., *et al*. (2013) The *Bacillus* BioBrick Box: generation and evaluation of essential genetic building blocks for standardized work with *Bacillus subtilis*. *J Biol Eng* **7**: 29.

Revilla-Guarinos, A., Gebhard, S., Mascher, T., and Zúñiga, M. (2014) Defence against antimicrobial peptides: different strategies in Firmicutes. *Environ Microbiol.* **16**: 1225–1237.

Rietkötter, E., Hoyer, D., and Mascher, T. (2008) Bacitracin sensing in *Bacillus subtilis*. *Mol Microbiol* **68**: 768–785.

Schmalisch, M., Maiques, E., Nikolov, L., Camp, A.H., Chevreux, B., Muffler, A., *et al*. (2010) Small genes under sporulation control in the *Bacillus subtilis* genome. *J Bacteriol* **192**: 5402–5412.

Schrecke, K., Staroń, A., Mascher, T. (2012) Two-component signalling in the Gram-positive envelope stress response: Intramembrane-sensing histidine kinases and

accessory membrane proteins, p. 426. *In* Gross, R., Beier, D. (eds.), *Two-component systems in bacteria*. Horizon Scientific Press.

Schrecke, K., Jordan, S., and Mascher, T. (2013) Stoichiometry and perturbation studies of the LiaFSR system of *Bacillus subtilis*. *Mol Microbiol* **87**: 769–788.

Staroń, A., Finkeisen, D.E., and Mascher, T. (2011) Peptide antibiotic sensing and detoxification modules of *Bacillus subtilis*. *Antimicrob Agents Chemother* **55**: 515–525.

Stein, T., Heinzmann, S., Solovieva, I., and Entian, K.-D. (2003) Function of *Lactococcus lactis* nisin immunity genes *nisI* and *nisFEG* after coordinated expression in the surrogate host *Bacillus subtilis*. *J Biol Chem* **278**: 89–94.

Storm, D.R., and Strominger, J.L. (1973) Complex formation between bacitracin peptides and isoprenyl pyrophosphates. The specificity of lipid-peptide interactions. *J Biol Chem* **248**: 3940–3945.

Suntharalingam, P., Senadheera, M.D., Mair, R.W., Lévesque, C.M., and Cvitkovitch, D.G. (2009) The LiaFSR system regulates the cell envelope stress response in *Streptococcus mutans*. *J Bacteriol* **191**: 2973–2984.

Wecke, T., Zühlke, D., Mäder, U., Jordan, S., Voigt, B., Pelzer, S., *et al*. (2009) Daptomycin versus Friulimicin B: in-depth profiling of *Bacillus subtilis* cell envelope stress responses. *Antimicrob Agents Chemother* **53**: 1619–1623.

Wolf, D., Kalamorz, F., Wecke, T., Juszczak, A., Mäder, U., Homuth, G., *et al*. (2010) In-depth profiling of the LiaR response of *Bacillus subtilis*. *J Bacteriol* **192**: 4680–4693.

Wolf, D., Domínguez-Cuevas, P., Daniel, R.A., and Mascher, T. (2012) Cell envelope stress response in cell wall-deficient L-forms of *Bacillus subtilis*. *Antimicrob Agents Chemother* **56**: 5907–5915.

Supporting information

Additional supporting information may be found in the online version of this article at the publishe's web-site.

Supplementary Information to:

Anatomy of the bacitracin resistance network in *Bacillus subtilis*

Jara Radeck[1,2], Susanne Gebhard[3], Peter Shevlin Orchard[2], Marion Kirchner[2,¶], Stephanie Bauer[2], Thorsten Mascher[1] and Georg Fritz[4]*

[1] *Technische Universität Dresden, Institute of Microbiology, Dresden, Germany*

[2] *Ludwig-Maximilians-Universität München, Department Biology I, München, Germany*

[3] *University of Bath, Milner Centre for Evolution, Department of Biology and Biochemistry, Bath, UK*

[4] *Philipps-Universität Marburg, LOEWE-Center for Synthetic Microbiology (SYNMIKRO), Marburg, Germany*

[¶] *Present affiliation: Technische Universität München, Department of Chemistry, Garching, Germany*

**For correspondence: Email thorsten.mascher@tu-dresden.de; Tel. (+49) 351 463-40420; Fax (+49) 351 463-37715*

Contents

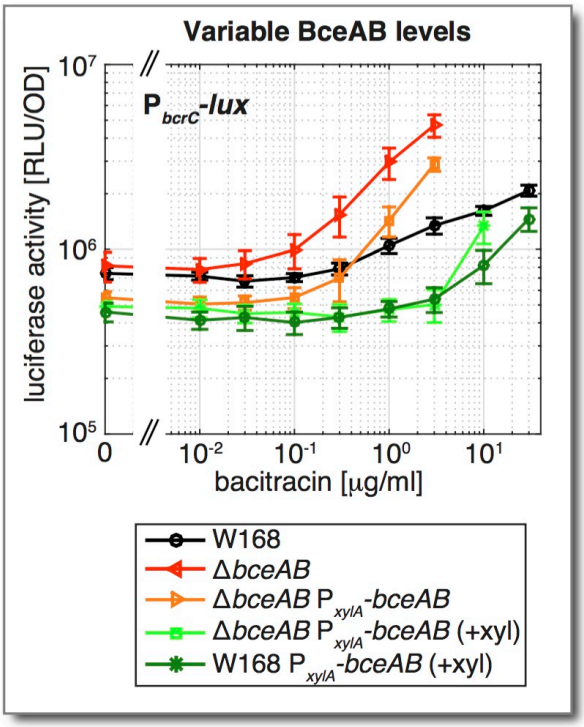

Figure S1. Regulatory crosstalk between BceAB and BcrC resistance module. Target promoter activities of P_{bcrC}-*lux* in strains producing different levels of BceAB, as given by specific luciferase activity (RLU/OD_{600}) one hour after addition of indicated amounts of bacitracin. Measurements were performed as described in Fig. 3 of the main text. Colors indicate different expression levels of *bceAB*, as obtained from strains TMB1620, TMB1624, TMB2745 and TMB2744 listed in Table S1.

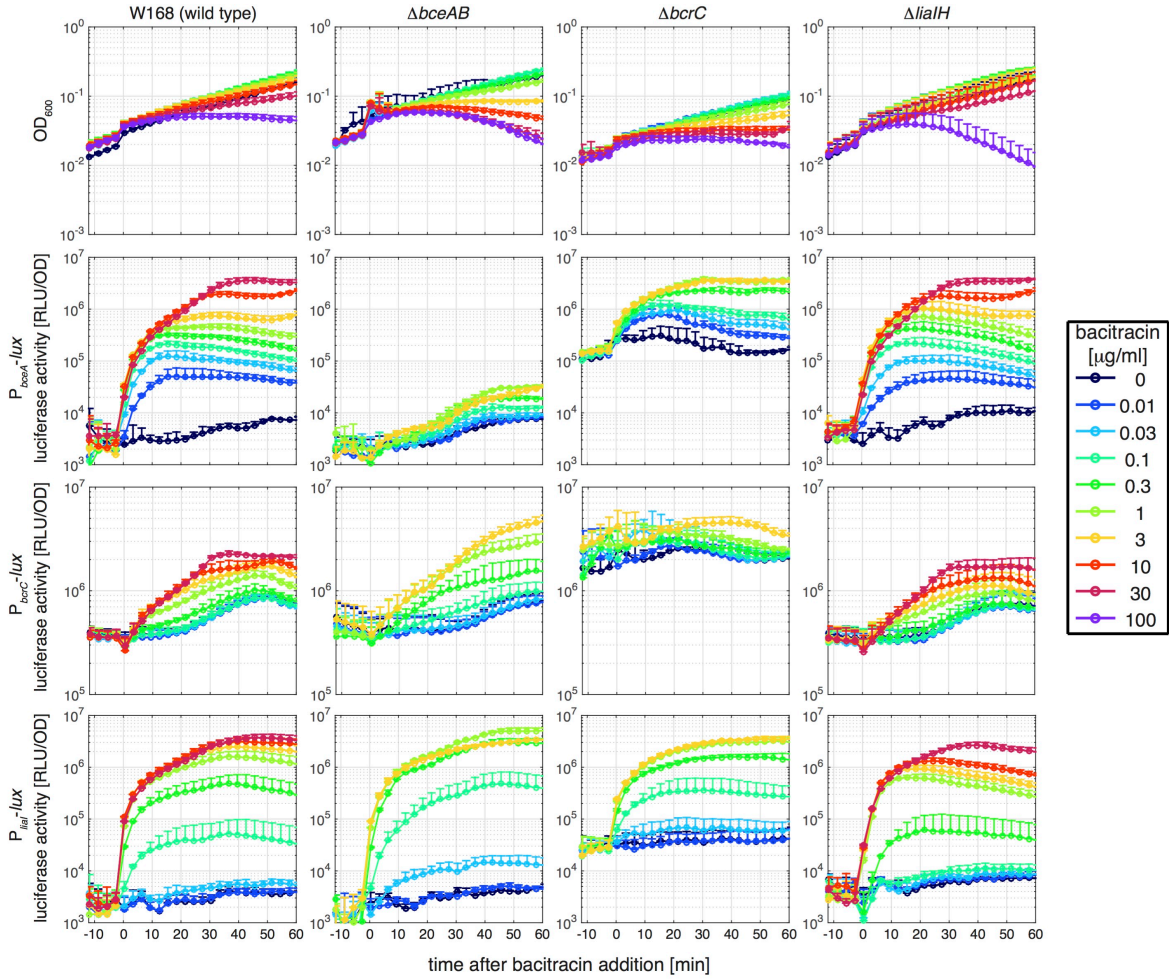

Figure S2. Expression dynamics of resistance modules in all mutant backgrounds. Dynamics of growth and target promoter activities of P_{bce}-*lux,* P_{bcrC}-*lux* and P_{liaI}-*lux* in strains carrying indicated deletions of CESR modules, as given by specific luciferase activity (RLU/OD_{600}) after addition of indicated amounts of bacitracin at t = 0 min. Measurements were performed during exponential growth phase in LB medium at 37°C in a microtiter plate reader. Data points and error bars indicate mean and standard deviation from at least three biological replicates. Data was obtained with strains TMB1619, TMB1620, TMB1617 (W168); TMB1623, TMB1624, TMB1621 (Δ*bceAB*); TMB1627, TMB1628, TMB1625 (Δ*bcrC*) and TMB1661, TMB1662, TMB1659 (Δ*liaIH*) containing P_{bceA}-*lux* , P_{bcrC}-*lux* or P_{liaI}-*lux*, respectively, listed in Table S1.

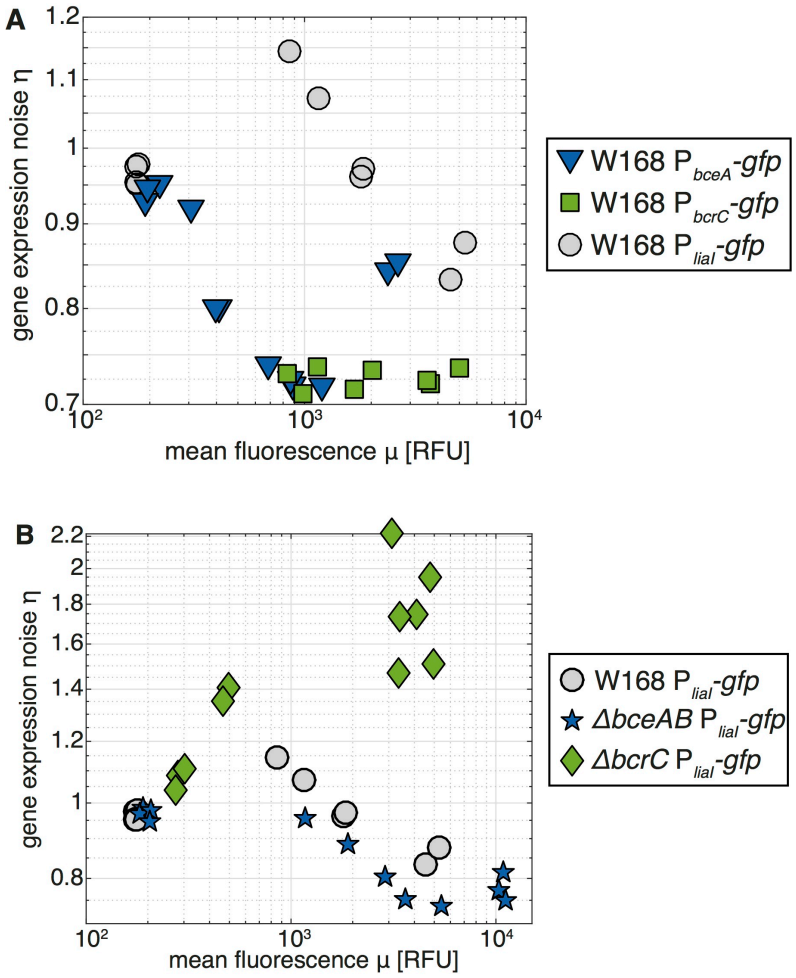

Figure S3. Quantification of gene expression noise in the three resistance modules. Scatterplot of gene expression noise η versus mean fluorescence values μ, as obtained from the fluorescence distributions in Fig. 5 of the main paper (each data point corresponds to the values of η and μ obtained for one fluorescence distribution). Here, gene expression noise was quantified by the coefficient of variation η, defined as the ratio of the standard deviation divided by the mean value of a fluorescence distribution. To exclude that differences in gene expression noise between different fluorescent distributions are the mere result of changes in the mean fluorescence level, we compare the values of η at identical mean fluorescence level, i.e., vertical lines in the graphs above. **(A)** Noise in P_{bceA}-*gfp*, P_{bcrC}-*gfp* and P_{liaI}-*gfp* reporter gene expression in a wild type (*B. subtilis* W168) strain background. **(B)** Noise in P_{liaI}-*gfp* reporter gene expression in W168, Δ*bceAB* and Δ*bcrC* strain background.

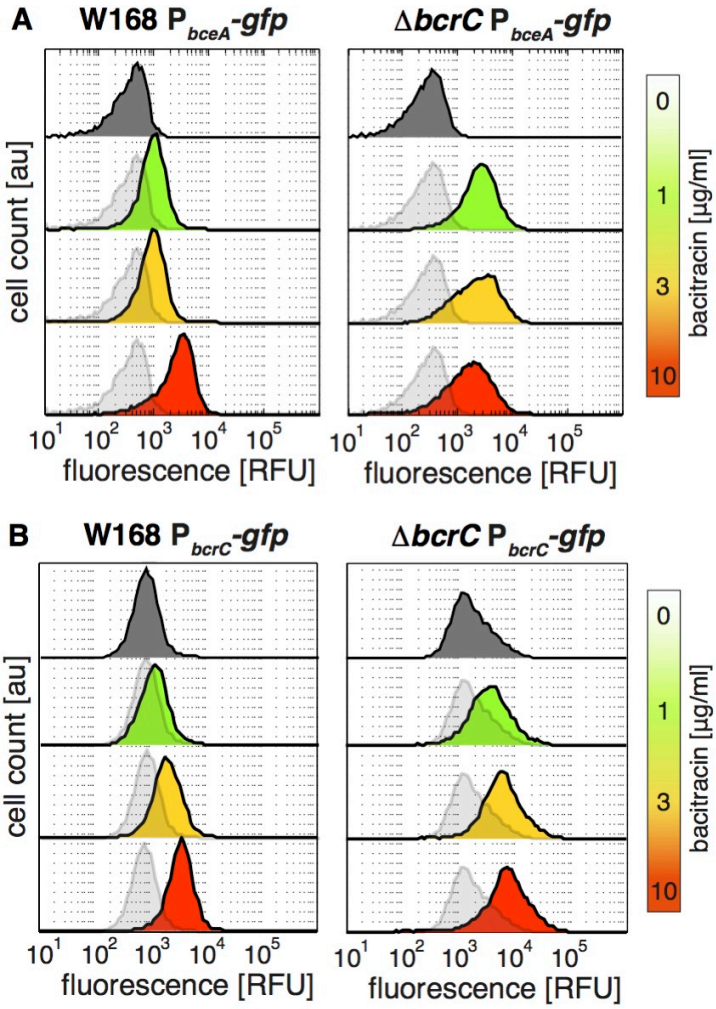

Figure S4. Influence of *bcrC* deletion on noise in P_{bceA} and P_{bcrC} promoter activity. Comparison of single cell bacitracin response in strains wild type and Δ*bcrC* deletion background for **(A)** P_{bceA}-*gfp and* **(B)** P_{bcrC}-*gfp* reporter plasmids (strains TMB2174, TMB2178, TMB2173 and TMB2177). Fluorescence distributions were quantified using flow cytometry, one hour after treatment of exponentially growing cells (37°C, LB medium) with bacitracin. Fluorescence distributions (*colored*) were obtained under bacitracin treatment indicated on the right, while transparent overlays (*gray*) are reference distributions obtained in the absence of bacitracin treatment. In every case one representative dataset of at least two independent biological replicates is shown.

Table S1. Bacterial strains used in this study

Name	Description[a]	Source
E. coli strains		
XL1-Blue	*recA1 endA1 gyrA96 thi-1 hsdR17 supE44 relA1 lac F'*::Tn*10* *proAB lacI*^{q} Δ(*lacZ*)M15]	Stratagene
DH5α	F– Φ80*lacZ*ΔM15 Δ(*lacZ*YA-*arg*F) U169 *rec*A1 *end*A1 *hsd*R17 (rK–, mK+) *pho*A *sup*E44 λ– *thi*-1 *gyr*A96 *rel*A1	Laboratory stock
NEB5α	*fhuA2 Δ(argF-lacZ)U169 phoA glnV44 Φ80 Δ(lacZ)M15 gyrA96 recA1 relA1 endA1 thi-1 hsdR17*	NEB
B. subtilis strains		
W168	Wild-type, *trpC2*	Laboratory stock
For determination of minimal inhibitory concentration		
TMB35	W168 *bceAB*::kan	(Rietkötter *et al.*, 2008)
TMB297	W168 *bcrC*::tet	(Rietkötter *et al.*, 2008)
TMB713	W168 *bcrC*::tet *bceAB*::kan	This study
TMB1151	W168 Δ*liaIH* clean deletion	(Toymentseva *et al.*, 2012)
TMB1829	W168 Δ*liaIH bceAB*::kan *bcrC*::tet	This study
TMB2127	W168 Δ*liaIH bceAB*::kan	This study
TMB2128	W168 Δ*liaIH bcrC*::tet	This study
For luminescence analysis		
TMB1617	W168 *sacA*::pCHlux101 (P_{liaI}-*lux*)	This study
TMB1621	W168 *bceAB*::kan *sacA*::pCHlux101 (P_{liaI}-*lux*)	This study
TMB1625	W168 bcrC::tet *sacA*::pCHlux101 (P_{liaI}-*lux*)	This study
TMB1659	W168 Δ*liaIH sacA*::pCHlux101 (P_{liaI}-*lux*)	This study
TMB2429	W168 *lacA*::pJNE2E01 (P_{xylA}-*bcrC*) sacA::pCHlux101 (P_{liaI}-*lux*)	This study
TMB2440	W168 Δ*liaIH lacA*::pJR2EF01 (P_{liaI}-*liaIH*) *sacA*::pCHlux101 (P_{liaI}-*lux*)	This study
TMB2589	W168 *bceAB*::kan *lacA*::pNT2E01 (P_{xylA}-*bceAB*) *sacA*::pCHlux101 (P_{liaI}-*lux*)	This study
TMB2591	W168 *bcrC*::tet *lacA*::pJNE2E01 (P_{xylA}-*bcrC*) *sacA*::pCHlux101 (P_{liaI}-*lux*)	This study
TMB2593	W168 *lacA*::pNT2E01 (P_{xylA}-*bceAB*) *sacA*::pCHlux101 (P_{liaI}-*lux*)	This study
TMB2690	W168 *lacA*::pJR2EF02 (P_{xylA}-*liaIH*) *sacA*::pCHlux101 (P_{liaI}-*lux*)	This study
TMB2692	W168 Δ*liaIH* lacA::pJR2EF02 (P_{xylA}-*liaIH*) *sacA*::pCHlux101 (P_{liaI}-*lux*)	This study
TMB1619	W168 *sacA*::pCHlux103 (P_{bceA}-*lux*)	(Höfler *et al.*, 2016)
TMB1623	W168 *bceAB*::kan *sacA*::pCHlux103 (P_{bceA}-*lux*)	This study
TMB1627	W168 *bcrC*::tet *sacA*::pCHlux103 (P_{bceA}-*lux*)	This study
TMB1661	W168 Δ*liaIH sacA*::pCHlux103 (P_{bceA}-*lux*)	This study
TMB2430	W168 *lacA*::pJNE2E01 (P_{xylA}-*bcrC*) *sacA*::pCHlux103 (P_{bceA}-*lux*)	This study
TMB2590	W168 *bceAB*::kan *lacA*::pNT2E01 (P_{xylA}-*bceAB*) *sacA*::pCHlux103 (P_{bceA}-*lux*)	This study
TMB2592	W168 *bcrC*::tet *lacA*::pJNE2E01 (P_{xylA}-*bcrC*) *sacA*::pCHlux103 (P_{bceA}-*lux*)	This study
TMB2594	W168 *lacA*::pNT2E01 (P_{xylA}-*bceAB*) *sacA*::pCHlux103 (P_{bceA}-*lux*)	This study
TMB2691	W168 *lacA*::pJR2EF02 (P_{xylA}-*liaIH*) *sacA*::pCHlux103 (P_{bceA}-*lux*)	This study
TMB2693	W168 Δ*liaIH lacA*::pJR2EF02 (P_{xylA}-*liaIH*) *sacA*::pCHlux103 (P_{bceA}-*lux*)	This study
TMB1620	W168 *sacA*::pCHlux104 (P_{bcrC}-*lux*)	(Höfler *et al.*, 2016)
TMB1624	W168 *bceAB*::kan *sacA*::pCHlux104 (P_{bcrC}-*lux*)	This study
TMB1628	W168 *bcrC*::tet *sacA*::pCHlux104 (P_{bcrC}-*lux*)	This study
TMB1662	W168 Δ*liaIH sacA*::pCHlux104 (P_{bcrC}-*lux*)	This study
TMB2744	W168 *lacA*::pNT2E01 (P_{xylA}-*bceAB*) *sacA*::pCHlux104 (P_{bcrC}-*lux*)	This study
TMB2745	W168 *bceAB*::kan *lacA*::pNT2E01 (P_{xylA}-*bceAB*) *sacA*::pCHlux104 (P_{bcrC}-*lux*)	This study
For flow cytometry analysis		
TMB1176	W168 pAT3803 (P_{liaI}-*gfp*)	(Toymentseva *et al.*, 2012)
TMB2056	W168 *bceAB*::kan pAT3803 (P_{liaI}-*gfp*)	This study
TMB2057	W168 *bcrC*::tet pAT3803 (P_{liaI}-*gfp*)	This study
TMB2173	W168 pJR3801 (P_{bcrC}-*gfp*)	This study
TMB2177	W168 *bcrC*::tet pJR3801 (P_{bcrC}-*gfp*)	This study
TMB2174	W168 pJR3802 (P_{bceA}-*gfp*)	This study
TMB2178	W168 *bcrC*::tet pJR3802 (P_{bceA}-*gfp*)	This study

[a] kan, kanamycin resistance; tet, tetracycline resistance.

Table S2. Primers used in this study

Primer name	Sequence (5'-3') [a]
TM1993	TTCC**TCTAGA**TGAGTAAAGGAGAAGAACTTTTC
TM1994	GGCC**GTCGAC**GA**ACTAGT**TTCATTTATTTG
TM2509	A**GCGGCCGC**ATCCAGACGTCTGTGGATAG
TM2510	TAA**GTCGAC**TCGTTTTCCTTGTCTTCATCTTA
TM2731	GATC**GAATTC**GCGGCCGCT**TCTAGA**AAGGAGGTG**GCCGGC**TTGAACTACGAAATTTTTAAAGCAATC
TM2732	GATC**ACTAGT**ATTA**ACCGGT**GAAATTTTGATCGGTTGGTTTTTTC
TM2968	GATC**GAATTC**GCGGCCGCT**TCTAGA**GAAGGCCAAAAAACTGCTGCC
TM2969	GATC**ACTAGT**ATTCGATAAGCTTGGGATCCC
TM3170	GATC**GAATTC**GAATCAATTTGAACATGTCATAAGCG
TM3171	GATC**TCTAGA**ATCCTCCTTATATATTGGATAATCTCATTATAAAAAGG
TM3172	GATC**GGTCTC**GA*ATT*CGCACTTTAATATCGGTACGAG
TM3173	GATC**TCTAGA**ATCCTCCTTATTACATTTTTATATTTAGTAGACTAATC
TM3415	GATC**TCTAGA**CCGGTGCGAGATACGACTC
TM3416	GATC**CTGCAG**TTTCATTCGGTTTCATCCTTCTC
TM3679	GATC**TCTAGA**GAAAACGAAAGGAGGATCTGC

[a] Recognition sites for endonuclease restriction enzymes are in bold, resulting overhangs for BsaI are in italics. The annealing part is underlined.

Table S3. Vectors and plasmids used in this study

Name	Description	Resistance in *E. coli* / *B. subtilis*[a]	Primers and Enzymes used for cloning[b]	Source
Vectors				
pAH328	*sacA*'…'*sacA, luxABCDE, cat, bla*	Amp^r / cm^r		(Schmalisch *et al.*, 2010)
pGP380	ori1030*, erm*, *bla*, Strep-Tag, PdegQ36 (Construction of N-term. Strep-tag in *B. subtilis* (SPINE))	Amp^r / MLS^r		(Herzberg *et al.*, 2007)
pBS2E	*lacA*'…'*lacA*, *erm*, *bla*	Amp^r / MLS^r		(Radeck *et al.*, 2013)
pBS4S	*thrC*'…'*thrC*, *spc*, *bla*	Amp^r / spc^r		(Radeck *et al.*, 2013)
pSG1151	*gfpmut*1, *cat*, *bla*, *ori-ColE*1, *ori-f*1	Amp^r / cm^r	Template for *gfp*-amplification	(Feucht and Lewis, 2001)
Plasmids				
pCHlux101	pAH328-derivative, *sacA*::P_{liaI}-*lux*, *cat*, *bla*	Amp^r / cm^r	P_{liaI}: TM2509/ TM2510; NotI, SalI	This study
pCHlux103	pAH328-derivative, *sacA*::P_{bceA}-*lux*, *cat*, *bla*	Amp^r / cm^r		(Höfler *et al.*, 2016)
pCHlux104	pAH328-derivative, *sacA*::P_{bcrC}-*lux*, *cat*, *bla*	Amp^r / cm^r		(Höfler *et al.*, 2016)
pAT3803	pGP380-derivative, P_{liaI}-*gfp*, *erm*, *bla*	Amp^r / MLS^r		(Toymentseva *et al.*, 2012)
pJR3801	pGP380-derivative, P_{bcrC}-*gfp*, *erm*, *bla*	Amp^r / MLS^r	P_{bcrC}: TM3172/ TM3173; BsaI(EcoRI), XbaI. *gfp*: TM1993/ TM1994; XbaI+SalI.	This study
pJR3802	pGP380-derivative, P_{bceA}-*gfp*, *erm*, *bla*	Amp^r / MLS^r	P_{bceA}: TM3170/ TM3171; EcoRI, XbaI. *gfp*: TM1993/ TM1994; XbaI+SalI.	This study
pJR2EF01	pBS2E-derivative, *lacA*::P_{liaI}-*liaIH*,*erm*, *bla*	Amp^r / MLS^r	P_{liaI}-*liaIH*:TM3415/ TM3416; XbaI+PstI	This study
pJR2EF02	pBS2E-derivative, *lacA*::P_{xylA}-*liaIH*,*erm*, *bla*	Amp^r / MLS^r	P_{xylA}:TM2968/ TM2969; EcoRI+SpeI. *liaIH*:TM3679/ TM3416; XbaI+PstI.	This study
pNT2E01	pBS2E-derivative, *lacA*::P_{xylA}-*bceAB*, *erm* , *bla*	Amp^r / MLS^r		(Fritz *et al.*, 2015)
pJNE2E01	pBS2E-derivative, *lacA*::P_{xylA}-*bcrC*,*erm*, *bla*	Amp^r / MLS^r	P_{xylA}:TM2968/ TM2969; EcoRI+SpeI. *bcrC*: TM2731/ TM2732; XbaI+PstI.	This study

[b]Amp^r, ampicillin resistance; cm^r, chloramphenicol resistance; MLS^r, erythromycin-induced resistance to macrolide, lincosamide and streptogramin B antibiotics; spc^r, spectinomycin resistance.

[b] Genomic DNA of B. subtilis W168 was used as template for PCR, except for amplification of *gfpmut1* where pSG1151 served as template. The vector was opened using the upstream restriction site of the promoter and the downstream restriction site of the gene, respectively, with the exception of pJR3801 where the vector was opened using EcoRI whereas P_{bcrC} was cut with BsaI.

Supplementary References

Feucht, A., and Lewis, P.J. (2001) Improved plasmid vectors for the production of multiple fluorescent protein fusions in *Bacillus subtilis*. *Gene* **264**: 289–297.

Fritz, G., Dintner, S., Treichel, N.S., Radeck, J., Gerland, U., Mascher, T., and Gebhard, S. (2015) A New Way of Sensing: Need-based activation of antibiotic resistance by a flux-sensing mechanism. *mBio* **6**: e00975.

Herzberg, C., Weidinger, L.A.F., Dörrbecker, B., Hübner, S., Stülke, J., and Commichau, F.M. (2007) SPINE: a method for the rapid detection and analysis of protein-protein interactions *in vivo*. *Proteomics* **7**: 4032–4035.

Höfler, C., Heckmann, J., Fritsch, A., Popp, P., Gebhard, S., Fritz, G., and Mascher, T. (2016) Cannibalism stress response in *Bacillus subtilis*. *Microbiology (Reading, Engl)*. [Epub ahead of print; doi: 10.1099/mic.0.000176].

Kallenberg, F., Dintner, S., Schmitz, R., and Gebhard, S. (2013) Identification of regions important for resistance and signalling within the antimicrobial peptide transporter BceAB of *Bacillus subtilis*. *J Bacteriol* **195**: 3287–3297.

Radeck, J., Kraft, K., Bartels, J., Cikovic, T., Dürr, F., Emenegger, J., *et al.* (2013) The *Bacillus* BioBrick Box: generation and evaluation of essential genetic building blocks for standardized work with *Bacillus subtilis*. *J Biol Eng* **7**: 29.

Rietkötter, E., Hoyer, D., and Mascher, T. (2008) Bacitracin sensing in *Bacillus subtilis*. *Mol Microbiol* **68**: 768–785.

Schmalisch, M., Maiques, E., Nikolov, L., Camp, A.H., Chevreux, B., Muffler, A., *et al.* (2010) Small genes under sporulation control in the *Bacillus subtilis* genome. *J Bacteriol* **192**: 5402–5412.

Toymentseva, A.A., Schrecke, K., Sharipova, M.R., and Mascher, T. (2012) The LIKE system, a novel protein expression toolbox for *Bacillus subtilis* based on the *liaI* promoter. *Microb Cell Fact* **11**: 143.

7.3 PUBLICATION III: THE CELL ENVELOPE STRESS RESPONSE OF *BACILLUS SUBTILIS*: FROM STATIC SIGNALING DEVICES TO DYNAMIC REGULATORY NETWORK

Publication III:

Radeck J, Fritz G, Mascher T (2016) The cell envelope stress response of *Bacillus subtilis*: from static signaling devices to dynamic regulatory network. **Curr Genet**. 63(1):79-90. doi: 10.1007/s00294-016-0624-0

Curr Genet
DOI 10.1007/s00294-016-0624-0

REVIEW

The cell envelope stress response of *Bacillus subtilis*: from static signaling devices to dynamic regulatory network

Jara Radeck[1] · Georg Fritz[2] · Thorsten Mascher[1]

Received: 16 May 2016 / Revised: 9 June 2016 / Accepted: 10 June 2016

Abstract The cell envelope stress response (CESR) encompasses all regulatory events that enable a cell to protect the integrity of its envelope, an essential structure of any bacterial cell. The underlying signaling network is particularly well understood in the Gram-positive model organism *Bacillus subtilis*. It consists of a number of two-component systems (2CS) and extracytoplasmic function σ factors that together regulate the production of both specific resistance determinants and general mechanisms to protect the envelope against antimicrobial peptides targeting the biogenesis of the cell wall. Here, we summarize the current picture of the *B. subtilis* CESR network, from the initial identification of the corresponding signaling devices to unraveling their interdependence and the underlying regulatory hierarchy within the network. In the course of detailed mechanistic studies, a number of novel signaling features could be described for the 2CSs involved in mediating CESR. This includes a novel class of so-called intramembrane-sensing histidine kinases (IM-HKs), which—instead of acting as stress sensors themselves—are activated via interprotein signal transfer. Some of these IM-HKs are involved in sensing the flux of antibiotic resistance transporters, a unique mechanism of responding to extracellular antibiotic challenge.

Communicated by M. Kupiec.

✉ Thorsten Mascher
Thorsten.Mascher@tu-dresden.de

[1] Institute of Microbiology, Technische Universität (TU) Dresden, Dresden, Germany

[2] LOEWE-Center for Synthetic Microbiology (SYNMIKRO), Philipps-Universität Marburg, Marburg, Germany

Keywords Cell wall antibiotic · ECF sigma factor · Lipid II cycle · Stress response · Signal transduction · Two-component system

Introduction: the cell envelope, its enemies and guardians

The envelope is an essential structure of any bacterial cell: it separates the cell from its environment and protects its content, serves as a molecular sieve, a diffusion barrier, a communication interface and counteracts the high internal osmotic pressure, thereby keeping the cell intact (Dufresne and Paradis-Bleau 2015; Silhavy et al. 2010). Because of its essential role, it is not surprising that the cell envelope, and in particular its biosynthesis, represents a primary target for antibiotic action—both for interspecies competition within the natural habitat and in clinical therapy. In fact, literally every step in the biosynthetic pathway leading from intracellular sugar and amino acid intermediates to the extracellular peptidoglycan is targeted by at least one antibiotic (Bugg et al. 2011; Schneider and Sahl 2010).

Cell wall biosynthesis encompasses three stages, ranging from the intracellular assembly of the building block, the membrane-anchored cyclic process of shuttling them to the outside (the lipid II cycle), and finally their incorporation in the growing peptidoglycan network. Of these stages, the lipid II cycle has gained particular attention in recent years, resulting in the development of a number of promising antimicrobial peptides (AMPs), such as lantibiotics or the lipo(depsi) peptides, daptomycin and friulimicin, that interfere with its individual steps (Schneider and Sahl 2010). In addition to these 'new kids on the block', a number of 'old goodies' of clinical relevance, such as tunicamycin, moenomycin, vancomycin or bacitracin, also interfere with the lipid II cycle.

Published online: 25 June 2016

The lipid II cycle starts on the cytoplasmic side of the membrane by hooking the soluble precursor molecule *N*-acetyl-muramic acid-pentapeptide onto the lipid carrier molecule undecaprenyl phosphate (UP), generating lipid I. Onto this first membrane-associated intermediate, *N*-acetyl-glucosamine is added, resulting in the formation of lipid II, which is then transferred to the extracytoplasmic side of the membrane by the action of flippases. Once on the outside, the disaccharide pentapeptide, which represents the bricks of the murein sacculus, is then incorporated in the growing peptidoglycan network, resulting in the release of undecaprenyl pyrophosphate (UPP). In order to be recharged, this lipid carrier needs to be dephosphorylated by UPP phosphatases and flipped back to the cytoplasmic side of the membrane, before the cycle can be re-initiated once again (Dufresne and Paradis-Bleau 2015; Silhavy et al. 2010).

To survive threats to their envelope, cells have evolved countermeasures to respond to antimicrobial challenge and thereby protect the integrity of the envelope. These responses are collectively referred to as cell envelope stress responses (CESR) (Jordan et al. 2008). So far, they are all based on the antibiotic-inducible expression of genes that encode protective cellular functions, including specific resistance determinants that detoxify or remove the antimicrobial compounds from their site of action. To this end, cells must be able to perceive the threat on the outside of the cell and then subsequently transmit this information to the cytoplasm. This event ultimately initiates a cellular response, usually in the form of differential gene expression. In order to be efficient, these signaling events need to be triggered way before severe damage can occur to the envelope, that is, at sublethal antibiotic concentrations. Hence, the sensory systems must be exquisitely sensitive and the resulting cellular responses need to be mounted fast to provide sufficient and timely protection to the cell.

Bacteria possess three different regulatory principles to connect extracellular inputs to cellular responses, and all three have been shown to be involved in mediating CESR. One-component systems (1CSs), such as the bacitracin-responsive regulator BcrR of *Enterococcus faecalis* (Gauntlett et al. 2008; Gebhard et al. 2009), combine an extracellular input domain with an intracellular effector domain within a single polypeptide chain. The two functional domains are connected by transmembrane helices that serve as intramolecular signal transmitters to convert the extracellular binding event with a structural change that activates the intracellular output domain. Because of the obvious molecular restriction of such simplified protein architectures, 1CSs are rarely found in bacterial CESRs. In fact, BcrR is so far the only known example of a membrane-anchored transcriptional regulator that responds to envelope stress. In contrast, two-component systems (2CSs) and extracytoplasmic function σ factors (ECFs) are widely used in bacterial CESR networks. Both types of signaling devices split the input and output domains on two separate proteins, one acting as a membrane-anchored sensor (histidine kinase or anti-σ factor, respectively), the other as a soluble transcriptional regulator (response regulator or σ factor, respectively). Members of both phylogenetically unrelated groups are commonly found among the signaling devices mediating the cellular response to AMP challenge (Jordan et al. 2008).

The CESR network in *Bacillus subtilis* is particularly well studied (Jordan et al. 2008) and will be the focus of this review. Our goal is to provide a chronological account of its dissection, split into five 'pictures' that represent the individual milestones that lead to our increasingly detailed insight into how this regulatory network behaves, using the best-understood *B. subtilis* CESR network, the response to bacitracin challenge, as a paradigm. We will start with summarizing the initial transcriptome-driven identification of the signaling systems involved (the 'static' picture). Next, we will describe the dynamic behavior of the bacitracin network (the 'dynamic' picture) and then continue with a summary of the mechanistic insight we have gained over the last 10 years into how the individual signaling devices perceive their stimuli and mediate their responses (the 'mechanistic' picture). After introducing this background knowledge, we will then highlight the most recent developments on the anatomy and regulatory interdependence within the CESR network (the 'interdependent' picture), before concluding this mini review with a brief description of current challenges followed by an outlook of what questions still need to be addressed in the future (the 'increasingly complex' picture).

The static picture: signaling devices and inducer spectra

The development of DNA microarrays allowed for the first time to gain a comprehensive picture of the genome-wide alterations in transcriptional profiles upon perceiving stress conditions. Not surprisingly, numerous transcriptome profiling studies were performed on antibiotic challenge of bacteria in the first decade of the twenty-first century, particularly using the Gram-positive model bacterium *B. subtilis* as the organism of choice [as summarized in Wecke and Mascher (2011)]. Such studies not only helped to identify compound-specific transcriptional profiles and putative resistance determinants encoded by the specifically induced genes, they also served as starting points for uncovering the underlying signal transduction and gene regulation.

A number of independent DNA microarray experiments compared the transcriptional profile of AMP-induced cultures versus uninduced control samples. Together with

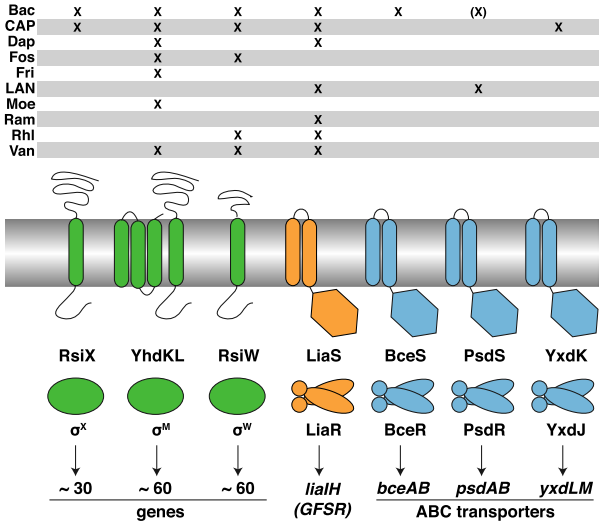

Fig. 1 The regulatory network of CESR in *B. subtilis*. In *B. subtilis*, three ECF σ factors (*green*) and four two-component systems (*orange* and *blue*) respond to antibiotics targeting the cell envelope and its biosynthesis. *X* indicates activation of the specific system by the indicated compound (Jordan et al. 2008; Wecke et al. 2011). *Bac* bacitracin, *CAP* cationic antimicrobial peptides, *Dap* daptomycin, *Fos* fosfomycin, *Fri* friulimicin, *LAN* lantibiotics, *Moe* moenomycin; *Ram* ramoplanin, *Rhl* rhamnolipids, *Van* vancomycin. Modified from Jordan et al. (2008)

detailed follow-up studies, four 2CSs and (at least) three ECFs were identified to be responsible for the observed CESR-specific differential gene expression (Fig. 1). Identification of the 2CSs was based on co-occurrence and genomic context conservation of the genes encoding the signaling devices next to their stress-inducible target genes. In contrast, the role of the ECFs was uncovered by the presence of specific target promoter motifs upstream of the differentially expressed genes (Cao et al. 2002; Mascher et al. 2003; Pietiäinen et al. 2005; Wecke et al. 2009).

Out of the four CESR-inducible 2CSs, three represent paralogous, so-called Bce-like systems, named for the best-understood example, BceRS-BceAB (Fig. 1, blue). These systems are each composed of a 2CS and an ABC transporter, which are functionally closely linked and encoded by two neighboring operons. Together, they form AMP-specific detoxification modules that efficiently remove (extracellular) AMPs from their site of action, thereby mediating high levels of resistance (Dintner et al. 2011; Mascher et al. 2003), as discussed below. Bce-like systems are highly conserved and widely distributed in the *Firmicutes* bacteria (Dintner et al. 2011; Joseph et al. 2002). Each responds to a small number of closely related AMPs: the Bce system responds primarily to bacitracin, the Psd system is preferentially induced by a number of lantibiotics, while the response of the Yxd system is triggered by the human AMP LL-37 (Pietiäinen et al. 2005; Staroń et al. 2011).

The fourth system, LiaRS, shows a much wider inducer spectrum. It strongly responds to a number of unrelated AMPs (Fig. 1, orange) that mostly interfere with the lipid II cycle of cell wall biosynthesis (hence the name: LiaRS stands for lipid II-interfering antibiotics regulator and sensor) (Mascher et al. 2004). In addition, a number of rather unspecific triggers of the Lia response, such as alkaline shock or detergents, interfere with membrane integrity. LiaRS, together with its membrane-anchored inhibitor protein LiaF, is also highly conserved in the low G+C Gram-positive bacteria (Mascher 2006). While homologous systems in streptococci and staphylococci are responsible for mounting general CESRs [summarized in Schrecke et al. (2012)], the Lia system of *B. subtilis* has evolved to coordinate a phage-shock protein-like response, with the neighboring *liaIH* operon representing the only relevant target of LiaR-dependent gene expression (Mascher et al. 2003, 2004). For many years after its initial characterization, the physiological role of this strictly regulated response remained elusive and a clear function of the LiaRS system in the CESR of *B. subtilis* could only be established very recently (see later sections).

A unifying feature of all HKs involved in orchestrating the CESR is their unique protein architecture. Their input domains consist of two transmembrane helices that are connected by a very short extracytoplasmic loop of less than 10–20 amino acids. Because of this minimalistic architecture, it was initially assumed that such kinases can only perceive envelope stress from within the membrane interface. Hence, they were named intramembrane-sensing HK (Mascher 2006; Mascher et al. 2003), a concept that has meanwhile been modified (Mascher 2014), as will also be described below.

In contrast to the clearly defined 2CS-dependent responses, the differential gene expression mediated by ECFs in response to cell envelope stress is much more complex (Fig. 1, green). This is due to the fact that the regulons controlled by the major ECFs involved in CESR—σ^M, σ^W, and σ^X—are rather complex (Helmann 2016): σ^M controls the largest regulon of about 60 genes, many of which are key for cell envelope homeostasis (Eiamphungporn and Helmann 2008). σ^W controls an 'antibiosis regulon' that also consists of about 60 genes, with many of the functions related to antibiotic resistance, especially against membrane-active agents. Some of the about 30 σ^X-target genes (most of which are also regulated by σ^V) are crucial for lantibiotic resistance and the homeostasis of the cytoplasmic membrane (Helmann 2016; Kingston et al. 2013). Due to the highly similar promoter motifs of the three ECFs, there is a significant degree of regulatory overlap between the different regulons at the level of promoter

recognition (Kingston et al. 2013; Mascher et al. 2007). Each of the three ECFs are activated by a number of different unrelated cell wall antibiotics and they most likely respond to some secondary effect of antibiotic action, such as the damage occurring in their presence. To a first approximation, the ECFs of *B. subtilis* orchestrate mostly general protective measures and homeostatic adaptations to envelope stress, while the 2CS-dependent responses are highly dynamic and rather specific, usually consisting of a single target operon each (Fig. 1). Taken together, this first stage of analyzing the CESR provided a detailed picture of the regulatory systems involved in responding to AMPs, the range of stressors activating them, and the genes controlled by them.

The dynamic picture: diffusion and temporal inducer gradients

The initial results described above are based on analyzing the response of *B. subtilis* to a whole array of different AMPs, targeting different steps of the lipid II cycle. This allowed gaining a comprehensive picture of the CESR regulation in this organism. In contrast, most of the increasingly detailed follow-up studies then focused on the response to a single compound, bacitracin. This cyclic non-ribosomally produced AMP is synthesized by strains of *B. subtilis* and *B. licheniformis* (Ming and Epperson 2002). While bacitracin is not produced by the laboratory wild-type strain of *B. subtilis* that was used for all studies, this antibiotic nevertheless is expected to play a role in the natural habitat. Hence, it is not surprising that *B. subtilis* evolved a multilayered response towards bacitracin, involving all three types of signaling systems described above: It strongly triggers the Lia and Bce response and, to weaker extend, also the Psd- and the ECF-dependent responses (Fig. 1). The latter also induces the expression of a second bacitracin resistance determinant, a UPP phosphatase encoded by the *bcrC* gene. In addition, the σ^B-dependent general stress response was also transiently induced, indicative for the severity of the stress applied (Mascher et al. 2003).

Some years after the initial description of the bacitracin stress response (Mascher et al. 2003), we returned to this regulatory network. We realized that the initial microarray studies, while providing a comprehensive picture on an organisms' capacity to respond to a certain antimicrobial compound, represented a highly artificial situation. Challenging growing cultures of *B. subtilis* with sublethal, but nevertheless high amounts of an antibiotic, represents a sudden and rather drastic antibiotic shock that does not reflect the natural situation for which the stress response networks have evolved for: in the natural environment, the soil, antibiotic challenge (e.g., production of the antibiotic by neighboring competitors) will most likely occur as an increasing antibiotic gradient over time. We, therefore, wondered how the well-known bacitracin stress network would respond when confronted with gradually increasing bacitracin concentrations (Rietkötter et al. 2008).

Indeed, detailed studies demonstrate that the individual signal systems within the bacitracin stress response network have very different sensitivities and response characteristics towards this compound (Fig. 2) (Rietkötter et al. 2008). The Bce system is the most sensitive system and also shows the highest rate of induction even at very low bacitracin concentrations. In contrast, the Lia system and ECF-dependent gene expression are only activated at higher concentrations. When faced with a bacitracin gradient increasing over time, this ultimately means that the Bce system is the first to respond. In many cases, *B. subtilis* will, therefore, only induce a single operon, *bceAB*, encoding the most efficient bacitracin resistance determinant, the ABC transporter BceAB, which removes bacitracin from its site of action. Only if this response is not sufficient, and bacitracin stress prevails or even increases, will the other systems be induced at all, thereby providing additional layers of protection. These results, therefore, suggest that the bacitracin network has evolved for efficiency, that is, maximizing the benefits while simultaneously minimizing the costs.

In addition to unraveling the regulatory dynamics within the bacitracin stress response network, this second study also provided first insights into the signaling mechanism and regulatory specificity of the Bce system and its paralogs (Rietkötter et al. 2008). It demonstrated that the ABC transporter BceAB—in addition to providing high-level resistance against bacitracin—is also mandatorily required for sensing this compound, as discussed in the next section. Moreover, we observed a regulatory crosstalk between the paralogous Bce and Psd systems at the level of the histidine kinase/response regulator interface: upon bacitracin treatment, the histidine kinase BceS is able to phosphorylate the non-cognate response regulator PsdR (Rietkötter et al. 2008). This observation represents one of the rare cases in which such a regulatory crosstalk has been observed in wild-type cells, that is, when both 2CSs involved still are intact. This result is indicative for the close phylogenetic relationship between the two systems, most likely as a result of a gene duplication event not too far away in the evolutionary history of *B. subtilis*.

The mechanistic picture: intramembrane-sensing histidine kinases, interprotein signal transfer and flux-sensing

Given that the inducer spectra of three CESR stress response modules (BceAB, LiaIH and BcrC) are very

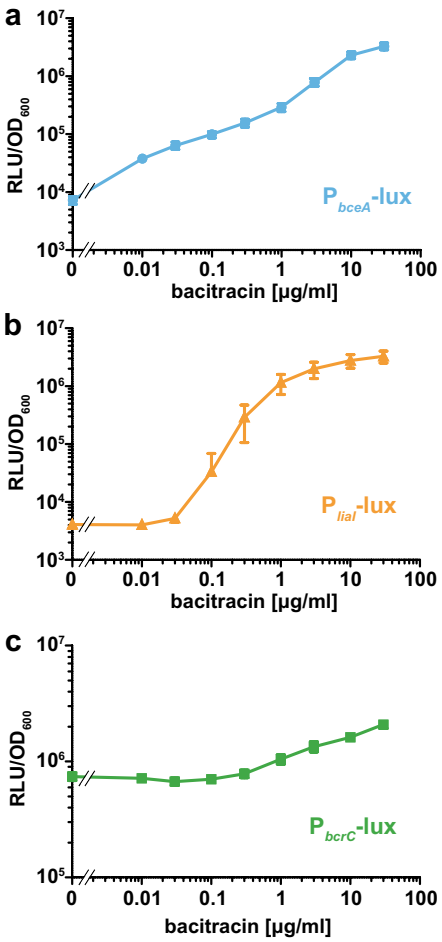

Fig. 2 Dose-dependent activation of resistance modules in an unperturbed CESR network. Target promoter activities of **a** P_{bceA}, **b** P_{lial} and **c** P_{bcrC} in *B. subtilis*, expressed as the specific luciferase activity (RLU/OD_{600}) 1 h after addition of indicated amounts of bacitracin. Measurements were performed during exponential growth phase in LB medium at 37 °C in a microtiter plate reader. *Data points* and *error bars* indicate means and standard deviations derived from at least three biological replicates. Data are based on Radeck et al. (2016)

diverse, and that even for the same inducer (e.g., bacitracin) the expression of these modules occurs at different induction thresholds, a salient question arises: what are the actual cues that trigger the induction of these systems? Do they all respond directly to the compound, or rather to downstream effects on cell physiology? First steps towards answering these questions were derived from genetic observations, noting that the 2CSs regulating the expression of the CESR modules feature unusual histidine kinases (HKs) (Fig. 3). As mentioned above, these HKs are characterized by an N-terminal input domain consisting of two transmembrane helices with a short extracellular linker of less than 10–20 amino acids (Mascher 2006), which is insufficient for stimulus perception per se. This originally led to the idea that these kinases sense their stimuli at or within the membrane interface, coining the term 'intramembrane-sensing histidine kinase' (IM-HK) (Mascher et al. 2003). However, it later became clear that IM-HKs are genetically and functionally linked to accessory membrane proteins (Mascher 2006; Mascher et al. 2006), which are essential for stimulus perception (Jeong et al. 2012; Jordan et al. 2006; Luttmann et al. 2012; Rietkötter et al. 2008). As detailed below for the Bce and the Lia system, these accessory membrane proteins typically act as sensors, whereas the role of the IM-HKs is reduced to their ability to transfer the signal to the downstream response regulator (Mascher 2014). Hence, understanding the function of these accessory membrane proteins and their interaction with their cognate IM-HK is key for understanding the nature of the stimulus perceived by these signaling devices.

The BceRS-BceAB complex acts as an antibiotic flux sensor

The expression of the ABC transporter BceAB is regulated by the histidine kinase BceS and the response regulator BceR, which are encoded in an operon upstream of *bceAB* (Mascher et al. 2003). Strikingly, deletion of the BceB permease completely abolished the ability of the BceRS 2CS to respond to bacitracin (Rietkötter et al. 2008), suggesting that the transporter itself might be involved in signaling. Moreover, a single point mutation in the Walker B motif of the ATPase BceA (exhibiting a highly reduced rate of ATP hydrolysis) also abolished signaling via BceRS, showing that ATP hydrolysis, and thus active transport of bacitracin, is required for stimulus perception (Rietkötter et al. 2008). Bacterial two-hybrid analyses together with in vitro pull-down assays further showed that the permease BceB forms a complex with the histidine kinase BceS (Dintner et al. 2014) (Fig. 3a), and amino acid residues crucial for this contact have been identified in the permease BceB (Kallenberg et al. 2013).

This lead to three plausible roles explaining the essentiality of the BceAB transporter in the regulatory pathway: in the simplest scenario, the transporter acts as a mere ligand-binding component in a sensory complex with the HK, allowing the cell to detect the ambient concentration of bacitracin (Bernard et al. 2007). Alternatively, it was proposed that the transporter may act as an importer of bacitracin, releasing it into the cytoplasm for degradation, where it might then be sensed by the HK (Hiron et al. 2011; Rietkötter et al. 2008). The third conceivable scenario was that the HK activity is determined by the transport activity of individual transporters (Rietkötter et al. 2008). Strikingly, using a systems approach combining quantitative gene expression analysis with computational modeling, we could

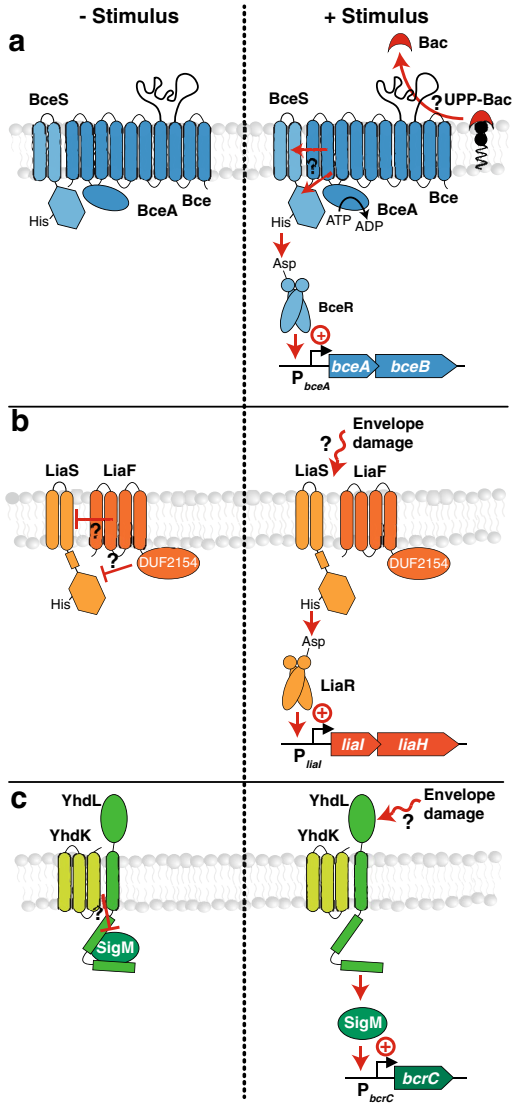

Fig. 3 Mechanism of signal transduction of the Bce and Lia systems and the ECF σ factor σ^M. **a** In the absence of bacitracin, the ABC Transporter BceAB and the associated IM-HK BceS remain inactive. After the addition of bacitracin and formation of the UPP-Bac complex, BceB recognizes UPP-Bac and removes bacitracin from its target employing a so far unknown transport mechanism dependent on ATP hydrolysis by BceA. This transport activity is transmitted via a yet unknown mechanism and acts as the stimulus for BceS activation. The HK in turn activates the cognate response regulator BceR via phosphotransfer which then upregulates transcription of *bceAB* (Fritz et al. 2015; Ohki et al. 2003). **b** In the absence of a stimulus, LiaF acts as an inhibitor of the IM-HK LiaS. Cell envelope damage triggers the activation of LiaS and hence phosphorylation of the cognate response regulator LiaR. LiaR dimerizes and activates transcription of *liaIH* (Jordan et al. 2006; Schrecke et al. 2013). **c** In the absence of stress, the anti-σ factor YhdKL sequesters σ^M to the membrane. Upon stimulus perception—triggered by cell envelope perturbations—YhdKL release σ^M into the cytoplasm where it recruits the RNA polymerase to its target promoters, including P_{bcrC} (Helmann 2016; Horsburgh and Moir 1999)

recently show that only the last scenario is compatible with all available data, suggesting that the sensory complex of BceB-BceS acts as a 'flux-sensor' that measures the load of individual transporters (Fritz et al. 2015). This sensory strategy then allows the cell to detect its current capacity to deal with the antibiotic challenge and thus precisely respond to the need for more transporters. Based on the fact that to date over 200 Bce-like systems are found in protein databases, and given that their HKs and ABC transporters have coevolved (Dintner et al. 2011), it seems likely that flux sensing is a widespread regulatory principle to control AMP resistance modules in *Firmicutes* bacteria.

The LiaRS-LiaF three-component system responds to inhibition of the lipid II cycle

The LiaRS 2CS regulates expression of the hexacistronic *liaIH-liaGFSR* operon (Jordan et al. 2006). In the absence of envelope stress, a weak constitutive promoter upstream of *liaG* ensures a basal expression level of *liaGFSR*, whereas inducing conditions lead to an upregulation of a major 1.1-kb transcript containing *liaIH* and a 4-kb transcript encompassing the entire locus. While the function of the small membrane protein LiaG is still elusive, the deletion of *liaF* resulted in a 'locked-ON' phenotype that displayed strong constitutive *liaIH-liaGFSR* expression even in the absence of envelope stress (Jordan et al. 2006), suggesting that LiaF acts as an inhibitor of LiaS in the absence of envelope stress (Fig. 3b). In line with these findings, increased production of LiaS was sufficient to overcome the inhibitory effect by LiaF, showing that the excess stoichiometry between LiaF and LiaS (~5:1) is important to keep LiaS in an inactive ('phosphatase ON') state (Schrecke et al. 2013). LiaF is a membrane protein that contains four membrane-spanning regions in its N-terminus and features a domain of unknown function (DUF2154) in its C-terminus, which displays structural homology to a putative cell adhesion protein and is predicted to reside in the cytoplasm. Spontaneous in-frame deletions in the C-terminus of LiaF revealed a locked-ON phenotype similar to the *liaF* deletion strain, suggesting that the C-terminus is functionally important for stimulus perception and/or signaling to LiaS (Jordan et al. 2006).

Although the precise stimulus for the LiaFSR system remains elusive to date, later work suggested that it is unable to sense AMPs directly (Wolf et al. 2012). Specifically, the response of the P_{lial} promoter towards its inducers bacitracin, mersacidin, vancomycin, nisin and daptomycin was completely absent in inducible L-forms of *B. subtilis*, which were depleted of cell wall precursors by repression of the *murE* operon (Wolf et al. 2012). This strongly suggested that the LiaFSR system requires the presence

of a functional cell wall biosynthetic machinery, potentially requiring lipid I and/or lipid II, to sense the downstream effects of the five antibiotics mentioned before. This prompted the notion that the LiaFSR system might act as an indirect, damage-sensing signal-transducing system, in line with its role as a secondary resistance determinant that is only activated if the primary resistance determinant BceAB provides incomplete protection (Radeck et al. 2016), as discussed below.

Regulation of cell wall homeostasis by the σ^M regulon

The third main player in the bacitracin stress response network is the UPP phosphatase BcrC, the corresponding *bcrC* gene being under control of σ^M regulation (Cao and Helmann 2002). The gene encoding σ^M is co-transcribed in an operon with the genes of the anti-σ factors YhdL and YhdK, which tightly control the activity of σ^M in response to cell envelope stress (Fig. 3c) (Horsburgh and Moir 1999). The small membrane protein YhdK features three transmembrane helices and was shown to interact with YhdL to negatively regulate σ^M in the absence of membrane stress (Yoshimura et al. 2004). Although the precise molecular mechanisms remain to be identified, it was demonstrated that the cytoplasmic N-terminus of YhdL is involved in σ^M binding, while the single transmembrane helix of YhdL is required for interaction with YhdK and the extracytoplasmic C-terminus might function as sensory domain (Fig. 3c) (Yoshimura et al. 2004). Like the LiaFSR system described above, σ^M is activated by a range of different cell envelope-perturbing conditions, but the precise molecular cues detected by YhdLK/σ^M are still a matter of debate, as discussed recently (Helmann 2016).

The interdependent picture: a network at last

More than a decade of studying the bacitracin-triggered CESR of *B. subtilis* has provided us with a detailed knowledge on the composition of the systems mediating the underlying gene regulation. As outlined in the previous sections, the dynamic behavior of the systems, as well as their mechanism of signal transduction, has been uncovered. But what was still missing was a proof that these signaling systems indeed form a regulatory network, that is, interact with and influence each other's behavior such that the overall response can only be described and understood in light of all of its constituents. Most recently, the first insights into this interdependence have been provided (Radeck et al. 2016). This work demonstrates a clear hierarchy, co-dependence and active redundancy of signaling systems involved in mediating the bacitracin CESR, as will be summarized below (Fig. 4).

BceAB is the primary bacitracin resistance module that masks the contribution of the other CESR modules

So far, a role in mediating bacitracin resistance had only been established for BceAB and BcrC, but not for LiaIH (Cao and Helmann 2002; Ohki et al. 2003; Wolf et al. 2010). This led to the question, if a potential role of LiaIH is masked by the efficiency of BceAB in removing bacitracin. To address the question of whether such masking effects exist within the bacitracin resistance network, mutants deleted of all possible combinations of the three resistance modules were tested for their susceptibility towards bacitracin. These experiments confirmed that BceAB indeed acts as the primary resistance determinant, while the (full) potential of the secondary resistance determinants LiaIH and BcrC was only revealed in a *bceAB* deletion mutant: in this genetic background, the presence of LiaIH increased the minimal inhibitory bacitracin concentration (MIC) by 6-fold, while BcrC mediated a 24-fold increased resistance. These data indicate that in wild-type cells, these two damage-induced systems act as "fallback"-mechanisms in a redundant manner to BceAB (Radeck et al. 2016). Strikingly, this redundancy is also reflected in the interconnections of the three systems on the regulatory level: in a *bceAB* deletion mutant, the P_{bcrC} and P_{liaI} promoters were strongly induced already at low bacitracin concentrations, whereas overproduction of BceAB shifted the responses of P_{bcrC} and P_{liaI} to much higher bacitracin levels (Radeck et al. 2016). This further supported the notion that the activities of the secondary, damage-sensing layer of the CESR are directly slaved to the exhaustion of the primary layer of bacitracin resistance.

BcrC and LiaIH provide a secondary and redundant layer of bacitracin resistance that influences the overall behavior of the network

As highlighted above, the contribution of BcrC and especially LiaIH to bacitracin resistance is only modest and partially—or in the case of LiaIH completely—masked by the action of the primary resistance layer BceAB. Nevertheless, these two determinants are functionally important, since they can partially compensate for the loss or exhaustion of BceAB activity. While the influence of BceAB levels on LiaRS- and σ^M-dependent gene regulation described above was not surprising, controlled modulations of BcrC and LiaIH levels revealed additional layers of complexity within the bacitracin stress response network.

In case of BcrC, the basal activity of both P_{bceA} and P_{liaI} was increased by an order of magnitude in a *bcrC* mutant, even in the absence of bacitracin. Overproduction of BcrC, on the other hand, only slightly reduced the response of both promoters, but only in the presence of

low concentrations of bacitracin (Radeck et al. 2016). This effect of BcrC levels is remarkable and highlights a tight integration of bacitracin stress response regulation with the native homeostasis of cell wall biosynthesis. Moreover, it indicates that a limitation in UPP-phosphatase levels can be perceived by both damage- (LiaRS) and drug-sensing (BceRS) CESR systems. Both aspects will be discussed in the last section of this review.

In contrast to BcrC and BceAB, LiaIH does not play a role in mediating bacitracin resistance in *B. subtilis* wild-type cells. Accordingly, varying the amounts of LiaIH does not influence P_{bceA} activity (Radeck et al. 2016). In contrast, elevated levels of LiaIH led to a tenfold increased basal activity of P_{liaI}, even in the absence of bacitracin, indicating that overproduction of these proteins already results in generating envelope stress that can be perceived by the Lia system (Radeck et al. 2016). Interestingly, the native control of LiaIH production seems to be required for full P_{liaI} activation at medium to high bacitracin concentrations. This observation indicates a potential auto-regulatory function of LiaIH output on LiaFSR sensing that has not been detected previously (Schrecke et al. 2013). The mechanism behind this phenomenon remains to be elucidated.

Interdependence of the bacitracin resistance determinants

Taken together, we propose the following model for the response to bacitracin (Fig. 4). In an unchallenged wild-type cell, BceAB and LiaIH are present at very low levels, whereas BcrC is highly expressed due to its crucial part in lipid II cycle progression. Upon addition of low amounts of bacitracin, it binds to a fraction of UPP, forming inactive UPP-Bac (Economou et al. 2013; Storm and Strominger 1974), which cannot be dephosphorylated by BcrC. Under such conditions, there is still enough unbound UPP available for normal carrier recycling to continue cell wall synthesis. Moreover, already at this early stage, BceAB detects UPP-Bac and removes bacitracin from its target, thereby stimulating its own expression via a flux-sensing mechanism (Fritz et al. 2015) and detoxifying the cell envelope before damage can occur. If the bacitracin level is increased further, despite upregulation of BceAB, cell wall synthesis is being affected and first damage to the cell envelope occurs. This induces the Lia system (Wolf et al. 2012), which is part of the secondary layer of resistance that protects the cell envelope by a mechanism yet to be identified (Radeck et al. 2016). Finally, at even higher bacitracin concentrations, perturbations of the lipid II cycle lead to activation of σ^M, which in turn upregulates the expression of cell envelope protecting proteins, amongst them BcrC (Cao and Helmann 2002; Helmann 2016). This UPP phosphatase reduces the pool levels of UPP, thereby diminishing the number of cellular targets for bacitracin binding (Cao and Helmann 2002; Radeck et al. 2016). The overall efficiency of this intricately regulated, triple-layered resistance network is underscored by the fact that wild-type cells are about 5000-fold more resistant towards bacitracin than a triple mutant devoid of all three resistance modules (Radeck et al. 2016).

The increasingly complex picture: stressed inside out and further on

As outlined by the sections above, over 15 years of research have painted an increasingly detailed picture of the bacitracin stress response network, but at the same time showed that we still seem to miss many pieces of the puzzle. Some of the most interesting questions that remain to be addressed are a direct result of the most recent study on the anatomy and interdependence of the bacitracin stress response network (Radeck et al. 2016). Others go back to earlier studies, as will be described below.

Intrinsic cell wall homeostasis versus extrinsic AMP challenge

Probably the most remarkable observation from the recent study is the significantly increased basal expression from P_{bceA} and P_{liaI} in a strain lacking BcrC. This UPP phosphatase was initially described as a non-essential stress-inducible protein (Cao and Helmann 2002; Petersohn et al. 2001). But the elevated levels of *bceA/liaI* promoter activity indicate that the absence of BcrC generates a bottleneck in cell wall biosynthesis that is perceived as cell envelope stress. BcrC, therefore, plays a crucial role in the normal cycling of cell envelope building blocks, in addition to its inducible expression in the presence of bacitracin and other inhibitors of the lipid II cycle. This demonstrates that the rate of lipid II cycling is an important parameter in perceiving envelope stress—at least in the case of AMPs interfering with these membrane-anchored processes. A deeper understanding of the physiology behind the CESR, therefore, requires going beyond a 'simple' analysis of the behavior of the underlying regulatory network. Instead, an integrative approach will be necessary that combines the analysis of lipid II cycle homeostasis with its inhibition by AMPs, using the CESR-inducible reporters as indicators of the overall cellular stress perceived.

Drug sensing versus target sensing

The results described in the previous section raise another issue that adds to the complexity of the CESR. As described in the mechanistic picture section, BceRS-like

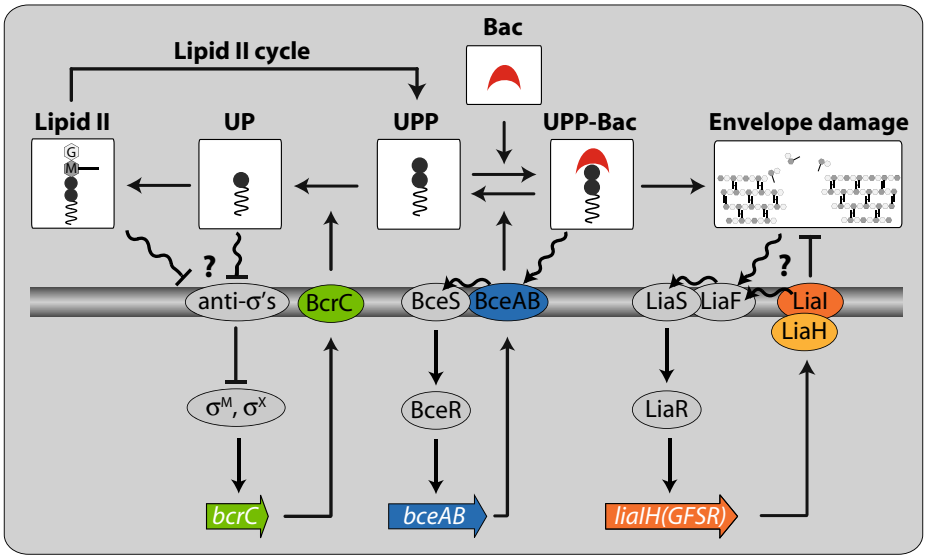

Fig. 4 Proposed architecture of the bacitracin resistance network in *B. subtilis*. Bacitracin tightly binds to UPP, resulting in an inactive UPP-Bac complex that prevents UPP recycling in the lipid II cycle. As a result, the pool of lipid carrier available for cell wall synthesis is drastically reduced, resulting in a cessation of cell wall biosynthesis. The presence of UPP-Bac is recognized by the ABC transporter BceAB, which in turn triggers upregulation of *bceAB* expression via the 2CS BceRS. BceAB efficiently removes bacitracin from UPP, which then allows BcrC to dephosphorylate UPP. Depletion of lipid II-cycle intermediates, such as UP or lipid II itself, might act as stimuli to induce *bcrC* expression (Inoue et al. 2013; Lee and Helmann 2013; Meeske et al. 2015), but the precise mechanisms remain to be identified. BcrC itself contributes to bacitracin resistance by competing for the mutual target UPP. The damage caused by bacitracin action is also perceived by the LiaFSR three-component system, resulting in a strong upregulation of *liaIH* expression. LiaIH, in turn, is needed to fully activate the Lia response by a so far unknown mechanism. *Bac* bacitracin, *UP* undecaprenyl phosphate, *UPP* undecaprenyl pyrophosphate

2CS sense their stimuli indirectly through their associated BceAB-like ABC transporters via a flux-sensing mechanism (Fritz et al. 2015). This mechanism not only allows the cell to accurately adjust the amount of BceAB transporters to the current need. It also represents a direct connection of the input (binding and hence sensing AMPs) with the output (removal of AMPs from their site of action) based on the transport mechanism itself. But what is the true nature of the substrate bound by the BceB permease? Initial evidence from cell wall-less L-forms of *B. subtilis* showed that the Bce system is triggered in the absence of cell wall biosynthesis (Wolf et al. 2012), arguing for a 'drug-sensing' mechanism of stimulus perception. This view was supported by in vitro results indicating that BceB is able to bind bacitracin directly (Dintner et al. 2014). In vivo results, on the other hand, argued for BceB binding UPP and even suggested that this transporter might play a role as a UPP flippase of the cycle (Kingston et al. 2014). The most recent observation that a tightened bottleneck in the lipid II cycle, provoked by the absence of the UPP phosphatase BcrC, increases P_{bceA} activity (Radeck et al. 2016) indeed points towards UPP as a possible binding partner for BceB. If taken together, the combined evidence can be interpreted such that BceB—while being able to bind to either bacitracin or UPP directly, but presumably with low affinity—most likely uses UPP-bound bacitracin as its natural high-affinity substrate. This would indeed be the physiologically most meaningful stimulus, since it provides a direct measure for the potentially 'harmful' fraction of bacitracin around a given cell. But further analysis will be necessary to prove this hypothesis.

Extrinsic AMP challenge versus intrinsic AMP production

As a soil organism, *B. subtilis* has to compete for the limited resources of this habitat. One aspect of this competition is the production of antibiotics that suppress the growth of other microbes trying to inhabit the same niche. Indeed, the genome of *B. subtilis* encodes a number of gene clusters that are predicted to be involved in the biosynthesis of antimicrobial compounds, including AMPs. These AMPs are controlled by the master regulator of sporulation, Spo0A, and are produced as part of the complex differentiation cycle that ultimately results in the production of highly resistant endospores. To delay the commitment to sporulate, *B. subtilis* produces two cannibalism toxins, the sporulation delay protein SDP and the sporulation killing factor SKF.

Both AMPs are secreted to the environment to kill sibling cells that have not yet activated Spo0A and hence neither produces the cannibalism toxins nor the corresponding auto-immunity proteins. In a multicellular context of a biofilm, for instance, this SDP/SKF-sensitive subpopulation is thus sacrificed. Their death releases nutrients that allow the cannibal subpopulation to overcome temporary phases of starvation without the need to sporulate (Gonzalez-Pastor 2011). In a recent report, it was demonstrated that the Bce and Psd system strongly respond to both cannibalism toxins (Höfler et al. 2016). In liquid cultures, SKF seems to be the predominant stimulus, but SDP also contributes to the overall response (Höfler et al. 2016). Likewise, the Lia system seems to be induced by yet another poorly characterized AMP encoded by the *yydF* gene (Butcher et al. 2007). The physiological relevance of the induction of multiple CESR modules by intrinsically produced AMPs remains to be identified, since no resistance phenotype could be demonstrated in any of these cases.

The link of intrinsically produced AMPs to differentiation might open another door into trying to understand the physiological relevance of the corresponding CESR: while sporulation and cannibalism are phenomena that can be observed in individual cells grown in liquid cultures, they nevertheless only start making sense in the context of multicellular communities. *B. subtilis* has emerged as a paradigm not only for understanding a complex regulatory cascade orchestrating a differentiation program, but also to studying this cascade in the context of bacteria as multicellular organisms (Kovács 2016). This aspect has been largely overlooked for the longest time, since the reference strains are highly domesticated after propagation in the defined laboratory environment over decades. This resulted in a loss of the more social phenotypes and complex behavioral (that is, multicellular) traits associated with differentiation and sporulation (Pollak et al. 2015). It is overdue, to return to the undomesticated ancestor strains for studying intrinsic AMP production and the corresponding stress responses in the light of such social, multicellular aspects of differentiation.

Interdependence between σ^W and Lia response

The recently published study on the interdependence within the bacitracin stress response network is not the first report demonstrating that individual CESR systems affect each other's activity. Indeed, it might be worthwhile to return to rather old observations that demonstrated a regulatory interference between the Lia response and σ^W-dependent gene expression. Challenging *B. subtilis* with alkaline shock (a sudden upshift of the external pH to about 9) strongly induces the σ^W response and also slightly triggers LiaR-dependent gene expression. Remarkably, this pH-dependent upregulation of *liaIH* expression completely disappears if *sigW* is deleted (Wiegert et al. 2001). A comparable observation has been made in a second study on the response of *B. subtilis* towards the AMP LL-37, which belongs to the cathelicidin family of amphipathic and α-helical peptides of the human immune defense. Again, a strong induction of the σ^W response and a moderate activation of LiaR-dependent gene expression are reported, while the Lia response is lost under the same experimental conditions if *sigW* is deleted (Pietiäinen et al. 2005). At first glance, both results are counter-intuitive, since loss of one stress-responsive system should increase the cellular stress observed by another damage-responsive system. But the fact that a strong induction of σ^W combines with a rather moderate activation of the Lia response might indicate that the Lia system in fact does not directly respond to the stressor applied in the above experiments (alkaline shock and LL-37, respectively), but instead indirectly responds to the sudden upregulation of some of the σ^W-controlled genes. The protein function encoded by these genes would then generate the stress that induces the Lia response. Given the size of the σ^W regulon, such a search may not be straightforward, but it might be a worthwhile endeavor in trying to identify the still elusive true stimulus sensed by the Lia system.

Acknowledgments The authors would like to acknowledge the contributions of numerous co-workers of the Mascher group, who by their dedication, hard work and intellectual input shaped our picture of the cell envelope stress response of *B. subtilis* in the past decade.

Compliance with ethical standards

Funding Work on the cell envelope stress response of *B. subtilis* in the Mascher and Fritz groups was continuously supported by Grants from the Deutsche Forschungsgemeinschaft (DFG) (Grants MA 3269, MA2837/1-3, and MA2837/3-1 to TM as well as Grant FR 3673/1-2 to GF).

Conflict of interest The authors declare that they have no conflict of interest.

References

Bernard R, Guiseppi A, Chippaux M, Foglino M, Denizot F (2007) Resistance to bacitracin in *Bacillus subtilis*: unexpected requirement of the BceAB ABC transporter in the control of expression of its own structural genes. J Bacteriol 189:8636–8642. doi:10.1128/jb.01132-07

Bugg TD, Braddick D, Dowson CG, Roper DI (2011) Bacterial cell wall assembly: still an attractive antibacterial target. Trends Biotechnol 29:167–173. doi:10.1016/j.tibtech.2010.12.006

Butcher BG, Lin Y-P, Helmann JD (2007) The *yydFGHIJ* operon of *Bacillus subtilis* encodes a peptide that induces the LiaRS two-component system. J Bacteriol 189:8616–8625. doi:10.1128/JB.01181-07

Cao M, Helmann JD (2002) Regulation of the *Bacillus subtilis bcrC* bacitracin resistance gene by two extracytoplasmic function sigma factors. J Bacteriol 184:6123–6129. doi:10.1128/JB.184.22.6123-6129.2002

Cao M, Kobel PA, Morshedi MM, Wu MF, Paddon C, Helmann JD (2002) Defining the Bacillus subtilis σ^W regulon: a comparative analysis of promoter consensus search, run-off transcription/macroarray analysis (ROMA), and transcriptional profiling approaches. J Mol Biol 316:443–457. doi:10.1006/jmbi.2001.5372

Dintner S, Staron A, Berchtold E, Petri T, Mascher T, Gebhard S (2011) Co-evolution of ABC-transporters and two-component regulatory systems as resistance modules against antimicrobial peptides in Firmicutes bacteria. J Bacteriol 193:3851–3862. doi:10.1128/JB.05175-11

Dintner S, Heermann R, Fang C, Jung K, Gebhard S (2014) A sensory complex consisting of an ATP-binding cassette transporter and a two-component regulatory system controls bacitracin resistance in *Bacillus subtilis*. J Biol Chem 289:27899–27910. doi:10.1074/jbc.M114.596221

Dufresne K, Paradis-Bleau C (2015) Biology and assembly of the bacterial envelope. In: Krogan PJN, Babu PM (eds) Prokaryotic systems biology. Springer, Cham, pp 41–76

Economou NJ, Cocklin S, Loll PJ (2013) High-resolution crystal structure reveals molecular details of target recognition by bacitracin. Proc Natl Acad Sci USA 110:14207–14212. doi:10.1073/pnas.1308268110

Eiamphungporn W, Helmann JD (2008) The *Bacillus subtilis* σ^M regulon and its contribution to cell envelope stress responses. Mol Microbiol 67:830–848. doi:10.1111/j.1365-2958.2007.06090.x

Fritz G, Dintner S, Treichel NS, Radeck J, Gerland U, Mascher T, Gebhard S (2015) A new way of sensing: need-based activation of antibiotic resistance by a flux-sensing mechanism. MBio 6:e00975. doi:10.1128/mBio.00975-15

Gauntlett JC, Gebhard S, Keis S, Manson JM, Pos KM, Cook GM (2008) Molecular analysis of BcrR, a membrane-bound bacitracin sensor and DNA-binding protein from *Enterococcus faecalis*. J Biol Chem 283:8591–8600. doi:10.1074/jbc.M709503200

Gebhard S, Gaballa A, Helmann JD, Cook GM (2009) Direct stimulus perception and transcription activation by a membrane-bound DNA binding protein. Mol Microbiol 73:482–491. doi:10.1111/j.1365-2958.2009.06787.x

Gonzalez-Pastor JE (2011) Cannibalism: a social behavior in sporulating *Bacillus subtilis*. FEMS Microbiol Rev 35:415–424. doi:10.1111/j.1574-6976.2010.00253.x

Helmann JD (2016) *Bacillus subtilis* extracytoplasmic function (ECF) sigma factors and defense of the cell envelope. Curr Opin Microbiol 30:122–132. doi:10.1016/j.mib.2016.02.002

Hiron A, Falord M, Valle J, Debarbouille M, Msadek T (2011) Bacitracin and nisin resistance in *Staphylococcus aureus*: a novel pathway involving the BraS/BraR two-component system (SA2417/SA2418) and both the BraD/BraE and VraD/VraE ABC transporters. Mol Microbiol 81:602–622. doi:10.1111/j.1365-2958.2011.07735.x

Höfler C, Heckmann J, Fritsch A, Popp P, Gebhard S, Fritz G, Mascher T (2016) Cannibalism stress response in *Bacillus subtilis*. Microbiology 162:164–176. doi:10.1099/mic.0.000176

Horsburgh MJ, Moir A (1999) σ^M, an ECF RNA polymerase sigma factor of *Bacillus subtilis* 168, is essential for growth and survival in high concentrations of salt. Mol Microbiol 32:41–50. doi:10.1046/j.1365-2958.1999.01323.x

Inoue H, Suzuki D, Asai K (2013) A putative bactoprenol glycosyltransferase, CsbB, in *Bacillus subtilis* activates SigM in the absence of co-transcribed YfhO. Biochem Biophys Res Commun 436:6–11. doi:10.1016/j.bbrc.2013.04.064

Jeong DW, Cho H, Jones MB, Shatzkes K, Sun F, Ji Q, Liu Q, Peterson SN, He C, Bae T (2012) The auxiliary protein complex SaePQ activates the phosphatase activity of sensor kinase SaeS in the SaeRS two-component system of *Staphylococcus aureus*. Mol Microbiol 86:331–348. doi:10.1111/j.1365-2958.2012.08198.x

Jordan S, Junker A, Helmann JD, Mascher T (2006) Regulation of LiaRS-dependent gene expression in *Bacillus subtilis*: identification of inhibitor proteins, regulator binding sites and target genes of a conserved cell envelope stress-sensing two-component system. J Bacteriol 188:5153–5166. doi:10.1128/JB.00310-06

Jordan S, Hutchings MI, Mascher T (2008) Cell envelope stress response in Gram-positive bacteria. FEMS Microbiol Rev 32:107–146. doi:10.1111/j.1574-6976.2007.00091.x

Joseph P, Fichant G, Quentin Y, Denizot F (2002) Regulatory relationship of two-component and ABC transport systems and clustering of their genes in the *Bacillus/Clostridium* group, suggest a functional link between them. J Mol Microbiol Biotechnol 4:503–513

Kallenberg F, Dintner S, Schmitz R, Gebhard S (2013) Identification of regions important for resistance and signalling within the antimicrobial peptide transporter BceAB of *Bacillus subtilis*. J Bacteriol 195:3287–3297. doi:10.1128/JB.00419-13

Kingston AW, Liao X, Helmann JD (2013) Contributions of the σ^W, σ^M and σ^X regulons to the lantibiotic resistome of *Bacillus subtilis*. Mol Microbiol 90:502–518. doi:10.1111/mmi.12380

Kingston AW, Zhao H, Cook GM, Helmann JD (2014) Accumulation of heptaprenyl diphosphate sensitizes *Bacillus subtilis* to bacitracin: implications for the mechanism of resistance mediated by the BceAB transporter. Mol Microbiol 93:37–49. doi:10.1111/mmi.12637

Kovács ÁT (2016) Bacterial differentiation via gradual activation of global regulators. Curr Genet 62:125–128. doi:10.1007/s00294-015-0524-8

Lee YH, Helmann JD (2013) Reducing the level of undecaprenyl pyrophosphate synthase has complex effects on susceptibility to cell wall antibiotics. Antimicrob Agents Chemother 57:4267–4275. doi:10.1128/aac.00794-13

Luttmann D, Gopel Y, Gorke B (2012) The phosphotransferase protein EIIA(Ntr) modulates the phosphate starvation response through interaction with histidine kinase PhoR in *Escherichia coli*. Mol Microbiol 86:96–110. doi:10.1111/j.1365-2958.2012.08176.x

Mascher T (2006) Intramembrane-sensing histidine kinases: a new family of cell envelope stress sensors in Firmicutes bacteria. FEMS Microbiol Lett 264:133–144. doi:10.1111/j.1574-6968.2006.00444.x

Mascher T (2014) Bacterial (intramembrane-sensing) histidine kinases: signal transfer rather than stimulus perception. Trends Microbiol 22:559–565. doi:10.1016/j.tim.2014.05.006

Mascher T, Margulis NG, Wang T, Ye RW, Helmann JD (2003) Cell wall stress responses in *Bacillus subtilis*: the regulatory network of the bacitracin stimulon. Mol Microbiol 50:1591–1604. doi:10.1046/j.1365-2958.2003.03786.x

Mascher T, Zimmer SL, Smith TA, Helmann JD (2004) Antibiotic-inducible promoter regulated by the cell envelope stress-sensing two-component system LiaRS of *Bacillus subtilis*. Antimicrob Agents Chemother 48:2888–2896. doi:10.1128/AAC.48.8.2888-2896.2004

Mascher T, Helmann JD, Unden G (2006) Stimulus perception in bacterial signal-transducing histidine kinases. Microbiol Mol Biol Rev 90:910–938. doi:10.1128/MMBR.00020-06

Mascher T, Hachmann AB, Helmann JD (2007) Regulatory overlap and functional redundancy among *Bacillus subtilis* extracytoplasmic function σ factors. J Bacteriol 189:6919–6927. doi:10.1128/JB.00904-07

Meeske AJ, Sham LT, Kimsey H, Koo BM, Gross CA, Bernhardt TG, Rudner DZ (2015) MurJ and a novel lipid II flippase are required

for cell wall biogenesis in *Bacillus subtilis*. Proc Natl Acad Sci USA 112:6437–6442. doi:10.1073/pnas.1504967112

Ming L-J, Epperson JD (2002) Metal binding and structure-activity relationship of the metalloantibiotic peptide bacitracin. J Inorg Biochem 91:46–58. doi:10.1016/S0162-0134(02)00464-6

Ohki R, Giyanto Tateno K, Masuyama W, Moriya S, Kobayashi K, Ogasawara N (2003) The BceRS two-component regulatory system induces expression of the bacitracin transporter, BceAB, in *Bacillus subtilis*. Mol Microbiol 49:1135–1144. doi:10.1046/j.1365-2958.2003.03653.x

Petersohn A, Brigulla M, Haas S, Hoheisel JD, Völker U, Hecker M (2001) Global analysis of the general stress response of *Bacillus subtilis*. J Bacteriol 183:5617–5631. doi:10.1128/JB.183.19.5617-5631.2001

Pietiäinen M, Gardemeister M, Mecklin M, Leskela S, Sarvas M, Kontinen VP (2005) Cationic antimicrobial peptides elicit a complex stress response in *Bacillus subtilis* that involves ECF-type sigma factors and two-component signal transduction systems. Microbiology 151:1577–1592. doi:10.1099/mic.0.27761-0

Pollak S, Omer Bendori S, Eldar A (2015) A complex path for domestication of *B. subtilis* sociality. Curr Genet 61:493–496. doi:10.1007/s00294-015-0479-9

Radeck J, Gebhard S, Orchard PS, Kirchner M, Bauer S, Mascher T, Fritz G (2016) Anatomy of the bacitracin resistance network in *Bacillus subtilis*. Mol Microbiol 100:607–620. doi:10.1111/mmi.13336

Rietkötter E, Hoyer D, Mascher T (2008) Bacitracin sensing in *Bacillus subtilis*. Mol Microbiol 68:768–785. doi:10.1111/j.1365-2958.2008.06194.x

Schneider T, Sahl H-G (2010) An oldie but a goodie—cell wall biosynthesis as antibiotic target pathway. Int J Med Microbiol 300:161–169. doi:10.1016/j.ijmm.2009.10.005

Schrecke K, Staroń A, Mascher T (2012) Two-component signaling in the Gram-positive envelope stress response: intramembrane-sensing histidine kinases and accessory membrane proteins. In: Gross R, Beier D (eds) Two component systems in bacteria. Horizon Scientific Press, Hethersett, pp 199–229

Schrecke K, Jordan S, Mascher T (2013) Stoichiometry and perturbation studies of the LiaFSR system of *Bacillus subtilis*. Mol Microbiol 87:769–788. doi:10.1111/mmi.12130

Silhavy TJ, Kahne D, Walker S (2010) The bacterial cell envelope. Cold Spring Harb Perspect Biol 2:a000414. doi:10.1101/cshperspect.a000414

Staroń A, Finkeisen DE, Mascher T (2011) Peptide antibiotic sensing and detoxification modules of *Bacillus subtilis*. Antimicrob Agents Chemother 55:515–525. doi:10.1128/AAC.00352-10

Storm DR, Strominger JL (1974) Binding of bacitracin to cells and protoplasts of *Micrococcus lysodeikticus*. J Biol Chem 249:1823–1827

Wecke T, Mascher T (2011) Antibiotic research in the age of omics: from expression profiles to interspecies communication. Antimicrob Chemother 66:2689–2704. doi:10.1093/jac/dkr373

Wecke T, Zühlke D, Mäder U, Jordan S, Voigt B, Pelzer S, Labischinski H, Homuth G, Hecker M, Mascher T (2009) Daptomycin versus friulimicin B: in-depth profiling of *Bacillus subtilis* cell envelope stress responses. J Antimicrob Chemother 53:1619–1623. doi:10.1128/aac.01046-08

Wecke T, Bauer T, Harth H, Mäder U, Mascher T (2011) The rhamnolipid stress response of *Bacillus subtilis*. FEMS Microbiol Lett. doi:10.1111/j.1574-6968.2011.02367.x

Wiegert T, Homuth G, Versteeg S, Schumann W (2001) Alkaline shock induces the *Bacillus subtilis* σ^W regulon. Mol Microbiol 41:59–71. doi:10.1046/j.1365-2958.2001.02489.x

Wolf D, Kalamorz F, Wecke T, Juszczak A, Mäder U, Homuth G, Jordan S, Kirstein J, Hoppert M, Voigt B, Hecker M, Mascher T (2010) In-depth profiling of the LiaR response of *Bacillus subtilis*. J Bacteriol 192:4680–4693. doi:10.1128/JB.00543-10

Wolf D, Dominguez-Cuevas P, Daniel RA, Mascher T (2012) Cell envelope stress response in cell wall-deficient L-forms of *Bacillus subtilis*. Antimicrob Agents Chemother 56:5907–5915. doi:10.1128/AAC.00770-12

Yoshimura M, Asai K, Sadaie Y, Yoshikawa H (2004) Interaction of *Bacillus subtilis* extracytoplasmic function (ECF) sigma factors with the N-terminal regions of their potential anti-sigma factors. Microbiology 150:591–599. doi:10.1099/mic.0.26712-0

7.4 MANUSCRIPT I: THE ESSENTIAL UPP PHOSPHATASE PAIR BCRC AND UPPP CONNECTS CELL WALL HOMEOSTASIS WITH CELL ENVELOPE STRESS RESPONSE IN *BACILLUS SUBTILIS*[$]

Manuscript I:

Radeck J, Lautenschläger N, Mascher T (2017) The essential UPP phosphatase pair BcrC and UppP connects cell wall homeostasis with cell envelope stress response in *Bacillus subtilis*. (submitted to Frontiers in Microbiology)

[&] was published in a revised form as: **Radeck J***, Lautenschläger N*, Mascher T (2017) The Essential UPP Phosphatase Pair BcrC and UppP Connects Cell Wall Homeostasis during Growth and Sporulation with Cell Envelope Stress Response in *Bacillus subtilis*. **Front. Microbiol.**, 8:2403. doi: 10.3389/fmicb.2017.02403

THE ESSENTIAL UPP PHOSPHATASE PAIR BCRC AND UPPP CONNECTS CELL WALL HOMEOSTASIS WITH CELL ENVELOPE STRESS RESPONSE IN *BACILLUS SUBTILIS*

Jara Radeck[1, $], Nina Lautenschläger[1,$], Thorsten Mascher[1,*]

[$] these authors contributed equally to this work
[1] Thorsten Mascher, General Microbiology, Institut für Mikrobiologie, Technische Universität Dresden, Dresden, Germany

*** Correspondence:**
Thorsten Mascher
thorsten.mascher@tu-dresden.de

Keywords: Lipid II, bactoprenol, undecaprenyl pyrophosphate, undecaprenol, undecaprenyl phosphate, bacitracin, cell wall biosynthesis

ABSTRACT

The bacterial cell wall separates the cell from its surrounding and protects it from environmental stressors. Its integrity is maintained by a highly regulated process of cell wall biosynthesis. The membrane-located lipid II cycle provides cell wall building blocks that are assembled inside the cytoplasm to the outside for incorporation. Its carrier molecule, undecaprenyl-phosphate (UP), is then recycled by dephosphorylation from undecaprenyl-pyrophosphate (UPP). In *Bacillus subtilis*, this indispensable reaction is catalyzed by the UPP-phosphatases BcrC and UppP. Here, we study the physiological function of both phosphatases with respect to morphology, cell wall homeostasis and the resulting cell envelope stress response (CESR). We demonstrate that *uppP* and *bcrC* represent a synthetic lethal gene pair, which encodes an essential physiological function. Accordingly, cell growth and morphology were severely impaired during exponential growth if the overall UPP-phosphatase level was limiting. UppP, but not BcrC, was crucial for normal

sporulation. Expression of *bcrC*, but not *uppP*, was upregulated in the presence of cell envelope stress conditions caused by bacitracin if UPP-phosphatase levels were limited. This homeostatic feedback renders BcrC more important during growth than UppP, particularly in defense against cell envelope stress.

INTRODUCTION

The bacterial cell wall is an essential structure that gives the cell its shape and counteracts the turgor pressure. The sacculus is one large macromolecule made up of peptidoglycan that has amazing properties: It is rigid, yet flexible and is constantly expanded and recycled during growth and cell division in a highly regulated manner, both spatially and temporally (Laddomada et al., 2016). Due to its essentiality, it is a prime antibiotic target at virtually any of the numerous steps leading to cell wall assembly.

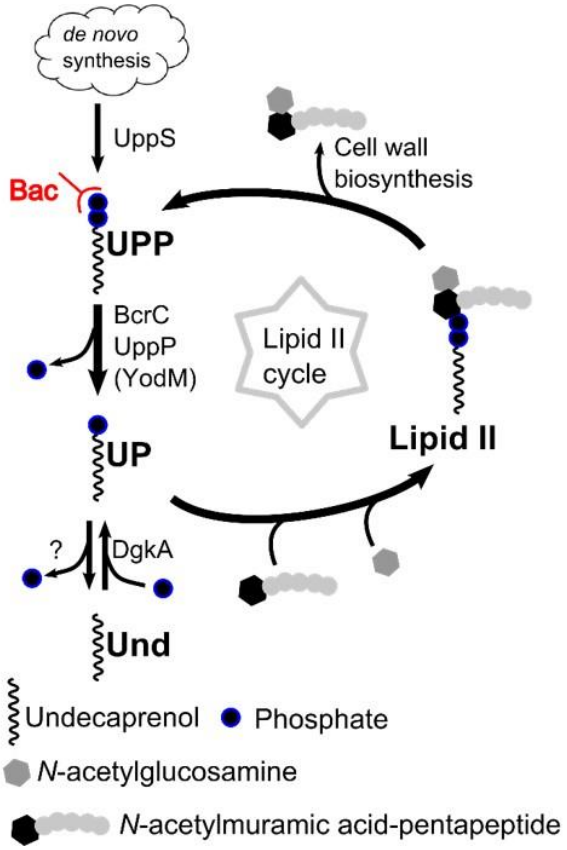

Figure 1. Simplified scheme of the Lipid II-cycle. UPP is dephosphorylated to UP by the UPP-phosphatases BcrC, UppP and YodM. The peptide antibiotic bacitracin specifically binds to UPP, thereby inhibiting its dephosphorylation. The carrier UP is loaded with a cell wall precursor, resulting in lipid II. After incorporation of the cell wall precursor into the existing cell wall, UPP is released and recycled by the UPP phosphatases. *De novo* synthesis of UPP occurs from isoprenoids via the enzyme UppS. Undecaprenol can also serve as an unphosphorylated carrier, which is phosphorylated by the kinase DgkA to UP.

Bac, Bacitracin; Und, Undecaprenol; UP, Undecaprenyl-phosphate; UPP, Undecaprenyl-pyrophosphate.

The lipid II cycle describes the membrane-associated steps of this process (Fig. 1). Briefly, *N*-acetylmuramic acid (MurNAc)-pentapeptide building blocks are assembled in the cytosol and linked to the lipid carrier, a C_{55}-phosphate called bactoprenol or undecaprenyl-phosphate (UP), thereby forming lipid I. An *N*-acetylglucosamine (GlcNAc) molecule is added, resulting in lipid II. This cell wall building block is subsequently shuttled across the membrane by the flippases Amj and MurJ (Meeske et al., 2015; Laddomada et al., 2016). On the outside, the GlcNac-MurNAc-

pentapeptide building block is incorporated into the existing cell wall by transgylcosylation and transpeptidation reactions, thereby releasing the lipid carrier in its pyrophosphate form (undecaprenyl-pyrophosphate, UPP). For its recycling, UPP is then dephosphorylated to UP by specialized UPP-phosphatases (Bernard et al., 2005; Manat et al., 2014) and flipped back to the cytosolic leaflet of the membrane, where it can be reloaded to enter the Lipid II cycle again.

Apart from this recycling, the cellular UP pool can also be replenished by *de novo* synthesis of UPP via the UPP synthetase UppS (Guo et al., 2005). The subsequent dephosphorylation to UP is likely performed by the same UPP-phosphatases that are required for recycling UPP (Manat et al., 2014). In Gram-positive bacteria, UP can also originate from phosphorylating undecaprenol, e.g. by the kinase DgkA in *B. subtilis* (Higashi et al., 1970; Jerga et al., 2007).

UP is the carrier for both peptidoglycan and wall teichoic acids (WTA) building blocks and its availability represents the central bottleneck for the synthesis of lipid II both *in vitro* and *in vivo* (Breukink et al., 2003; Breukink and de Kruijff, 2006; Egan et al., 2015). Only ~ $2*10^5$ UP molecules (0.5-1 % of all phospholipids) are present per cell (Kramer et al., 2004) and it has been estimated that each of the carriers shuttles one to three cell wall building blocks per seconds during exponential growth (McCloskey and Troy, 1980). The amount of WTA and peptidoglycan synthesis is reduced under UP-limitation, especially if conditions favor the competing pathway (Anderson et al., 1972). Antibiotics that target the lipid II cycle benefit from this bottleneck, because blocking any step will lead to accumulation of intermediates, shortage of free carrier molecules and impaired cell wall biosynthesis that depends on UP.

Because of the essentiality of the cell envelope, any threats are potentially lethal to bacteria. Consequently, bacteria have evolved appropriate countermeasures to detect and remove threats or damages. These responses are collectively termed cell envelope stress response (CESR) (Jordan et al., 2008). *Bacillus subtilis* is one of the main model organisms for studying the Gram-positive cell wall and member of the *Firmicutes* phylum (low G+C Gram-positives). In this organism, the CESR is orchestrated by two-component systems and extracytoplasmic sigma factors (ECFs)

(Radeck et al., 2016a). While many antibiotics can trigger the CESR, the molecular nature behind these stimuli has only been identified for very few cases. The antibiotic itself seems rarely to be detected directly. Instead, downstream effects of antibiotic threat, such as envelope damage or – more importantly – the accumulation of certain intermediates, are suspected to be the actual triggers of CESR (Meeske et al., 2015; Helmann, 2016). A similar effect to such an antibiotic-mediated blockade can also be achieved by reducing the availability of the corresponding enzyme. Consequently, the lipid II cycle, cell wall homeostasis and cell envelope stress (CES) are interconnected processes that can hardly be studied independently. In fact, a *B. subtilis* mutant with reduced UppS acitivity (and therefore reduced *de novo* synthesis of UPP) had altered antibiotic resistance properties and elevated σ^M-acitvity (Lee and Helmann, 2013). Here, we will focus on the CESR caused by limitations of the crucial UPP-phosphatase activity, provided e.g. by BcrC.

The expression of *bcrC* is controlled by multiple stress-inducible alternative sigma factors, including σ^M, σ^I, σ^X, σ^V, and potentially also σ^W (Cao and Helmann, 2002; Tseng and Shaw, 2008; Guariglia-Oropeza and Helmann, 2011; Zweers et al., 2012). σ^M controls approx. 60 genes involved in cell wall synthesis, shape determination, detoxification and DNA damage response (Eiamphungporn and Helmann, 2008). It is activated by multiple triggers, including antibiotics, high salt, heat stress and acidic pH (Thackray and Moir, 2003). While all of these inducers affect cell envelope synthesis or integrity, the molecular cue for the activation of this and other ECFs is yet to be identified (as reviewed in Helmann, 2016).

Induction of P_{bcrC} can be triggered e.g. by the addition of the antibiotic bacitracin (Cao and Helmann, 2002; Radeck et al., 2016b). Bacitracin is a cyclic antimicrobial peptide produced by some strains of *Bacillus licheniformis* and *B. subtilis* (Azevedo et al., 1993; Ishihara et al., 2002). It was shown that bacitracin tightly binds UPP, thereby blocking the dephosphorylation reaction mediated by UPP-phosphatases and consequently slowing down the lipid II cycle (Siewert and Strominger, 1967; Storm and Strominger, 1973; Economou et al., 2013). The deletion of *bcrC* may have similar consequences, since the loss of one UPP-phosphatase might reduce the rate of UPP dephosphorylation to UP.

A very sensitive indicator of CES is the LiaR-controlled *liaI* promoter (P_{liaI}) (Mascher et al., 2004). The cognate three-component system, LiaFSR reacts to a broad range of cell envelope stressors, including alkaline shock, oxidative stress, or bacitracin addition (Jordan et al., 2006; Wolf et al., 2010). In turn, it regulates a phage-shock protein-like response that provides a secondary layer of protection against CES (Radeck et al., 2016b). The low basal activity and strong, highly dynamic induction of P_{liaI} made this promoter an ideal candidate for the development of a highly sensitive CESR-inducible whole cell biosensor (Mascher et al., 2004; Wolf and Mascher, 2016; Kobras et al., 2017). Recently, we demonstrated that P_{liaI} activity in response to bacitracin is elevated in a *bcrC* deletion mutant and decreased in a *bcrC* overexpression strain. These findings indicate that the CES caused by bacitracin is relieved in the presence of the UPP-phosphatase BcrC (Radeck et al., 2016b).

In the same study, we observed that P_{bcrC} activities were increased in a *bcrC* null mutant. Together, this lead to the hypothesis that changes in UP and UPP levels can be sufficient to create CES (Radeck et al., 2016b). Due to their crucial role in the lipid II cycle, we hypothesize that impaired UPP-phosphatase activity leads to a limitation in cell wall synthesis, which in turn should increase the CESR.

Here, we aimed at challenging this hypothesis by studying the effects of enzymes potentially involved in UP turnover on *B. subtilis* physiology and stress responses in detail. Towards that end, we analyzed strains depleted for (combinations of) both the UPP-phosphatases BcrC/UppP and the undecaprenol kinase DgkA on cell physiology and morphology. First, we demonstrate the synthetic lethality of BcrC and UppP and a severe morphological defect in UPP-phosphatase depleted strains. Next, UppP is shown to be indispensable for efficient sporulation. Unexpectedly, *uppP* or *bcrC* deletion and complementation mutants did not activate a classical CESR, as judged by the lack of P_{liaI} induction. Instead, the resulting limitation in UPP-phosphatase levels is perceived by the broader ECF-dependent signaling network. As a result, P_{bcrC} activity was increased in those mutants, thereby providing a homeostatic feedback mechanism by which the cell can autoregulate its UPP-phosphatase level according to needs. Furthermore, we provide the first evidence that DgkA is indeed involved in UPP homeostasis: While a lack of this predicted undecaprenol kinase did not result in

an observable deficiency, a (most likely minor) role in UP turnover is indicated by an increased activity of P_{bcrC} in a *dgkA* mutant in stationary phase. Taken together, our data provides the first insight into the fine-tuning of UP homeostasis that adjusts the Lipid II cycle, and hence cell wall biosynthesis, in response to growth rates and envelope stress levels.

RESULTS

High level expression of UPP-phosphatases BcrC and UppP in *B. subtilis*

The genome of *B. subtilis* encodes three UPP-phosphatases, BcrC, UppP and YodM. YodM and BcrC belong to the large group of type II phosphatidic acid phosphatases (PAP2s) that share their catalytic mechanism while pursuing a wide range of functions from signaling to export. Both proteins are homologues to the crystalized UPP-phosphatase PgpB of *E. coli* (El Ghachi et al., 2005; Fan et al., 2014; Kelley et al., 2015). While YodM seems to be dysfunctional due to insufficient expression (Zhao et al., 2016), BcrC has been studied to some extent. It seems to be the major *B. subtilis* UPP-phosphatase (Bernard et al., 2005; Inaoka and Ochi, 2012) and is highly expressed at most culture conditions, as judged by a comprehensive tiling array study (Fig. 2) (Nicolas et al., 2012). The monocistronic gene *bcrC* (Fig. 2A) is regulated by the CES-inducible ECFs σ^M and σ^X (Cao and Helmann, 2002). The latter respond to CES that might be caused by changing UP levels or other intermediates of the lipid II cycle (Helmann, 2016). Under our experimental conditions, the activity of P_{bcrC} remained at high levels (Fig. 2C) from early exponential to late stationary phase - with exception of the known decrease during transition state, which is frequently observed for online promoter activity measurements (Radeck et al., 2013). As discovered previously, P_{bcrC} activity was increased by the addition of bacitracin (30 µg ml^{-1}; Fig. 2C) (Mascher et al., 2003; Radeck et al., 2016b).

The minor UPP-phosphatase UppP (Inaoka and Ochi, 2012) is homologous to BacA from *E. coli*. The latter accounts for about 75% of the UPP-phosphatase activity in this organism (El Ghachi et al., 2004). *uppP* is the second gene of the *yubA-uppP* operon and its P_{yubA}-dependent expression is not induced by bacitracin (Cao and Helmann, 2002). YubA is predicted to be a membrane protein belonging to the autoinducer-2 exporter (ai-2e) family and might be associated with cell wall synthesis (Fenton et al., 2016; UniProt, 2017). The activity of P_{yubA} is comparable to P_{bcrc} during exponential growth, but about 3-fold higher during stationary phase (Fig. 2B). In contrast to P_{bcrc}, and in agreement with a previous study, P_{yubA} was not significantly induced by bacitracin (Fig. 1C, Cao and Helmann, 2002). Our data based on the promoter-*lux*

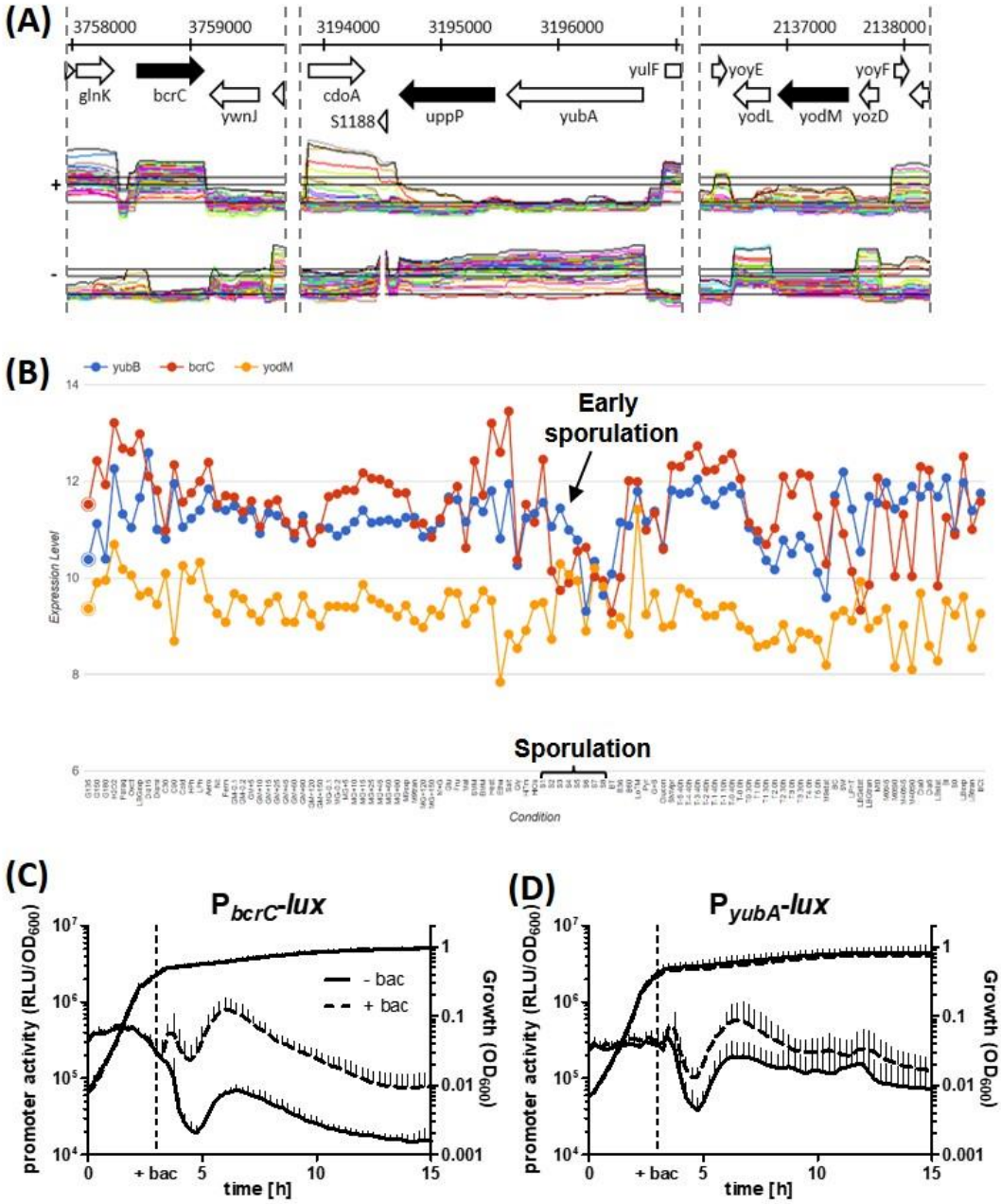

Figure 2. Expression of UPP phosphatase genes. **(A, B)** Figures modified from subtiwiki 2.0 (Nicolas et al., 2012; Michna et al., 2016). Details on the experimental conditions can be obtained from (URL) by clicking on the points of interest. **(A)** Genomic context of UPP-phosphatase genes and respective mRNA levels (+ or – strand, respectively) across 104 conditions. The scale indicates the genomic position. **(B)** Comparison of expression profiles for *uppP*, *bcrC* and *yodM*. Sporulation and early sporulation are indicated with a bracket and arrow, respectively. **(C, D)** Growth (OD_{600}) and activity levels of P_{bcrC} and P_{yubA} (RLU/OD_{600}) in *B. subtilis* W168 (TMB1620 and TMB3688) from early exponential to late stationary phase in absence or presence of 30 µg ml^{-1} bacitracin (+ bac; dashed lines), respectively. P_{bcrC} actictivity was significantly increased upon bacitracin addition (p=0.021, 2-way ANOVA), but not P_{yubA} (p=0.29, 2-way ANOVA). Measurements were obtained in a microtiter plate reader at 37°C in MCSEC medium. Data is shown for three independent biological replicates (mean and SD).

fusions agrees well with the tiling array data on mRNA levels of *uppP* and *bcrC* (Fig. 2B, Nicolas et al., 2012). At most conditions, *bcrC* (red) is expressed at a slightly higher level than *uppP* (*yubB*, in blue). One exception is sporulation, during which *bcrC* expression drops at early sporulation and *uppP* only at late sporulation (see arrow).

For the third UPP-phosphatase, the tiling array data shows that there is almost no transcription of *yodM* (yellow), but instead high levels of counter-transcription (Fig. 2A). This finding has recently been verified (Zhao et al., 2016). Due to these observations, YodM and its promoter, P_{yodM}, were not considered further for our analysis.

In summary, there are two well-transcribed UPP-phosphatase genes in *B. subtilis* cells, BcrC and UppP. We therefore decided to study their role in cell wall homeostasis and CES in *B. subtilis*. Towards that goal, we investigated single and combined deletion and complementation strains for their effect on cell morphology, sporulation, CESR and antibiotic resistance.

uppP and _bcrC_ are a synthetic lethal gene pair

Initially, we aimed at replacing all three UPP-phosphatase genes with resistance cassettes (*bcrC*::*tet*, *uppP*::*MLS* and *yodM*::*spec*) in single and double mutants. For simplicity reasons, all allelic replacements are noted as deletions throughout the manuscript and figure legends. All single mutants and double mutants with Δ*yodM* were readily obtained. Since the lack of any observable phenotype during the initial characterization of all Δ*yodM* strains can readily be explained by the lack of *yodM* expression (Fig. 2A and (Zhao et al., 2016)), these strains were not considered further.

In contrast to the single mutants, multiple attempts to construct a *ΔuppP ΔbcrC* double mutant failed, indicative of synthetic lethality of *bcrC* and *uppP.* To support this assumption, we constructed complementation strains, in which *uppP* or *bcrC* were ectopically integrated into the *thrC* locus under control of the xylose-inducible promoter P_{xylA}. In strains carrying a complementation copy of either *bcrC* or *uppP*, the deletion of both native genes was possible in the presence of xylose. These strains (Δ*uppP* Δ*bcrC* P_{xylA}-*bcrC* and Δ*uppP* Δ*bcrC* P_{xylA}-*uppP*) will be referred to as depletion

strains to distinguish them from the complementation strains Δ*bcrC* P_{xylA}-*bcrC and* Δ*uppP* P_{xylA}-*uppP*. Our findings are in agreement with a recent study from the Helmann laboratory, which independently demonstrated the synthetic lethality of the *bcrC*/*uppP* gene pair using a CRISPR-dCas9 knockdown approach (Zhao et al., 2016).

Cell morphology is impaired in UPP-phosphatase mutants during exponential growth

Depletion of essential envelope-associated proteins often leads so bulging, filamentation or lysis of cells (Peters et al., 2016). Since *uppP* and *bcrC* are synthetic lethal and the lipid II-cycle and cell wall synthesis depend on the recycling of UP by UPP-phosphatases, we hypothesized that a depletion of UPP-phosphatases in fast-growing cells leads to a morphological phenotype similar to that observed for other essential cell envelope functions.

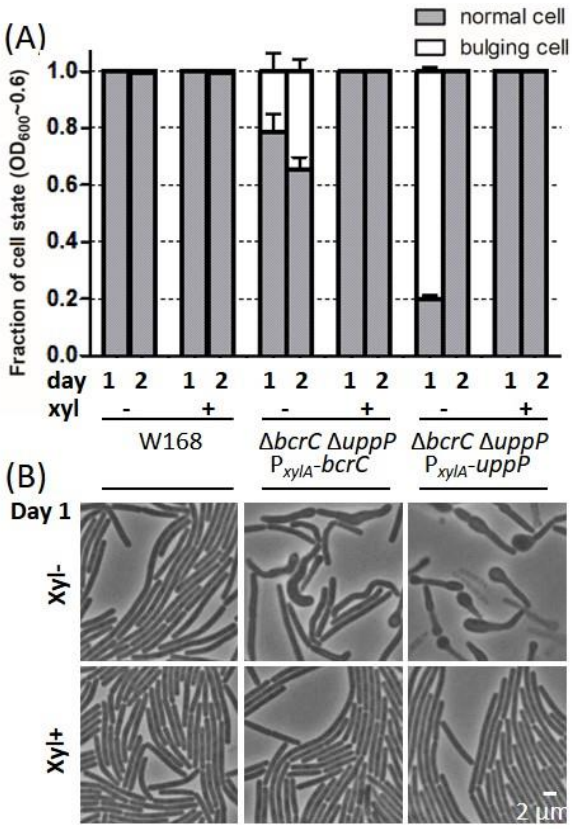

Figure 3. Cell morphology during exponential growth in *bcrC* and *uppP* complementation mutants.

Strains W168, TMB3739, TMB3740 were inoculated from fresh overnight cultures (day 1) or 24h-cultures (on day 2), grown in MCSEC at 37°C, 220 rpm without xylose (xyl-) to deplete the respective UPP phosphatase or with 0.2% xylose (xyl+) to fully induce the production in complementation mutants. Overnight cultures were always supplemented with xylose, whereas the inoculum for day 2 was taken from samples either with (xyl+) or without (xyl-) xylose added. Phase contrast pictures were taken in late exponential phase (OD_{600}~0.6, ~6 h post-inoculation). **(A)** Fraction of cells with normal (grey) or bulging morphology (white). At least 1000 cells were counted for each of the three independent biological replicates. **(B)** Representative pictures of cells with normal or bulging morphology. Samples were taken from day 1. The scale bar represents 2 µm.

Single *uppP* or *bcrC* deletions, the respective complementation mutants, and the wild type showed no or less than 0.1% misshaped cells (data not shown). In contrast, both UPP phosphatase depletion strains TMB3739 (Δ*uppP* Δ*bcrC* P_{xylA}-*bcrC*) and TMB3740 (Δ*uppP* Δ*bcrC* P_{xylA}-*uppP*) showed a severe phenotype during exponential growth phase (Fig. 3). In the absence of xylose, about 20-30% (TMB3739) or 80% (TMB3740) of the cells are bulging and sometimes bending (Fig. 3A). This phenotype could be completely suppressed by the addition of xylose, resulting in high expression levels of the complemented UPP-phosphatase (Fig. 3B). This phenotype could not be observed at slow growth e.g. in stationary phase (Fig. S1) even though some cells look swollen compared to wild type cells (e.g. the Δ*uppP* mutant TMB3408).

In summary, we could show that a very low expression of only *uppP* or *bcrC* lead to severe morphological changes, e.g. bulging cells during exponential growth – concomitant with depleted peptidoglycan or WTA synthesis (Muchova et al., 2011; Botella et al., 2014) caused by a lack of UP. This phenotype was most severe for the *uppP* depletion strain.

UppP is important for efficient sporulation

During the morphology studies, we observed altered sporulation rates between the wild type and UPP phosphatase mutants, especially Δ*uppP*. We therefore quantified the sporulation efficiency in our strains by determining the fractions of vegetative versus sporulating cells and endospores in a culture 24 h after inoculation (summarized in Fig. 4, see Fig. S2 for the complete dataset). Under our experimental conditions, about 30% of the wild type cells (Fig. 4B, i) were in the process of sporulation or had already sporulated. Mutants with a native copy of *uppP* (ii-iv), and mutants with wild type copy of *bcrC* in combination with an ectopic inducible copy of *uppP* (viii, ix) had similar sporulation rates. Sporulation was impaired (<7%), if the native copy of *uppP* was lost and no ectopic copy was introduced (v, vi), or if *uppP* was depleted in the phosphatase double mutant (x). The sporulation deficiency of the latter could partially be restored by the addition of xylose to induce *uppP* expression (xi).

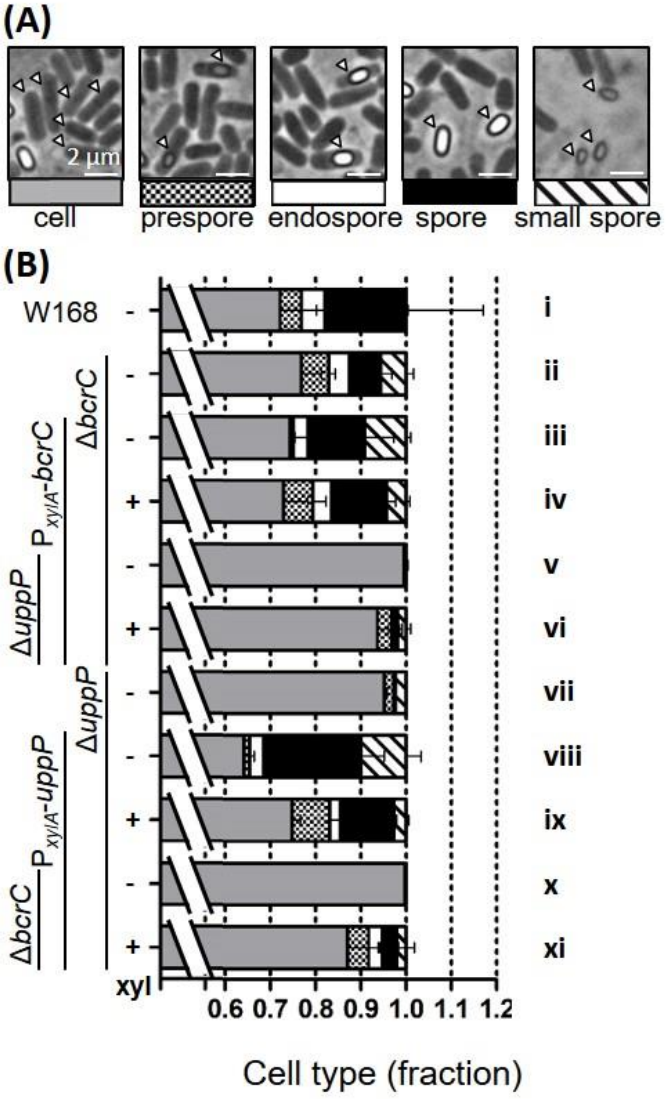

Figure 4. Sporulation efficiencies of *bcrC* and *uppP* deletion and complementation mutants. Strains (W168, TMB0297, TMB3694, TMB3739, TMB3408, TMB3695, and TMB3740) were grown as described in Fig. 3 and phase contrast microscopy pictures were taken 24 hours post-inoculation. **(A)** Representative pictures for normal cells (grey), prespores without fully established phase-bright endospore (small checkered), completed endospores (white), free spores (black) and small free spores (striped). **(B)** Cell type fractions are shown as stacked bar graphs. Data is shown for at least 1000 cells per measurement and the error bars represent the standard deviation between independent biological triplicates. The full data set is shown in Fig. S2.

The reduced sporulation frequencies in Δ*uppP* mutants did not originate from delayed sporulation, since a similar reduction in sporulation rates (2-5% compared to > 30% in the wild type) was also observed after 48h (data not shown). However, using a spore-crust marker (GFP-CotZ), we detected that some of the phase-grey particles in a Δ*uppP* mutant were spores instead of cells (Fig. S3). This phenotype is indicative of alterations in stage IV or V of sporulation, where mutants have thinner or no germ cell wall or cortex (Coote, 1972; Piggot and Coote, 1976). Both spore layers consist of peptidoglycan, a defect in their synthesis therefore points towards UppP being the responsible UPP-phosphatase for the lipid II cycle during sporulation. This observation is in agreement with a recent screen for sporulation mutants, in which a

reduced sporulation efficiency and phase-grey spores were also detected in a *uppP* mutant (Meeske et al., 2016).

Here we could show that the rates of normal, phase bright spores drastically decreased in absence of UppP. In the presence of BcrC, low levels of UppP still allow a normal sporulation (Fig. 4, vii, viii), while this residual UppP amount is not sufficient in the absence of BcrC (x). Either the native copy of *uppP* or the combination of native *bcrC* and an ectopic version of *uppP* is required for efficient sporulation.

The combined results from our sporulation counts (Fig. 4) and the cell morphology study (Fig. 3) demonstrate that limited amounts of either UPP-phosphatase alone (TMB3739, TMB3740 without xylose) are not sufficient to retain normal cell shape during fast growth or ensure efficient sporulation. While each native phosphatase is sufficient to keep normal cell shape in exponential growth, BcrC cannot compensate for the lack of UppP during sporulation. Both phenotypes point towards defects in cell wall synthesis. This provoked the question if under such circumstances this bottleneck in cell wall synthesis leads to a CESR, which is normally triggered by the external addition of cell wall antibiotics, such as bacitracin (Radeck et al., 2016a). To address this question, two well established reporters for CESR (the P_{lial} and P_{bcrC} promoters fused to the *lux* reporter cassette (Radeck et al., 2016b)) were combined with the mutant collection and probed for their activity under UPP phosphatase-limiting conditions.

Limitations in UPP-phosphatases are perceived as envelope stress by the P_{bcrC} reporter

P_{lial} is a very sensitive reporter of cell envelope damage due to its wide inducer spectrum and high dynamic activity range (Mascher et al., 2004; Rietkötter et al., 2008). But we did not observe any UPP phosphatase-dependent induction of the P_{lial}-controlled CESR, even if we additionally challenged the cells with bacitracin (data not shown).

In contrast to the damage-sensing P_{lial} reporter, the P_{bcrC}-derived reporter is postulated to respond to alterations/limitations in cell wall homeostasis (Minnig et

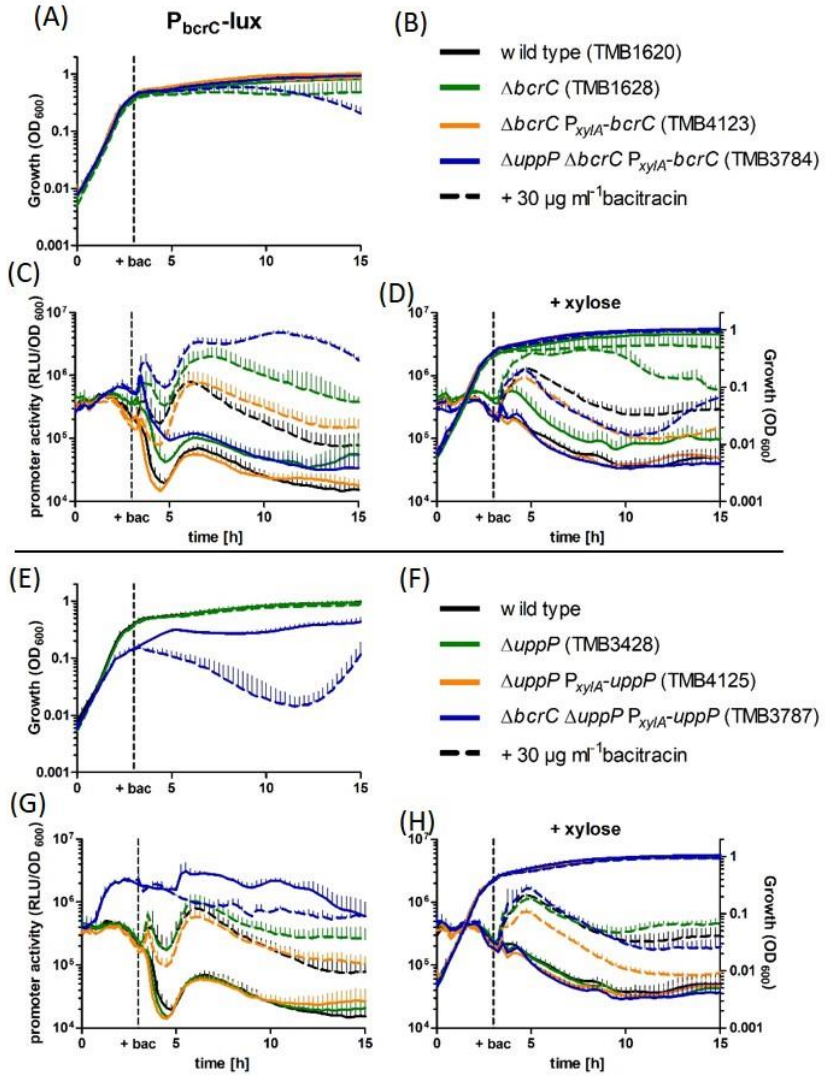

Figure 5. Growth and P_{bcrC} promoter activities in the wild type and *bcrC* and *uppP* complementation mutants. Strains were grown in MCSEC at 37°C in 96-well plates in a microtiter plate reader. OD_{600} and luminescence was measured every 15 minutes for 15 hours. **(A-D)** Growth and P_{bcrC}-activity in *bcrC* deletion, complementation and depletion strains. **(E-H)** Growth and P_{bcrC}-activity in *uppP* deletion, complementation and depletion strains. The strains are defined by the color, while solid or dashed lines indicate the absence or presence of 30 µg ml^{-1} bacitracin. **(D, H)** Samples were grown with 0.2 % xylose to fully induce P_{xylA}-driven gene expression. In these cultures, promoter activity steadily decreased from the transition phase onwards. This phenomenon was observed for all strains either harboring P_{bcrC} or the constitutive reference promoter P_{lepA} (data not shown). We therefore postulate that the change in promoter dynamics is caused by the presence of an additional C-source (xylose). Thin lines represent the standard deviation of at least three biological replicates

al., 2003) and could therefore be more suitable to detect stress caused by changes in the UPP-phosphatase levels. In light of this study, P_{bcrC} is particularly relevant since it controls the expression of one of the two UPP phosphatases, BcrC. It therefore provides a direct read-out for the cells ability to respond to limitations in UPP

phosphatases by upregulating *bcrC* expression. Towards this end, we measured P_{bcrC}-activity in the wild type as well as *bcrC* and *uppP* deletion, complementation and depletion strains. Promotor activity as relative luminescence units normalized to cell density (RLU/OD_{600}) and growth (OD_{600}) were measured in a microtiter plate reader for 15 hours (Fig. 5).

For the wild type reporter strain (TMB1620), P_{bcrC} activity of $3\text{-}5*10^5$ RLU/OD_{600} was observed during exponential growth and the transition phase (Fig. 5 A, C; black lines, 0-3 h). The activity decreased about 10-fold during early stationary phase (4-6 h), briefly increased (6-8 h) and then steadily declined during late stationary phase. Upon bacitracin addition (30 µg ml^{-1}), the promotor activity was increased about 10-fold, while no change in growth behavior was detected.

In the *ΔbcrC* mutant (TMB1628, green) and the *bcrC* depletion strain (TMB3784, blue), the P_{bcrC} activity increased without and especially with bacitracin addition and a slightly reduced optical density was observed during stationary phase compared to the wild type (Fig. 5A-D). These effects were revoked by the addition of xylose (TMB3784) or the introduction of a complementing copy of *bcrC* (TMB4123, orange), even without xylose.

Deletion of *uppP* (TMB3428, green) only had a minor effect on P_{bcrC} activity (approx. three-fold elevation during late stationary phase upon bacitracin addition, Fig. 5 E, G). However, in the *uppP* depletion strain (TMB3787, blue) impaired growth – especially in the presence of bacitracin – and strongly increased P_{bcrC} activity was observed throughout growth, even without bacitracin addition. A subsequent in-depth analysis supported these findings: The *uppP* depletion strain (TMB3740), but not the *bcrC* depletion strain (TMB3739) showed a clear growth defect in absence of xylose. All phenotypes of complementation mutants reverted to wild type levels in presence of xylose (see Fig. S4 for details).

Taken, the single *bcrC* deletion, as well as two phosphatase depletion strains (Δ*bcrC* Δ*uppP* P_{xylA}-*bcrC* and Δ*bcrC* Δ*uppP* P_{xylA}-*uppP*) had the strongest effect on P_{bcrC} activity, especially in the presence of bacitracin.

The undecaprenol kinase DgkA contributes to the cellular UP pool

The results described in the previous section demonstrate that the cell is indeed capable of perceiving limitations in UPP phosphatase levels, most likely at the level of the resulting UP shortage. A second enzymatic activity potentially contributing to the cellular UP pool is the undecaprenol kinase DgkA that phosphorylates undecaprenol to UP (Jerga et al., 2007). Based on the results of the previous section, the activity of the P_{bcrC} reporter might provide an ideal read-out to probe if DgkA indeed provides a measurable contribution to the UP pool, particularly if the cellular amount of UPP phosphatases is severely limited. We therefore deleted *dgkA* in the wild type and all phosphatase deletion, complementation and depletion strains and then measured the P_{bcrC} activity throughout the growth cycle.

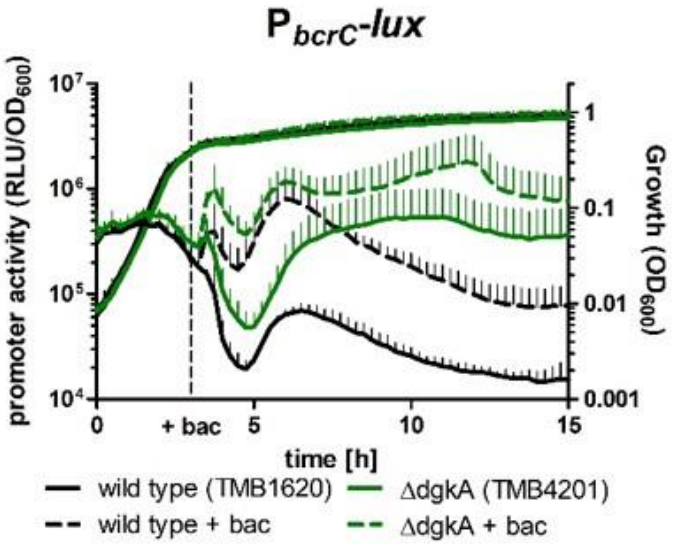

Figure 6. P_{bcrC} promoter activity depends on DgkA. Strains were grown as described in Fig. 5. Black, wild type; green, *dgkA* mutant. Samples induced with bacitracin are shown as dashed lines. Thin lines represent the standard deviation of three biological replicates.

Surprisingly, a strong DgkA-dependent effect was already observed in the wild type reporter strain: the P_{bcrC} activity was elevated ~10-fold in the *dgkA* mutant during late stationary phase relative to the wild type, both in the presence or absence of bacitracin (Fig. 6). A similar effect was observed for all phosphatase mutants (Fig. S5). This result indicates that a DgkA-dependent phosphorylation of undecaprenol indeed detectably contributes to the cellular UP pool, even though a *dgkA* mutant did not show any (additional) morphological phenotype during fast growth (data not shown). It has previously been shown that a *B. subtilis dgkA* mutant produces less and cortex-deficient endospores – a peptidoglycan structure that depends on UP for its synthesis

(Amiteye et al., 2003 and Fig. S2). This suggests that the role of DgkA to contribute to the UP-pool is rather during sporulation.

Deletion and Depletion of UPP-phosphatases increases sensitivity towards the UPP-binding antibiotic bacitracin

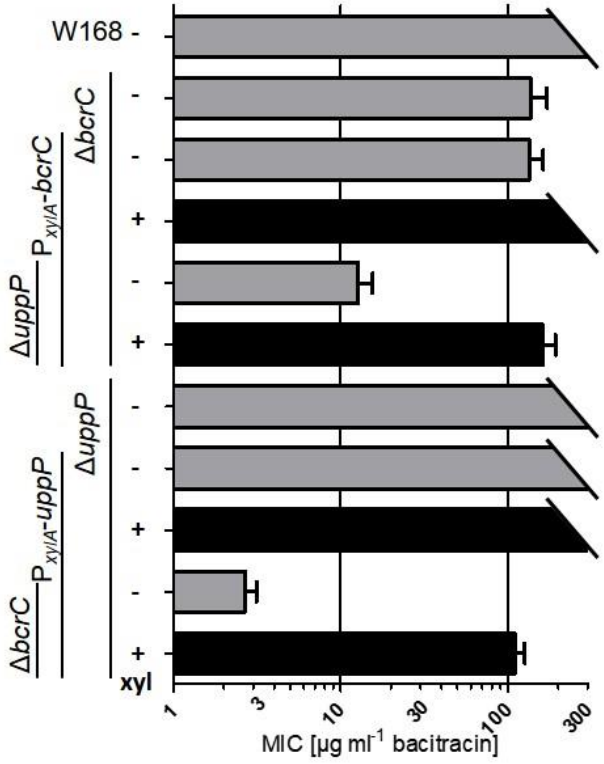

Figure 7. Minimal inhibitory bacitracin concentration of *bcrC* and *uppP* deletion and complementation mutants. Strains (W168, TMB297, TMB3694, TMB3739, TMB3408, TMB3695, and TMB3740) were inoculated from fresh overnight cultures (xyl+) in MCSEC at 37°C with or without 0.2% xylose. During exponential growth, cells were embedded in soft agar and plated as an overlay on MCSEC agar. One Etest® strip (bacitracin 0.016-256 µg ml^{-1}) was placed on the soft agar (see Material and Methods). The MIC was determined after 24h of incubation at 37°C. Data is shown for at least three independent biological replicates (two replicates, if MIC>256 µg ml^{-1}) with mean and standard deviation. The full data set is depicted in Fig. S6.

B. subtilis wild type cells are highly resistant against the UPP-binding antibiotic bacitracin (minimal inhibitory concentration, MIC, >256 µg ml^{-1}). The primary resistance determinant is the bacitracin-specific ABC-transporter BceAB (Mascher et al., 2003; Ohki et al., 2003; Rietkötter et al., 2008). But BcrC provides a (secondary) layer of bacitracin resistance, most likely by competing with the antibiotic for the same target molecule, UPP (Bernard et al., 2005; Radeck et al., 2016a; Radeck et al., 2016b). The inhibitory effect of bacitracin is based on depleting the UP pool by formation of a UPP-bacitracin complex, finally leading to an arrest of the lipid II cycle (Fig. 1). It stands to reason to postulate that deletions in genes encoding UPP phosphatases or undecaprenol kinases might also contribute to the sensitivity of the cells towards bacitracin. We therefore measured the MIC for bacitracin in UPP-phosphatase deletion and depletion mutants, using Etest® strips (Fig. 7 and Fig. S6).

While the individual deletion of *uppP* had no measurable effect on bacitracin MIC, the deletion of *bcrC* lead to the known reduction of the MIC to ~ 120 µg ml^{-1}. This phenotype could be complemented by the addition of xylose, thereby inducing the ectopically integrated P$_{xylA}$-*bcrC*. Without xylose, the MIC of this strain is comparable to the *bcrC* deletion mutant, indicating very little background activity of P$_{xylA}$ under non-inducing conditions. If *uppP* is deleted in this genetic background, the MIC was even further decreased to ~ 15 mg ml^{-1}. In this depletion strain, the P$_{xylA}$-mediated expression of *bcrC* can no longer fully compensate for the loss of both UPP-phosphatases (MIC of ~150 compared to >256 µg ml^{-1} in Δ*uppP*). The *uppP* depletion mutant (TMB3739, Δ*bcrC* Δ*uppP* P$_{xylA}$-*uppP*) exhibited the lowest MIC (~3 µg ml^{-1}). Upon addition of xylose, a 35-fold increase in bacitracin MIC could be observed (Fig. 7).

Taken together, the resistance towards the UPP-binding bacitracin is indeed severely reduced in mutants limited for UPP-phosphatases. This phenotype can be (almost fully) compensated for by induction of ectopically integrated UPP-phosphatase genes under control of P$_{xylA}$. Again, the phenotype of the *uppP*-depletion strain (TMB3740) is more severe than that of the *bcrC*-depletion (TMB3739), in line with the morphological defects observed above (Fig. 3). The additional deletion of *dgkA* or *yodM* had no effect on the observed MIC in any of the mutants tested, again indicating a very minor contribution of these two gene products. Removing the main bacitracin resistance determinant, *bceAB*, lead to an overall lower basal MICs, but had no additional influence on the behavior described above (Fig. S6).

DISCUSSION

Together, *bcrC* and *uppP* encode the essential UPP phosphatase function of *B. subtilis*

In our study, we demonstrated that *uppP* and *bcrC* constitute a synthetic lethal gene pair – a result that is perfect agreement with an independent study performed in parallel using CRISPR-dCas9 knock-downs to study the effect of UPP-phosphatase levels in *B. subtilis* (Zhao et al., 2016). These observations thereby correct two

previous studies, which independently reported the successful construction of a *uppP/bcrC* double deletion mutant that showed the same phenotype as a single *bcrC* deletion mutant (Bernard et al., 2005; Inaoka and Ochi, 2012). Both groups used deletion constructs based on the vector pMUTIN, which disrupted either *uppP* or *bcrC* by integrating via single homologous recombination (Vagner et al., 1998; Kobayashi et al., 2003; Bernard et al., 2005; Inaoka and Ochi, 2012). Based on their data, it must be postulated that these deletion constructs generated a gene fragment up- or downstream the integration site, which was still large enough to maintain (residual) UPP phosphatase activity. In contrast, both recent studies only used complete allelic replacement mutants based on double homologous recombination of a resistance cassette (this study and Zhao et al., 2016).

According to our results, the basal expression of *bcrC* driven by P_{xylA} is still sufficient for growth at normal doubling times. This is in agreement with the parallel study, which initially failed to generate *uppP* or *bcrC* depletion strains due to the high basal activity of $P_{spac(hy)}$ which was used for complementation: The strains still grew in the absence of IPTG, despite the knock-out of the native *uppP* and *bcrC* genes (Zhao et al., 2016).

In contrast, the third UPP phosphatase, YodM, did not provide a measurable contribution to the cellular UP pool. While the Zhao *et al.* study demonstrated that the gene product of *yodM* indeed has UPP phosphatase activity, this was only sufficient to support growth if expression was artificially improved (Zhao et al., 2016), in line with our own observations. This is not surprising, considering the expression profiles from a comprehensive transcriptome study, which demonstrates a lack of *yodM* expression, but instead a strong counter-transcription (Fig. 2). Together, the data provided in this study and the recent report from the Helmann group unequivocally demonstrates that the UPP phosphatase activity in *B. subtilis* is primarily – if not exclusively – provided by BcrC and UppP. While both can functionally complement each other, our study indicates that the two phosphatases have slightly different functions in wild type cells.

BcrC is more relevant during vegetative growth, while UppP is important for efficient sporulation

Table 1 summarizes the main findings of our study with regard to bacitracin sensitivity, P_{bcrC} activity, cell morphology and growth rates. While our data demonstrates that either phosphatase is sufficient to support growth, the respective mutants do show significant differences in their overall behavior. The Δ*bcrC* single mutant had a decreased MIC for bacitracin and an elevated P_{bcrC} activity, in contrast to the Δ*uppP* strain. If the UPP phosphatase levels are further reduced or if the cultures are additionally challenged with bacitracin, the phenotypes are overall less severe if BcrC is complemented compared to UppP under similar conditions. Hence,the *uppP* depletion strain (that completely lacks BcrC) shows a severe growth defect and strong CESR in the absence of xylose. While an elevated P_{bcrC} activity is also measured for the *bcrC* depletion strain, this effect is rather weak in the absence of bacitracin and only a mild growth defect is observed. Our data therefore not only supports previous findings that BcrC is the major UPP phosphatase during vegetative growth in *B. subtilis* (Bernard et al., 2005; Inaoka and Ochi, 2012), but also demonstrates that an ectopically complementing copy of *bcrC* is more efficient in providing the UPP phosphatase activity than a similar construct for *uppP*.

In contrast, UppP seems to play the more prominent role with regard to sporulation. At strongly reduced levels of UppP, BcrC can support but never fully compensate the function of UppP. Its role in the formation of mature spores was recently also observed in a screen for sporulation mutants (Meeske et al., 2016).

When triggering a CESR, as monitored by an increased σ^M-dependent P_{bcrC} activity (this study,Cao and Helmann, 2002; Radeck et al., 2016b), we recently observed that a deletion of *bcrC* further increases the CESR (Radeck et al., 2016a; Radeck et al., 2016b). Here, we could demonstrate that this effect holds true for UPP phosphatases in general: While a *uppP* deletion alone does not trigger the CESR, very low levels of UPP phosphatase activity (especially in the *uppP* depletion strain) cause a stronger CESR than the *bcrC* single mutant (Fig. 5). This finding perfectly fits to the working model that low levels of UP (or downstream effects thereof) are the stimulus for σ^M

activation, rather than the protein levels of BcrC (Lee and Helmann, 2013; Zhao et al., 2016). It is also supported by the finding that P_{bcrC} is induced in presence of bacitracin, which blocks the dephosphorylation to UP by binding to UPP (Cao and Helmann, 2002).

Outlook and open questions

Our study clearly demonstrates the essential role of UPP phosphatases for the lipid II cycle, in perfect agreement with results from an independent study performed in parallel (Zhao et al., 2016). In addition, we could demonstrate that these phosphatases also provide a direct link in connecting cell envelope homeostasis with CESR. Nevertheless, some questions are still open and need to be addressed in subsequent studies.

Quite surprisingly, P_{bcrC} activity is unchanged in the *uppP* depletion strain treated with xylose, while the native *uppP* copy present in *ΔbcrC* is not sufficient to prevent CESR. This phenomenon could not be observed with regard to the bacitracin sensitivity and provokes the question if and how *uppP* is regulated during growth and CES. For further investigations, protein and/or activity levels of UPP-phosphatases and the abundance of UPP and UP in challenged and non-challenged cells will help to better understand the stoichiometry of UPP dephosphorylation, a crucial step of the lipid II cycle.

Another aspect that needs to be taken into account is the substantial contribution of UPP *de novo* synthesis to the lipid II cycle: Reducing the UppS protein levels by 50% significantly altered cell wall antibiotic sensitivities (Lee and Helmann, 2013). But so far, very little is known about the stoichiometry between UPP recycling and *de novo* synthesis, which are both essential and depend on UPP phosphatases.

Two reactions are known to generate UP independent of UPP phosphatases: (i) recycling from WTA-shuttling, which depends on UP and is therefore not self-sustaining (Brown et al., 2013), and (ii) phosphorylation of undecaprenol, e.g. via DgkA (Jerga et al., 2007; Van Horn and Sanders, 2012). The cellular abundance and dynamics of undecaprenol has so far not been studied for *B. subtilis*, but data from

other species indicates that this molecule is present in the membrane of Gram-positive bacteria and absent in Gram-negative bacteria (Higashi et al., 1970; Barreteau et al., 2009). In *Staphylococcus aureus*, a UP phosphatase activity was detected, but could not be assigned to a certain protein (Willoughby et al., 1972). Future studies – particularly for *B. subtilis* – will hopefully address the source of undecaprenol and its role as a possible resource for the lipid II cycle.

The localization and cellular dynamics of UPP phosphatases throughout the growth cycle and into sporulation might provide further insights into their activity pattern and hence their cellular roles. Such studies would also allow studying their proximity to active cell wall biosynthesis clusters (peptidoglycan and WTA), which could be a relevant proxy for efficient carrier supply (Kawai et al., 2011; Typas et al., 2012). Unfortunately, our initial attempts to generate functional translational GFP-fusions to the N- or C-terminus of UppP or BcrC were not successful. Some fusion constructs did not provide (sufficient) UPP phosphatase activity to complement the synthetic lethal gene pair in a *uppP* and *bcrC* deletion background. And those constructs that maintained the phosphatase activity lacked a fluorescent signal, potentially due to the fluorophore localizing to the extracellular side of the membrane (data not shown). Future studies, that employ linkers or fluorophors that mature in the periplasm (such as mCherry or superfolder GFP (Dammeyer and Tinnefeld, 2012)) will hopefully circumvent these obstacles.

The data provided by our and other recent studies (Meeske et al., 2016; Zhao et al., 2016) are an important first step in gaining a mechanistic understanding on UPP phosphatases. But despite the insights gained during these studies, there is still a lot to be learned about the dynamics of the UP pool and how the functions that make and break this essential intermediate of cell envelope biosynthesis contribute to cell growth, differentiation and cellular stress responses.

EXPERIMENTAL PROCEDURES

Bacterial strains and growth conditions

E. coli strains were routinely grown in lysogeny broth (LB) and *B. subtilis* in *M*OPS-based *c*hemically defined medium with *s*uccinate and glutamate (MCSE) (Radeck et al., 2013), supplemented with casamino acids (1%, CAA) and L-threonine (50 µg ml^{-1}) (MCSEC) at 37°C with agitation (220 rpm). Addition of CAA was necessary to prevent background activity of P_{hom}, which is located upstream of the integration site of the *uppP* and *bcrC* complementation constructs (Radeck et al., 2013). Transformations of *B. subtilis* were carried out as described previously (Harwood and Cutting, 1990). All *B. subtilis* strains used in this study are derivatives of the laboratory wild type strain W168 and are listed in Table S1. All allelic replacements are shown as gene deletions in the main text and figure captions for better readability. Selective media for *E. coli* contained ampicillin (100 µg ml^{-1}) or chloramphenicol (35 µg ml^{-1}). Selective media for *B. subtilis* contained chloramphenicol (5 µg ml^{-1}), kanamycin (10 µg ml^{-1}), spectinomycin (200 µg ml^{-1}), tetracycline (12.5 µg ml^{-1}) and/or a combination of erythromycin (1 µg ml^{-1}) and lincomycin (25 µg ml^{-1}) for macrolide-lincosamide-streptogramin B (MLS) resistance. Solid media additionally contained 1.5% (w/v) agar. For complementation studies, full induction of the promoter P_{xylA} was achieved by adding xylose to a final concentration of 0.2% (w/v). Overnight cultures contained xylose per default to ensure normal growth of depletion strains.

DNA manipulation

Plasmids were generated by using standard cloning techniques (Sambrook and Russell, 2001) with enzymes and buffers from New England Biolabs® (NEB) according to the manufacturer's protocols. Phusion® polymerase was used for polymerase chain reaction (PCR) amplification for cloning purposes, otherwise OneTaq® was used. PCR purification was performed with *HiYield PCR Gel Extraction/PCR Clean-up Kit* (Süd-Laborbedarf Gauting, SLG®). For complementation studies, *uppP* or *bcrC* were placed under control of the xylose-inducible promoter P_{xylA} inserted into the *thrC*-integration vector pBS4S. For measurements of promoter activity, promoter fragments spanning

about 400 bp upstream of the Shine-Dalgarno sequence of the respective gene were cloned into pAH328, which carried the *luxABCDE* operon as an online luminescence reporter (Schmalisch et al., 2010). All plasmids generated during this study and a brief description of the construction are provided in Table S2.

Allelic replacement mutations of *bcrC* and *uppP* were generated via long flanking homology PCRs, as described previously (Mascher et al., 2003). The integration of plasmids or DNA fragments into the *B. subtilis* genome via double recombination was verified with threonine auxotrophy (*thrC*) or colony PCR (*sacA, uppP, bcrC, yodM, dgkA*). All primer sequences are listed in Table S3.

Luciferase assay

Luciferase activities of *B. subtilis* strains harboring promoter-*lux* fusions were assayed using a Synergy™ NEOALPHAB multi-mode microplate reader from BioTek® (Winooski, VT, USA). The reader was controlled using the software Gen5™ (version 2.06). 100 µl culture volume were used per well in 96-well plates (black wall, clear bottom, clear lid, Greiner Bio-One). Incubation in the reader occurred at 37°C with linear agitation (567cpm) and luminescence and OD_{600} were measured every 5 min. Strains were grown in MCSEC medium. Overnight cultures contained 0.2% xylose, to ensure protein production in complementation strains. (i) Day cultures (containing 0.2 % xylose) were inoculated 1:5,000 from fresh overnight cultures, and strains were grown until exponential phase (OD_{600}= 0.1-0.4) (ii) Cells were harvested by centrifugation, washed twice in MCSEC, resuspended in MCSEC and the optical density was adjusted to OD_{600}=0.025. (iii) 0.2 % xylose was added if indicated and incubation in the reader occurred for 3 hours. (iv) 30 µg ml^{-1} of bacitracin was added, if applicable, and the incubation and measurement continued for 17 hours. Specific luminescence activity is given by the raw luminescence output (RLU) normalized by cell density (RLU/OD) (Radeck et al., 2013). For the depletion assay, cultures were handled as described, but the resuspended cultures (ii) were set to OD_{600}=0.1 and 1:2, 1:4, 1:8, 1:16, and 1:100 dilutions thereof.

Microscopy

Cell morphologies and sporulation frequencies were studied with an Olympus Microscope (AX70, 100x oil objective, camera XC10) and the accompanying software (Olympus cellSens Dimension 1.14). Phase contrast and GFP fluorescence channels (filter cube: U-MNIB, FF blue longpass, Ex. 470-490 nm, Em. 515-∞) were used. The exposure time for the GFP-channel was 100 ms. Strains were grown as described above, but day cultures were supplemented with 0.2% xylose (as indicated in figure legends), and incubated for up to 48 hours in flasks. Samples were taken at late exponential phase (OD_{600} ~0.6-0.8, typically after 5-6 h), late / very late stationary phase (24 h/48 h post inoculation). Phase contrast pictures were adjusted in brightness and contrast to improve cell shape detection. All GFP-channel pictures were adjusted in brightness and contrast with the identical settings.

Determination of minimal inhibitory concentration

Bacitracin resistance in *B. subtilis* strains was determined using Etest® strips on bacterial lawns (bioMérieux, Marcy l'Etoile, France), as described previously (Radeck et al., 2016b), with the following changes: (i) MCSEC medium was used instead of MH, (ii) overnight cultures contained 0.2 % xylose, and (iii) day cultures, soft agar and agar plates contained 0.2 % xylose, if applicable (see figure legends).

Conflict of Interest

The authors declare that the research was conducted in the absence of any commercial or financial relationships that could be construed as a potential conflict of interest.

Author contributions

JR and TM conceptualized the study. NL and JR designed the experiments and generated the *B. subtilis* strains. JR performed MIC assays and coordinated the experimental work, NL performed all remaining experiments. JR and TM wrote the manuscript. All authors approved the manuscript and agree to be accountable for the content of the work.

Funding

This project was funded by the Deutsche Forschungsgemeinschaft (DFG) priority program SPP1617 'Phenotypic Heterogeneity and Sociobiology of Bacterial Populations' (grant MA 2837/3-2 to TM).

Acknowledgements

We thank Vanessa Gilly for obtaining some of the micrographs shown in Fig. S1 and S3 and Philipp Popp for the construction of TMB4201-4205.

References

Amiteye, S., Kobayashi, K., Imamura, D., Hosoya, S., Ogasawara, N., and Sato, T. (2003). Bacillus subtilis Diacylglycerol Kinase (DgkA) Enhances Efficient Sporulation. *Journal of Bacteriology* 185(17), 5306-5309. doi: 10.1128/jb.185.17.5306-5309.2003.

Anderson, R.G., Hussey, H., and Baddiley, J. (1972). The mechanism of wall synthesis in bacteria. The organization of enzymes and isoprenoid phosphates in the membrane. *Biochem J* 127(1), 11-25. doi: 10.1042/bj1270011.

Azevedo, E.C., Rios, E.M., Fukushima, K., and Campos-Takaki, G.M. (1993). Bacitracin production by a new strain of *Bacillus subtilis*. Extraction, purification, and characterization. *Appl Biochem Biotechnol* 42(1), 1-7.

Barreteau, H., Magnet, S., El Ghachi, M., Touze, T., Arthur, M., Mengin-Lecreulx, D., et al. (2009). Quantitative high-performance liquid chromatography analysis of the pool levels of undecaprenyl phosphate and its derivatives in bacterial membranes. *J Chromatogr B Analyt Technol Biomed Life Sci* 877(3), 213-220. doi: 10.1016/j.jchromb.2008.12.010.

Bernard, R., El Ghachi, M., Mengin-Lecreulx, D., Chippaux, M., and Denizot, F. (2005). BcrC from *Bacillus subtilis* acts as an undecaprenyl pyrophosphate phosphatase in bacitracin resistance. *J Biol Chem* 280(32), 28852-28857. doi: 10.1074/jbc.M413750200.

Botella, E., Devine, S.K., Hubner, S., Salzberg, L.I., Gale, R.T., Brown, E.D., et al. (2014). PhoR autokinase activity is controlled by an intermediate in wall teichoic acid metabolism that is sensed by the intracellular PAS domain during the PhoPR-mediated phosphate limitation response of Bacillus subtilis. *Mol Microbiol* 94(6), 1242-1259. doi: 10.1111/mmi.12833.

Breukink, E., and de Kruijff, B. (2006). Lipid II as a target for antibiotics. *Nat Rev Drug Discov* 5(4), 321-332. doi: 10.1038/nrd2004.

Breukink, E., van Heusden, H.E., Vollmerhaus, P.J., Swiezewska, E., Brunner, L., Walker, S., et al. (2003). Lipid II is an intrinsic component of the pore induced by nisin in bacterial membranes. *J Biol Chem* 278(22), 19898-19903. doi: 10.1074/jbc.M301463200.

Brown, S., Santa Maria, J.P., Jr., and Walker, S. (2013). Wall teichoic acids of gram-positive bacteria. *Annu Rev Microbiol* 67, 313-336. doi: 10.1146/annurev-micro-092412-155620.

Cao, M., and Helmann, J.D. (2002). Regulation of the *Bacillus subtilis bcrC* bacitracin resistance gene by two extracytoplasmic function s factors. *J Bacteriol* 184(22), 6123-6129. doi: 10.1128/JB.184.22.6123–6129.2002.

Consortium, T.U. (2017). UniProt: the universal protein knowledgebase. *Nucleic Acids Research* 45(D1), D158-D169. doi: 10.1093/nar/gkw1099.

Coote, J.G. (1972). Sporulation in *Bacillus subtilis*. Characterization of oligosporogenous mutants and comparison of their phenotypes with those of asporogenous mutants. *J Gen Microbiol* 71(1), 1-15. doi: 10.1099/00221287-71-1-1.

Dammeyer, T., and Tinnefeld, P. (2012). Engineered fluorescent proteins illuminate the bacterial periplasm. *Comput Struct Biotechnol J* 3, e201210013. doi: 10.5936/csbj.201210013.

Economou, N.J., Cocklin, S., and Loll, P.J. (2013). High-resolution crystal structure reveals molecular details of target recognition by bacitracin. *Proc Natl Acad Sci U S A* 110(35), 14207-14212. doi: 10.1073/pnas.1308268110.

Egan, A.J., Biboy, J., van't Veer, I., Breukink, E., and Vollmer, W. (2015). Activities and regulation of peptidoglycan synthases. *Philos Trans R Soc Lond B Biol Sci* 370(1679). doi: 10.1098/rstb.2015.0031.

Eiamphungporn, W., and Helmann, J.D. (2008). The Bacillus subtilis sigma(M) regulon and its contribution to cell envelope stress responses. *Mol Microbiol* 67(4), 830-848. doi: 10.1111/j.1365-2958.2007.06090.x.

El Ghachi, M., Bouhss, A., Blanot, D., and Mengin-Lecreulx, D. (2004). The *bacA* gene of *Escherichia coli* encodes an undecaprenyl pyrophosphate phosphatase activity. *J Biol Chem* 279(29)**,** 30106-30113.

El Ghachi, M., Derbise, A., Bouhss, A., and Mengin-Lecreulx, D. (2005). Identification of multiple genes encoding membrane proteins with undecaprenyl pyrophosphate phosphatase (UppP) activity in *Escherichia coli*. *J Biol Chem* 280(19)**,** 18689-18695.

Fan, J., Jiang, D., Zhao, Y., Liu, J., and Zhang, X.C. (2014). Crystal structure of lipid phosphatase *Escherichia coli* phosphatidylglycerophosphate phosphatase B. *Proc Natl Acad Sci U S A* 111(21)**,** 7636-7640. doi: 10.1073/pnas.1403097111.

Fenton, A.K., El Mortaji, L., Lau, D.T.C., Rudner, D.Z., and Bernhardt, T.G. (2016). CozE is a member of the MreCD complex that directs cell elongation in Streptococcus pneumoniae. 2**,** 16237. doi: 10.1038/nmicrobiol.2016.237.

Guariglia-Oropeza, V., and Helmann, J.D. (2011). Bacillus subtilis sigma(V) confers lysozyme resistance by activation of two cell wall modification pathways, peptidoglycan O-acetylation and D-alanylation of teichoic acids. *J Bacteriol* 193(22)**,** 6223-6232. doi: 10.1128/JB.06023-11.

Guo, R.T., Ko, T.P., Chen, A.P., Kuo, C.J., Wang, A.H., and Liang, P.H. (2005). Crystal structures of undecaprenyl pyrophosphate synthase in complex with magnesium, isopentenyl pyrophosphate, and farnesyl thiopyrophosphate: roles of the metal ion and conserved residues in catalysis. *J Biol Chem* 280(21)**,** 20762-20774. doi: 10.1074/jbc.M502121200.

Harwood, C.R., and Cutting, S.M. (1990). *Molecular Biological Methods for Bacillus.* Chichester: John Wiley & Sons.

Helmann, J.D. (2016). Bacillus subtilis extracytoplasmic function (ECF) sigma factors and defense of the cell envelope. *Curr Opin Microbiol* 30**,** 122-132. doi: 10.1016/j.mib.2016.02.002.

Higashi, Y., Strominger, J.L., and Sweeley, C.C. (1970). Biosynthesis of the peptidoglycan of bacterial cell walls. XXI. Isolation of free C55-isoprenoid alcohol and of lipid intermediates in peptidoglycan synthesis from *Staphylococcus aureus*. *J Biol Chem* 245(14)**,** 3697-3702.

Inaoka, T., and Ochi, K. (2012). Undecaprenyl pyrophosphate involvement in susceptibility of Bacillus subtilis to rare earth elements. *J Bacteriol* 194(20)**,** 5632-5637. doi: 10.1128/JB.01147-12.

Ishihara, H., Takoh, M., Nishibayashi, R., and Sato, A. (2002). Distribution and variation of bacitracin synthetase gene sequences in laboratory stock strains of *Bacillus licheniformis*. *Curr Microbiol* 45(1)**,** 18-23.

Jerga, A., Lu, Y.J., Schujman, G.E., de Mendoza, D., and Rock, C.O. (2007). Identification of a soluble diacylglycerol kinase required for lipoteichoic acid production in Bacillus subtilis. *J Biol Chem* 282(30)**,** 21738-21745. doi: 10.1074/jbc.M703536200.

Jordan, S., Hutchings, M.I., and Mascher, T. (2008). Cell envelope stress response in Gram-positive bacteria. *FEMS Microbiol Rev* 32(1)**,** 107-146. doi: 10.1111/j.1574-6976.2007.00091.x.

Jordan, S., Junker, A., Helmann, J.D., and Mascher, T. (2006). Regulation of LiaRS-dependent gene expression in bacillus subtilis: identification of inhibitor proteins, regulator binding sites, and target genes of a conserved cell envelope stress-sensing two-component system. *J Bacteriol* 188(14)**,** 5153-5166. doi: 10.1128/JB.00310-06.

Kawai, Y., Marles-Wright, J., Cleverley, R.M., Emmins, R., Ishikawa, S., Kuwano, M., et al. (2011). A widespread family of bacterial cell wall assembly proteins. *EMBO J* 30(24)**,** 4931-4941. doi: 10.1038/emboj.2011.358.

Kelley, L.A., Mezulis, S., Yates, C.M., Wass, M.N., and Sternberg, M.J. (2015). The Phyre2 web portal for protein modeling, prediction and analysis. *Nat Protoc* 10(6)**,** 845-858. doi: 10.1038/nprot.2015.053.

Kobayashi, K., Ehrlich, S.D., Albertini, A., Amati, G., Andersen, K.K., Arnaud, M., et al. (2003). Essential *Bacillus subtilis* genes. *Proc Natl Acad Sci U S A* 100(8)**,** 4678-4683.

Kobras, C.M., Mascher, T., and Gebhard, S. (2017). "Application of a Bacillus subtilis Whole-Cell Biosensor (PliaI-lux) for the Identification of Cell Wall Active Antibacterial Compounds," in *Antibiotics: Methods and Protocols,* ed. P. Sass. (New York, NY: Springer New York), 121-131.

Kramer, N.E., Smid, E.J., Kok, J., De Kruijff, B., Kuipers, O.P., and Breukink, E. (2004). Resistance of Gram-positive bacteria to nisin is not determined by Lipid II levels. *FEMS Microbiol Lett* 239(1)**,** 157-161. doi: 10.1016/j.femsle.2004.08.033.

Laddomada, F., Miyachiro, M.M., and Dessen, A. (2016). Structural Insights into Protein-Protein Interactions Involved in Bacterial Cell Wall Biogenesis. *Antibiotics (Basel)* 5(2). doi: 10.3390/antibiotics5020014.

Lee, Y.H., and Helmann, J.D. (2013). Reducing the Level of Undecaprenyl Pyrophosphate Synthase Has Complex Effects on Susceptibility to Cell Wall Antibiotics. *Antimicrob Agents Chemother*. doi: 10.1128/AAC.00794-13.

Manat, G., Roure, S., Auger, R., Bouhss, A., Barreteau, H., Mengin-Lecreulx, D., et al. (2014). Deciphering the metabolism of undecaprenyl-phosphate: the bacterial cell-wall unit carrier at the membrane frontier. *Microb Drug Resist* 20(3)**,** 199-214. doi: 10.1089/mdr.2014.0035.

Mascher, T., Margulis, N.G., Wang, T., Ye, R.W., and Helmann, J.D. (2003). Cell wall stress responses in *Bacillus subtilis*: the regulatory network of the bacitracin stimulon. *Mol Microbiol* 50(5)**,** 1591-1604. doi: 10.1046/j.1365-2958.2003.03786.x.

Mascher, T., Zimmer, S.L., Smith, T.A., and Helmann, J.D. (2004). Antibiotic-inducible promoter regulated by the cell envelope stress-sensing two-component system LiaRS of Bacillus subtilis. *Antimicrob Agents Chemother* 48(8)**,** 2888-2896. doi: 10.1128/AAC.48.8.2888-2896.2004.

McCloskey, M.A., and Troy, F.A. (1980). Paramagnetic isoprenoid carrier lipids. 2. Dispersion and dynamics in lipid membranes. *Biochemistry* 19(10)**,** 2061-2066. doi: 10.1021/bi00551a009,.

Meeske, A.J., Rodrigues, C.D., Brady, J., Lim, H.C., Bernhardt, T.G., and Rudner, D.Z. (2016). High-Throughput Genetic Screens Identify a Large and Diverse Collection of New Sporulation Genes in Bacillus subtilis. *PLoS Biol* 14(1)**,** e1002341. doi: 10.1371/journal.pbio.1002341.

Meeske, A.J., Sham, L.T., Kimsey, H., Koo, B.M., Gross, C.A., Bernhardt, T.G., et al. (2015). MurJ and a novel lipid II flippase are required for cell wall biogenesis in Bacillus subtilis. *Proc Natl Acad Sci U S A* 112(20)**,** 6437-6442. doi: 10.1073/pnas.1504967112.

Michna, R.H., Zhu, B., Mader, U., and Stulke, J. (2016). SubtiWiki 2.0--an integrated database for the model organism Bacillus subtilis. *Nucleic Acids Res* 44(D1)**,** D654-662. doi: 10.1093/nar/gkv1006.

Minnig, K., Barblan, J.L., Kehl, S., Moller, S.B., and Mauel, C. (2003). In *Bacillus subtilis* W23, the duet s^X s^M, two sigma factors of the extracytoplasmic function subfamily, are required for septum and wall synthesis under batch culture conditions. *Mol Microbiol* 49(5)**,** 1435-1447. doi: 10.1046/j.1365-2958.2003.03652.x.

Muchova, K., Wilkinson, A.J., and Barak, I. (2011). Changes of lipid domains in Bacillus subtilis cells with disrupted cell wall peptidoglycan. *FEMS Microbiol Lett* 325(1)**,** 92-98. doi: 10.1111/j.1574-6968.2011.02417.x.

Nicolas, P., Mäder, U., Dervyn, E., Rochat, T., Leduc, A., Pigeonneau, N., et al. (2012). Condition-dependent transcriptome reveals high-level regulatory architecture in *Bacillus subtilis*. *Science* 335(6072)**,** 1103-1106. doi: 10.1126/science.1206848.

Ohki, R., Giyanto, Tateno, K., Masuyama, W., Moriya, S., Kobayashi, K., et al. (2003). The BceRS two-component regulatory system induces expression of the bacitracin transporter, BceAB, in Bacillus subtilis. *Molecular Microbiology* 49(4)**,** 1135-1144. doi: 10.1046/j.1365-2958.2003.03653.x.

Peters, J.M., Colavin, A., Shi, H., Czarny, T.L., Larson, M.H., Wong, S., et al. (2016). A Comprehensive, CRISPR-based Functional Analysis of Essential Genes in Bacteria. *Cell* 165(6)**,** 1493-1506. doi: 10.1016/j.cell.2016.05.003.

Piggot, P.J., and Coote, J.G. (1976). Genetic Aspects of Bacterial Endospore Formation. *Bacteriol Rev* 40(4)**,** 908-962.

Radeck, J., Fritz, G., and Mascher, T. (2016a). The cell envelope stress response of Bacillus subtilis: from static signaling devices to dynamic regulatory network. *Current Genetics***,** 1-12. doi: 10.1007/s00294-016-0624-0.

Radeck, J., Gebhard, S., Orchard, P.S., Kirchner, M., Bauer, S., Mascher, T., et al. (2016b). Anatomy of the bacitracin resistance network in *Bacillus subtilis*. *Mol Microbiol* 100(4)**,** 607-620. doi: 10.1111/mmi.13336.

Radeck, J., Kraft, K., Bartels, J., Cikovic, T., Dürr, F., Emenegger, J., et al. (2013). The *Bacillus* BioBrick Box: generation and evaluation of essential genetic building blocks for standardized work with *Bacillus subtilis*. *J Biol Eng* 7(1)**,** 29. doi: 10.1186/1754-1611-7-29.

Rietkötter, E., Hoyer, D., and Mascher, T. (2008). Bacitracin sensing in *Bacillus subtilis*. *Mol Microbiol* 68(3)**,** 768-785. doi: 10.1111/j.1365-2958.2008.06194.x.

Sambrook, J., and Russell, D.W. (2001). *Molecular Cloning - a laboratory manual.* Cold Spring Harbor, N.Y.: Cold Spring Harbor Laboratory Press.

Schmalisch, M., Maiques, E., Nikolov, L., Camp, A.H., Chevreux, B., Muffler, A., et al. (2010). Small genes under sporulation control in the *Bacillus subtilis* genome. *J Bacteriol* 192(20)**,** 5402-5412. doi: 10.1128/JB.00534-10.

Siewert, G., and Strominger, J.L. (1967). Bacitracin: an inhibitor of the dephosphorylation of lipid pyrophosphate, an intermediate in the biosynthesis of the peptidoglycan of bacterial cell walls. *Proc Natl Acad Sci U S A* 57(3)**,** 767-773.

Storm, D.R., and Strominger, J.L. (1973). Complex formation between bacitracin peptides and isoprenyl pyrophosphates. The specificity of lipid-peptide interactions. *J Biol Chem* 248(11)**,** 3940-3945.

Thackray, P.D., and Moir, A. (2003). SigM, an extracytoplasmic function sigma factor of *Bacillus subtilis*, is activated in response to cell wall antibiotics, ethanol, heat, acid, and superoxide stress. *J Bacteriol* 185(12)**,** 3491-3498. doi: 10.1128/JB.185.12.3491-3498.2003.

Tseng, C.L., and Shaw, G.C. (2008). Genetic evidence for the actin homolog gene *mreBH* and the bacitracin resistance gene *bcrC* as targets of the alternative sigma factor SigI of *Bacillus subtilis*. *J Bacteriol* 190(5)**,** 1561-1567. doi: 10.1128/JB.01497-07.

Typas, A., Banzhaf, M., Gross, C.A., and Vollmer, W. (2012). From the regulation of peptidoglycan synthesis to bacterial growth and morphology. *Nat Rev Microbiol* 10(2)**,** 123-136. doi: 10.1038/nrmicro2677.

Vagner, V., Dervyn, E., and Ehrlich, S.D. (1998). A vector for systematic gene inactivation in *Bacillus subtilis*. *Microbiology* 144 (Pt 11)**,** 3097-3104.

Van Horn, W.D., and Sanders, C.R. (2012). Prokaryotic diacylglycerol kinase and undecaprenol kinase. *Annu Rev Biophys* 41**,** 81-101. doi: 10.1146/annurev-biophys-050511-102330.

Willoughby, E., Higashi, Y., and Strominger, J.L. (1972). Enzymatic Dephosphorylation of C55-Isoprenylphosphate. *J Biol Chem* 247(16)**,** 5113-5115.

Wolf, D., Kalamorz, F., Wecke, T., Juszczak, A., Mäder, U., Homuth, G., et al. (2010). In-depth profiling of the LiaR response of *Bacillus subtilis*. *J Bacteriol* 192(18)**,** 4680-4693. doi: 10.1128/JB.00543-10.

Wolf, D., and Mascher, T. (2016). The applied side of antimicrobial peptide-inducible promoters from Firmicutes bacteria: expression systems and whole-cell biosensors. *Applied Microbiology and Biotechnology* 100(11)**,** 4817-4829. doi: 10.1007/s00253-016-7519-3.

Zhao, H., Sun, Y., Peters, J.M., Gross, C.A., Garner, E.C., and Helmann, J.D. (2016). Depletion of undecaprenyl pyrophosphate phosphatases (UPP-Pases) disrupts cell envelope biogenesis in *Bacillus subtilis*. *J Bacteriol*. doi: 10.1128/JB.00507-16.

Zweers, J.C., Nicolas, P., Wiegert, T., van Dijl, J.M., and Denham, E.L. (2012). Definition of the sigma(W) regulon of Bacillus subtilis in the absence of stress. *PLoS One* 7(11)**,** e48471. doi: 10.1371/journal.pone.0048471.

SUPPLEMENTAL MATERIAL

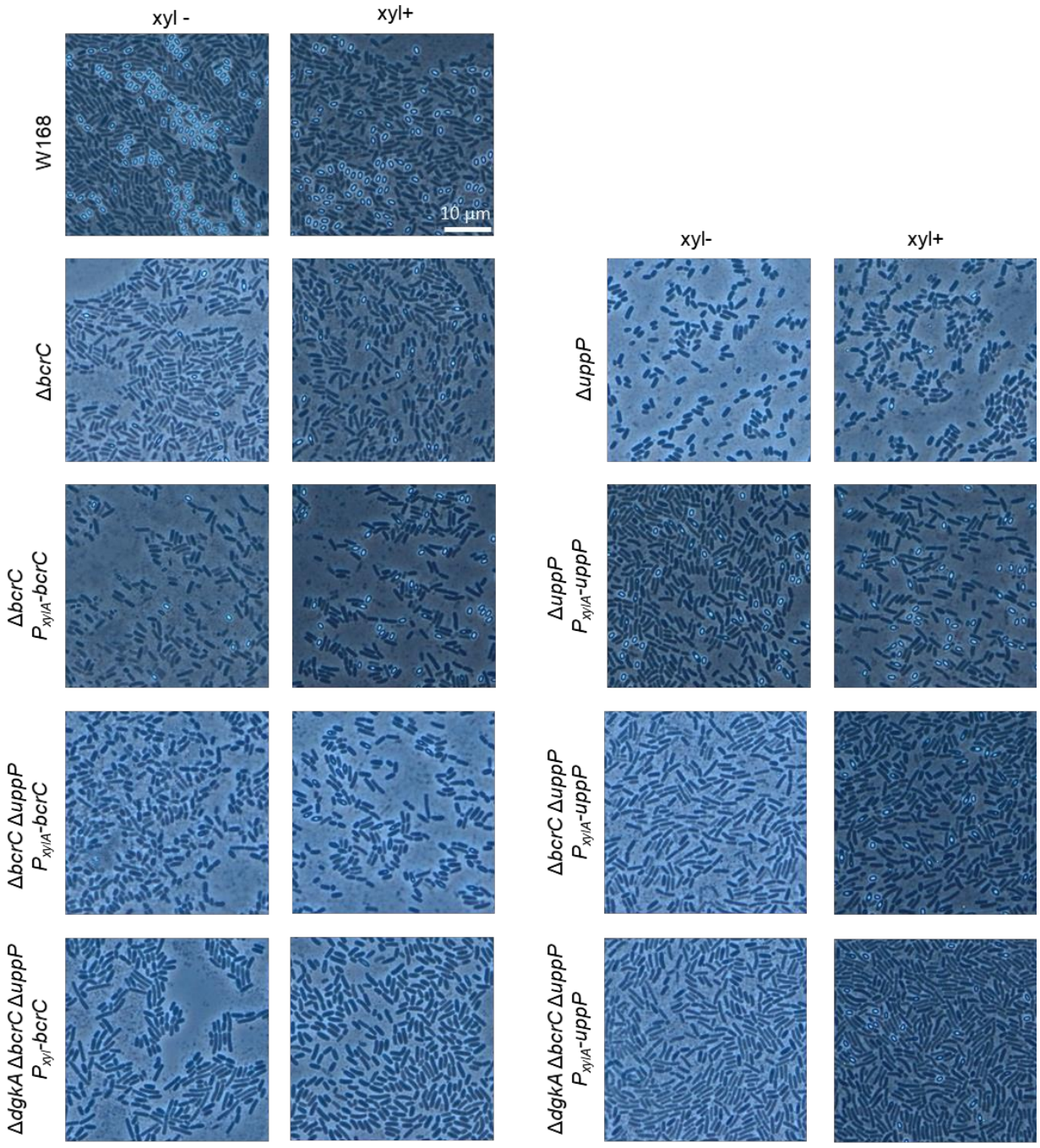

Figure S1. Sporulation efficiency of *bcrC* and *uppP* deletion and complementation mutants.

Strains (W168, TMB297, TMB3694, TMB3739, TMB3957, TMB3408, TMB3695, TMB3740, and TMB3958) were grown as described in Fig. 2 and phase contrast microscope pictures were taken 24 h post-inoculation. The scale bar is 10 µm.

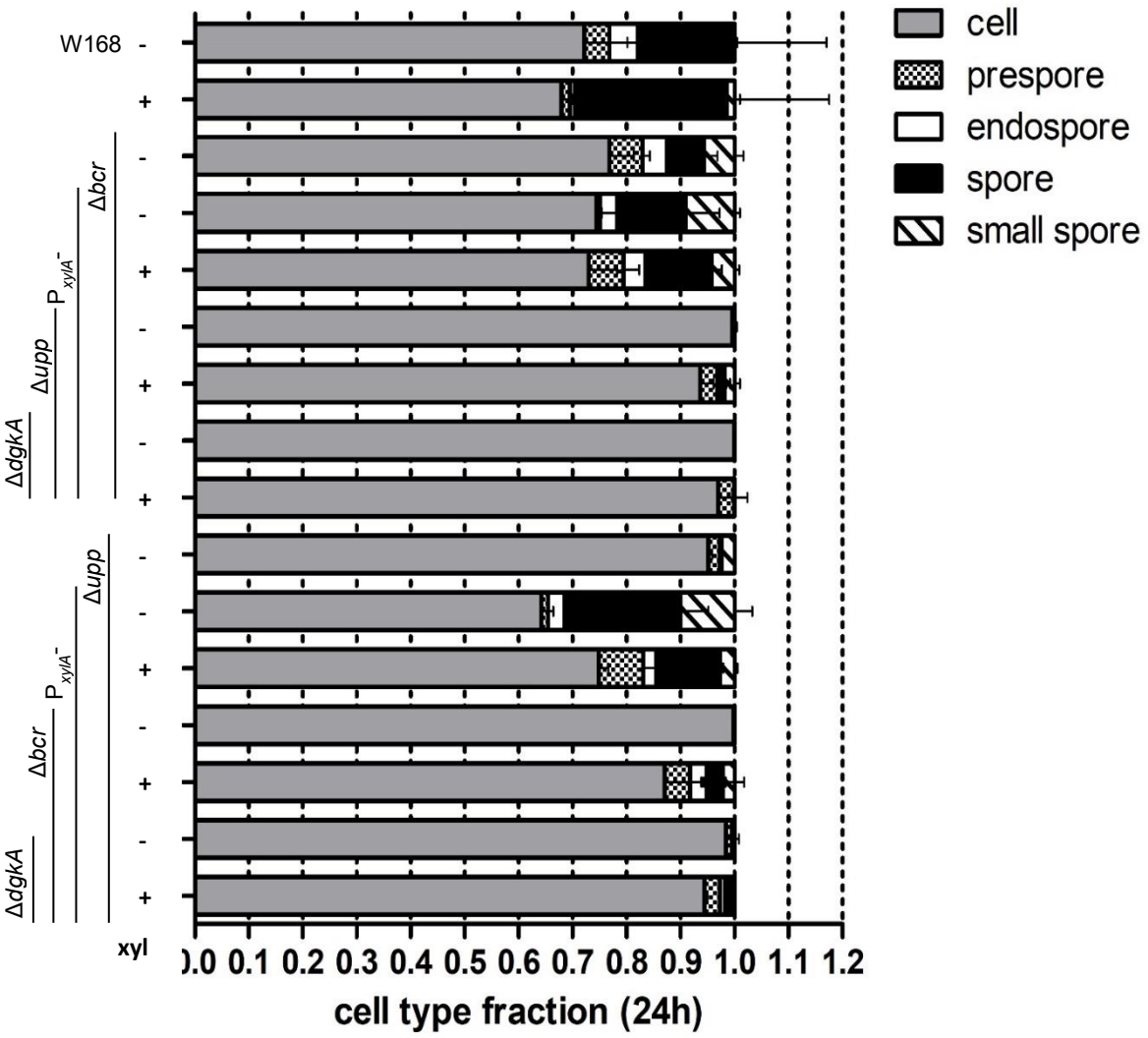

Figure S2. Sporulation efficiency of *bcrC* and *uppP* deletion and complementation mutants.

Strains (W168, TMB297, TMB3694, TMB3739, TMB3957, TMB3408, TMB3695, TMB3740, and TMB3958) were grown as described in Fig. 2 and phase contrast microscopy pictures were taken 24 h post-inoculation. Legend: normal cells (grey), prespores without fully established phase-bright endospore (small checkered), completed endospores (white), free spores (black) and small free spores (striped). xyl+, 0.2% xylose supplemented in the day culture.

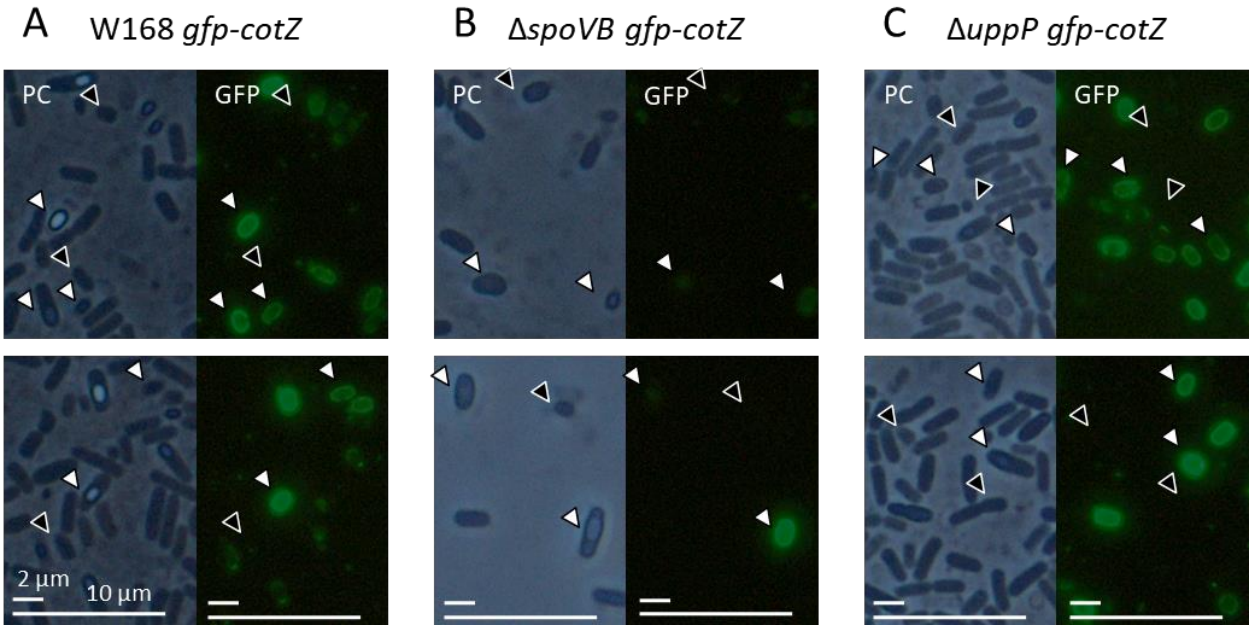

Figure S3. Detection of spores in *uppP* mutant via crust marker GFP-CotZ

Strains (TMB2112, TMB4150, and TMB4151) were grown as described in Fig. 3 and phase contrast as well as green fluorescence were documented 24 h post-inoculation. Prespores, endospores, free spores, phase-dark free spores, and small free spores can have fully developed spore crusts where GFP-CotZ is located (see white arrowheads with black border). However, not all small phase-dark particles can be classified as spores with this marker (see black arrowheads with white border, no GFP signal). **A**. **Wild type**. Please note that small spores only appear small in the phase contrast picture, but their crust has (almost) normal size as visualized in the GFP-channel. **B**. ***spoVB* mutant** (lipidII flippase, active during sporulation). Sporulation is strongly impaired. This strain was used as a control. **C**. ***uppP* mutant**. Hardly any developed phase-bright spores were formed. But prespores as well as some phase-dark spores (which could be mistaken for small cells) clearly show a spore crust. The scale bars are 2 or 10 µm, respectively.

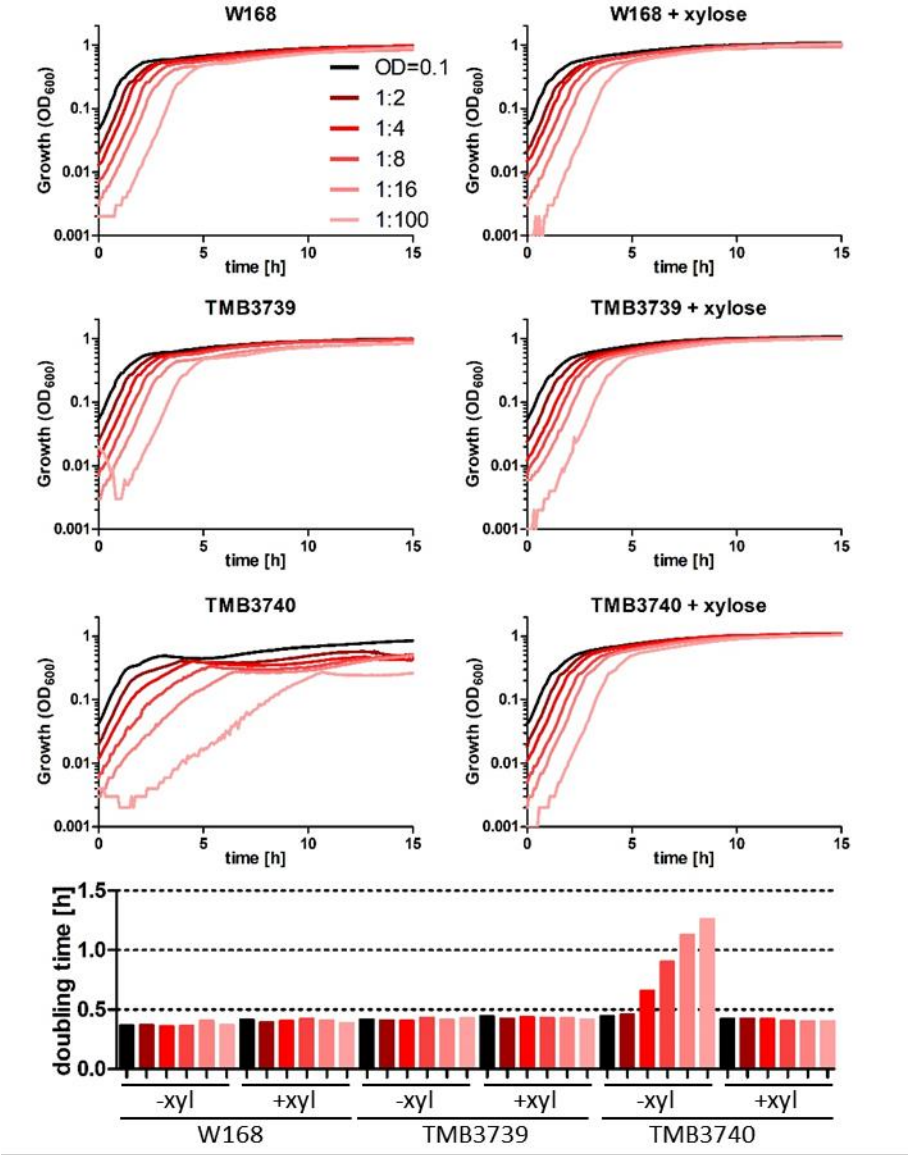

Figure S4. Growth of the wild type and *bcrC* and *uppP* complementation mutants. Strains were grown in MCSEC supplemented with 0.2% xylose at 37°C to OD_{600}=0.2-0.6, washed and resuspended to an optical density of OD_{600} = 0.1 in MCSEC (A, C, E), or MCSEC + 0.2% xylose (B, D, F). Cultures, as well as their 1:2, 1:4, 1:8, 1:16 and 1:100 dilutions were grown in 96-well plates in a microtiter plate reader at 37° where OD_{600} was measured every 5 minutes for 15 hours. **A-F.** Graphs show the OD_{600}-values as a measure for cell density, or the doubling time during exponential growth, with the color saturation decreasing with increasing dilutions. **A, B.** W168. **C, D.** TMB3739, Δ*bcrC* Δ*uppP* P_{xylA}-*bcrC.* **E, F.** TMB3740, Δ*bcrC* Δ*uppP* P_{xylA}-*uppP.* Data was obtained in biological triplicates, of which one representative sample is shown. **G.** The doubling times were calculated with Prism5, using the exponential growth equation and OD_{600}-values from 0.007 to 0.15 (TMB3740 –xyl) or 0.24 (all other strains), respectively.

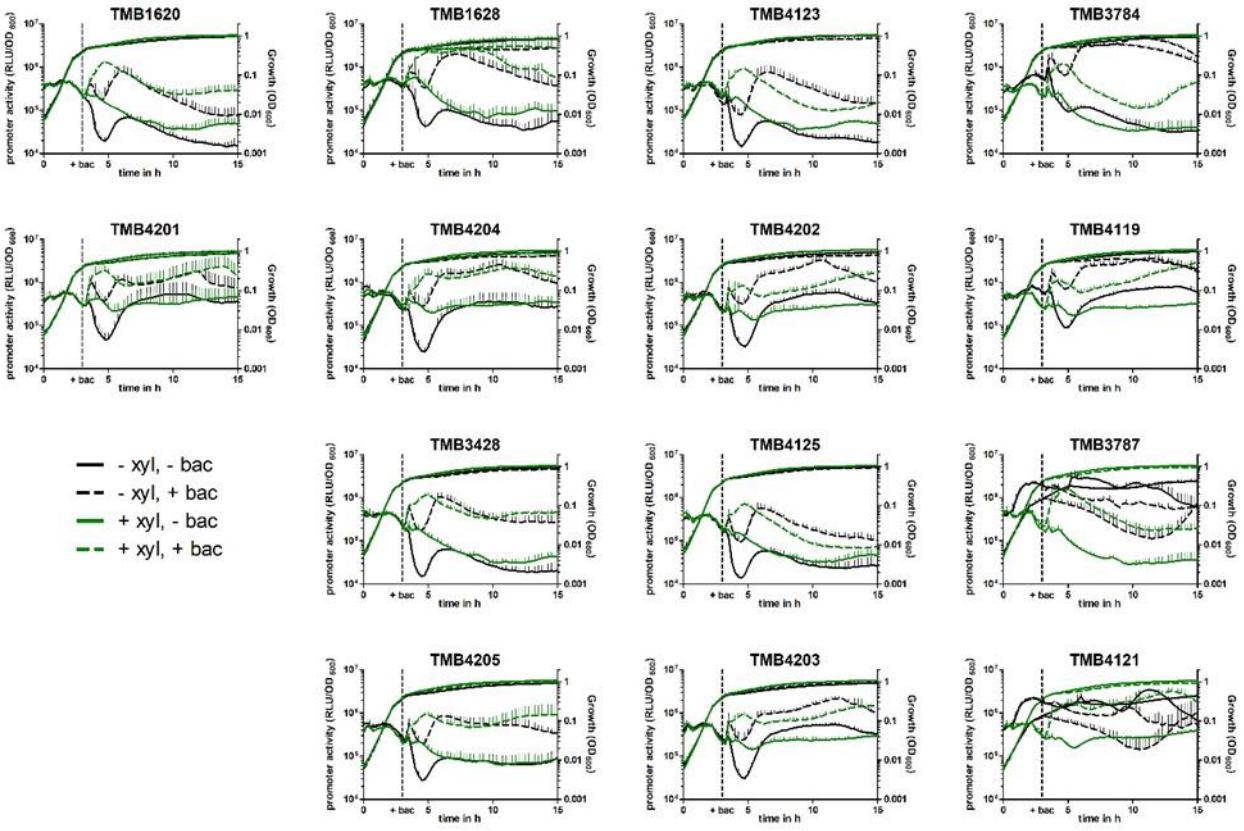

Figure S5. Growth and P_{bcrC} promoter activities in the wild type and *bcrC* and *uppP* complementation mutants. See legend of Fig. 5. Black, without xylose; green, + 0.2% xylose; solid line, without bacitracin; dashed line, + 30 µg ml^{-1} bacitracin. Thin lines represent the standard deviation of three biological replicates.

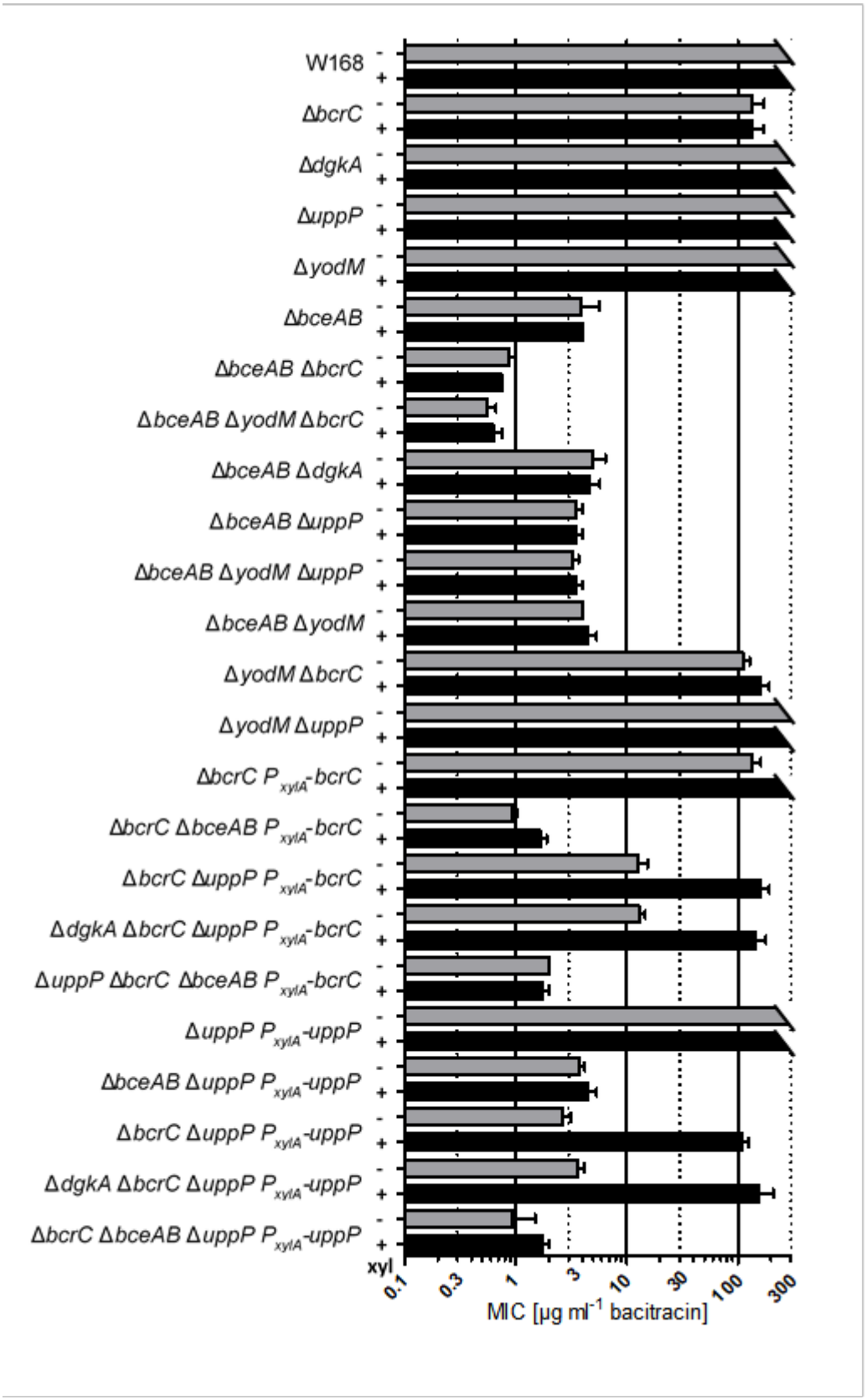

Figure S6. Minimal inhibitory bacitracin concentration of *bcrC* and *uppP* deletion and complementation mutants. Description, see Fig. 7.

Table S1: Bacterial strains used in this study

Name	Description[a]	Source
E. coli strains		
XL1-Blue	*recA1 endA1 gyrA96 thi-1 hsdR17 supE44 relA1 lac F'*::Tn*10* *proAB lacI*^{q} Δ(*lacZ*)M15]	Stratagene
NEB5α	*fhuA2 Δ(argF-lacZ)U169 phoA glnV44 Φ80 Δ(lacZ)M15 gyrA96 recA1 relA1 endA1 thi-1 hsdR17*	NEB
B. subtilis strains		
W168	wild type, *trpC2*	Laboratory stock
For luminescence analysis		
TMB3688	W168 *sacA*::pJRlux101 (P_{yubA}-*lux*)	This study
TMB1620	W168 *sacA*::pCHlux104 (P_{bcrC}-*lux*)	(Höfler et al., 2016)
TMB1628	W168 *bcrC*::*tet sacA*::pCHlux104 (P_{bcrC}-*lux*)	This study
TMB4123	W168 *bcrC*::*tet thrC*::pJR4S01 (P_{xylA}-*bcrC*) *sacA*::pCHlux104 (P_{bcrC}-*lux*)	This study
TMB3784	W168 *bcrC*::*tet uppP*::*MLS thrC*::pJR4S01 (P_{xylA}-*bcrC*) *sacA*::pCHlux104 (P_{bcrC}-*lux*)	This study
TMB3428	W168 *uppP*::*MLS sacA*::pCHlux104 (P_{bcrC}-*lux*)	This study
TMB4125	W168 *uppP*::*MLS thrC*::pJR4S02 (P_{xylA}-*uppP*) *sacA*::pCHlux104 (P_{bcrC}-*lux*)	This study
TMB3787	W168 *bcrC*::*tet uppP*::*MLS thrC*::pJR4S02 (P_{xylA}-*uppP*) *sacA*::pCHlux104 (P_{bcrC}-*lux*)	This study
TMB4201	W168 *dgkA*::*kan sacA*::pCHlux104 (P_{bcrC}-*lux*)	This study
TMB4204	W168 *dgkA*::*kan bcrC*::*tet sacA*::pCHlux104 (P_{bcrC}-*lux*)	This study
TMB4202	W168 *dgkA*::*kan bcrC*::*tet thrC*::pJR4S01 (P_{xylA}-*bcrC*) *sacA*::pCHlux104 (P_{bcrC}-*lux*)	This study
TMB4119	W168 *dgkA*::*kan bcrC*::*tet uppP*::*MLS thrC*::pJR4S01 (P_{xylA}-*bcrC*) *sacA*::pCHlux104 (P_{bcrC}-*lux*)	
TMB4205	W168 *dgkA*::*kan uppP*::*MLS sacA*::pCHlux104 (P_{bcrC}-*lux*)	This study
TMB4203	W168 *dgkA*::*kan uppP*::*MLS thrC*::pJR4S02 (P_{xylA}-*uppP*) *sacA*::pCHlux104 (P_{bcrC}-*lux*)	This study
TMB4121	W168 *dgkA*::*kan bcrC*::*tet uppP*::*MLS thrC*::pJR4S02 (P_{xylA}-*uppP*) *sacA*::pCHlux104 (P_{bcrC}-*lux*)	
Cell morphology, sporulation efficiency, and bacitracin MIC		
TMB0297	W168 *bcrC*::*tet*	(Rietkötter et al., 2008)
TMB3694	W168 *bcrC*::*tet thrC*::pJR4S01 (P_{xylA}-*bcrC*)	This study
TMB3739	W168 *bcrC*::*tet uppP*::*MLS thrC*::pJR4S01 (P_{xylA}-*bcrC*)	This study
TMB3957	W168 *dgkA*::*kan bcrC*::*tet uppP*::*MLS thrC*::pJR4S01 (P_{xylA}-*bcrC*)	This study
TMB3408	W168 *uppP*::*MLS*	This study
TMB3695	W168 *uppP*::*MLS thrC*::pJR4S02 (P_{xylA}-*uppP*)	This study
TMB3740	W168 *bcrC*::*tet uppP*::*MLS thrC*::pJR4S02 (P_{xylA}-*uppP*)	This study
TMB3958	W168 *dgkA*::*kan bcrC*::*tet uppP*::*MLS thrC*::pJR4S02 (P_{xylA}-*uppP*)	This study
GFP-CotZ		
TMB4517	W168 *amyE*::p1CSV-CotZ-N-GFP (P_{cotYZ}-*gfp-cotZ*)	(Julia Bartels, unpublished)
TMB4150	W168 *spoVB*::*MLS amyE*::p1CSV-CotZ-N-GFP (P_{cotY}-*gfp-cotZ*)	This study
TMB4151	W168 *uppP*::*MLS amyE*::p1CSV-CotZ-N-GFP (P_{cotY}-*gfp-cotZ*)	This study
Supplemental bacitracin MIC		
TMB3923	W168 *dgkA*::*kan*	This study
TMB3568	W168 *yodM*::*spec*	This study
TMB0035	W168 *bceAB*::*kan*	(Rietkötter et al., 2008)
TMB0713	W168 *bceAB*:*kan bcrC*::*tet*	(Radeck et al., 2016)
TMB4104	W168 *yodM*::*spec bcrC*::*tet bceAB*::*kan*	This study
TMB4110	W168 *dgkA*::*cat bceAB*::*kan*	This study
TMB4102	W168 *uppP*::*mls bceAB*::*kan*	This study
TMB4105	W168 *yodM*::*spec uppP*::*mls bceAB*::*kan*	This study
TMB4103	W168 *yodM*::*spec bceAB*::*kan*	This study
TMB3716	W168 *yodM*::*spec bcrC*::*tet*	This study
TMB3738	W168 *yodM*::*spec uppP*::*mls*	This study
TMB4106	W168 *bcrC*::*tet thrC*::pJR4S01 (P_{xylA}-*bcrC*) *bceAB*::*kan*	This study
TMB4108	W168 *bcrC*::tet *uppP*::*MLS thrC*::pJR4S01 (P_{xylA}-*bcrC*) *bceAB*::*kan*	This study
TMB4107	W168 *uppP*::*MLS thrC*::pJR4S02 (P_{xylA}-*uppP*) *bceAB*::*kan*	This study
TMB4109	W168 *bcrC*::*tet uppP*::*MLS thrC*::pJR4S02 (P_{xylA}-*uppP*) *bceAB*::*kan*	This study

Table S2. Vectors and plasmids used in this study

Name	**Description**	**Resistance in *E. coli* / *B. subtilis*[a]**	**Primers and Enzymes used for cloning[b]**	**Source**
Vectors				
pAH328	*sacA*'...'*sacA, luxABCDE, cat, bla*	Amp^r / cm^r		(Schmalisch et al., 2010)
pBS4S	*thrC*'...'*thrC, spc, bla*	Amp^r / spc^r		(Radeck et al., 2013)
pBS1C	*amyE'...'amyE, cat, bla*	Amp^r / cm^r		(Radeck et al., 2013)
Plasmids				
pCHlux104	pAH328-derivative, *sacA*::P$_{bcrC}$-*lux*, *cat*, *bla*	Amp^r / cm^r		(Höfler et al., 2016)
pJRlux101	pAH328-derivative, *sacA*::P$_{yubA}$-*lux*, *cat*, *bla*	Amp^r / cm^r	P$_{yubA}$: TM4738/TM5121; EcoRI, SalI	This study
pJR4S01	pBS4S-derivative, *thrC*::P$_{xylA}$-*bcrC*, *spc*, *bla*	Amp^r / spc^r	P$_{xylA}$:TM2968/ TM2969; EcoRI, SpeI. *bcrC*: TM2731/ TM2732; XbaI ,PstI	This study
pJR4S02	pBS4S-derivative, *thrC*::P$_{xylA}$-*uppP, spc, bla*	Amp^r / spc^r	P$_{xylA}$:TM2968/ TM2969; EcoRI, SpeI. *uppP*: 3 fragments (TM5122/ TM5125, TM5124/ TM5127, TM5126/ TM5123) were PCR-fused (TM5122/ TM5123)[c]; XbaI, PstI.	This study
p1CSV-CotZ-N-GFP	pBS1C-derivative, *amyE*::P$_{cotYZ}$-*gfp-cotZ, cat, bla*	Amp^r / cm^r		(Julia Bartels, unpublished)

[b] Amp^r, ampicillin resistance; cm^r, chloramphenicol resistance; spc^r, spectinomycin resistance.

[b] Genomic DNA of *B. subtilis* W168 was used as template for PCR. SpeI and XbaI generate compatible DNA overhangs. If two DNA-pieces were inserted, the vector was opened using the upstream restriction site of the promoter and the downstream restriction site of the gene, respectively.

[c] Two silent mutations with similar codon usage were introduced into *uppP* to allow cloning in BioBrick™ standard: P103: CCT→CCA, A195: GCA→GCG.

Table S3. Primers used in this study

Primer name	Description	Sequence (5'->3') [a]
Primers used for cloning		
TM4738	P_{yubA}-fwd	GATC**GAATTC**GCGGCCGCT**TCTAGA**GTTCGGGCTCGCTATGTATAC
TM5121	P_{yubA}-rev	TAA**GTCGAC**TCATACATAGTTTAATTAAATTGTACAC
TM2968	P_{xylA}-fwd	GATC**GAATTC**GCGGCCGCT**TCTAGA**GAAGGCCAAAAAACTGCTGCC
TM2969	P_{xylA}-rev	GATC**ACTAGT**ATTCGATAAGCTTGGGATCCC
TM2731	*bcrC*-fwd	GATC**GAATTC**GCGGCCGCT**TCTAGA**AAGGAGGTG**GCCGGC**TTGAACTACGAAATTTTTAAAGCAATC
TM2732	*bcrC*-rev	GATC**ACTAGT**ATTA**ACCGGT**GAAATTTTGATCGGTTGGTTTTTTC
TM5122	*uppP*-fwd	CCTA**GAATTC**GCGGCCGCT**TCTAGA**AAGGAGGTG**GCCGGC**ATGACTCTATGGGAATTGTTTG
TM5123	*uppP*-rev	GCCGGA**CTGCAG**CGGCCGCT**ACTAGT**ATTA**ACCGGT**TTACATCATGATCAAAAGTAAAATCAC
TM5124	*uppP*-PstImut1-fwd	CCGTCGGACTCGTGCC**a**GCAGCTGTTCTCGGCTTTTTG
TM5125	*uppP*-PstImut1-rev	CAAAAAGCCGAGAACAGCTGC**t**GGCACGAGTCCGACGG
TM5126	*uppP*-PstImut2-fwd	GATTAAACCACCGAGCTGC**g**GCCGACTTTACGTTTATTATGG
TM5127	*uppP*-PstImut2-rev	CCATAATAAACGTAAAGTCGGC**c**GCAGCTCGGTGGTTTAATC
Primers used for LFH-PCRs		
TM4749	*uppP*-up-fwd	GAGATTATCATTTCGATCGTCAC
TM4750	*uppP*-up-rev	CCTATCACCTCAAATGGTTCGCTGGTACTCTGTTAATCCTTCTACG
TM4751	*uppP*-do-fwd	CGAGCGCCTACGAGGAATTTGTATCGTTGCAATCTATCGAATTATTCTC
TM4752	*uppP*-do-rev	AATGGAACTGTATGAGTGTATCC
TM0139	MLS-fwd	CAGCGAACCATTTGAGGTGATAGGGATCCTTTAACTCTGGCAACCCTC
TM0140	MLS-rev	CGATACAAATTCCTCGTAGGCGCTCGGGCCGACTGCGCAAAAGACATAATCG
TM0057	MLS-check-fwd	CCTTAAAACATGCAGGAATTGACG
TM0148	MLS-check-rev	GTTTTGGTCGTAGAGCACACGG
TM5303	*dgkA*-up-fwd	CAAGAGTCGGCGCATATTATC
TM5304	*dgkA*-up-rev	CCTATCACCTCAAATGGTTCGCTGGAAATTCCGCTCCGTCCG
TM5305	*dgkA*-down-fwd	CGAGCGCCTACGAGGAATTTGTATCGCAGCCATTGAACATACGGTTG
TM5306	*dgkA*-down-rev	GGATAGAATTGCGGCCCTTC
TM0137	kan-fwd	CAGCGAACCATTTGAGGTGATAGG
TM0138	kan-rev	CGATACAAATTCCTCGTAGGCGCTCGG
TM0056	kan-check-fwd	CATCCGCAACTGTCCATACTCTG
TM0147	kan-check-rev	CTGCCTCCTCATCCTCTTCATCC
TM0135	cat-fwd	CAGCGAACCATTTGAGGTGATAGGCGGCAATAGTTACCCTTATTATCAAG
TM0136	cat-rev	CGATACAAATTCCTCGTAGGCGCTCGGCCAGCGTGGACCGGCGAGGCTAGTTACCC
TM0173	cat-check-fwd	CTAATGTCACTAACCTGCCC
TM0146	cat-check-rev	GTCTGCTTTCTTCATTAGAATCAATCC

[a] Recognition sites for endonuclease restriction enzymes are in bold. Introduced mutations are in bold lower case. The annealing part is underlined.

Supplemental References

Höfler, C., Heckmann, J., Fritsch, A., Popp, P., Gebhard, S., Fritz, G., et al. (2016). Cannibalism stress response in Bacillus subtilis. *Microbiology* 162(1)**,** 164-176. doi: 10.1099/mic.0.000176.

Radeck, J., Gebhard, S., Orchard, P.S., Kirchner, M., Bauer, S., Mascher, T., et al. (2016). Anatomy of the bacitracin resistance network in *Bacillus subtilis*. *Mol Microbiol* 100(4)**,** 607-620. doi: 10.1111/mmi.13336.

Radeck, J., Kraft, K., Bartels, J., Cikovic, T., Dürr, F., Emenegger, J., et al. (2013). The *Bacillus* BioBrick Box: generation and evaluation of essential genetic building blocks for standardized work with *Bacillus subtilis*. *J Biol Eng* 7(1)**,** 29. doi: 10.1186/1754-1611-7-29.

Rietkötter, E., Hoyer, D., and Mascher, T. (2008). Bacitracin sensing in *Bacillus subtilis*. *Mol Microbiol* 68(3)**,** 768-785. doi: 10.1111/j.1365-2958.2008.06194.x.

Schmalisch, M., Maiques, E., Nikolov, L., Camp, A.H., Chevreux, B., Muffler, A., et al. (2010). Small genes under sporulation control in the *Bacillus subtilis* genome. *J Bacteriol* 192(20)**,** 5402-5412. doi: 10.1128/JB.00534-10.

7.5 MANUSCRIPT II: *BACILLUS* SEVA SIBLINGS: A GOLDEN GATE-BASED TOOLBOX TO CREATE PERSONALIZED INTEGRATIVE VECTORS FOR *BACILLUS SUBTILIS*[$]

Manuscript II:

Radeck J, Meyer D, Lautenschläger N, Mascher T (2017) *Bacillus* SEVA siblings: A Golden Gate-based toolbox to create personalized integrative vectors for *Bacillus subtilis*. (submitted to Scientific Reports)

[&] was published in a revised form in: **Sci. Rep.** 7:14134. doi: 10.1038/s41598-017-14329-5

Bacillus SEVA siblings: A Golden Gate-based toolbox to create personalized integrative vectors for *Bacillus subtilis*

Jara Radeck[1,2], Daniel Meyer[2], Nina Lautenschläger[1], Thorsten Mascher [1,*]

[1] Institute of Microbiology, Technische Universität (TU) Dresden, 01062 Dresden, Germany

[2] Department of Biology I, Ludwig-Maximilians-Universität (LMU) München, 82152 Planegg-Martinsried, Germany

* To whom correspondence should be addressed. Tel: +49 351 463-40420; Fax: +49 351 463-37715; Email: Thorsten.Mascher@tu-dresden.de

ABSTRACT

Bacillus subtilis combines natural competence for genetic transformation with highly efficient homologous recombination. These features allow using vectors that integrate into the genome via double homologous recombination. So far, their utilization is restricted by the fixed combination of resistance markers and integration loci, as well as species- or strain-specific regions of homology. To overcome these limitations, we developed a toolbox for the creation of personalized *Bacillus* vectors in a standardized manner with a focus on fast and easy adaptation of the sequences specifying the integration loci. We based our vector toolkit on the Standard European Vector Architecture (SEVA) to allow the usage of their vector parts. The *Bacillus* SEVA siblings are assembled via efficient one-pot Golden Gate reactions from four *entry* parts with the choice of four different enzymes. The toolbox contains seven *Bacillus* resistance markers, two *Escherichia coli* origins of replication, and a free choice of integration loci. Vectors can be customized with a cargo, before or after vector assembly, and could be used in different *B. subtilis* strains and potentially beyond. Our adaptation of the SEVA-standard provides a powerful and standardized toolkit for the convenient creation of personalized *Bacillus* vectors.

KEYWORDS

Integrative vector, *Bacillus* vector, exchange integration sites, customize integration loci

INTRODUCTION

The diversity of plasmid vectors in molecular cloning

In molecular cloning, vectors are vehicles to transfer foreign nucleic acids into a living cell. In the context of this article, we restrict the term "vector" to "plasmid vectors", small circular DNA molecules that originate from bacteria. They are easy to handle for inserts up to 10-15 kb, replicate independently of the bacterial chromosome and can be isolated in large amounts through standard plasmid preparation procedures. Over the last decades, vectors were increasingly modified to meet custom needs. For instance, they may contain promoters for ready-to-use gene expression, or reporter genes to measure transcription or translation rates, respectively. More elaborated vector types can contain biosafety features, internal measuring standards or may be used for clean chromosomal gene deletions or dual expression systems [1-4]. Synthetic biology strives to implement and extend the principles of engineering (standardization, decoupling, abstraction) into biology [5]. Especially standardization in vector and plasmid construction offers the clear advantage of comparability, compatibility, flexibility and reusability of single parts and whole vectors, as exemplified by the Standard European Vector Architecture (SEVA).

The Standard European Vector Architecture provides standardized vectors for Gram-negative bacteria

In 2013, the group of Victor de Lorenzo developed a standardized vector toolbox for the use in Gram-negative bacteria, with a special interest in *Pseudomonas putida*. With SEVA, they set the stage for a community-driven development platform and for evolving a standardized vector collection. This platform facilitates finding, creating, and naming of suitable vectors as well as their downstream handling [6,7]. Currently, the SEVA database lists 135 SEVA vectors and 49 SEVA siblings [8] (http://seva.cnb.csic.es/, March 2017). Subsequently, linker sequences were developed to make the vectors compatible to different cloning methods [9].

Each SEVA vector contains at least three functional elements (Fig. 1a), (i) the origin of replication (ori) for vector replication in the host cell, (ii) a selectable marker, e.g.

an antibiotic resistance cassette to select for vector uptake and maintenance, and (iii) a multiple cloning site (MCS) for insertion of the DNA of interest. In the SEVA standard, the latter part is called cargo, irrespective of the size and nature of the insert. The cargo is isolated by flanking double transcriptional terminators (T1, T0), to avoid unwanted transcriptional read-through into other elements of the backbone. All parts are flanked by defined rare endonuclease restriction sites and assemble in a fixed order and orientation (Fig. 1a). They must not contain these and further restriction endonuclease recognition sites. Additionally, the transcriptional terminators and the origin of transfer (*oriT*, for plasmid conjugation) are predefined, whereas the selectable marker, ori and cargo can be chosen freely, as long as they adhere to the standard. An easy number-based nomenclature assures the fast determination of vector features from the vector's name [6,7].

Distinct features of vectors for *Bacillus subtilis*

Bacillus subtilis is the best studied low-G+C Gram-positive bacterium (phylum *Firmicutes*) and one of the leading workhorses of the biotechnological industry [10-12]. Its ease of genetic manipulation is based on its natural competence, which includes the active uptake of (any) DNA and recombination of homologous regions into the chromosome [13]. These features enable to routinely use integrative instead of replicative vectors. This ensures genetic stability even without maintaining a constant selective pressure. Moreover, copy number effects are avoided, which can otherwise influence the promoter activity on replicative vectors, particularly at the single cell level [14,15].

For cloning convenience, vectors designed for integration into the *B. subtilis* genome usually replicate in *E. coli* but do not contain an ori for *B. subtilis*. Instead, two homology regions of at least 400 bp, which define the insertion locus, flank the cargo and the resistance marker for *B. subtilis*. The plasmids are linearized in the *E. coli* part of the vector before *B. subtilis* transformation to avoid integration via single crossing over events. Consequently, only the DNA segment that is located between the homology regions will integrate into the chromosome, resulting in genetic stability of single copy number inserts even in the absence of selective pressure.

The currently available vectors combine known and effective selection cassettes with well-characterized integration loci [16-20]. This status quo limits the combination of resistance markers and integration sites, and does not allow targeting entirely new chromosomal regions. Moreover, existing vectors cannot be used in another *Bacillus* strain, which differs in the nucleotide sequence at the specified integration site.

Due to the genetic accessibility of *B. subtilis*, PCR-based methods, such as long-flanking homology (LFH)-PCR [21], can be used to target new or strain-specific loci. While this approach is very convenient for generating knock-out mutants, it is restricted with respect to the cargo: fusing several PCR products, and obtaining large fragments, e.g. the *luxABCDE* bioluminescence reporter operon (5.7 kb) that allows online measurement [17,19], with sufficient yield for efficient transformation (> 1 µg [22]) can be tedious. In these cases, transformants have to be sequenced each time to ensure the integrity of the cargo (e.g. lack of mutations). In order to combine the advantages of vectors (stability and reusability) with those of PCR-based methods (flexibility) for the use in *B. subtilis* and related species, we designed, constructed and tested a new vector concept: the *Bacillus* SEVA siblings.

Concept of *Bacillus* SEVA siblings as customized vectors

Here, we describe a toolkit that was developed for the fast and easy generation of genomic integration vectors for *B. subtilis*, thereby overcoming the traditional limitations described above. Each vector contains a resistance marker, cargo and flanking homology regions of choice. To ensure compatibility and reusability of already existing parts for replication in *E. coli*, we based our system on SEVA and added flanking homology regions as well as *Bacillus* resistance markers at defined positions (Fig. 1b). Our vectors will be named *Bacillus* SEVA siblings, which is in line with the current SEVA regulations [6].

Our toolbox offers seven functional antibiotic resistance cassettes for selection in *B. subtilis* and high and medium copy number *E. coli* vectors modified to be assembled with your homology regions of interest in a one-pot Golden Gate assembly [23,24]. We tested the assembly efficiencies for five different enzymes and the *B. subtilis* transformability of every part provided. As proof of concept for efficient assembly

and functionality, we analyzed the expression levels of the red fluorescing protein mKate2 under control of the xylose-inducible promoter P_{xylA} at different chromosomal insertion loci.

RESULTS

Vector layout for double cross-over homologous recombination in *B. subtilis*

We designed and constructed our vector building toolkit with the main goal to easily exchange the target loci for double homologous integration into the genome. This is important for two major reasons: Current vector collections do not allow the free combination of integration loci and selectable markers. Moreover, they omit the use of *Bacillus* strains if they differ from the reference lab strains in their nucleotide sequence, so that the integration sites of standard vectors are not compatible. For our collection of customizable vectors, we focus on allelic replacement via double recombination, where the DNA-sequence to be integrated into the chromosome (here termed *integration part*) is flanked by two regions of homology (Fig. 1b).

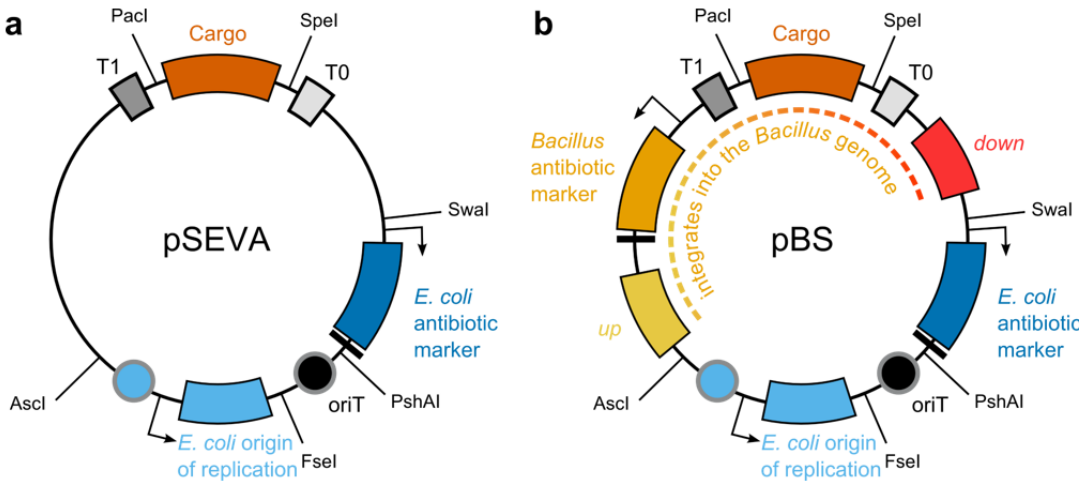

Figure 1. Configuration of a SEVA vector and its *Bacillus* SEVA sibling. (**a**) The basic SEVA vector is composed of six parts, separated by defined endonuclease restriction sites. The transcriptional terminators T0 and T1 as well as the origin of transfer *oriT* are fixed, whereas the cargo, the ori and the antibiotic marker can be chosen freely from a pool of SEVA-compatible parts. (**b**) For genomic integration, three parts were added to the SEVA layout to create the *Bacillus* SEVA sibling pBS: Flanking homology regions *up* and *down*, as well as an antibiotic marker for *Bacillus*. Vector verification and propagation occurs in *E. coli* and only the part in between the homology regions will integrate into the genome. Vectors are drawn not to scale. Functional transcriptional units are indicated with an arrow (promoter) and black bar (terminator).

For *B. subtilis,* approximately 400 bp of identical sequence are required for efficient integration. Shorter sequences (70 bp) can sometimes be sufficient, but are not recommended due to the significantly reduced efficiency [25]. For ease of construction, the *integration part* is combined with an ori and selectable marker for *E. coli* (here

termed *replication part*). Before *B. subtilis* transformation, the vector is linearized in the *replication part* to avoid single cross-over events and ensure double cross-over integration.

Although our toolkit was optimized for the exchange of integration sites, it can be customized in manifold ways as will be outlined in the discussion. A quick user manual with helpful information for vector construction can be found in the supplemental material (Text S2).

The customizable vector collection is based on SEVA to allow re-use of *E. coli* parts

Currently, most vectors and plasmids used for genetic manipulation of *B. subtilis* are propagated in *E. coli*. As demonstrated for NarK and β-carotene production, the *E. coli* vector propagation strongly depends on the ori and resistance markers in ways that cannot be foreseen yet [9]. Consequently, we designed our vectors to be flexible not only with respect to their cargo, but also their ori and *E. coli* resistance marker. For this purpose, we based our vector toolkit on SEVA. This standard was designed for vectors to allow exchanging of the cargo, resistance marker and ori, using defined rare type II restriction enzymes [7]. The accompanying vector collection was very well-received by scientists and is still growing. It can be used to adapt the vectors of our toolbox, which are therefore named *Bacillus* SEVA siblings. SEVA restriction sites were removed from critical parts of the *entry vectors*, so that *the final vectors* adhere to the SEVA standard, if no forbidden restriction sites are present in the customized parts.

***Bacillus* SEVA siblings are assembled *de novo* from multiple fragments via Golden Gate cloning**

As depicted in Fig. 1b, the *integration* and *replication parts* of an integration vector are separated by the regions of homology, called *up* and *down*. Consequently, the exchange of both *up* and *down* fragments with standard cloning techniques would involve two cloning and verification steps without a selectable marker. To avoid laborious stepwise cloning, advanced cloning techniques for the easy, fast, efficient and directed one-pot assembly of multiple fragments are available, such as Gibson

assembly [26,27] or Golden Gate cloning [23,24]. The latter is based on a ligase and type IIS endonucleases (e.g. BsaI), which cut outside (next to) their recognition site. Consequently, the restriction site can be designed according to need and separated from the recognition site during the cloning procedure. The reaction mix can include linear and circular DNA, containing restriction sites for the same enzyme but different overhangs. This allows the easy and efficient assembly of up to ten parts in the correct order and loss of the recognition sites in the *final vector* [23]. For our vector toolbox, we chose Golden Gate assembly for the following reasons: (i) Gibson assembly usually must be established in a lab to run smoothly, whereas restriction based cloning is more robust. (ii) The *up* and *down* regions need to be PCR-generated and Gibson assembly asks for longer overhangs thus increasing the primer costs.

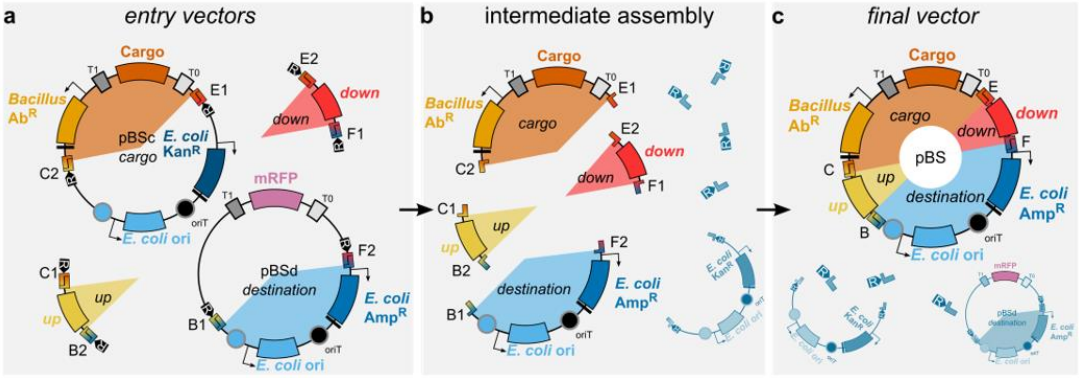

Figure 2. Assembly of a *Bacillus* SEVA sibling pBS. (**a**) Collection of *entry* parts needed for the assembly of a pBS vector: one *cargo vector*, one *destination vector*, one *up* and one *down* flanking homology fragment. The latter two are depicted as PCR fragments, but can also be located on a vector. Each of the desired fragments is flanked by IIS-restriction sites where the recognition site (R) is located outside the desired fragment. The compatibility of the resulting overhangs is indicated with letters and a color gradient, e.g. E1 and E2 overhangs can anneal. (**b**) Intermediate stage of the Golden Gate assembly, showing the desired fragments and some of the by-products (grey). (**c**) Creation of the *final vector*, including some possible by-products (grey). Only the *destination vector* and the *final vector* carry the ampicillin resistance marker and will be selected for after transformation of the reaction mix into *E. coli*. The *destination vector* will be counter-selected by a red/white screen based on an mRFP-marker.

Instead of re-using and modifying preexisting vectors, each new vector will be freshly assembled by combining four fragments via Golden Gate assembly (Fig. 2): the *up* and *down* fragments, the *replication part*, and the *cargo* which includes an antibiotic marker for selection in *Bacillus* and a MCS. Therefore, all vectors and sequences offered through the *Bacillus* Genetic Stock Center (BGSC) and the SEVA collection (see

Table 1 and supplementary data S3) are *entry* vectors to allow customized assembly, but no *final Bacillus* vectors.

Architecture of *Bacillus* SEVA siblings

Fig. 1 compares a *final* ***B****acillus* SEVA **s**ibling (pBS), with a standard SEVA vector for *E. coli*. SEVA suggests a designated location for the insertion of special features that are not part of the cargo. They are positioned at the terminator sequences and next to, but not obstructing the AscI and SwaI recognition sites which allow the exchange of SEVA vector parts. In line with this regulation, the homology regions and resistance marker are located at both terminator sequences. The respective *Bacillus* resistance cassette is placed between the cargo and the T0-terminator and directed counter-clockwise in order to not interfere with the transcription of the cargo. SEVA-vectors are named according to their features in a number-based code, see SEVA 2.0 for a comprehensive description [6]. We suggest the naming of *final vectors* to be based on the SEVA-standard, in which the *E. coli* features are specified in three digits: the first digit describes the *E. coli* resistance marker, e.g. 1 for Ampicillin resistance or 2 for kanamycin. The second digit indicates the ori, e.g. 4 for pRO1600/ColE1 or 9 for pBR322/ROP. The third digit encodes the cargo, e.g. 1 for the default MCS or 3 for the *lacZα*-pUC18 MCS. pSEVA243 consequently is a vector mediating kanamycin resistance [2] with a high copy number [4= pRO1600/ColE1] that carries a MCS for blue/white screening [3=*lacZα*-pUC18]. *Bacillus*-specific features should be added behind, so pBS143K-amyE is a vector with an *E. coli* ampicillin resistance marker [1], pRO1600/ColE1 ori [4] and *lacZα*-pUC18 MCS [3] that carries a kanamycin *Bacillus* resistance marker [K] and integrates into the *amyE*-locus [amyE].

We conceptualized the assembly so that SEVA-parts can be exchanged before or after the assembly of the *final vectors*, e.g. to accommodate the presence of either SEVA- or Golden Gate-forbidden restriction sites.

Table 1: Vectors of the *Bacillus* SEVA siblings toolbox

BGSC*	Name[$]	Description[#]	Resistance in *E. coli* / *B. subtilis*	Source
Vectors for default assembly				
Destination vectors				
ECE701	pBSd141R	*mRFP1,* MCS-IIS F2, *bla*, ori pRO1600/ColE1, MCS-IIS B1	Amp^r / -	This study
ECE702	pBSd191R	*mRFP1,* MCS-IIS F2, *bla*, ori pBR322/ROP, MCS-IIS B1	Amp^r / -	This study
Vectors for flanking homology regions[§]				
	pSEVA243	*lacZα*-pUC18 MCS, *neo*, ori pRO1600/ColE1	Kan^r/-	SEVA[7]
ECE703	pSEVA243X	*lacZα***-pUC18 MCS incl. MCS-IIS B2+C1 for *up*, *neo*, ori pRO1600/ColE1	Kan^r/-	This study
ECE704	pSEVA243Y	*lacZα***-pUC18 MCS incl. MCS-IIS E2+F1 for *down*, *neo*, ori pRO1600/ColE1	Kan^r/-	This study
Cargo-Resistance vectors				
ECE706	pBSc241B	MCS-default, MCS-IIS E1, *neo*, ori pRO1600/ColE1, MCS-IIS C2, *bleO*	Kan^r/ble^r	This study
ECE707	pBSc241C	MCS-default, MCS-IIS E1, *neo*, ori pRO1600/ColE1, MCS-IIS C2, *cat*	Kan^r/cm^r	This study
ECE708	pBSc241M	MCS-default, MCS-IIS E1, *neo*, ori pRO1600/ColE1, MCS-IIS C2, *ermC*	Kan^r/MLS^r	This study
ECE709	pBSc241S	MCS-default, MCS-IIS E1, *neo*, ori pRO1600/ColE1, MCS-IIS C2, *aad(9)*	Kan^r/spc^r	This study
ECE710	pBSc241T	MCS-default, MCS-IIS E1, *neo*, ori pRO1600/ColE1, MCS-IIS C2, *tetL*	Kan^r/tet^r	This study
ECE711	pBSc241Z	MCS-default, MCS-IIS E1, *neo*, ori pRO1600/ColE1, MCS-IIS C2, *ble-Sh*	Kan^r/zeo^r	This study
ECE720	pBSc291K	MCS-default, MCS-IIS E1, *neo*, ori pBR322/ROP, MCS-IIS C2, *aph(3')IIIa*	Kan^r/kan^r	This study
ECE713	pBSc243B	*lacZα**-pUC18 MCS, MCS-IIS E1, *neo*, ori pRO1600/ColE1, MCS-IIS C2, *bleO*	Kan^r/ble^r	This study
ECE714	pBSc243C	*lacZα**-pUC18 MCS, MCS-IIS E1, *neo*, ori pRO1600/ColE1, MCS-IIS C2, *cat*	Kan^r/cm^r	This study
ECE715	pBSc243M	*lacZα**-pUC18 MCS, MCS-IIS E1, *neo*, ori pRO1600/ColE1, MCS-IIS C2, *ermC*	Kan^r/MLS^r	This study
ECE716	pBSc243S	*lacZα**-pUC18 MCS, MCS-IIS E1, *neo*, ori pRO1600/ColE1, MCS-IIS C2, aad(9)	Kan^r/spc^r	This study
ECE717	pBSc243T	*lacZα**-pUC18 MCS, MCS-IIS E1, *neo*, ori pRO1600/ColE1, MCS-IIS C2, *tetL*	Kan^r/tet^r	This study
ECE718	pBSc243Z	*lacZα**-pUC18 MCS, MCS-IIS E1, *neo*, ori pRO1600/ColE1, MCS-IIS C2, *ble-Sh*	Kan^r/zeo^r	This study
ECE721	pBSc293K	*lacZα**-pUC18 MCS, MCS-IIS E1, *neo*, ori pBR322/ROP, MCS-IIS C2, *aph(3')IIIa*	Kan^r/kan^r	This study
Vectors for customizable resistance markers				
ECE705	pBSc241	MCS-default, MCS-IIS E1, *neo*, ori pRO1600/ColE1, MCS-IIS C2	Kan^r/-	This study
ECE712	pBSc243	*lacZα**-pUC18 MCS, MCS-IIS E1, *neo*, ori pRO1600/ColE1, MCS-IIS C2	Kan^r/-	This study
ECE719	pBSc291	MCS-default, MCS-IIS E1, *neo*, ori pBR322/ROP, MCS-IIS C2	Kan^r/-	This study
ECE725	pBSc293	*lacZα**-pUC18 MCS, MCS-IIS E1, *neo*, ori pBR322/ROP, MCS-IIS C2	Kan^r/-	This study
ECE722	pBSc391	MCS-default, MCS-IIS E1, *cat*, ori pBR322/ROP, MCS-IIS C2	Cm^r/-	This study
ECE726	pBSc393	*lacZα**-pUC18 MCS, MCS-IIS E1, *cat*, ori pBR322/ROP, MCS-IIS C2	Cm^r/-	This study
Plasmids for activity-test				
pSEVA243X-amyE		pSEVA243X-derivative carrying a 550bp *amyE up* fragment	Kan^r/-	This study
pSEVA243Y-amyE		pSEVA243Y-derivative carrying a 580bp *amyE down* fragment	Kan^r/-	This study
pBSc241M_P_{xylA}-*mkate2* (2195)		pBSc241M-derivative carrying *mkate2* under the control of xylose-inducible P_{xylA}	Kan^r/-	This study
pBS141M-amyE_mkate2		P_{xylA}-*mkate2*,'*amyE*, *bla*, ori pRO1600/ColE1, *amyE'*, *erm*	Amp^r/MLS^r	This study
pBS141M-ypqP_mkate2		P_{xylA}-*mkate2*,'*ypqP*, *bla*, ori pRO1600/ColE1, *ypqP'*, *erm*	Amp^r/MLS^r	This study
pBS141M-ykoS_mkate2		P_{xylA}-*mkate2*,'*ykoS*, *bla*, ori pRO1600/ColE1, *ykoS'*, *erm*	Amp^r/MLS^r	This study
pBS191M-ndk_mkate2		P_{xylA}-*mkate2*,'*ndk*, *bla*, ori pBR322/ROP, *ndk'*, *erm*	Amp^r/MLS^r	This study
pBS141M-thrC_mkate2		P_{xylA}-*mkate2*,'*thrC*, *bla*, ori pRO1600/ColE1, *thrC'*, *erm*	Amp^r/MLS^r	This study
Vectors used for vector construction (templates for PCR reactions)				
pDG148		*bla*, *kan*, *ble/phle*, P_{spac}	Amp^r/kan^r	[37,40]
pDG780		pBluescriptKS+, *kan*	Kan^r/kan^r	[41]
pBS3Clux		pAH328 derivative; *sacA'…'sacA, luxABCDE, bla, cat*	Amp^r/cm^r	[17]
pBS4S		pDG1731 derivative; *thrC'…'thrC, 'hom, thrB', spc, bla*	Amp^r/spc^r	[17]
pSB1A3-mkate-B0014		*bla*, BBa_K823051 (Bsu codon-adapted red fluorescing protein *mkate2*, terminator B0014), pMB1 ori (high copy number)	Amp^r/-	Lab stock

* *Bacillus* Genetic Stock Center (BGSC, http://www.bgsc.org/)

[$] The vector names act as identifiers for the SEVA or SEVA siblings collection. **p**, **P**lasmid. **BS**, ***B****acillus* SEVA **s**ibling. **d**, ***d****estination vector* / **c**, ***c****argo vector* / **f**, ***f****inal vector*. Numbers according to SEVA standard: 1st position, resistance marker (1, amp. 2, kan). 2nd position, origin of replication (4, pRO1600/ColE1, a narrow-host-range ori with high copy number in *E. coli* and varying copy number in *Pesudomonas aeruginosa* and close relatives[7]). 9, pBR322/ROP (medium copy number ori in *E. coli* and few other bacteria[42]).). 3rd position, cargo (1, MCS default. 3, *lacZα*-pUC18 MCS which allows for blue-white screening with X-Gal).

[#] *lacZα**, premature stop codon (C202A, Q68Stop). *lacZα***, premature stop codon (pSEVA243X: G390A, W130Stop, pSEVA243Y: G399A, W133Stop). Both variants are still suitable for blue-white screening. Genes encoding antibiotic resistance markers are explained in detail in Table 2.

[§] Flanking homology regions can be stored in those vectors. If the PCR fragment contains the restriction sites needed for assembly, it can be ligated blunt end into pSEVA243 via SmaI. If restriction sites should be added for all enzymes, the PCR fragments can be ligated blunt end into pSEVA243X (for *up*) or pSEVA243Y (for *down*) via EcoRV. In this case, the correct orientation needs to be verified by sequencing.

Golden Gate shuffling to assemble *Bacillus* SEVA siblings with type IIS restriction enzymes

In our current set-up, four different fragments are needed to assemble the *final vector*: the *up* and *down* homology fragments, the *cargo* with the *Bacillus* resistance cassette and the part for replication and selection in *E. coli*, which we call *destination vector*. These *entry* parts can be combined using Golden Gate assembly as detailed in Fig. 2. The *up* and *down* homology fragments can be used either as PCR products (as depicted) or as cargo of the specialized vectors containing the *up* (pSEVA243X) and *down* (pSEVA243Y) fragments, respectively. Each entry part is flanked by recognition sites for a type IIS restriction endonuclease, which creates overhangs that allow for the directional assembly of all *entry* parts. Compatible overhangs are named with the same capital letter in Fig. 2a.

As necessary for Golden Gate assembly, the recognition sites are located "outside" of the part desired for the assembly, so that correctly assembled parts cannot be re-cleaved – in contrast to the re-ligation products of *entry* vectors. By this means, assembly of mostly correct *final vectors* is ensured. The *destination vector* carries a different antibiotic marker than all other *entry* vectors to select for vectors carrying the correct backbone. An mRFP1-cassette present on the original *destination vector* is used for red/white screening. This part is removed during assembly of the *final vector* so that colonies carrying the original vector appear red and colonies carrying the correct *final vector* appear white.

Classic Golden Gate assembly uses BsaI and BbsI (=BpiI) as type IIS restriction enzymes [23,28], but BsmBI and BtgZI were recently found to also be suitable [29,30]. Our *Bacillus* SEVA siblings toolbox accommodates all four of them for assembly to circumvent compatibility issues with the desired genomic region, e.g. the presence of one or more recognition sites in the *up* and *down* fragments. In addition to BsaI, BbsI, BsmBI and BtgZI, we also included a fifth restriction enzyme (AarI)– not reported previously for its use in Golden Gate assembly.

Golden Gate assembly restriction sites are arranged in special MCS-IIS

All four *entry* parts are flanked by MCSs that contain recognition sites for all five type IIS restriction enzymes (MCS-IIS). Inside each MCS-IIS, recognition and restriction sites are designed so that the same overhang sequence is created, independent of the enzyme used. The overhangs are non-palindromic and differ in at least two nucleotides to ensure the correct assembly of the desired vector. For ease of understanding, fusion sites were named with capital letters B, C, E, and F as indicated in Fig. 2. Fig. 3 shows the annotated MCS-IIS C2, in which all five enzymes create the overhang GCGA. For the detailed sequence of all 8 MCS-IIS, see Fig. S1.

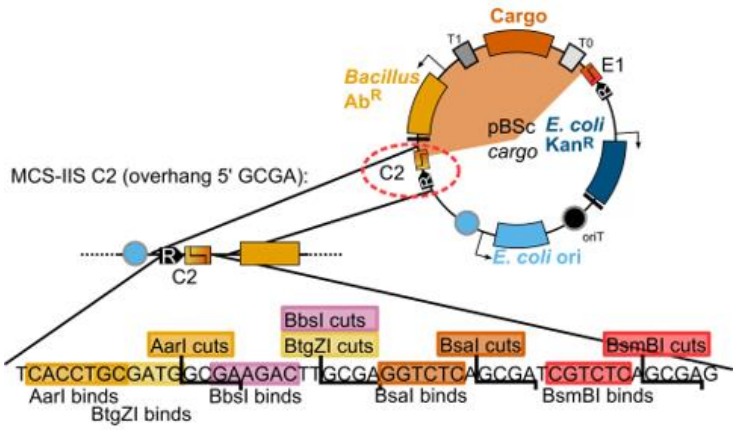

Figure 3. Architecture of the MCS-IIS C2. This DNA-sequence is located on the *cargo vector* between the *E. coli* ori and the *Bacillus* antibiotic marker. The recognition sites for five type IIS restriction enzymes (AarI, BtgZI, BbsI, BsaI, BsmBI), each designed to create a 5' GCGA-overhang are encoded on the DNA stretch. Architecture of all MCS-IIS can be found in Fig. S1.

To compare the assembly efficiency as a function of the enzyme of choice, we used one set of *entry* vectors to construct *final* vectors with identical features. However, nucleotide sequences differ at the assembly scar sites, due to the MCS-IIS. We used pSEVA23X-amyE (*up*), pSEVA243Y-amyE (*down*), pBSc243M and pBSd141R as *entry* vectors. In this case, the cargo carries a *lacZα*-fragment that allows for blue-white screening and colonies carrying the correct vector appear blue in the presence of 5-bromo-4-chloro-3-indolyl-β-D-galactopyranoside (X-Gal). Red colonies carry the original *destination vector* and white colonies an incorrect vector. We checked colony color, test digest and sequencing results and found good assembly efficiencies for four enzymes: AarI, BbsI, BsaI and BsmBI (Table 3). For BtgzI however, we failed in finding conditions allowing the correct assembly of the *final vector*. This was surprising, since its use in Golden Gate assembly has been described previously in combination with BsmBI [30]. Even if the desired fragments were digested and gel

purified separately, the ligation yielded no correct vector. But in principle, BtgZI can be used for assembly once suitable conditions are found. In contrast, BsaI, BpiI and BsmBI were particularly well-suited with efficiencies of >95% in routinely vector assembly (data not shown). The optimized conditions we used for each enzyme are given briefly in the Methods section and are described in more detail in the Supplemental Text S2.

Taken together, *Bacillus* SEVA siblings vectors can be efficiently assembled using one of four type IIS restriction endonucleases. In addition to the established enzymes (BsaI, BbsI and BsmBI), AarI was also found to be suitable for Golden Gate assembly. Because of its 7 bp recognition site, it should be found less frequently in genomic sequences compared to the "classical" enzymes with a 6bp recognition site.

Our collection of *entry* parts for the assembly of *Bacillus* SEVA siblings

For the assembly of *Bacillus* SEVA siblings vectors, four different categories of *entry* parts are needed: *cargo and resistance*, *up*, *down*, and the *replication part*. They will be described in more detail below. The *entry* vectors offered with our toolbox are depicted in Fig. 4 and listed with detailed descriptions in Table 1.

pBSc: Cargo and resistance. Since for most experiments the same cargo will usually be combined with the same resistance marker, both are located on the *cargo vector pBSc*. As a result, only four instead of five parts have to be assembled, thereby increasing cloning efficiency. For our collection of *cargo vectors*, we used well-established antibiotic resistance markers to enable selection on phleomycin D, chloramphenicol, kanamycin, macrolide and streptogramin B antibiotics (MLS), spectinomycin, tetracycline, and zeocin (Table 2). Forbidden restriction sites were removed and transcriptional terminators were added where necessary. Transcription occurs in the opposite direction to the cargo. Per default, the *cargo vector* uses the high copy number ori pRO1600/ColE1. For the kanamycin resistance marker, this vector was unstable, so the medium copy number ori pBR322/ROP was used. All *cargo vectors* are offered with the default SEVA MCS (pUC18-related polylinker without *lacZα*, [7]) or the *lacZα**-pUC18 MCS (Table 1). The cargo of choice can be

Table 2: Description of antibiotic markers used in this study

Abbr.		Gene	Description*	Antibiotic	Conc. [µg ml^{-1}]	Source
	amp^r	*bla*	β-lactamase (Eco)	Ampicillin	100	pSEVA143 [7]
	kan^r	*neo*	neomycin-kanamycin phosphotranferase type I (Eco)	Kanamycin	50	pSEVA241 [7]
	cm^r	*cat*	chloramphenicol *O*-acetyltransferase (Eco)	Chloramphenicol	35[$]	pSEVA341 [7]
B	ble^r	*bleO*[#]	bleomycin binding protein (phleomycin D)	Phleomycin D1	100	pDG148 [40]
C	cm^r	*cat*	chloramphenicol *O*-acetyltransferase	Chloramphenicol	5	pBS3Clux [17,19]
K	kan^r	*aph(3')IIIa*	aminoglycoside *O*-phosphotransferase APH(3')-IIIa	Kanamycin	10	pDG780 [41]
M	MLS^r	*ermC*	23S rRNA (adenine(2058)-*N*(6))-methyltransferase	Erythromycin & Lincomycin	1 25	pDG647 [41]
S	spc^r	*aad(9*	aminoglycoside nucleotidyltransferase ANT9	Spectinomycin	200	pBS4S [16,17]
T	tet^r	*tetL*	tetracycline efflux MFS transporter	Tetracycline	12.5	pDG1513 [41]
Z	zeo^r	*ble-Sh*[#]	phleomycin/bleomycin binding protein (codon-optimized for Bsu)	Zeocin	100	This study

* Eco, *E. coli*; Bsu, *B. subtilis*

[$] 5 µg ml^{-1} were used for medium copy number vectors.

[#] *bleO* and *ble-Sh* both mediate resistance against phleomycin or zeocin (both from the bleomycin family) by binding to the antibiotic, respectively. There are differences in amino acid sequence of the encoded proteins and in the properties of the antibiotics, but mediation of cross-resistance cannot be excluded.

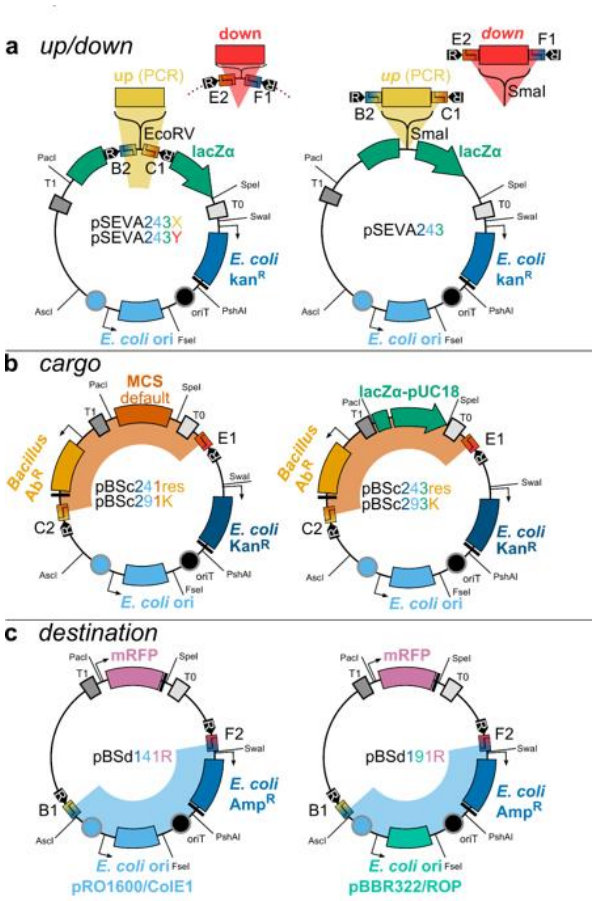

Figure 4. Vector suite for the generation of *Bacillus* SEVA siblings. Schematic representation of the vector architectures, details are listed in Table 1. (**A**). Vectors for flanking homology regions. *Up* fragments (PCR product) can be stored in pSEVA243X and *down* in pSEVA243Y, each linearized with EcoRV. The respective MCS-IIS are encoded on the vectors. If required restriction site are already encoded on the primer overhangs, fragments can be stored in pSEVA243 or used directly for Golden Gate assembly. (**B**) *Cargo vectors* carry one of the following *Bacillus* antibiotic markers: Ble, Cat, Kan, MLS, Spc, Tet, Zeo and either the default MCS (pBSc241res) or the *lacZα**-pUC18 MCS for blue/white-screening. Vectors carrying the *Bacillus* kanamycin resistance marker utilize the medium copy number pBR322/ROP ori, all others the high copy number pRO1600/ColE1. Backbones are also available without *Bacillus* marker to allow insertion of a new or customized marker. (**C**) *Destination vectors* carry an mRFP1-cassette as cargo for red/white screening and an ampicillin resistance marker for selection in *E. coli*. They are available with high (pRO1600/ColE1) or medium (pBR322/ROP) copy number origins of replication.

inserted into the *cargo vector* or into the *final vector*, depending on enzyme compatibility and cloning strategy.

Up and down flanking homology regions. The choice of *up* and *down* flanking homology regions depends on and needs to be adjusted to the *Bacillus* strain and experiment. The regions need specific overhangs for the subsequent assembly. This can be achieved by either of the following two strategies: (i) PCR-amplified fragments of choice (without overhangs) are cloned blunt end into the EcoRV-linearized pSEVA243X (*up*) or pSEVA243Y (*down*), respectively. As a result, the insert receives the matching MCS-IIS encoded on these vectors which can be used for Golden Gate assembly. (ii) Incorporation of one restriction site to the primers will directly allow the use of the PCR product for Golden Gate assembly.

pBSd: replication part in E. coli. The *destination vector* carries the *replication part* of the *final vector*. Its resistance (ampicillin marker) differs from all other *entry vectors* to allow selection for the correct backbone after vector assembly. A high copy number (pBSd141R) and medium copy number version (pBSd191R) are provided. Both carry an mRFP cassette in their default MCS, thereby allowing red/white screening: After Golden Gate assembly, colonies with the original *destination vector* will appear red and therefore can be discarded. If different *E. coli* features are required for the *final vector*, they can be exchanged in the *destination vector* or the *final vector*, depending on needs and enzyme compatibilities.

Assembly, transformation and integration of pBS vectors

The reaction for the vector assembly contains the *entry* parts, one of the type IIS restriction enzymes, ligase and buffer. The specific protocols depend on the enzyme used and can be found in the Materials and Method section. Competent *E. coli* cells are subsequently transformed with the reaction mix and plated on selective media containing ampicillin (and X-Gal in case of blue/white screening). Verification of the *final vector* can be achieved in a two-step procedure using test digests followed by sequencing. For the latter, primers TM3782 and TM3783 (if pBSd141R was used as *destination vector*) or TM3783 and TM5128 (pBSd191R) are recommended. The sequencing results should cover the *up* and *down* region as well as the adjacent

assembly scars to ensure correct assembly of all parts. We tested all *entry* parts of the toolbox (Table 1) for their assembly efficiencies (Tables S4-S6) and found that in all cases it was more than sufficient to test six colonies of the correct color to obtain a correct *final vector*. If the high copy number *destination vector* is used, or selection for the correct cargo is possible, e.g. via blue/white screening, assembly efficiencies are even higher.

Table 3: Assembly efficiencies* depending on restriction enzyme

Enzyme	**% Blue**[$]	% White	% Red	Total colonies	Corr. test digest[#]	Corr. Sequencing	*B. subtilis* transf.[§]	
AarI	**36.8 (±26.1)**	0.9 (±0.9)	62.2 (±25.5)	3017 (±1292)	14/18	3/3	++	4/4
BbsI	**41.5 (±34.2)**	0.7 (±0.1)	57.7 (±34.1)	3568 (±1084)	15/18	3/5	++	4/4
BsaI	**52.8 (±13.1)**	6.1 (±2.2)	41.1 (±13.9)	4004 (±1443)	15/18	3/3	++	4/4
BsmBI	**49.8 (±11.0)**	3.7 (±0.5)	46.5 (±10.9)	2000 (±412)	13/18	3/3	++	4/4
BtgZI	**0**	0	100	182	0/6	0/3	n.a.	n.a.

* *entry* parts: pBSc243M, pBSd141R, pSEVA243X-amyE (*up*) and pSEVA243Y-amyE (*down*).
[$] Colonies appear blue if carrying the correct *final vector* and red if the *destination vector* is unchanged. If available, only blue colonies were used for test digest and correct test digests were used for sequencing. Data is shown for 3 independent Golden Gate assemblies with AarI, BbsI, BsaI or BsmBI. The total number of colonies as well as their apparent color is shown as average and standard deviation. BtgZI did not lead to correct assemblies of *final vector* and data is derived from a single experiment only.
[#] Test digests, sequencing and transformation results are given in total.
[§] ++ indicates >1000 colonies per 100 µl of *B. subtilis* W168 transformation mixture. The correct insertion locus was verified with a starch test.

Prior to transformation of *B. subtilis* W168, all vectors have to be linearized, e.g. using ApaI, to ensure chromosomal integration by double homologous recombination. All transformations were successful – except for vectors carrying the tetracycline resistance marker where only for one of two loci could be targeted (Tables S4, S5). The transformation efficiencies depended on the selection marker (Tables 2,3 and S4-S6). Correct integration was verified by colony PCR or physiological tests; e.g. a starch test for integration into the *amyE* locus.

As a proof of concept, we analyzed the expression of the reporter gene *mkate2* under control of the xylose-inducible promoter P_{xylA} at five loci spread across the chromosome (Table 4): *amyE*, *ykoS*, *ypqP* (prophage SPβ), *nkd*, and *thrC* at positions 28, 111, 183-195, 203, and 283° on the circular chromosome, respectively. *amyE* and *thrC* are early-discovered and frequently used integration loci close to the ori, encoding a starch-hydrolyzing alpha-amylase and the threonine synthase, respectively. The 130 kb-large prophage SPβ, which itself is inserted at the *ypqP* locus,

is known to be not essential and was targeted to demonstrate the possibility of deleting large genomic regions. The two remaining genes, *ndk* and *ykoS*, encode a nucleoside diphosphate kinase and a gene of unknown function, respectively. Those non-essential genes were chosen based on their chromosomal location.

Table 4: Assembly efficiencies* and reporter activity depending on integration sites

Locus	**% Light red** [$]	% White	% Red	Total colonies	Correct test digest	Correct Sequencing	*B. subtilis* transf. [#]	
amyE	**69.8**	19.8	10.3	1160	6/6	1/1	+	4/4
ypqP	**92.2**	2.9	4.9	1236	6/6	1/1	+	4/4
ykoS	**91.6**	3.2	5.3	1900	6/6	1/1	++	4/4
ndk [&]		**75**	25	496	12/12	1/1	++	4/4
thrC	**92.1**	5.2	2.6	4580	6/6	1/1	+	4/4

* Data is shown for one Golden Gate assembly using BsaI and the following *entry* parts: PCR products *up* and *down* with BsaI-overhangs, pBSd141R and pBSc141M_P_{xyl}-*mkate2*.

[$] Colonies appear light red if carrying the correct *final vector* and red if the *destination vector* is unchanged. Only light red colonies were used for test digest and correct test digests were used for sequencing. The correct chromosomal integration was verified as described in Material and Methods.

[#] Number of colonies per 100 µl of transformation mixture: ++, >1000; +, >100 and number of colonies with verified chromosomal integration from number of tested colonies.

[&] pBSd191R was used as *destination vector*. No colonies of "light red" color could be identified due to lower copy number of the *final vector*, in comparison to the other constructs. As a consequence, white colonies were used for further verification.

Since the same reporter was used in all vector constructs, the reporter-cargo was added at the *entry vector* level to pBSc241M, resulting in pBSc241M-P_{xylA}-*mkate2*. pBSd141R (ori pRO/ColE1, high copy number) was chosen as the *destination vector* and primers were designed for PCR-product assembly of *up* and *down* fragments via BsaI. Assembly and verification of four *final vectors* was achieved within five working days. The vector carrying homology regions for integration into *ndk* was instable (small colonies), necessitating a change to pBSd191R (ori pBR322/ROP, medium copy number) as a *destination vector.* After transformation of *B. subtilis* W168, the resulting integrants were verified by starch or threonine auxotrophy tests (*amyE* and *thrC*, respectively), or colony PCR for the remaining loci (Table 4). The xylose-inducible promoter P_{xylA} was fully induced with xylose in exponentially growing cultures. The fluorescence intensity of *B. subtilis* cells was quantified in triplicates in a microtiter plate reader as a measure for mKate2 production (Fig. 5). The results highlight a dependence of the expression levels on the chromosomal location: As demonstrated previously, genes close to the ori (0°/360°) tend to be expressed at higher levels than those close to the termination region (180°).

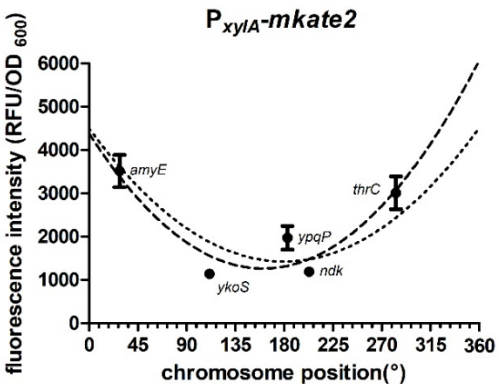

Figure 5. Maximal promoter activity of P_{xylA} depends on chromosomal location. The reporter construct P_{xylA}-*mkate2* was integrated into the *B. subtilis* genome at five different chromosomal loci, as indicated. mKate expression was maximally induced with the addition of 0.2% xylose and fluorescence intensity was measured as an indicator for mKate abundance. The fluorescence intensity is given as a function of the chromosome position. The error bars show the standard deviation of three independent biological replicates. The data was fitted to two second order polynomial functions: dashed line: no constrains, R^2=0.85; dotted line: minimum was set to X=180, R^2=0.72.

One exception was the *ykoS*-locus, located at the replication termination site, which had a higher reporter activity than the constructs inserted at the ori-proximal *ypqP* or *ndk* sites. Nevertheless, these results are in good agreement with a recent study [31], thereby demonstrating that our vector toolbox can for example be used to study the effect of chromosome location on expression levels in a simple and straightforward manner.

DISCUSSION

B. subtilis is a versatile heterologous host with powerful genetics allowing precise genomic manipulation. But so far, the available integrative vectors could not easily be adapted to different strains or, more importantly, other *bacilli*, since no modular toolbox was available to allow free combination of resistance markers and integration sites. To fill this gap, we present a rigorously evaluated toolbox for the construction of integrative vectors with customizable flanking homology regions for *Bacillus sp*. The *final* pBS *vector* can be assembled within one week from four *entry* parts via efficient Golden Gate cloning. Our vector suite offers the choice of four type IIS restriction endonucleases (AarI, BbsI, BsaI and BsmBI) for Golden Gate assembly, seven *Bacillus* antibiotic resistance markers, and two different MCSs, available on either a high or medium copy number *E. coli* backbone. The toolbox is adjusted to and widely compatible with the *E. coli* SEVA standard to allow reusability of its cargos or vector parts. All components provided in this toolbox were successfully tested for assembly efficiency, functionality, and usability in *B. subtilis*. The supplementary assembly guide (Text S2) provides necessary information to facilitate a fast and efficient cloning process.

In the course of developing our vectors, a few combinations were discovered which were difficult to handle on high copy number vectors (ori pRO1600/ColE1): (i) The *Bacillus* kanamycin resistance marker was prone to mutations and is therefore offered with the medium copy number ori pBR322/ROP. (ii) The *lacZα**-pUC18 MCS differs from the original *lacZα*-pUC18 MCS in a single-nucleotide polymorphism causing a premature stop codon in *lacZα* that does not impair blue/white screening. There was a strong selection pressure against the original *lacZα*-pUC18 MCS (very small colonies), which caused transposon integrations and single nucleotide polymorphisms in *lacZα*. Consequently, we used the mutated but fully functional *lacZα**-pUC18 MCS for our constructs. (iii) The *final ndk*-vectors only contained the *ndk down* fragment when using the high copy number pBSd141R as *destination vector*. However, assembly with the medium copy number vector pBSd191R was successful in the first attempt.

Based on our experience, the use of a medium copy number vector is highly recommended as the first trouble shooting strategy in case of cloning issues, especially if slowly growing colonies occur. Also, low copy number oris (e.g. p15A and pSC101) or different directionality of the inserts could be used in case toxicity issues occur, which result in genetic instabilities even on medium copy number vectors.

Furthermore, the tetracycline resistance marker could not confer resistance in *B. subtilis* W168 when the *amyE* locus was targeted. However, when using a different integration locus (*lacA*), the transformation was successful. Due to the dependence of expression levels on the chromosomal region, we suspect this to be causing the transformation issues.

The *Bacillus* SEVA siblings toolbox was developed to provide a versatile starting point for the efficient construction of personalized, yet standardized vectors. Both, the *entry* parts as well as *final vectors* can be customized to meet personal needs. The MCS or cargo and ori can easily be exchanged according to the SEVA standard and new or modified resistance markers can be inserted in markerless *cargo vectors* via MluI, e.g. markers flanked with target sites for recombinases. These systems would allow directed, recombinase-mediated removal of the marker after chromosomal integration (for reviews on recombinase-mediated cassette exchange, e.g. by Flp and Cre/*loxP*, see [32,33]).

It should also be pointed out that the free choice of chromosomal integration loci provided by our vector toolbox allows for replacing even larger (non-essential) chromosomal areas directly in the process of plasmid integration. We have demonstrated this possibility by integrating an *mkate2*-expressing plasmid into the *ypqP* locus of the *B. subtilis* chromosome, thereby deleting the 130kb prophage SPβ (Table 4). This combined integration/deletion at any desired chromosomal position will greatly enhance the possibilities in genetically manipulating *B. subtilis*.

The current resistance markers located on *cargo vectors* were tested for their functionality only in *B. subtilis* W168. Since they originate from broad host range vectors, they are expected to be functionally expressed in many low G+C Gram-positive bacteria (phylum *Firmicutes*). The *Bacillus* SEVA siblings might therefore be

suitable for e.g. other bacilli, increasing the number of species where customized vectors can be used for genetic manipulation. Indeed, preliminary results from an ongoing study using our vectors reported similar or even better vector assembly efficiencies as those described in Table 3. Choramphenicol- or erythromycin-resistant mutants were readily obtained in *Paenibacillus polymyxa* (order: *Bacillales*, family: *Paenibacillaceae*) (Christoph Engl, personal communication).

If transformation efficiencies are too low, conjugation can be performed using the *oriT* already included in the SEVA standard, which provides efficient transfer into various Gram-negative and -positive hosts[7,34,35]. It can be exchanged with a conjugation marker of choice in the *destination* or *final vector* to meet the needs of the target organism. Recombination efficiency of homologous sequences into the chromosome varies more than 30-fold along the *B. subtilis* chromosome [36], and even more between species. In general, integration rates can be improved by using longer stretches of DNA or a vector with a temperature-sensitive replicon (e.g. based on pMAD [3,37]). Vector replication not only increases the number of vectors per cell and number of cells carrying a vector (by passing it on to the next generation), but also supports the second recombination event during which the vector backbone is excised from the chromosome [3]. A temperature-sensitive origin of replication can therefore be added to the *destination* or *final vector* to improve recombination with the chromosome.

Moreover, the construction logic described for the *Bacillus* SEVA siblings – that is, the restriction enzymes used for the assembly of the final integrative plasmids – can of course also be applied for developing other SEVA-compatible integration vectors for completely unrelated microorganisms in a similar fashion. But this would require adjusting the corresponding resistance cassettes applicable to these bacteria.

Here, we present the first fully modular, yet standardized vector toolkit for integrative vectors in *B. subtilis* and beyond. We hope that the *Bacillus* SEVA siblings vector toolbox will prove to be useful for projects throughout the *Bacillus* world. In case personalized *entry vectors* (*pBSc*, *pBSd*) are created, we would like to encourage sharing them with the *Bacillus* community, e.g. via the SEVA or BGSC collections, to

further improve the tools available for genetically manipulating these powerful organisms.

MATERIAL AND METHODS

Bacterial strains and growth conditions

All strains used in this study are listed in Table S1. *B. subtilis* and *E. coli* were routinely grown in lysogeny broth (LB) medium (1% (w/v) tryptone, 0.5 % (w/v) yeast extract, 1 % (w/v) NaCl) at 37°C with agitation (220 rpm). Solid media additionally contained 1.5 % (w/v) agar. Selective media contained appropriate antibiotics, as provided in Table 2.

Transformation

E. coli (XL1 blue, Agilent Technologies, Santa Clara, CA, USA) competent cells were prepared and transformed according to the rubidium chloride method [38], achieving ~$5*10^6$ colony forming units (CFU) per µg pUC18 DNA. Transformations of *B. subtilis* were carried out as described previously [17,22]. The integration of plasmids into the *B. subtilis* genome was checked on starch plates (*amyE*), with minimal medium lacking threonine (*thrC*) or colony PCR (*lacA*, *ypqP, ykoS, ndk*). Detailed protocols were published previously [17,39].

DNA manipulation

Vectors and plasmids used in this study are listed in Table 1. General cloning procedure, such as endonuclease restriction digest, ligation and PCR, was performed with enzymes and buffers from New England Biolabs® (NEB; Ipswich, MA, USA) or Thermo Scientific™ (Waltham, MA, USA) according to the respective protocols. Phusion® polymerase was used for PCRs if the resulting fragment was further used, otherwise OneTaq® was the polymerase of choice. PCR-purification was performed with the *HiYield PCR Gel Extraction/PCR Clean-up Kit* (Süd-Laborbedarf GmbH (SLG), Gauting, Germany). Plasmids were prepared using alkaline lysis and subsequent DNA precipitation. All plasmids created during this study are listed in Table 1, their construction is described in supplemental Table S2 and all primer sequences are given in Table S3.

Golden Gate assemblies of *final vectors*

Golden Gate assemblies were performed using T4 DNA ligase (30 WU) from Thermo Scientific™ with the accompanied buffer. BsaI, BbsI, BsmBI and BtgZI were purchased from NEB, AarI from Thermo Scientific™. *Entry* parts were diluted to 20 or 40 nM stock concentrations and 2 or 1 µl were used per 15 µl reaction, respectively. For all enzymes, 0.5 µl were used per reaction, except for AarI where 1.5 µl were necessary because of its lower activity. BsaI and AarI are active in ligase buffer, but for AarI the accompanying oligonucleotides were supplemented for optimal efficiency. For BbsI half of the ligase buffer was replaced by NEBuffer 2.1 and for BsmBI half was replaced by NEBuffer 3.1.

The general assembly protocol was 37°C, 30 min; 16°C, 30 min; (37°C, 3 min; 16°C, 5 min) x 15; 37°C, 10 min; 50°C, 10 min; 80°C, 10 min. The exception was BsmBI, where 55°C were required for the first incubation step and ligase was only added afterwards. 7.5 µl of the final reaction were used for *E. coli* transformation.

Measurement of P_{xylA} activity

Fluorescence intensity of strains carrying a transcriptional fusion of the xylose-inducible promoter P_{xylA} and the fluorescence reporter *mkate2* were assayed using a Synergy™ NEOALPHAB multi-mode microplate reader from BioTek ® (Winooski, VT, USA). The reader was controlled using the software Gen5™ (version 2.06). Cells were inoculated 1:1000 from fresh overnight cultures and grown to OD_{600} ~ 0.2, treated with 0.2% xylose and grown for two hours. Cells were harvested by centrifugation and resuspended in phosphate buffered saline (137 mM NaCl, 2.7 mM KCl, 10 mM Na2HPO4, 1.8 mM KH2PO4, pH 7.4). 200 µl per well in 96-well plates (black walls, clear bottom; Greiner Bio-One, Frickenhausen, Germany) were measured for their OD_{600}, and mKate-fluorescence using the monochromator with following parameters: endpoint measurement, gain: 100, excitation wavelength: 588 nm, emission wavelength: 633 nm.

Data availability

The vectors generated in this study are available from the Bacillus Genetic Stock Center (BGSC, http://www.bgsc.org/ , accession numbers ECE701-26) and the SEVA collection (http://wwwuser.cnb.csic.es/~seva/?page_id=19). For sequence information, the following accession numbers apply: GenBank, KY995178 to KY995203; ACS Synthetic Biology Registry (https://acs-registry.jbei.org/ , JPUB_008862 to JPUB_008887).

Supplementary data

Text S1 (.pdf): Figure S1 (Architecture of all MCS-IIS) and Tables S1-S7 (Strains and oligonucleotides used in this study, details on plasmid construction, and assembly efficiencies of further pBS vectors).

Text S2 (.pdf): Protocol for *Bacillus* SEVA siblings vector assembly.

Supplementary Data S3 (.zip that contains .gbk-files): Annotated vector sequences.

Acknowledgements

We thank Wilfried Meijer for fruitful initial design discussions and Beate Lüdke for assistance with *B. subtilis* transformations. This work was supported by the Deutsche Forschungsgemeinschaft (DFG) priority program SPP1617 'Phenotypic Heterogeneity and Sociobiology of Bacterial Populations' [grant number MA 2837/3-2 to TM]. Funding for open access charge: dito.

Author contributions statement

JR and TM conceptualized Bacillus SEVA siblings. JR detailed and planned the experiments, analyzed the data and created the figures. JR, DM and NL cloned the vectors and JR performed Golden Gate assemblies. JR and TM wrote the manuscript. All authors reviewed the manuscript.

Conflict of interest

All authors declare no conflict of interest.

REFERENCES

1 Wright, O., Delmans, M., Stan, G. B. & Ellis, T. GeneGuard: A modular plasmid system designed for biosafety. *ACS Synth Biol* **4**, 307-316, doi:10.1021/sb500234s (2015).

2 Shimada, T. *et al.* Classification and strength measurement of stationary-phase promoters by use of a newly developed promoter cloning vector. *J Bacteriol* **186**, 7112-7122, doi:10.1128/JB.186.21.7112-7122.2004 (2004).

3 Arnaud, M., Chastanet, A. & Debarbouille, M. New vector for efficient allelic replacement in naturally nontransformable, low-GC-content, gram-positive bacteria. *Appl Environ Microbiol* **70**, 6887-6891, doi:10.1128/AEM.70.11.6887-6891.2004 (2004).

4 Sinah, N., Williams, C. A., Piper, R. C. & Shields, S. B. A set of dual promoter vectors for high throughput cloning, screening, and protein expression in eukaryotic and prokaryotic systems from a single plasmid. *BMC Biotechnol* **12**, 54, doi:10.1186/1472-6750-12-54 (2012).

5 Andrianantoandro, E., Basu, S., Karig, D. K. & Weiss, R. Synthetic biology: new engineering rules for an emerging discipline. *Mol Syst Biol* **2**, 2006 0028, doi:10.1038/msb4100073 (2006).

6 Martinez-Garcia, E., Aparicio, T., Goni-Moreno, A., Fraile, S. & de Lorenzo, V. SEVA 2.0: an update of the Standard European Vector Architecture for de-/re-construction of bacterial functionalities. *Nucleic Acids Res* **43**, D1183-1189, doi:10.1093/nar/gku1114 (2015).

7 Silva-Rocha, R. *et al.* The Standard European Vector Architecture (SEVA): a coherent platform for the analysis and deployment of complex prokaryotic phenotypes. *Nucleic Acids Res* **41**, D666-675, doi:10.1093/nar/gks1119 (2013).

8 *Standard European Vector Architecture*, <http://wwwuser.cnb.csic.es/~seva/?page_id=17 and http://wwwuser.cnb.csic.es/~seva/?page_id=19> (accessed March 2017)

9 Kim, S. H., Cavaleiro, A. M., Rennig, M. & Norholm, M. H. SEVA Linkers: A Versatile and Automatable DNA Backbone Exchange Standard for Synthetic Biology. *ACS Synth Biol* **5**, 1177-1181, doi:10.1021/acssynbio.5b00257 (2016).

10 van Dijl, J. M. & Hecker, M. *Bacillus subtilis*: from soil bacterium to super-secreting cell factory. *Microb Cell Fact* **12**, 3, doi:10.1186/1475-2859-12-3 (2013).

11 Hohmann, H.-P., van Dijl, J. M., Krishnappa, L. & Prágai, Z. in *Industrial Biotechnology*, 221-297 (Wiley-VCH Verlag GmbH & Co. KGaA, 2017).

12 Liu, Y., Li, J., Du, G., Chen, J. & Liu, L. Metabolic engineering of *Bacillus subtilis* fueled by systems biology: Recent advances and future directions. *Biotechnol Adv* **35**, 20-30, doi:10.1016/j.biotechadv.2016.11.003 (2017).

13 Mell, J. C. & Redfield, R. J. Natural competence and the evolution of DNA uptake specificity. *J Bacteriol* **196**, 1471-1483, doi:10.1128/JB.01293-13 (2014).

14 Zucca, S., Pasotti, L., Mazzini, G., De Angelis, M. G. & Magni, P. Characterization of an inducible promoter in different DNA copy number conditions. *BMC Bioinformatics* **13 Suppl 4**, S11, doi:10.1186/1471-2105-13-S4-S11 (2012).

15 Adams, C. W. & Hatfield, G. W. Effects of Promoter Strengths and Growth Conditions on Copy Number of Transcription-Fusion Vectors. *J Biol Chem* **259**, 7399-7403 (1984).

16 Guerout-Fleury, A. M., Frandsen, N. & Stragier, P. Plasmids for ectopic integration in *Bacillus subtilis*. *Gene* **180**, 57-61 (1996).

17 Radeck, J. *et al.* The *Bacillus* BioBrick Box: generation and evaluation of essential genetic building blocks for standardized work with *Bacillus subtilis*. *Journal Biol Eng* **7**, 29, doi:10.1186/1754-1611-7-29 (2013).

18 Hartl, B., Wehrl, W., Wiegert, T., Homuth, G. & Schumann, W. Development of a new integration site within the *Bacillus subtilis* chromosome and construction of compatible expression cassettes. *J Bacteriol* **183**, 2696-2699, doi:10.1128/JB.183.8.2696-2699.2001 (2001).

19 Schmalisch, M. *et al.* Small genes under sporulation control in the *Bacillus subtilis* genome. *J Bacteriol* **192**, 5402-5412, doi:10.1128/JB.00534-10 (2010).

20 Stülke, J. *et al.* Induction of the *Bacillus subtilis ptsGHI* operon by glucose is controlled by a novel antiterminator, GlcT. *Mol Microbiol* **25**, 65-78 (1997).

21 Wach, A. PCR-synthesis of marker cassettes with long flanking homology regions for gene disruptions in *S. cerevisiae*. *Yeast* **12**, 259-265 (1996).

22 Harwood, C. R. & Cutting, S. M. *Molecular Biological Methods for Bacillus*. (John Wiley & Sons, 1990).

23 Engler, C., Kandzia, R. & Marillonnet, S. A one pot, one step, precision cloning method with high throughput capability. *PLoS One* **3**, e3647, doi:10.1371/journal.pone.0003647 (2008).

24 Engler, C., Gruetzner, R., Kandzia, R. & Marillonnet, S. Golden gate shuffling: a one-pot DNA shuffling method based on type IIs restriction enzymes. *PLoS One* **4**, e5553, doi:10.1371/journal.pone.0005553 (2009).

25 Khasanov, F. K., Zvingila, D. J., Zainullin, A. A., Prozorov, A. A. & Bashkirov, V. I. Homologous recombination between plasmid and chromosomal DNA in *Bacillus subtilis* requires approximately 70 bp of homology. *Mol Gen Genet* **234**, 494-497, doi:10.1007/bf00538711 (1992).

26 Gibson, D. G. Synthesis of DNA fragments in yeast by one-step assembly of overlapping oligonucleotides. *Nucleic Acids Res* **37**, 6984-6990, doi:10.1093/nar/gkp687 (2009).

27 Gibson, D. G., Smith, H. O., Hutchison, C. A., 3rd, Venter, J. C. & Merryman, C. Chemical synthesis of the mouse mitochondrial genome. *Nat Methods* **7**, 901-903, doi:10.1038/nmeth.1515 (2010).

28 Weber, E., Engler, C., Gruetzner, R., Werner, S. & Marillonnet, S. A Modular Cloning System for Standardized Assembly of Multigene Constructs. *PLoS ONE* **6**, e16765, doi:10.1371/journal.pone.0016765 (2011).

29 Sarrion-Perdigones, A. *et al.* GoldenBraid: An Iterative Cloning System for Standardized Assembly of Reusable Genetic Modules. *PLoS ONE* **6**, e21622, doi:10.1371/journal.pone.0021622 (2011).

30 Sarrion-Perdigones, A. *et al.* GoldenBraid 2.0: a comprehensive DNA assembly framework for plant synthetic biology. *Plant Physiol* **162**, 1618-1631, doi:10.1104/pp.113.217661 (2013).

31 Sauer, C. *et al.* Effect of Genome Position on Heterologous Gene Expression in *Bacillus subtilis*: An Unbiased Analysis. *ACS Synthetic Biology* **5**, 942-947, doi:10.1021/acssynbio.6b00065 (2016).

32 Turan, S., Zehe, C., Kuehle, J., Qiao, J. & Bode, J. Recombinase-mediated cassette exchange (RMCE) - a rapidly-expanding toolbox for targeted genomic modifications. *Gene* **515**, 1-27, doi:10.1016/j.gene.2012.11.016 (2013).

33 Dong, H. & Zhang, D. Current development in genetic engineering strategies of *Bacillus* species. *Microb Cell Fact* **13**, 63, doi:10.1186/1475-2859-13-63 (2014).

34 Martinez-Garcia, E., Calles, B., Arevalo-Rodriguez, M. & de Lorenzo, V. pBAM1: an all-synthetic genetic tool for analysis and construction of complex bacterial phenotypes. *BMC Microbiol* **11**, 38, doi:10.1186/1471-2180-11-38 (2011).

35 Trieu-Cuot, P., Carlier, C., Martin, P. & Courvalin, P. Plasmid transfer by conjugation from *Escherichia coli* to Gram-positive bacteria. *FEMS Microbiol Lett* **48**, 289-294, doi:10.1111/j.1574-6968.1987.tb02558.x (1987).

36 Vagner, V. & Ehrlich, S. D. Efficiency of homologous DNA recombination varies along the *Bacillus subtilis* chromosome. *J Bacteriol* **170**, 3978-3982 (1988).

37 Rachinger, M. *et al.* Size unlimited markerless deletions by a transconjugative plasmid-system in *Bacillus licheniformis*. *J Biotechnol* **167**, 365-369, doi:10.1016/j.jbiotec.2013.07.026 (2013).

38 Mülhardt, C. *Der Experimentator. Molekularbiologie/Genomics*. 6 edn, (Spektrum Akademischer Verlag, 2009).

39 Sambrook, J. & Russell, D. W. *Molecular Cloning - a laboratory manual*. (Cold Spring Harbor Laboratory Press, 2001).

40 Joseph, P., Fantino, J. R., Herbaud, M. L. & Denizot, F. Rapid orientated cloning in a shuttle vector allowing modulated gene expression in *Bacillus subtilis*. *FEMS Microbiol Lett* **205**, 91-97 (2001).

41 Guerout-Fleury, A. M., Shazand, K., Frandsen, N. & Stragier, P. Antibiotic-resistance cassettes for *Bacillus subtilis*. *Gene* **167**, 335-336 (1995).

42 Balbás, P. & Bolívar, F. in *Recombinant Gene Expression: Reviews and Protocols* (eds Paulina Balbás & Argelia Lorence) 77-90 (Humana Press, 2004).

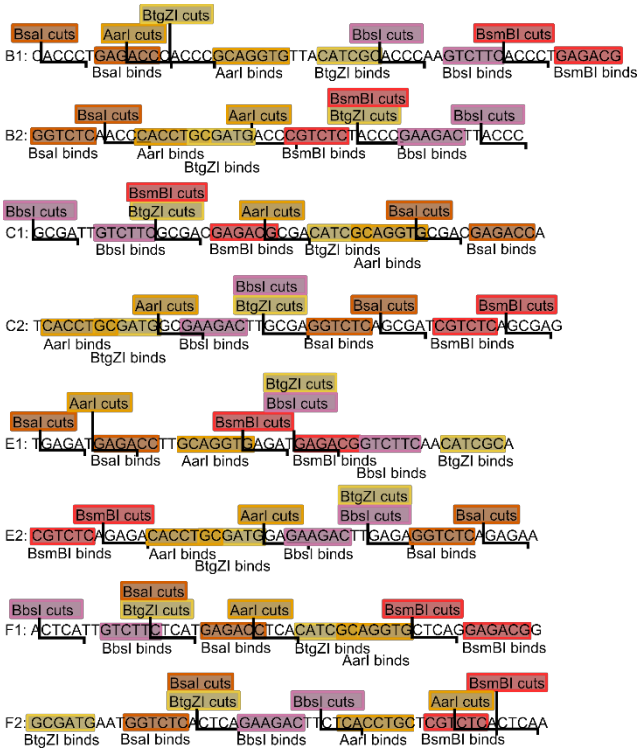

Figure S1: Architecture of all MCS-IIS. These DNA-sequences are located on the *entry vectors* (see Figure 2) and allow the Golden Gate assembly of the *final vector* via one of five type IIS restriction enzymes (AarI, BtgZI, BbsI, BsaI, BsmBI). In each MCS-IIS, the same 4-nt overhang is created, irrespective of the enzyme used. The overhangs are designed to allow assembly in the specified order depicted in Figure 2.

Table S1. Bacterial strains used in this study

Name	Description	Source
E. coli strains		
XL1-Blue	*recA1 endA1 gyrA96 thi-1 hsdR17 supE44 relA1 lac F'*::Tn*10 proAB lacI*^{q} Δ(*lacZ*)M15]	Agilent Technologies
NEB5α	*fhuA2 Δ(argF-lacZ)U169 phoA glnV44 Φ80 Δ(lacZ)M15 gyrA96 recA1 relA1 endA1 thi-1 hsdR17*	New England Biolabs®
DH5α	*F– Φ80lacZΔM15 Δ(lacZYA-argF) U169 recA1 endA1 hsdR17 (rK–, mK+) phoA supE44 λ– thi-1 gyrA96 relA1*	Thermo Scientific™
B. subtilis strains		
W168	Wild-type, *trpC2*	Laboratory stock
TMB3717	W168 *amyE*::pBSf141mls-amyE_mkate2 (P_{xylA}-*mkate2*, *ermC*)	This study
TMB3718	W168 *ypqP*::pBSf141mls-ypqP_mkate2 (P_{xylA}-*mkate2*, *ermC*)	This study
TMB3719	W168 *ykoS*::pBSf141mls-ykoS_mkate2 (P_{xylA}-*mkate2*, *ermC*)	This study
TMB3720	W168 *ndk*::pBSf191mls-ndk_mkate2 (P_{xylA}-*mkate2*, *ermC*)	This study
TMB3721	W168 *thrC*::pBSf141mls-thrC_mkate2 (P_{xylA}-*mkate2*, *ermC*)	This study

Table S2. Construction of Vectors and Plasmids used in this study

Name	Primers and Enzymes used for cloning[a]
pBSd141R	800bp DNA-fragment (synthesized by Thermo Scientific™ containing MCS-IIS B1, T1, MCS default, T2, MCS-IIS F2) was ligated into pSEVA243 via SwaI+AscI to create vector pSEVA141BF. Monomeric red fluorescent protein (mRFP BBa_E1010)) was codon-optimized for expression in *Bacillus* with *B. subtilis* W168 *rpsB* promoter and *yvtI* terminator from *Bacillus licheniformis* DSM13, synthesized, cut with KpnI+BbsI and ligated into pSEVA141BF (BamHI+KpnI).
pBSd191R	BsmBI-free pBR322 origin of replication was created by PCR-joining two fragments with primers TM4150+TM4153: TM4150+TM4151, pMAD and TM4152+4153, pMAD. This fragment was cut with FseI+AscI and ligated with the 1500bp and 600bp fragments of pSEVA141BF cut with SwaI, FseI and AscI. mRFP from pBSd141R was inserted via EcoRI+XbaI.
pSEVA243X	DNA-fragment containing MCS-IIS B2, EcoRV and MCS-IIS C1 was synthesized by Thermo Scientific™ and cloned into pSEVA243 via EcoRI+SpeI.
pSEVA243Y	DNA-fragment containing MCS-IIS E2, EcoRV and MCS-IIS F1 was synthesized by Thermo Scientific™ and cloned into pSEVA243 via EcoRI+SpeI.
pBSc241B	*ble*-cassette was amplified by PCR (TM3773+TM3774, pDG148), cut with MluI and ligated into pBSc241 (cut with AscI).
pBSc241C	*cat*-cassette was amplified by PCR (TM3771+TM3772, pBS3Clux), cut with MluI and ligated into pBSc241 (cut AscI).
pBSc241M	SacI-free *mls*-cassette was created by PCR-joining 2 fragments with TM3767+TM3768: TM3767+TM3770, pDG647 and mls-back TM3769+TM3768, pDG647, cut with MluI and ligated into pBSc241 (cut with AscI).
pBSc241S	KpnI+SwaI-free *spec*-cassette (incl. terminator BBa_B0014) was created by PCR-joining 3 fragments with TM3762+TM3761: TM3762+TM3764, pBS4S, TM3763+TM3765, pBS4S and TM3766+TM3761, pSB1A3-mkate-B0014, cut with MluI and ligated into pSEVA241EC (cut with AscI).
pBSc241T	BsmBI+AarI-free *tet*-cassette was created by PCR-joining 2 fragments with TM3752+TM3753: TM3752+TM3755, pDG1513 and TM3754+TM3753, pDG1513, cut with MluI and ligated into pBSc241 (cut with AscI).
pBSc241Z	*zeo*-cassette was synthesized by Thermo Scientific™ (codon adapted for *B. subtilis*, with *kan*-promoter from pDG780 and *cat*-terminator from pBS3Clux flanked with MluI restriction sites), cut with MluI and ligated into pBSc241 (cut with AscI).
pBSc291K	BbsI-free *kan*-cassette (incl. terminator BBa_B0014) was created by PCR-joining of 3 fragments with TM3756+TM3761: TM3756+TM3758, pDG780, TM3757+TM3759, pDG780 and TM3760+TM3761, pSB1A3-mkate-B0014, cut with MluI and ligated into pBSc291 (cut with AscI).
pBSc243B	*lacZα**-pUC18-MCS from pSEVA143* was ligated into pBSc241B via PacI+SpeI.
pBSc243C	*lacZα**-pUC18-MCS from pSEVA143* was ligated into pBSc241C via PacI+SpeI.
pBSc243M	*lacZα**-pUC18-MCS from pSEVA143* was ligated into pBSc241M via PacI+SpeI.
pBSc243S	*lacZα**-pUC18-MCS from pSEVA143* was ligated into pBSc241S via PacI+SpeI.
pBSc243T	*lacZα**-pUC18-MCS from pSEVA143* was ligated into pBSc241T via PacI+SpeI.
pBSc243Z	*lacZα**-pUC18-MCS from pSEVA143* was ligated into pBSc241Z via PacI+SpeI.
pBSc293K	*lacZα**-pUC18-MCS from pBSc243 was ligated into pBSc291K via PacI+SpeI.
pBSc241	DNA-fragment containing MCS-IIS C2, T1, MCS default, T0, MCS-IIS E1 was synthesized by Thermo Scientific™, cut with MluI+ScaI and ligated into pSEVA243 (cut with SwaI+AscI).
pBSc243	*lacZα**-pUC18-MCS from pSEVA143* was ligated into pBSc241 via PacI+SpeI.
pBSc291	BsmBI-free ori pBR322 from pBSd191R cut with AscI+FseI was ligated into pSEVA243 cut with AscI+FseI+SpeI (both 800bp and 1300bp fragments), creating pSEVA293*. DNA-fragment containing MCS-IIS C2, T1, MCS default, T0, MCS-IIS E1 was synthesized by Thermo Scientific™, cut with MluI+ScaI and ligated into pSEVA293* (cut with SwaI+AscI).
pBSc293	*lacZα**-pUC18-MCS from pBSc243 was ligated into pBSc291via PacI+SpeI.
pBSc391	BtgZI/BsmBI/ScaI-free *cat* cassette was synthesized by Thermo Scientific™ and ligated into pSEVA243 via PshAI+SwaI, creating pSEVA343*. BsmBI-free ori pBR322 cut from pBSd191R with AscI+FseI ligated into pSEVA343* cut with AscI+FseI+SpeI (both: 800+1500bp bands were used), creating pSEVA393*. DNA-fragment containing MCS-IIS C2, T1, MCS default, T0, MCS-IIS E1 was synthesized by Thermo Scientific™, cut with MluI+ScaI and ligated into pSEVA393* (SwaI+AscI).
pBSc393	*lacZα**-pUC18-MCS from pBSc243 was ligated into pBSc392 via PacI+SpeI.
pSEVA243X-amyE	"*amyE*-up" fragment (600bp) amplified from W168 with TM4230+TM4231 was ligated into EcoRV-linearized pSEVA243X.
pSEVA243Y-amyE	"*amyE*-do" fragment (600bp) amplified form W168 with TM4981+TM4982 was ligated into EcoRV-linearized pSEVA243Y.
pBSc141M_P$_{xylA}$-*mkate2*	Insert P$_{xylA}$ (BBa_K1351039, EcoRI+SpeI) and red fluorescent protein *mkate2* (BBa_K823029, codon-adapted to *B. subtilis*, XbaI+PstI) were ligated into pBSc241mls (EcoRI+PstI).
pBS141M-amyE_mkate2	Golden Gate reaction with BsaI and the vectors pBSc141M_P$_{xylA}$-*mkate2* and pBSd141R, as well as the PCR fragments (~500 bp) BsaI-*amyE*-up (TM4518+TM4519, W168) and BsaI-*amyE*-do (TM4983+TM4984, W168).
pBS141M-ypqP_mkate2	Golden Gate reaction with BsaI and the vectors pBSc141M_P$_{xylA}$-*mkate2* and pBSd141R, as well as the PCR fragments (~500 bp) BsaI-*ypqP*-up (TM5100+TM5101, W168) and BsaI-*ypqP*-do (TM5102+TM5103, W168).
pBS141M-ykoS_mkate2	Golden Gate reaction with BsaI and the vectors pBSc141M_P$_{xylA}$-*mkate2* and pBSd141R as well as the PCR fragments (~500 bp) BsaI-*ykoS*-up (TM5108+TM5109, W168) and BsaI-*ykoS*-do (TM5110+TM5111, W168).
pBS191M-ndk_mkate2	Golden Gate reaction with BsaI and the vectors pBSc141M_P$_{xylA}$-*mkate2* and pBSd191R as well as the PCR fragments (~500 bp) BsaI-*ndk*-up (TM5112+TM5113, W168) and BsaI-*ndk*-do (TM5114+TM5115, W168).
pBS141M-thrC_mkate2	Golden Gate reaction with BsaI and the vectors pBSc141M_P$_{xylA}$-*mkate2* and pBSd141R as well as the PCR fragments (~500 bp) BsaI-*thrC*-up (TM5116+TM5117, W168) and BsaI-*thrC*-do (TM5118+TM5119, W168).

[a] *lacZα**-pUC18: contains a premature stop codon (C202T => Q68*) in the *lacZα*-open reading frame. *lacZα* is still functional for blue-white screening. Non-mutated fragments (can) lead to plasmid instability if combined with the high copy number ori pRO1600/ColE1.

Table S3: Oligonucleotides used in this study

Number	Name	Sequence[a] (5' to 3')
TM0057	mls-check-fwd	CCTTAAAACATGCAGGAATTGACG
TM0718	cat-check-fwd	AATAGCGACGGAGAGTTAGG
TM0498	kan-check-fwd	GCCGGTATAAAGGGACCACC
TM0058	spec-check-fwd	GTTATCTTGGAGAGAATATTGAATGGAC
TM5222	tet-check-fwd	TGTTTTAGGTGGGCTTTCGTTC
TM3680	pSEVA PS1	AGGGCGGCGGATTTGTCC
TM3681	pSEVA PS2	GCGGCAACCGAGCGTTC
TM3682	pSEVA PS3	GAACGCTCGGTTGCCGC
TM3683	pSEVA PS4	CCAGCCTCGCAGAGCAGG
TM3684	pSEVA PS5	CCCTGCTTCGGGGTCATT
TM3685	pSEVA PS6	GGACAAATCCGCCGCCCT
TM3782	pSEVAcheck-sites1	CGCAAAAAACGCACCACTACG
TM3783	pSEVAcheck-sites2	GGTTATTGTCTCATGAGCGG
TM3784	pSEVAcheck-sites3	CTTGTATTACTGTTTATGTAAGCAG
TM4154	SEVA141BF-T0SpeI-fwd	CTGGCGACTAGTCTTGGAC
TM5128	pSEVAcheck-sites4	GGTTACTGATGATGAACATGC
TM3752	MluI-Tet-fwd	GATC*ACGCGT*GGATTTTATGACCGATGATGAAG
TM3753	MluI-Tet-rev	GATC*ACGCGT*TAAAAAAAGGATCAATTTTGAACTCTC
TM3754	Tet-BsmBI,AarI mut fwd	GAAATGGTTTTGAACGTCagcTTACCTGATATTGCAAATGATTTTAATAAA CCtCCTGCGAGTACAAACTGG
TM3755	Tet-BsmBI,AarI mut rev	CCAGTTTGTACTCGCAGGaGGTTTATTAAAATCATTTGCAATATCAGGTA AgctGACGTTCAAAACCATTTC
TM3756	MluI-kan-fwd	GATC*ACGCGT*TTCTGGTATTTAAGGTTTTAGAATGC
TM3757	Kan-BbsI mut fwd	GGATTGCGAAAACTGGGAAGAgGACACTCCATTTAAAGATCCGC
TM3758	Kan-BbsI mut rev	GCGGATCTTTAAATGGAGTGTCcTCTTCCCAGTTTTCGCAATCC
TM3759	Kan w/o term rev	GAGCCAGTGTGAGGTACTAAAACAATTCATCCAG
TM3760	B0014-kan-fusion fwd	GAATTGTTTTAGTACCTCACACTGGCTCACCTTCG
TM3761	MluI-B0014-rev	GATC*ACGCGT*AAAATAATAAAAAAGCCGGATTAATAATC
TM3762	MluI-spec-fwd	GATC*ACGCGT*TAACAACTATGGATATAAAATAGG
TM3763	Spec-KpnImut fwd	CAATTATTATTCAGCAAGAAATGGTtCCGTGGAATCATCCTCCC
TM3764	Spec-KpnImut rev	GGGAGGATGATTCCACGGaACCATTTCTTGCTGAATAATAATTG
TM3765	Spec-SwaImut-w/oterm rev	TTATAATTTTTTTAATCTGTTgTTTAAATAGTTTATAGTTAAATTTAC
TM3766	B0014-spec-fusion fwd	CTATTTAAAcAACAGATTAAAAAAATTATAATCACACTGGCTCACCTTCG
TM3767	MluI-mls- fwd	GATC*ACGCGT*GATCCTTTAACTCTGGCAACCCTC
TM3768	MluI-mls-rev	GATC*ACGCGT*GCCGACTGCGCAAAAGACATAATC
TM3769	MLS-SacImut fwd	CTCATCATGTTCATATTTATCAGAGgTCGTGCTATAATTATACTAATTTTA TAAGG
TM3770	MLS-SacImut rev	CCTTATAAAATTAGTATAATTATAGCACGAcCTCTGATAAATATGAACATG ATGAG
TM3771	MluI-cat-fwd	GATC*ACGCGT*AAGTGGGATATTTTTAAAATATATATTTATG
TM3772	MluI-cat-rev	GATC*ACGCGT*CAGGTTAGTGACATTAGAAAACC
TM3773	MluI-bleo-fwd	GATC*ACGCGT*ACGATGACCTCTAATAATTGTTAATC
TM3774	MluI-bleo-rev	GATC*ACGCGT*TCTTTTATTCAGCAATCGCGC
TM4150	pBR322-AscI fwd	TATTTTGGCGCGCCAATATCCCGCCGCATCCATACC
TM4151	pBR322-BsmBImut rev	GCTTACAGACAAGCTGTGACgcTCTCCGGGAGCTGCATG
TM4152	pBR322-BsmBImut fwd	CATGCAGCTCCCGGAGAgcGTCACAGCTTGTCTGTAAGC

TM4153	pBR322-FseI-rev	TTAAATGGCCGGCCCGTAGAAAAGATCAAAGGATC
TM4230	SEVA-amyE-up-fwd	ATGTTTGCAAAACGATTCAAAACC
TM4231	SEVA-amyE-up-rev	CGATCAGACCAGTTTTTAATTTG
TM4981	SEVA-amyE-do fwd	CTGGGCGGTGATAGCTTC
TM4982	SEVA-amyE-do rev	CTTTTGTTGTATTCGCATCTGC
TM4518	BsaI-amyE-up-fwd	CTCAAGG*GGTCTCC***ACCC**ATGTTTGCAAAACGATTCAAAACC
TM4519	BsaI -amyE-up-rev	CTCAAGG*GGTCTCC***TCGC**CGATCAGACCAGTTTTTAATTTG
TM4983	BsaI -amyE-do-fwd	CTCAAGG*GGTCTCC***GAGA**CTGGGCGGTGATAGCTTC
TM4984	BsaI -amyE-do-rev	CTCAAGG*GGTCTCC***TGAG**CTTTTGTTGTATTCGCATCTGC
TM5100	BsaI-ypqP-up-fwd	CTCAAGG*GGTCTCC***ACCC**CAAAGTTGAACATATGATGCATGG
TM5101	BsaI-ypqP-up-rev	CTCAAGG*GGTCTCC***TCGC**GTACTGATATTAATGACATGCTGC
TM5102	BsaI-ypqP-do-fwd	CTCAAGG*GGTCTCC***GAGA**GTATCTCCTGTGAACACAATGG
TM5103	BsaI-ypqP-do-rev	CTCAAGG*GGTCTCC***TGAG**GATGCAATTCTTCAATAATCTGAGC
TM5108	BsaI-ykoS-up-fwd	CTCAAGG*GGTCTCC***ACCC**AAAGGAAGATGCCCATATCCG
TM5109	BsaI-ykoS-up-rev	CTCAAGG*GGTCTCC***TCGC**CGTCATAAATGCAATACTGCCT
TM5110	BsaI-ykoS-do-fwd	CTCAAGG*GGTCTCC***GAGA**TTGTTATATACGTGAGCTTTGCG
TM5111	BsaI-ykoS-do-rev	CTCAAGG*GGTCTCC***TGAG**CGTTTACCGAGTTCATCGAC
TM5112	BsaI-ndk-up-fwd	CTCAAGG*GGTCTCC***ACCC**CGCAGGAACAGCTTGAACC
TM5113	BsaI-ndk-up-rev	CTCAAGG*GGTCTCC***TCGC**TGTTCGGCGTAGTGTTTCTC
TM5114	BsaI-ndk-do-fwd	CTCAAGG*GGTCTCC***GAGA**ACCTGTATTCGCAATGGTGTG
TM5115	BsaI-ndk-do-rev	CTCAAGG*GGTCTCC***TGAG**AGTCTCGCTGTCTTTTTGTCC
TM5116	BsaI-thrC-up-fwd	CTCAAGG*GGTCTCC***ACCC**GCGTGAGCTTTGAAAAAATCC
TM5117	BsaI-thrC-up-rev	CTCAAGG*GGTCTCC***TCGC**AATGCATTTCATGTTAGCACGG
TM5118	BsaI-thrC-do-fwd	CTCAAGG*GGTCTCC***GAGA**GAAAATCCGGAAACAATAGCG
TM5119	BsaI-thrC-do-rev	CTCAAGG*GGTCTCC***TGAG**GCTTTCAAAGACGGTCAGC

[a] Endonuclease restriction enzyme recognition sites in italics, restriction site in bold for IIS enzymes; Underlined nucleotides do not anneal with the original template. Introduced mutated nucleotides in lower case.

Tables S4-6. Assembly efficiencies for BSs vectors. Colonies appear blue (Table S4 and first five constructs of Table S6) or white (Table S5 and remaining constructs of Table S6) if carrying the correct *final vector* and red if the *destination vector* is unchanged. Only colonies of the correct color were used for test digest and correct test digests were used for sequencing. Data is shown for one Golden Gate assembly each. Number of colonies per 100 µl of *B. subtilis* W168 transformation mixture: ++, >1000; +, >100; o,>10; θ, <10; -, no colony with verified chromosomal integration. Number of colonies with correct insertion locus as verified with a starch test (out of colonies tested) is given in the last column.

Table S4. Assembly efficiencies for pBSc241-derivatives with pSEVA243XamyE (*up*) , pSEVA243YamyE (*down*), pBSd141R and BsaI.

Cargo vector	% white	% red	Total colonies	Correct test digest	Correct Sequencing	*B. subtilis* transformation	
pBSc241	**90.8**	9.2	8592	3/6	1/1	n.a.	n.a.
pBSc241B	**93.6**	6.4	6336	4/6	1/1	o	2/4
pBSc241C	**86.5**	13.5	4384	3/6	1/2	++	3/4
pBSc291K	**84.5**	15.5	3564	4/6	1/2	o	2/11
pBSc241M	**84.1**	15.9	3328	2/6	1/1	++	3/4
pBSc241S	**90.6**	9.4	6816	5/6	1/1	o	3/10
pBSc241T	**90.3**	9.7	1480	2/6	1/1	-; θ*	0/1;3/3[a]
pBSc241Z	**91.2**	8.8	2448	6/6	1/1	o	4/4

[a] *B. subtilis* transformation was not successful for integration into the *amyE* locus. However, transformation was successful if the *lacA* locus was targeted (data only shown in column "*B. subtilis* transformation").

Table S5. Assembly efficiencies for pBSc243-derivatives with pSEVA243XamyE (*up*) , pSEVA243YamyE (*down*), pBSd141R and BsaI.

Cargo vector	% blue	% white	% red	Total colonies	Correct test digest	Correct Sequencing	*B. subtilis* transformation	
pBSc243	**81.5**	9.6	8.9	7248	6/6	1/1	n.a.	n.a.
pBSc243B	**75.4**	17.8	6.8	4224	6/6	1/1	o	4/4
pBSc243C	**68.0**	18.4	13.6	5056	3/6	1/2	++	4/4
pBSc293K	**76.8**	11.8	11.4	2640	4/6	1/1	o	4/4
pBSc243M	**71.3**	7.2	21.5	6024	3/6	1/1	++	4/4
pBSc243S	**82.8**	4.4	12.8	3248	6/6	1/1	o	7/20
pBSc243T	**78.9**	5.0	16.1	2576	5/6	1/1	-; θ[a]	0/7;9/9[a]
pBSc243Z	**77.9**	16.1	6.0	2988	6/6	1/1	o	4/4

[a] *B. subtilis* transformation was not successful for integration into the *amyE* locus. However, transformation was successful if the *lacA* locus was targeted (data only shown in column "*B. subtilis* transformation").

Table S6. Efficiencies for BsaI-mediated pBS assembly with mixed combinations of *cargo*, *up*, *down* and *destination* vectors and parts.

Abb.[a]	% blue	% white	% red	Total colonies	Correct test digest	Correct Sequencing	*B. subtilis* transformation	
34V	**44.8**	3.0	52.2	3248	6/6	1/1	++	4/4
34P	**73.4**	10.8	15.8	3336	6/6	1/2	+	4/4
39V	**67.7**	19.4	12.9	744	6/6	1/1	++	4/4
39P	**68.0**	30.9	1.1	4200	6/6	1/1	++	4/4
39Pkan	**62.1**	36.6	1.3	3672	6/6	1/1	o	4/4
14V	n.a.	**38.1**	61.9	2560	4/6	1/1	+	4/4
14P	n.a.	**82.0**	18.0	2000	3/6	1/1	++	4/4
19V	n.a.	**95.7**	4.3	1128	3/6	1/1	++	4/4
19P	n.a.	**99.2**	0.8	2380	1/6	1/1	++	4/4
19Pkan	n.a.	**98.6**	1.4	2840	1/6	1/1	o	4/4

[a] The abbreviations encode for *entry* parts and are outlined in Table S7.

Table S7. Legend for Table S6.

Name	Cargo	Destination	Up	Down
34V	pBSc243M	pBSd141R	pSEVA243XamyE	pSEVA243YamyE
34P	pBSc243M	pBSd141R	BsaI-amyE-up (PCR)	BsaI-amyE-down (PCR)
39V	pBSc243M	pBSd191R	pSEVA243XamyE	pSEVA243YamyE
39P	pBSc243M	pBSd191R	BsaI-amyE-up (PCR)	BsaI-amyE-down (PCR)
39Pkan	pBSc293K	pBSd191R	BsaI-amyE-up (PCR)	BsaI-amyE-down (PCR)
14V	pBSc241M	pBSd141R	pSEVA243XamyE	pSEVA243YamyE
14P	pBSc241M	pBSd141R	BsaI-amyE-up (PCR)	BsaI-amyE-down (PCR)
19V	pBSc241M	pBSd191R	pSEVA243XamyE	pSEVA243YamyE
19P	pBSc241M	pBSd191R	BsaI-amyE-up (PCR)	BsaI-amyE-down (PCR)
19Pkan	pBSc291K	pBSd191R	BsaI-amyE-up (PCR)	BsaI-amyE-down (PCR)

HOW TO BUILD YOUR OWN *BACILLUS* SEVA SIBLING (PBS)

EXPLANATION OF *BACILLUS* SEVA SIBLINGS

1) *Bacillus* SEVA siblings (pBS) are vectors that are made for *Bacillus sp*. and are based on the Standard European Vector Architecture (SEVA) for replicative *E. coli* vectors.

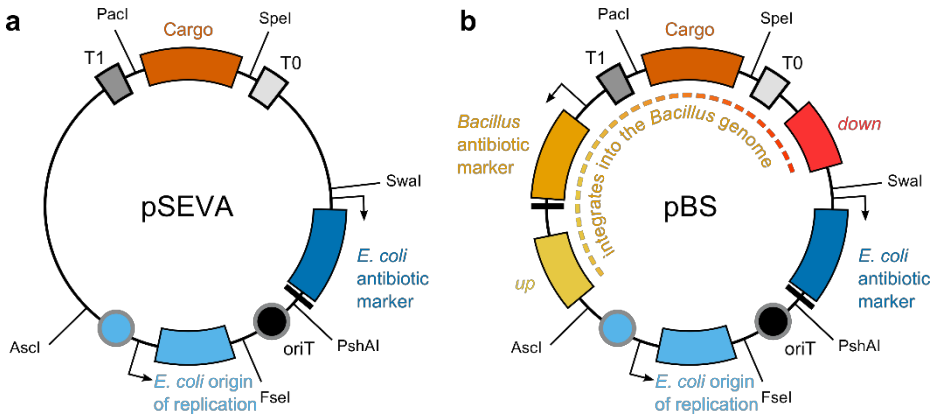

Figure 1. Comparison of SEVA vector (a) and Bacillus SEVA sibling (b)

2) They are assembled from 4 parts (*up*, *cargo-resistance pBSc*, *down*, and *destination pBSd*) via the one-pot Golden Gate assembly (compatible overhangs are marked with the same letter, see Fig. 2), so that the homology regions for genomic integration can be easily adjusted to your strain of interest.
3) Single parts of the vector can be exchanged before or after the assembly according to the SEVA-Standard.
4) List of available *Entry vectors*, see Table 1 and 2: *destination vectors* (*pBSd*); *up* and *down vectors*; *cargo-resistance vectors* (*pBSc*). Sequences can be downloaded from the SEVA and Bacillus Genetic Stock Center (BGSC) collections.

Table 1. Quick guide of *entry* vectors

Name	description	Remarks/What to do with it?
pSEVA243X	For *up* fragments	Linearize (EcoRV) and insert your PCR product to receive appropriate MCS-IIS (B2+C1). Allows blue/white screening.
pSEVA243Y	For *down* fragments	Linearize (EcoRV) and insert your PCR product to receive appropriate MCS-IIS (E2+F1). Allows blue/white screening.
pSEVA243[a]	For *up* and *down* fragments	Linearize (SmaI) and insert PCR product that includes IIS overhangs.
pBSc241res* **pBSc243res***	***Cargo-resistance vector*** with - default MCS (pUC18) - MCS lacZα-pUC18 *Resistances available: -, *ble*, *cat*, *kan*, *mls*, *spec*, *tet*, *zeo*. *kan* is offered in a medium copy vector	Adjust cargo before or after BSs assembly
pBSd141R **pBSd191R**	***Destination vectors*** with - high copy ori: pRO1600/ColE1 - medium copy ori: pBR322/ROP Both carry *mRFP1* for red/white screening	Adjust *E. coli* ori before or after BSs assembly

[a] pSEVA243 seems to be prone to transposal integration in the *lacZα*-region in some *E. coli* strains, as manifesting in white (and only small blue) colonies on X-Gal. In this case, consider changing the strain, ori or lacZα-version.

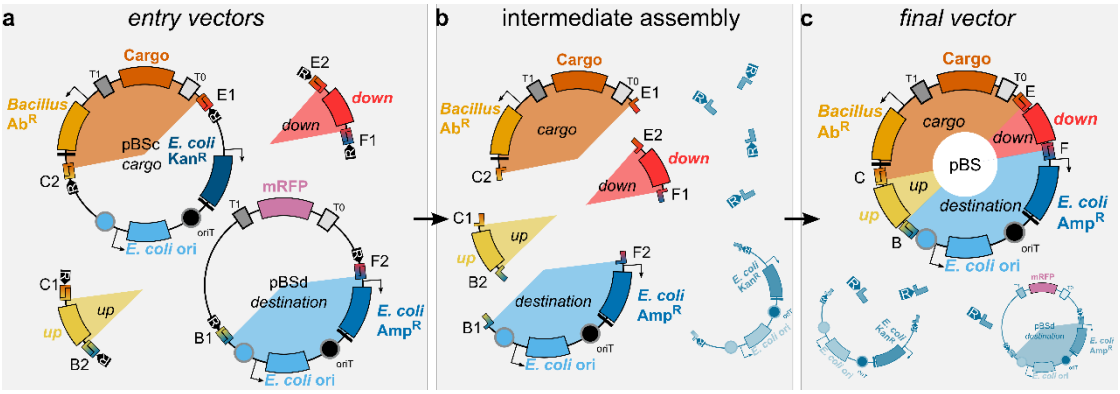

Figure 2. Schematic assembly of *Bacillus* SEVA sibling from *entry* parts

PLANNING THE ASSEMBLY

Useful questions to plan your vector assembly

1) Is it helpful to insert "your" construct of interest into the cargo region before or after pBS assembly? (test same construct/promoter etc. in different loci or rather use one locus and different cargos?) →both is possible
2) Which resistance marker to choose? (The *tet* marker was not working properly for integration into the *amyE* locus.)
3) Which MCS to choose (with lacZa (= encoded by "3" as a third digit) for blue-white screening, or without (encoded by "1"))?

Table 2. Entry vectors available for BSs assembly

BGSC[a]	Name[b]	Description	Resistance in *E. coli* / *B. subtilis*
Vectors for default assembly			
Destination vectors			
ECE701	pBSd141R	*mRFP1*, MCS-IIS F2, *bla*, ori pRO1600/ColE1, MCS-IIS B1	Amp^r / -
ECE702	pBSd191R	*mRFP1*, MCS-IIS F2, *bla*, ori pBR322/ROP, MCS-IIS B1	Amp^r / -
Vectors for flanking homology regions			
	pSEVA243	*lacZα*-pUC18 MCS, *neo*, ori pRO1600/ColE1	Kan^r/-
ECE703	pSEVA243X	*lacZα**-pUC18 MCS incl. MCS-IIS B2+C1 for *up*, *neo*, ori pRO1600/ColE1	Kan^r/-
ECE704	pSEVA243Y	*lacZα**-pUC18 MCS incl. MCS-IIS E2+F1 for *down*, *neo*, ori pRO1600/ColE1	Kan^r/-
Cargo-Resistance vectors			
ECE706	pBSc241B	MCS-default, MCS-IIS E1, *neo*, ori pRO1600/ColE1, MCS-IIS C2, *bleO*	Kan^r/ble^r
ECE707	pBSc241C	MCS-default, MCS-IIS E1, *neo*, ori pRO1600/ColE1, MCS-IIS C2, *cat*	Kan^r/cm^r
ECE708	pBSc241M	MCS-default, MCS-IIS E1, *neo*, ori pRO1600/ColE1, MCS-IIS C2, *ermC*	Kan^r/mls^r
ECE709	pBSc241S	MCS-default, MCS-IIS E1, *neo*, ori pRO1600/ColE1, MCS-IIS C2, *aad(9)*	Kan^r/spc^r
ECE710	pBSc241T	MCS-default, MCS-IIS E1, *neo*, ori pRO1600/ColE1, MCS-IIS C2, *tetL*	Kan^r/tet^r
ECE711	pBSc241Z	MCS-default, MCS-IIS E1, *neo*, ori pRO1600/ColE1, MCS-IIS C2, *ble-Sh*	Kan^r/zeo^r
ECE720	pBSc291K	MCS-default, MCS-IIS E1, *neo*, ori pBR322/ROP, MCS-IIS C2, *aph(3')IIIa*	Kan^r/kan^r
ECE713	pBSc243B	*lacZα**-pUC18 MCS, MCS-IIS E1, *neo*, ori pRO1600/ColE1, MCS-IIS C2, *bleO*	Kan^r/ble^r
ECE714	pBSc243C	*lacZα**-pUC18 MCS, MCS-IIS E1, *neo*, ori pRO1600/ColE1, MCS-IIS C2, *cat*	Kan^r/cm^r
ECE715	pBSc243M	*lacZα**-pUC18 MCS, MCS-IIS E1, *neo*, ori pRO1600/ColE1, MCS-IIS C2, *ermC*	Kan^r/mls^r
ECE716	pBSc243S	*lacZα**-pUC18 MCS, MCS-IIS E1, *neo*, ori pRO1600/ColE1, MCS-IIS C2, aad(9)	Kan^r/spc^r
ECE717	pBSc243T	*lacZα**-pUC18 MCS, MCS-IIS E1, *neo*, ori pRO1600/ColE1, MCS-IIS C2, *tetL*	Kan^r/tet^r
ECE718	pBSc243Z	*lacZα**-pUC18 MCS, MCS-IIS E1, *neo*, ori pRO1600/ColE1, MCS-IIS C2, *ble-Sh*	Kan^r/zeo^r
ECE721	pBSc293K	*lacZα**-pUC18 MCS, MCS-IIS E1, *neo*, ori pBR322/ROP, MCS-IIS C2, *aph(3')IIIa*	Kan^r/kan^r

[a] Bacillus Genetic Stock Center (http://www.bgsc.org/order.php)

[b] Numbers according to SEVA standard: 1st position, resistance marker (1, amp; 2, kan). 2nd position, origin of replication (4, pro1600/colE1 (high copy number). 9, pBR322/ROP (medium copy number). 3rd position, cargo (1, MCS default. 3, lacZα-pUC18 MCS which allows for blue-white screening with X-Gal). For further annotations, please see main publication.

4) Which locus and homology regions to choose? (For *B. subtilis* >400 bp is recommended; <800 bp is useful for sequencing reasons)
5) Which enzyme (BsaI, BbsI, BsmBI, AarI) to choose for the Golden Gate assembly (check Cargo and homology regions for the respective recognition sites!)? → BsaI is a good default. BtgZI was not working as intended. [Personal experience: the assembly can work fine, even if one unwanted restriction site is present, as long as it is incompatible to the overhangs used for assembly.]
6) Choose destination vector (high ("4" as second digit) or medium copy number("9")). For assemblies with parts known to be difficult to handle on high copy number vectors (e.g. the *Bacillus* kan-cassette), the medium copy number version should be chosen.
7) Reusability of integration sites
    a) Use once/few times or only with one of the enzmyes? → use PCR product with overhangs containing the necessary restriction sites. It can also be stored in a vector that does not mediate ampicillin resistance in *E. coli*, e.g. pSEVA243.
    b) Flexibility in choosing the enzyme for the assembly? → use primers without overhangs and insert into pSEVA243X and pSEVA243Y to add overhangs for all enzymes (check for correctly directed insertion!).

Primer design (and cloning) of *up* and *down* integration sites

8) If you choose to only use one enzyme sites (7a): Add the respective overhangs to primers for *up* and *down* integration site (see example primers below) → the fragment can still be stored e.g. in pSEVA243 (via SmaI; direction of ligation into vector is not important) and either the PCR product or the vector can be used for Golden Gate assembly.

Table 3. Example primers with Golden Gate overhangs.

Primer Name	Sequence[a] (5' to 3')
BsmBI-sacA-up-fwd	taggct**CGTCTC**t**ACCC**GACAGCACATGACCAGGAG
BsmBI-sacA-up-rev	taggct**CGTCTC**t**TCGC**CCAAAATCGTCCAGCCCG
BsmBI-sacA-do-fwd	taggct**CGTCTC**t**GAGA**CCCATCCGACCATTGACTG
BsmBI-sacA-do-rev	taggct**CGTCTC**t**TGAG**GATTTCCCGGTCGCACTG
BbsI-lacA-up-fwd	taggct**GAAGAC**tt**ACCC**GTGATGTCAAAGCTTGAAAAAAC
BbsI-lacA-up-rev	taggct**GAAGAC**tt**TCGC**ATAAATCACAGTGGCAATCTCC
BbsI-lacA-do-fwd	taggct**GAAGAC**tt**GAGA**TTCAAGCTATATTTGGAGTTGAG
BbsI-lacA-do-rev	taggct**GAAGAC**tt**TGAG**CTAATGTGTGTTTACGACAATTC
BsaI-amyE-up-fwd	ctcaagg**GGTCTC**C**ACCC**ATGTTTGCAAAACGATTCAAAACC
BsaI -amyE-up-rev	ctcaagg**GGTCTC**C**TCGC**CGATCAGACCAGTTTTTAATTTG
BsaI -amyE-do-fwd	ctcaagg**GGTCTC**C**GAGA**ATGGATGAGCGATGATGATATC
BsaI -amyE-do-rev	ctcaagg**GGTCTC**C**TGAG**TCAATGGGGAAGAGAACCG
AarI-amyE-up-fwd	ctcaagg**CACCTGC**aatg**ACCC**ATGTTTGCAAAACGATTCAAAACC
AarI -amyE-up-rev	ctcaagg**CACCTGC**aatg**TCGC**CGATCAGACCAGTTTTTAATTTG
AarI -amyE-do-fwd	ctcaagg**CACCTGC**aatg**GAGA**ATGGATGAGCGATGATGATATC
AarI -amyE-do-rev	ctcaagg**CACCTGC**aatg**TGAG**TCAATGGGGAAGAGAACCG

[a] The **recognition site**, **restriction site** (in all cases a 3' overhang will be generated), and annealing part are indicated. The annealing part needs to specified for "your" fragments. Lower case letters ensure binding of the enzyme to the PCR-product and can be changed, but work fine as they are.

9) If you choose to be flexible with the restriction enzyme (7b): Amplify your *up* and *down* fragment with primers without overhang and ligate into EcoRV-site of pSEVA243X (*up*) or pSEVA243Y (*down*). Check for correct direction of integration via sequencing. Use the vector for Golden Gate assembly.

10) If desired, different directionality of the integration part can be achieved by adding overhangs to the *up* and *down* fragments using primer overhangs vice versa to the default version.

Preparation

1) Make sure that you have all fragments/vectors and the enzymes ready for your assembly. All *entry* vectors except for the destination vector (= *pBSc* and pSEVA243X, pSEVA243Y) mediate kanamycin resistance in *E. coli* (50 µg ml^{-1}), whereas the *destination vectors pBSd* mediate ampicillin resistance (100 µg ml^{-1}).
2) Enzyme supplier: Thermo Scientific™: T4 DNA ligase 30 WU + buffer, AarI + Oligo; New England Biolabs®: BsaI (not "HF"), BsmBI, BbsI, NEBuffer 2.1, 3.1

ASSEMBLY

Preparation

1) Prepare and purify vectors or PCR products (Midi, Mini plasmid or PCR prep kits with DNA-binding columns). If you use PCR products, please ensure to clean the product from primer-dimers via gel extraction, since those carry the restriction sites needed for assembly and will be inserted into the *final vector* instead of the correct part.
2) Dilute all vectors and fragments to 40 nM (=fmol/µl), or 20 nM.

Calculation from µg/ml to nM: c (nM) = x (conc. in ng μl^{-1}) *1520/ length (bp)

We recommend estimating the DNA concentration on an agarose gel. For PCR products please ensure there are no "primer clouds" or other fragments as they all contain the correct overhangs and will be part of the assembly!

Golden Gate assembly

For each assembly (in µl)

Cargo (40nM)	1
Destination (40nM)	1
Up (40nM)	1
Down (40nM)	1
T4 DNA-Ligase (30WU)*	0.5
10x BSA	1.5
H_2O	Ad 15[+]

Programm:

37°C*	30min	
16°C	30min	
37°C	3min	X 15
16°C	5min	
50°C	10min	
80°C	10min	

[+]taking into account the enzyme-specific volume given below

Add the following components according to the enzyme to be used:

AarI	1.5	BsaI	0.5	BbsI	0.5	BsmBI*	0.5
50x Oligo	0.3			Puffer 2.1	0.75	Puffer 3.1	0.75
Ligase buffer	1.5	Ligase buffer	1.5	Ligase buffer	0.75	Ligase buffer	0.75

* For BsmBI: initial restriction takes place at 55°C. Add ligase **AFTER** that step.

E. coli transformation into and selection

3) Use competent cells of at least $5*10^6$ CFU/µg DNA. Below 10^6 is not recommended.
4) Plate on selective media (100 µg ml^{-1} ampicillin). For vectors containing *lacZα*, IPTG (1µM) and X-Gal (100 µg ml^{-1}) can be supplemented to allow blue/white-screening.
5) Colonies containing the original destination vector will appear red, those containing the correct vector will be white or blue (if *lacZα* is present). Prolonged incubation or storage can enhance colors of the colonies.
6) Pick colonies for Colony PCR or plasmid preparation (for lacZα also use a replica plate without X-Gal, since "blue" is the "dominant" phenotype over "red") and perform test digest. (e.g. with PvuII or enzymes cutting "your" *up* and *down* fragments or cargo).
7) Verify the correct insert and assembly break points via sequencing (TM3782 and TM3783 for high copy number, TM5128 and TM 3783 for medium copy number vectors).

Table 3. Oligonucleotides recommended for sequencing

Primer Name	Sequence (5' to 3')
TM5128	GGTTACTGATGATGAACATGC
TM3782	CGCAAAAAACGCACCACTACG
TM3783	GGTTATTGTCTCATGAGCGG

Trouble shooting

8) If the ratio of colonies displaying the correct color is far off (20 red: 1 white e.g.), the procedure should be optimized, because most likely those white colonies contain wrong vectors.
9) Correct colonies might be small or not present, if some parts of the vector are toxic in *E. coli*. In this case, the medium copy number destination vector should be chosen.

Naming

The central features of all *entry* and *final vectors* can be described in the SEVA number code.

They do not comply with the standard perfectly, so they are called SEVA siblings and will be named:

10) *Entry vectors*: pBSd### for destination vector, pBSc###*res* for cargo vector, pSEVA243X*locus* (=*up*) or pSEVA243-*enzyme*-*locus*-up (if restriction sites were added by primer overhangs), pSEVA243Y*locus* (=*down*) or pSEVA243-*enzyme*-*locus*-down
11) *Final vectors*: pBS###*res*-*locus*_*cargo (res* = capital letter representing the resistance marker)

USE OF THE VECTOR

1) Modification of the *final* vector, e.g. by changing the cargo, if applicable.
2) Transformation of your desired organism according to the respective protocols. For *B. subtilis* W168 natural competence can be used (check Radeck *et al*., 2013 for detailed protocols in supplemental material S3)
3) Usually, in the replication part of the vector (=not integrative part), linearization should occur before transformation. Towards that end, e.g. ApaI can be used (check your cargo and integration sites!).
4) Check for spontaneous antibiotic resistant mutants using a "no DNA" control.
5) Verify the correct insertion via Colony PCR of up-fwd Primer / TM3685 (or resistance specific, see below) and TM3682 / down-rev.

Table 4. Oligonucleotides for integration check PCR

Primer Name	Sequence (5' to 3')
TM3682	GAACGCTCGGTTGCCGC
TM3685	GGACAAATCCGCCGCCCT
TM0057 (mls)	CCTTAAAACATGCAGGAATTGACG
TM0718 (cat)	AATAGCGACGGAGAGTTAGG
TM0498 (kan)	GCCGGTATAAAGGGACCACC
TM0058 (spec)	GTTATCTTGGAGAGAATATTGAATGGAC
TM5222 (tet)	TGTTTTAGGTGGGCTTTCGTTC

After performing your experiments & demonstrating functionality:

6) Please submit customized entry vectors to BGSC (http://www.bgsc.org) and/or SEVA (http://wwwuser.cnb.csic.es/~seva/).

7.6 SUPPLEMENTAL DATA

Some of the open questions presented in the publications and manuscript were addressed and the corresponding data is presented in this section. The corresponding strains are listed in Table 1 at the end of this section.

7.6.1 P_{BCRC}-RESPONSE DOES NOT DEPEND ON LIAIH

P_{bcrC} activity dependends on σ^M which is activated by CESR. The molecular cue is still unknown. LiaIH is activated upon cell envelope stress caused by bacitracin and it was shown to mediate resistance against its inducer in the absence of BceAB. This newly-found feature raised the question, if the presence of LiaIH reduces the CESR caused

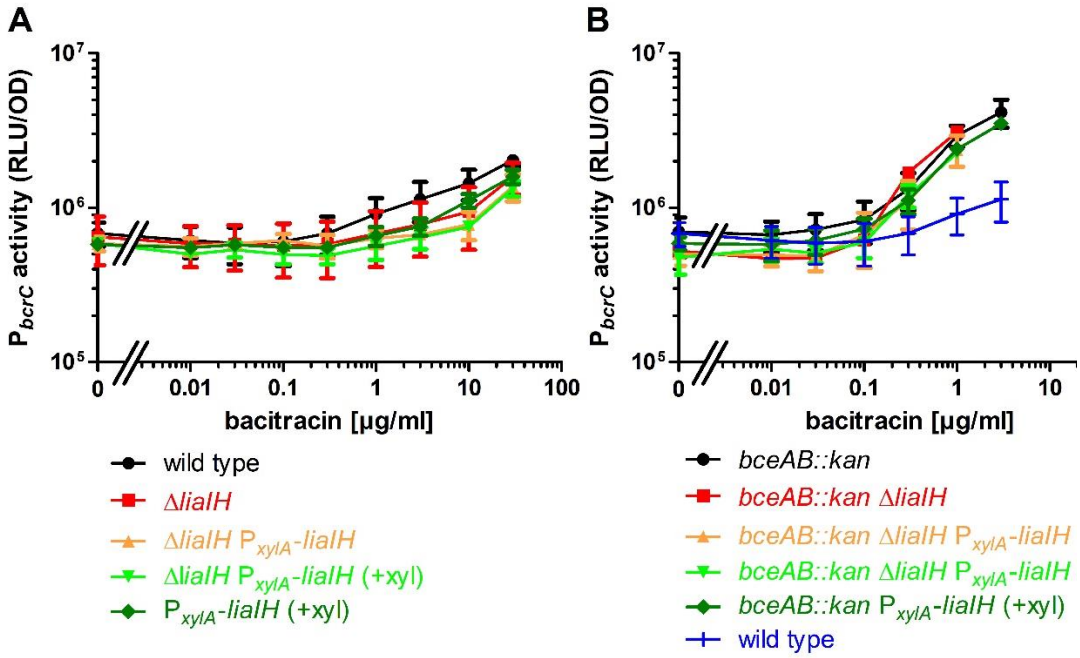

Figure 6. Activity of the *bcrC*-promoter depending on LiaIH-levels in the presence and absence of BceAB. Target promoter activity of P_{bcrC} -*lux* in strains expressing different levels of LiaIH in wild type (A) or *bceAB*-disruption background (B), as given by specific luciferase activity (RLU/OD_{600}) one hour after addition of indicated amounts of bacitracin. Measurements were performed as described in Fig. 3 of **publication II**. Colors code for different expression levels of *liaIH*, as driven by the xylose-inducible promoter P_{xylA}: (red) No expression, via deletion of LiaIH; (orange) Low constitutive expression, via complementation of the deletion mutant with P_{xylA}-*liaIH* in the absence of xylose; (light green) High constitutive expression, via complementation of the deletion mutant P_{xylA}-*liaIH* in the presence of 0.2% xylose; (dark green) overexpression in W168 wild type background, via expression of P_{xylA}-*liaIH* in the presence of 0.2% xylose. The corresponding strains are (A) TMB1620, TMB1662, TMB3684, TMB3685 and (B) TMB1620, TMB1624, TMB2195, TMB3686, and TMB3687, as listed in Table 1. Error bars indicate the standard deviation between at least three biological replicates.

by bacitracin as detected by P_{bcrC}. Consequently, the activity of P_{bcrC} was measured as described in **publication II**, and the level of LiaIH was adjusted using the xylose-inducible promoter P_{xylA}. This was also performed in strains missing *bceAB*, to exclude that any measurable effect is covered by the presence of the main resistance determinant. Figure 6 shows P_{bcrC}-activity 1 hour after addition of increasing amounts of bacitracin. P_{bcrC}-activity shows a high basal activity and low dynamic range, from about $7 * 10^5$ to $1.5 * 10^6$ (A, with native *bceAB*) or $4 * 10^6$ RLU/OD (B, without *bceAB*). In the absence and presence of *bceAB*, the amount of LiaIH did not significantly influence the promoter activity of P_{bcrC}, suggesting that these proteins protect the cell envelope in a distinct manner, compared to the cell envelope stress sensed by σ^M. Since the dynamic range is so low, it is still conceivable that influencing patterns could not be detected.

7.6.2 P_{BCEA}-RESPONSE TO LOSS OF BCRC DOES NOT DEPEND ON PRODUCTION OF ANTIMICROBIAL PEPTIDES

In **publication II**, it was found that P_{bceA} is activated in the absence of BcrC, which was puzzling because P_{bceA} was normally activated in response to the flux of bacitracin transport (**publication I**). It was suggested that in case of *bcrC* deletion, P_{bceA} is activated by intrinsically produced AMPs under these experimental conditions. To address this question, P_{bceA}-activity was measured as described in **publication II** in strains where the operons known to encode for toxin production of SdpC, SkfA, and YydF were disrupted by antibiotic cassettes, as described in (Höfler *et al.*, 2016). Strains were measured as described in **publication II**. Figure 7 shows P_{bceA}-activity of the wild type and AMP-defective strains 1 hour after bacitracin addition with (blue) and without presence of BcrC (red). Without bacitracin, P_{bceA}-activity is low (10^4 RFU/OD) and it gradually increases for all strains with increasing bacitracin concentrations, reaching a maximum of $2.5*10^6$ RFU/OD, in line with previous descriptions (**publications I, II**). All strains missing BcrC (red) show an about 10-fold higher P_{bceA}-activity than their counterparts with BcrC, if bacitracin is added. So, the presence or absence of all three AMPs investigated did not influence P_{bceA}-activity, neither in the absence, nor presence of BcrC.

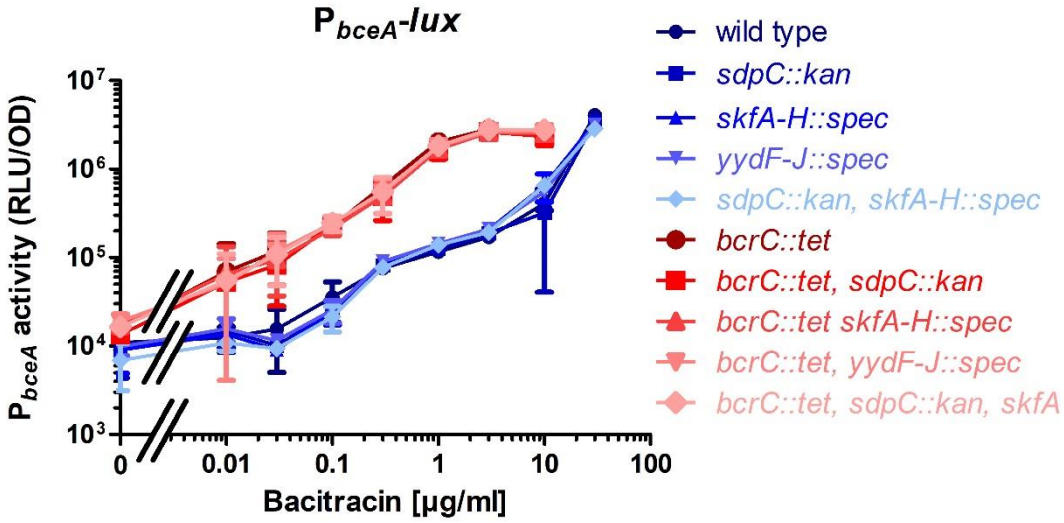

Figure 7. Influence of Cannibalism toxins SdpC, SkfA and YydF on P_{bceA}-activity in the presence and absence of BcrC. Target promoter activity of P_{bceA}-*lux* in wild type or strains missing the genes necessary for functional cannibalism toxin production in wildtype (red), or *bcrC*-disruption background (blue), as given by specific luciferase activity (RLU/OD_{600}) one hour after addition of indicated amounts of bacitracin. Measurements were performed as described in Fig. 3 of **publication II**. Genotypes are given in the legend, corresponding to TMB1619, TMB1627, TMB1770, TMB 1773, TMB1775, TMB2015, and TMB3570-TMB3573 (Table 1). Error bars indicate the standard deviation between at least three biological replicates.

7.6.3 LIST OF ADDITIONAL STRAINS

Table 1: *B. subtilis* strains used for additional data in this study

Strain	Description	Source
Strains used for Figure 6		
TMB1620	W168 *sacA*::pCHlux104 (P_{bcrC}-*lux*)	(Höfler *et al.*, 2016)
TMB1624	W168 *bceAB::kan sacA*::pCHlux104 (P_{bcrC}-*lux*)	publication II
TMB1662	W168 Δ*liaIH* (clean deletion) *sacA*::pCHlux104 (P_{bcrC}-*lux*)	publication II
TMB2159	W168 Δ*liaIH bceAB::kan sacA*::pCHlux104 (P_{bcrC}-*lux*)	This study
TMB3684	W168 *lacA*::pJR2EF02 (pBS2E-P_{xylA}-*liaIH*) *sacA*::pCHlux104 (P_{bcrC}-*lux*)	This study
TMB3685	W168 Δ*liaIH lacA*::pJR2EF02 (pBS2E-P_{xylA}-*liaIH*) *sacA*::pCHlux104 (P_{bcrC}-*lux*)	This study
TMB3686	W168 *bceAB::kan lacA*::pJR2EF02 (pBS2E- P_{xylA}-*liaIH*) *sacA*::pCHlux104 (P_{bcrC}-*lux*)	This study
TMB3687	W168 Δ*liaIH bceAB::kan lacA*::pJR2EF02 (pBS2E- P_{xylA}-*liaIH*) *sacA*::pCHlux104 (P_{bcrC}-*lux*)	This study
Strains used for Figure 7		
TMB1619	W168 *sacA*::pCHlux103 (P_{bceA}-*lux*)	(Radeck *et al.*, 2013)
TMB1627	W168 *bcrC::tet sacA*::pCHlux103 (P_{bceA}-*lux*)	(Radeck *et al.*, 2013)
TMB1770	W168 *sdpC::kan sacA*::pCHlux103 (P_{bceA}-*lux*)	(Höfler *et al.*, 2016)
TMB1773	W168 *skfA-H::spec sacA*::pCHlux103 (P_{bceA}-*lux*)	(Höfler *et al.*, 2016)
TMB1775	W168 sacA::pCHlux103 (PbceA-lux)) *yydFGHIJ::spec sacA*::pCHlux103 (P_{bceA}-*lux*)	(Höfler *et al.*, 2016)
TMB2015	W168 *sdpC::kan skfA-H*::*spec sacA*::pCHlux103 (P_{bceA}-*lux*)	(Höfler *et al.*, 2016)
TMB3570	W168 *bcrC::tet sdpC::kan sacA*::pCHlux103 (P_{bceA}-*lux*)	This study
TMB3571	W168 *bcrC::tet skfA-H::spec sacA*::pCHlux103 (P_{bceA}-*lux*)	This study
TMB3572	W168 *bcrC::tet yydFGHIJ::spec sacA*::pCHlux103 (P_{bceA}-*lux*)	This study
TMB3573	W168 *bcrC::tet sdpC::kan skfA-H::spec sacA*::pCHlux103 (P_{bceA}-*lux*)	This study

8 ACKNOWLEDGEMENTS

Vielen Dank an die Gutachter (Thorsten Mascher, Ralf Heermann) und Prüfer der LMU, sowie an Julia Bartels, Diana Wolf, Marion Kirchner und Carolin Höfler für die kritische Durchsicht dieser Arbeit. Ich bin der LMU und sämtlichen Dozenten für die exzellente Ausbildung während meines Bachelor- und Masterstudiums, sowie für die Ermöglichung der Teilnahme an den iGEM-Wettbewerben sehr dankbar.

In den Jahren der Arbeit an der Dissertation hatte ich viele Gelegenheiten mich fachlich und persönlich zu entwickeln und ich möchte allen danken, die mir dabei unterstützend zur Seite standen. Es war eine gute Zeit, eine leichte Zeit und auch eine schwere Zeit, eine wichtige Zeit.

Mein Dank geht an Thorsten, den ich als Betreuer des iGEM-Wettbewerbs kennengelernt habe und der mich von Beginn an gefördert hat – ohne Dich hätte ich nie so viel von der Wissenschaft und Akademie gelernt, wie es der Fall war. Ich dachte, ich hätte einen guten Schreibstil – bis Du zum ersten Mal einen Abstract und dann ein Manuskript korrigiert hattest. Dieser Stolz, als das erste Mal, ein kompletter Satz genau so stehen bleiben durfte – den werde ich nie vergessen. Genausowenig wie den Frust, dass der Satz danach wieder komplett zerlegt wurde ;-).

Lange habe ich nicht gezögert, als ich mich entscheiden musste, ob ich mit nach Dresden gehe. Obwohl die Entscheidung schwer war, war das einzig vernünftige. Und es war eine sehr gute Zeit. Ich durfte viele Erfahrungen machen, die ich sonst nicht gemacht hätte und das weiß ich sehr zu schätzen. Und doch war es anstrengend und ich musste mich erneut entscheiden: wann wird es Zeit, Dresden wieder zu verlassen? Ich habe mich für eher früher entschieden und es war trotzdem eine schwere Zeit. Ich vermute, dass es auch andersherum so gewesen wäre. Doch wer weiß das schon. Thorsten, ich bin Dir dankbar, dass Du mich meinen Weg gehen lässt und mich unterstützt, auch wenn es nicht Deine Wahl gewesen wäre. Ich weiß, dass Du gibst, was Du kannst.

Ich danke allen Kollegen im Labor, ehemaligen und jetzigen, für's Aufleben, für's da sein, für die gute Zusammenarbeit. Susanne und Schorsch, Julia, Dayane, Daniela, Diana, Franzi, Ainhoa, Xiaoluo, Stephan, Philipp, Qiang, Mona, Niko, Roman, Caro, Caro2, Vanessa, Annett, Susanne, Stephan, Zsolt uvm. Vor allem Julia – wir haben so viel zusammen erlebt: vom ersten Semester, ersten iGEM, erfolgreichem 2012er iGEM, erstem iGEM-Betreuen, bis hin zum PhD in der gleichen Arbeitsgruppe. Leider konnten wir nicht mehr so (viel) zusammenarbeiten und zusammen erleben, wie wir uns gewünscht hatten. Ich drücke Dir die Daumen, dass Du deine Ziele erreichst!

Ein großes Danke geht an Nina, für die Geduld und die vielen Überstunden und ich fürchte auch Nachtschichten am Mikroskop und plate reader, um die Daten zu generieren seit ich nicht mehr in Dresden bin!

Ich danke meinen Eltern Hanne und Uwe für ihr Vertrauen in mich und die Unterstützung, wann immer ich sie brauche. Meinem Bruder Marcis für die ersten Einsichten in die Wissenschaft und Felix, Polina und Ian für all die Exkursionen und Ideen zur Lebensfreude. Meiner Oma Ruth, der aus Geldmangel die höhere Bildung verwehrt blieb und deren Stolz so ehrlich ist. Du verstehst mich und findest die richtigen Worte, wenn ich im Selbstmitleid zu versinken drohe. Danke Klaus für die Umarmungen, danke Sabine für die Aufnahme, obwohl es nicht einfach war.

Ich danke meinen Freunden für die Geduld mit mir und meinen Schreibkrisen, und vor allem für die Ablenkung.

Mein größter Dank gilt Phil, für alles. Deine Zurückhaltung gibt mir den Raum, mich selbst zu finden, Dein fester Stand und Deine Ehrlichkeit sorgen dafür, dass ich mich dabei nicht verliere. Deine Geduld und Dein Einfühlungsvermögen lassen mich immer wieder schwach werden.

Stefan Sagmeister (österreichischer Künstler) hat mir mit seinen “things that I have learned in my life so far” hilfreiche Denkanstöße gegeben. Mit zweien davon, die mich besonders berühren, möchte ich die Danksagung und dieses Werk beenden:

“Having guts always works out for me.”

“Everybody always thinks they are right.”